Bimodal Mechanism of DNA Repair Stimulation by DDB2 (XPE) in Chromatin

Dissertation

zur

Erlangung der naturwissenschaftlichen Doktorwürde

(Dr. sc. nat.)

vorgelegt der

Mathematisch-naturwissenschaftlichen Fakultät

der

Universität Zürich

von

Jia Fei

aus der

Volksrepublik China

Promotionskomitee
Prof. Dr. Josef Jiricny (Vorsitz)
Prof. Dr. Hanspeter Nägeli (Leitung der Dissertation)
Prof. Dr. Michael Hengartner

Zürich, 2011

1. Table of content

Contents

2. Summary

Deleterious covalent bonds are generated between adjacent pyrimidine bases in DNA when skin cells are bombarded with the ultraviolet (UV) component of sunlight. All living organisms have evolved multiple strategies to cope with the resulting pyrimidine dimers, because these DNA lesions cause mutations that lead to cell death or threaten genome integrity. In the human skin, UV lesions are removed by the nucleotide excision repair (NER) machinery that is generally initiated when the XPC sensor subunit recognizes offending DNA lesions. However, to excise cyclobutane pyrimidine dimers (CPDs), which is the most abundant UV lesion, the NER complex depends on an accessory factor referred to as DDB or UV-DDB (for UV-damaged DNA-binding). The actual DNA-binding subunit of this heterodimer (DDB2) binds avidly to the chromatin of UV-irradiated cells but, until now, inconsistent data have been reported as to how this protein stimulates DNA repair. Mutations of DDB2 cause xeroderma pigmentosum complementation group E (XP-E), an inherited disease associated with sunlight hypersensitivity and predisposition to skin cancer. The present thesis first demonstrates that the formation of a stable XPC protein-DNA recognition complex at UV lesions depends on the insertion of a β-hairpin of XPC into the DNA double helix. Next, the thesis shows that DDB2 interacts directly with the DNA-binding domain of XPC protein to promote this thermodynamically unfavorable β-hairpin insertion. Finally, this thesis demonstrates a previously unknown ubiquitin-dependent function whereby DDB2 sorts out solubilizable nucleosomes as hotspots for NER activity. Through ubiquitylation by the DDB1-CUL4 ligases, DDB2 prevents the XPC partner from penetrating into insoluble chromatin that is refractory to the recruitment of downstream NER subunits. To summarize, the present thesis describes DDB2 as a bivalent organizer of DNA repair in human cells and identifies a new task of ubiquitin in controlling the spatiotemporal chromatin distribution of a key guardian of the genome.

3. Summary (in German)

DDB2 (XPE) stimuliert die DNA Reparatur im Chromatin durch einen bimodalen Mechanismus

Nach UV Bestrahlung von Zellen bindet DDB2 sofort an Chromatin; bislang findet sich in der Literatur keine uebereinstimmenden Daten, wie dieser Faktor die DNA Reparatur stimuliert. In dieser Arbeit koennen wir eine vorher unbekannte Ubiquitin- abhaengige Funktion von DDB2 zeigen: DDB2 erkennt loesbares Chromatin als Hotspot fuer DNA Exzisions Aktivitaet. Durch DDB1-CUL4A vermittelte Ubiquitinierung verhindert DDB2, dass das XPC Protein in unloeslichen Nukleosomen verschwindet, die die schnelle Akkumulation von nachfolgenden Reparatur Komplexen nicht erlauben. Eine Ubiquitin-unabhaengige, direkte Interaktion ueber die beiden DNA- Bindedom?nen von XPC ermoeglicht DDB2 eine kurzweilige Rekrutierung von XPC zu den UV Schaeden. Dort erleichtert DDB2 das thermodynamisch unguenstige Einfuegen des beta Hairpins von XPC in die geschaedigte DNA Helix. In dieser Studie konnten wir zeigen, dass Ubiquitin auch eine Rolle bei der raeumlich-zeitlichen Verteilung des Hauptwaechters des Genoms im Chromatin uebernimmt, als auch, dass DDB2 eine vielseitige Funktion bei der Organisation der DNA Reparatur einnimmt.

4. Introduction

4.1 UV damage responses

DNA molecules are under continuous attack by spontaneous decay events, endogenous reactive metabolites and exogenous genotoxic agents (Lindahl, 1993; Kirkwood, 2005; Luch, 2005). Against these multiple sources of DNA damage, the genome stability is ensured by a network of DNA repair pathways collaborating over the whole cell division cycle. Proper maintenance of genomic stability is critical for normal development as well as the prevention of premature aging and diverse cancer-prone diseases (**Fig. 1**) (Hoeijmakers, 2001; Friedberg et al, 2006b; Hoeijmakers, 2009; Jackson & Bartek, 2009).

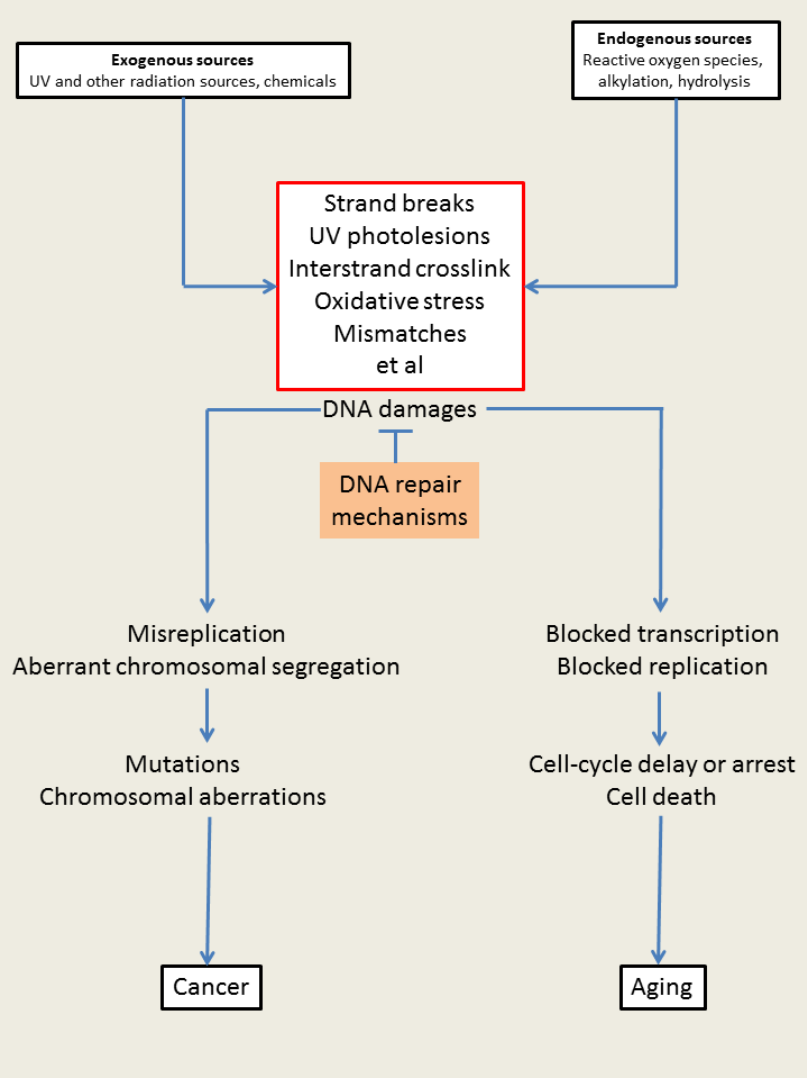

Figure 1. *Proper repair of DNA is required for the maintenance of genome stability. Mutations caused by a failure of DNA repair trigger either replication arrest or mutagenesis, leading to cell death, cellular senescence, contributing to aging, or carcinogenesis. Adapted from (Hoeijmakers, 2009).*

Five major DNA repair machineries have been discovered that cope with mutagenic DNA insults. These DNA damage responses include nucleotide excision repair (NER) to eliminate bulky lesions, base excision repair (BER) to remove modified or incorrect bases, mismatch repair (MMR) to rectify DNA replication errors, homologous recombination (HR) as well as non-homologous-end-joining (NHEJ) to process DNA double strand breaks and rescue missing genetic information (Lindahl & Wood, 1999; Harper & Elledge, 2007).

Nucleotide excision repair (NER) is a central component of this repair network that displays an extraordinary versatility in recognizing and eliminating a wide variety of DNA helix-distorting base lesions. The most intensively studied targets of NER activity are ultraviolet light (UV)-induced crosslinks between adjacent pyrimidines, referred to as pyrimidine dimers, mainly cyclobutane pyrimidine dimers (CPDs) and the more DNA helix-distorting 6-4 pyrimidine-pyrimidone photoproducts (6-4PPs) (**Fig. 2**).

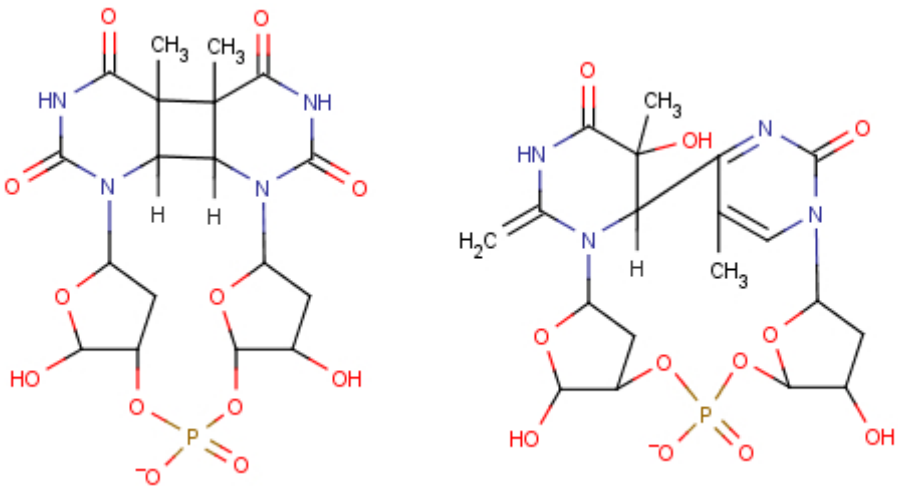

Figure 2. Chemical structure of the major UV-induced photolesions, CPDs (left) and 6-4PPs (right).

These photodimers can stall the elongation of DNA polymerases during DNA replication and suppress the transcription of genes (Mitchell et al, 1990; Mouret et al, 2006). In addition, most of the cellular UV-induced mutations leading to skin cancer are due to the slowly repaired CPDs (Tang et al, 2000). However, in addition to UV lesions, the NER machine also recognizes and

removes a number of other bulky base adducts which are generated by exogenous mutagens (Friedberg et al, 2006a), including for example polycyclic aromatic hydrocarbons or other harmful components of tobacco smoke, food carcinogens like for example heterocyclic amines or aflatoxins, and even some chemotherapeutic drugs like cisplatin and psoralens (Sancar, 1996; Hoeijmakers, 2009). Further NER substrates are oxidative base lesions, such as 8,5′-cyclopurine nucleosides, that cannot be removed by the action of DNA glycosylases (Satoh et al, 1993; Reardon et al, 1997; Kuraoka et al, 2000), protein-DNA crosslinks (Reardon & Sancar, 2006) and DNA lesions generated by lipid peroxidation products such as malondialdehyde (Johnson et al, 1997). The NER pathway is initiated when the DNA substrate displays two obligate and distinguishable features, i.e., a local base pair disruption and a chemically altered deoxyribonucleotide residue (Hess et al, 1997a; Hess et al, 1997b; Buterin et al, 2005). Once initiated, the NER apparatus proceeds with damage recognition, DNA duplex unwinding, damage verification, damage excision, gap filling and ligation (Wood, 1999; Gillet & Scharer, 2006; Guo et al, 2010).

The NER reaction involves a multiprotein complex of around 10 factors comprising 30 different subunits that are assembled at DNA lesion sites in a sequential manner (Wood, 1999). The precise order of recruitment of these core NER players is still debated, but a favored model illustrated in **Fig. 3** proposes that the initiation of NER activity can be divided into two distinct subpathways, transcription-coupled repair (TCR) and global genome repair (GGR). The major difference between these two subpathways is the mechanism by which the DNA damage is initially recognized in the genome. The TCR process senses and removes base damages only from the transcribed DNA strand of transcriptionally active genes. It takes place when the RNA polymerase II (RNAPII) is stalled by obstructing DNA lesions (Tornaletti & Hanawalt, 1999; Svejstrup, 2002). RNAPII, in turn, recruits Cockayne syndrome A protein (CSA), Cockayne syndrome B protein (CSB), transcription factor IIH (TFIIH) and XPG to the lesion sites (Venema et al, 1990; van Hoffen et al, 1993). CSA is the component of a Cullin ubiquitin E3

ligase that ubiquitinates RNA polymerase II, CSA itself and histones upon UV irradiation (Groisman et al, 2003).

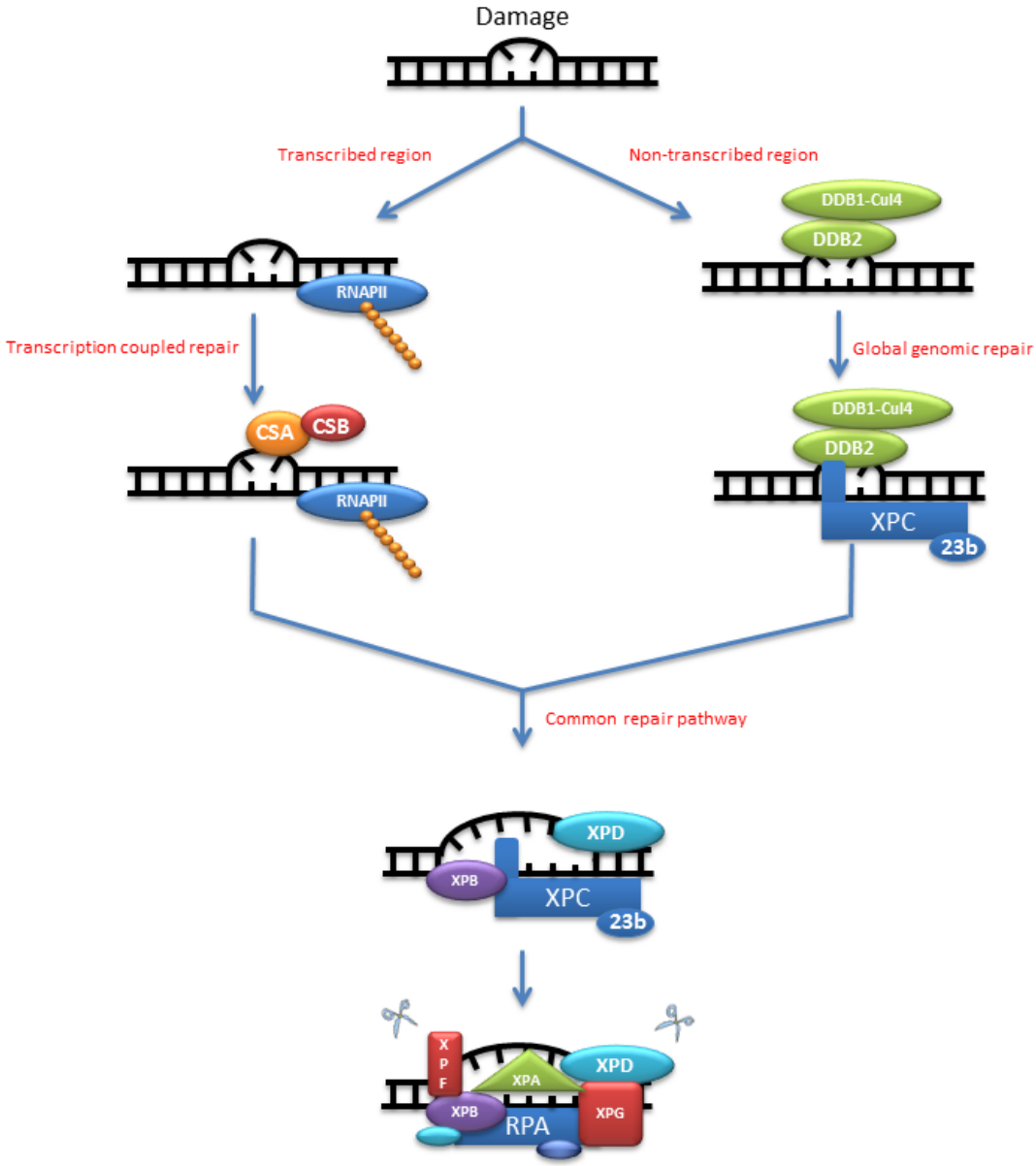

Figure 3. Scheme of the mammalian NER system. Model adapted from (Cleaver et al, 2009)

Instead, CSB belongs to the SWI2/SNF2 family of DNA-dependent ATPase with chromatin remodeling activity (Troelstra et al, 1992) and also displays a

ubiquitin-binding domain (UBD). A CSB deletion mutant that lacks this UBD is unable to mediate the TCR process and fails to support the rapid reactivation of transcription following DNA damage (Anindya et al, 2010). Possible roles of the CSA and CSB proteins are to remove the stalled transcription complex, or induce its retraction from the lesion site, and act as a scaffold to facilitate the recruitment of repair proteins. This TCR process allows for the fast removal of transcription-obstructing lesions from transcribed DNA sequences and avoids that stalled RNAPII complexes result in the induction of cell death by apoptosis (Ljungman & Zhang, 1996; van Oosten et al, 2000).

Unlike TCR, the GGR subpathway operates throughout the whole genome and is triggered by binding of the XPC complex (consisting of XPC, RAD23B and centrin 2) to damaged DNA sites (Sugasawa et al, 1998; Volker et al, 2001; Riedl et al, 2003). As will be outlined below, DDB (including the *XPE* gene product) is also involved in the initial damage recognition during GGR and plays a very important role in the removal of UV lesions. The major biological significance of GGR is that it prevents the DNA replication machinery from encountering damaged templates, thus reducing the frequency of mutations due to lesion bypass by translesion DNA synthesis. As a consequence, GGR represents an important defense line against DNA damage-induced mutagenesis and carcinogenesis (Friedberg, 2001; Hoeijmakers, 2001). Indeed, it is important to point out that the vast majority of cancer-associated mutations arise from DNA damage in non-transcribed sequences. The mechanism by which XPC protein initiates the GGR response through the detection of damaged DNA sites will be discussed in detail in section 3.3. How exactly this protein and its partners are able to rapidly sense a few damaged lesions among more than 6000 million bases of each mammalian cell is one of the most fascinating questions in modern biology.

After damage recognition by either RNAPII (in TCR) or XPC (in GGR), the subsequent excision repair reactions take place by a common cascade. A central component at this stage of the NER pathway is the TFIIH complex (Yokoi et al, 2000; Volker et al, 2001). In TCR, RNAPII, in conjunction with CSA and CSB proteins, promotes the loading of TFIIH onto damaged sites

(Tantin, 1998) whereas, in GGR, TFIIH is recruited by the carboxy-terminal domain of XPC protein, (Yokoi et al, 2000; Araujo et al, 2001; Uchida et al, 2002). The whole TFIIH complex is composed of ten subunits including the two ATP-dependent DNA unwinding enzymes XPB and XPD. XPB displays a weak 3'–5' helicase activity, while XPD shows the opposite 5'–3' polarity (Schaeffer et al, 1993; Schaeffer et al, 1994). The more downstream NER factors XPA and replication protein A (RPA) stimulate this unwinding function of TFIIH, which results in an opened nucleoprotein intermediate where 25-30 base pairs are unwound around the damaged site (Holstege et al, 1996; Evans et al, 1997).

Very recent results from our laboratory demonstrate that, besides the formation of this open intermediate, the 5'–3' helicase activity of XPD is responsible for a damage-specific and strand-selective lesion demarcation process (Sugasawa et al, 2009; Mathieu et al, 2010). The mechanism by which the XPD helicase interacts with damaged DNA has been studied with a monomeric homolog from the mesophilic archaeon *Ferroplasma acidarmanus* incubated with DNA substrates containing a site-directed CPD lesion. This experimental approach demonstrated that the collision of XPD with a single CPD is sufficient to inhibit its helicase function and that the presence of this lesion stimulates its concurrent ATPase activity. The resulting unwinding junctions were probed by digestion with restriction endonucleases or with a CPD-specific DNA glycosylase (T4 DNA endonuclease V). These protection assays showed that XPD remains tightly bound to a CPD located in the translocated strand along which the enzyme moves in the 5'–3' direction. In contrast, the XPD enzyme readily dissociates from the DNA substrate when it runs into a CPD located in the displaced 3'–5' strand. Taken together, these recent results reveal a damage verification and demarcation mechanism mediated by a strand-selective immobilization of the XPD helicase. This enzyme is thought to use its iron-sulfur cluster (Fan et al, 2008; Liu et al, 2008; Wolski et al, 2008) as a molecular "ploughshare" to search for obstructing lesions. An attractive feature of this strand-selective verification and demarcation model is that a stable pre-incision intermediate that allows for DNA incision can only be formed by damage-specific immobilization of the

XPD subunit, such that its unwinding activity is focused on the lesion site without further translocation of the TFIIH complex (Sugasawa et al, 2009; Mathieu et al, 2010).

After the formation of an immobilized unwinding intermediate, the “Y-shaped” double-stranded to single-stranded DNA junctions on either side of the lesion are recognized by the endonucleases XPF-ERCC1 and XPG (O'Donovan et al, 1994; Sijbers et al, 1996). XPF-ERCC1 carries out the 5′ incision, which precedes the 3′ incision by XPG (Staresincic et al, 2009). This coordinated double cleavage of damaged strands generates oligonucleotide excision products of 24–32 residues containing the offending damage (Huang et al, 1992; Moggs et al, 1996). The undamaged template strand is protected by RPA (Wold, 1997) and repair synthesis is accomplished by the action of DNA polymerases delta, epsilon and kappa (Ogi et al, 2010), in conjunction with replication factor C (RFC) and proliferating cell nuclear antigen (PCNA). Finally, the remaining nick is joined by DNA ligase I and DNA ligase III (Aboussekhra et al, 1995; Moser et al, 2007). This sequential repair process is sustained by a network of protein-protein interactions illustrated in **Fig. 4**.

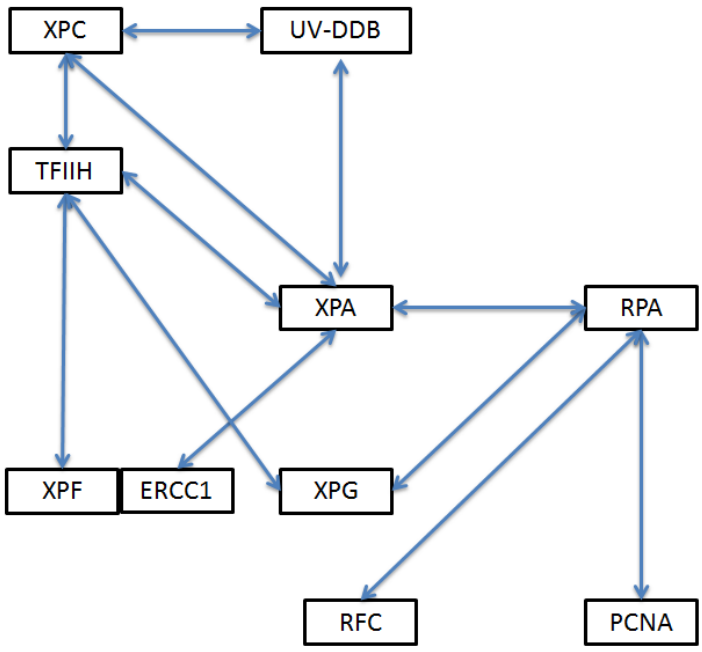

Figure 4. Interactions between GGR factors (Sugasawa, 2010).

In addition to the elimination of DNA damage induced by genotoxic reactions, some authors propose that the NER pathway has also been adopted for a more general function in transcription by mediating gene activation through the removal of an inhibitory DNA methylation code in regulatory sequences (Barreto et al, 2007; Le May et al, 2010).

4.2 Xeroderma pigmentosum and Cockayne syndrome

In humans, hereditary defects in one of seven NER genes (designated *XPA* to *XPG*) cause a devastating disease, known as xeroderma pigmentosum (XP), that is characterized by hypersensitivity to sunlight, a dramatic predisposition to skin cancer (~1,000 times higher than in the normal population), neurological deficits and also ophthalmologic manifestations (Kraemer et al, 1987; Friedberg, 2001; Hoeijmakers, 2001). The incidence of this autosomal recessive syndrome is about 1:250000 in the United States and Europe, whereas it is higher (1:40000) in Japan (Hengge & Emmert, 2008). Various laboratory methods like the measurement of UV sensitivity of cultured fibroblasts, the assessment of chromosome breaks, cell fusion and complementation studies, unscheduled DNA synthesis as well as gene sequencing have been adapted for the diagnosis of this syndrome in patients. Based on genetic or biochemical complementation experiments, NER-deficient XP patients are classified into seven groups (XP-A to XP-G). An additional complementation group (XP-V for variant) involves a defective DNA polymerase eta (POLη) that leads to high rates of mutagenesis following exposure to UV light. Thus, although XP-V patients have normal NER activity, they exhibit similar symptoms as the classical XP complementation groups (Johnson et al, 1999; Masutani et al, 1999). With regard to the TCR process, mutations in the *CSA* or *CSB* genes cause Cockayne syndrome characterized by UV hypersensitivity, severe developmental abnormalities, segmental premature aging but no overt risk of cancer (Nance & Berry, 1992; Bootsma et al, 2001; Friedberg, 2001).

4.3 DNA damage recognition by the XPC complex

The *XPC* gene was originally cloned by correction of the UV hypersensitivity of XP-C fibroblasts (Legerski & Peterson, 1992). The human *XPC* gene

encodes a protein of 940 amino acids that forms a heterotrimer with centrin 2 (an 18-kDa centrosomal protein) and RAD23B [A 58-kDa homolog of yeast RAD23 (for RADiation-sensitive)] (van der Spek et al, 1996).

RAD23B was one of the first indications hinting to a possible link between NER and the ubiquitin-proteasome system (Schauber et al, 1998). In fact, RAD23B displays an amino-terminal ubiquitin-like (UBL) domain and two carboxy-terminal ubiquitin association (UBA) domains besides an XPC-binding domain (Dantuma et al, 2009). The UBA domains interact with K-48/63-linked polyubiquitination chains or UBL domains of other interacting proteins. It has been proposed that RAD23B inhibits the recognition of ubiquitinated target proteins by the proteasome complex (Bertolaet et al, 2001; Chen et al, 2001a; Wilkinson et al, 2001; Raasi & Pickart, 2003). In addition, the UBL domain, which interacts with proteasome subunits such as Rpn1, Ufd2 and Pth2, is more directly involved in the NER system by stimulating its overall activity (Russell et al, 1999; Lambertson et al, 2003). The combined deletion of RAD23A and RAD23B, the two mammalian homologs of RAD23 (Ng et al, 2003) causes a dramatic reduction of the cellular amount of XPC protein, in turn leading to a strong reduction in NER activity, an effect that can be compensated by XPC over-expression (Ng et al, 2002; Okuda et al, 2004). Because XPC protein is ubiquitinated upon UV irradiation by the Cullin 4A ubiquitin ligase (Sugasawa et al, 2005; Wang et al, 2005), it has been concluded that the function of RAD23B is to stabilize its XPC partner through protection from proteasomal degradation. However, this hypothesis has been challenged by protein interaction analyses, using the fluorescence resonance energy transfer (FRET) technique, where after UV exposure the amount of RAD23B in complex with XPC protein strongly dropped (Bergink, 2006). Therefore, the precise role of RAD23B during DNA damage recognition remained unclear.

Centrin 2 is a highly abundant and conserved multifunctional Ca^{2+}-binding protein, belonging to the calmodulin superfamily (Salisbury, 2007) that is involved in centriole duplication (Salisbury et al, 2002). However, about 90% of centrin 2 are not associated with centrosomal structures (Paoletti et al, 1996), suggesting that it has additional cellular functions. A recent study

showed that SUMOylation of centrin 2 by conjugation with SUMO2/3 moieties generates a nucleus localization signal, thus stimulating the interaction with XPC protein (Klein & Nigg, 2009). Although centrin 2 is dispensable for NER both *in vivo* and *in vitro*, an interaction between centrin 2 and the carboxy-terminus of XPC has been shown to stimulates the damaged DNA-binding activity of the XPC complex (Popescu et al, 2003; Nishi et al, 2005).

4.3.1 XPC protein

The XPC polypeptide is the DNA-binding subunit of the XPC complex. Electrophoretic mobility shift assays (EMSA) reveal that XPC displays a modest binding preference for DNA containing many different types of base lesions, including 6-4PPs, benzo[*a*]pyrene (B[*a*]P) diol epoxide adducts, cisplatin crosslinks and N-acetoxy 2-acetylaminofluorescence (AAF) adducts (Batty et al, 2000; Sugasawa et al, 2001; Sugasawa et al, 2002). Nevertheless, XPC on its own is unable to discriminate between native DNA and duplexes containing CPDs, which are the most abundant products generated by UV irradiation. The mechanism of how XPC protein recognizes various helix-distorting base lesions that do not share a common chemical structure has been addressed in several biochemical studies. In particular, studies from our group show that XPC protein interacts preferentially with the unpaired bases of single stranded DNA over double stranded DNA (Maillard et al, 2007a; Maillard et al, 2007b). We further demonstrated that XPC protein recognizes damaged sites in duplex DNA by sensing the presence of unpaired nucleotides located in the undamaged complementary strand across bulky lesions. This indirect readout of DNA targets, by which XPC protein detects damage-induced distortions of the double helix rather then the base lesions themselves, accounts for the striking substrate versatility of the GGR process. Also, scanning force microscopy studies revealed that the binding of XPC protein to DNA induces a 39-49° kink in the DNA backbone and partial melting of the duplex of 4-7 base pairs (Evans et al, 1997; Janicijevic et al, 2003; Mocquet et al, 2007).

These biochemical analyses have been confirmed by subsequent X-ray analyses of a co-crystal of RAD4 (the yeast *Saccharomyces cerevisiae* XPC

homolog) with RAD23 and an artificial DNA substrate containing a CPD embedded in a cluster of three adjacent base mismatches (**Fig. 5**) (Min & Pavletich, 2007; Sugasawa & Hanaoka, 2007).

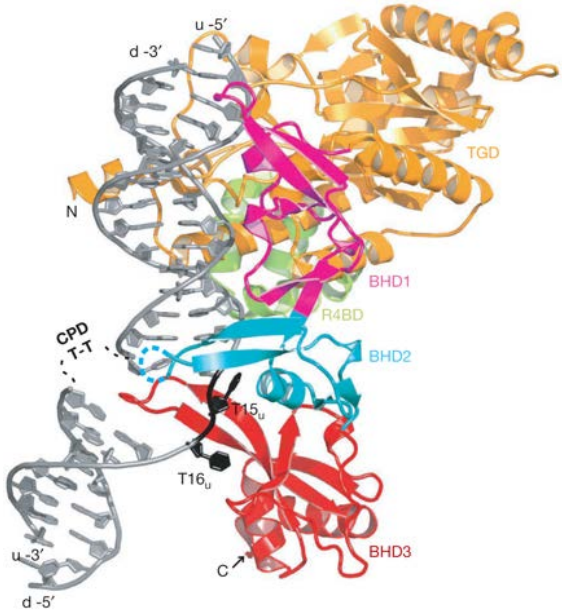

Figure 5. Ribbon structure of the RAD4-RAD23-DNA complex. TGD, gold; BHD1, magenta; BHD2, cyan; BHD3, red; R4BD (RAD4-binding domain), green.

These structural investigations revealed that the DNA-binding region of RAD4/XPC comprises a transglutaminase homology domain (TGD) and three consecutive β-hairpin domains (BHDs). In the co-crystal, RAD4 protein binds to the substrate in a bimodal manner (Min & Pavletich, 2007). The N-terminal TGD and BHD1 motifs form a C-clamp-like structure that holds a portion (11 base pairs) of native double-stranded DNA on the 3′ side of the lesion. The TGD motif also acts as a docking platform for RAD23. Although TGD displays a similarity to the transglutaminase fold of peptide-*N*-glycanases, it does not show any glycanase activity due to the lack of a Cys-His-Asp catalytic triad (Anantharaman et al, 2001). It should also be noted that the homologous TGD segment of human XPC protein is divided into two individual parts by a an intervening sequence of 180 amino acids, whose function is unknown. The other two β-hairpin domains, BHD2 and BHD3, form a hand-like structure that binds much closer to the damaged site. However, as illustrated in **Fig. 5**, this BHD2-BHD3 region interacts exclusively with residues located in the

undamaged single strand and thereby flips-out two nucleotides opposite to the the CPD. A long β-hairpin of BHD3 is inserted into the DNA duplex, which results in the formation of a stable complex with the DNA substrate (Camenisch et al, 2009; Clement et al, 2010a). Importantly, the damaged bases are extruded into an extrahelical position so that they are optimally exposed to downstream NER reactions. Interestingly, a comparison of amino acid sequences showed that the BHD region of XPC protein has a strong similarity to the oligonucleotide/oligosaccharide-binding fold (OB-fold) of RPA-B (a single-stranded DNA-binding domain of the large subunit of RPA) and also to the OB-fold of BRCA2 (Maillard et al, 2007b), indicating that the damaged DNA-recognition function of XPC protein may have evolved during evolution from an ancient single-stranded DNA-binding protein (Maillard et al, 2007b).

Further studies from our laboratory indicate that human XPC protein searches for DNA damage in the genome by a facilitated diffusion process (Clement et al, 2010b). The BHD1/BHD2 motifs sense the presence of unpaired bases and give rise to a dynamic intermediate at damaged sites (**Fig. 6**) but, on their own, are unable to form a stable recognition complex (Camenisch et al, 2009). Within this region, an amino acid substitution (Trp690Ser) has been found in an XP patient. Although the affected residue does not make a direct contact with DNA, it is thought to be important for the correct protein folding and, hence, for protein stability (Bunick et al, 2006; Maillard et al, 2007b; Yasuda et al, 2007). The work of Camenisch et al. (2009) led to the identification of a minimal sensor peptide, comprising ~15% of human XPC protein (residues 607-766), that retains a DNA damage recogntion activity in the chromatin of living cells. Intriguingly, the shorter polypeptide $XPC_{607-741}$ failed to recognize DNA damage, emphasizing the importance of residues 742-766, which are located at the transition between BHD2 and BHD3 and predicted to fold into a β-turn structure. This short β-turn motif of XPC protein is essential to support the dynamic search for unpaired bases in complex mammalian genomes (Camenisch et al, 2009). Two types of protein-DNA interactions have been identified within the β-turn motif. Residues 754 and 756 make direct contacts with one of the flipped out bases in the undamaged strand (Clement et al,

2010b). Instead, residue 755 has an opposite repulsive effect and we identified an amino acid change at this position (Glu755Lys) that increases the affinity of human XPC protein for the native double helix. Fluorescence recovery after photobleacheaching (FRAP) measurements showed that this Glu755Lys mutation reduces the protein mobility necessary to effectively find lesion sites in living cells and, as a consequence, impedes an efficient DNA repair response. We concluded that the BHD1/BHD2 region of human XPC protein, in conjunction with the β-turn motif, provides a dynamic sensor surface that mediates a very rapid movement of XPC protein across nuclear DNA to search for unpaired bases in the genome. At lesion sites, the additional BHD3 motif is then inserted into the double helix to anchor XPC protein and generate a stable recognition complex (**Fig. 6**).

As mentioned above, XPC on its own is unable to sense the small helical distortion induced by CPDs. Therefore, full repair of CPDs by GGR is carried out through the additional assistance of UV-DDB. However, the mechanism by which UV-DDB stimulates the repair of UV lesions had not yet been elucidated.

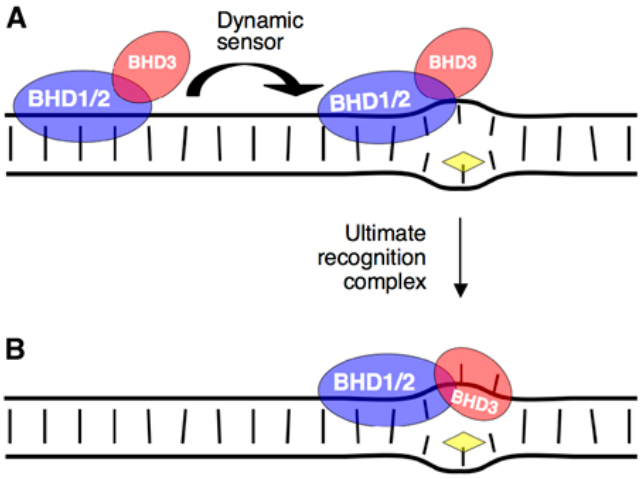

Figure 6. Two-stage detection of DNA lesions by XPC protein. (A) The initial search for unpaired bases is carried out by BHD1/BHD2 in conjunction with the β-turn motif, resulting in the formation of an unstable nucleoprotein intermediate. (B) Recognition of undamaged single-stranded DNA by BHD3 and insertion of its β-hairpin into the double helix leads to the formation of a stable recognition complex.

4.4 UV-DDB

The UV-DDB (or DDB) complex (consisting of DDB1 and DDB2) was originally identified by virtue of its extraordinary affinity for UV-irradiated DNA (Feldberg & Grossman, 1976; Chu & Chang, 1988; Takao et al, 1993; Dualan et al, 1995). DDB1 (1140 amino acids) is a constitutive interaction partner of DDB2, identified from early purification experiments, where DDB2 always co-purified with a 127-kDa protein (Takao et al, 1993; Dualan et al, 1995; Hwang et al, 1996). DDB1 is strongly conserved among eukaryotes, does not have any detectable DNA-binding activity and no disease-associated mutations have been reported so far. By interaction with Cullin ubiquitin ligases, DDB1 plays a much broader role than DDB2 in regulating cellular functions (Li et al, 2006b; Liu et al, 2009). Accordingly, a DDB1 knockout in mice causes severe growth defects, genomic instability and massive apoptosis during early embryonic development (Cang et al, 2006; Wakasugi et al, 2007).

Unlike DDB1, DDB2 plays a very specific role in DNA damage recognition. This accessory subunit is found only in plants and higher vertebrates (Chu & Yang, 2008). In humans, DDB2 is a 48-kDa WD40 repeat-containing protein composed of 427 amino acids, which is not stable or not soluble *in vitro* when DDB1 is absent (Scrima et al, 2008). Mutations of DDB2 have been found in XP-E patients (Itoh et al, 1999; Rapic-Otrin et al, 2003), whose clinical features are characterized by mild dermatological abnormalities and late skin cancer development compared to other XP complementation groups (Bennett & Itoh, 2008). XP-E patients lack DDB activity (Chu & Chang, 1988; Keeney et al, 1992) predominantly due to mutations and absence of DDB2 protein. In one case, the XP-E patient (XP82TO) bears a single amino acid mutation (Lys244Glu) that is compatible with normal cellular amounts of DDB2 protein, although the mutant is not able to bind to DNA substrates (Rapic-Otrin et al, 2003). Due to the low incidence of the XP-E syndrome, it is so far difficult to obtain a deep insight into the molecular pathology of this disease (Hengge & Emmert, 2008). The major DNA repair defect of XP-E cells is an overall reduced excision of CPDs (50% efficiency of wild-type controls) accompanied, during the first 1-4 hours after UV irradiation, by a delayed removal of 6-4PPs (Ford & Hanawalt, 1997; Hwang et al, 1999). Complementation of XP-E cells

by microinjection or ectopic expression of DDB2 protein restores the normal kinetics of CPD and 6-4PP excision (Tang et al, 2000; Moser et al, 2005). Similarly, over-expression of DDB2 in DDB2-deficient *Drosophila*, Chinese hamster ovarian (CHO) or mouse cells increases their resistance against the deleterious effects of UV light (Tang et al, 2000; Fitch et al, 2003a; Alekseev et al, 2005; Moser et al, 2005; Sun et al, 2010). It has been noted that DDB2 expression is induced by p53 in human cells but not in rodent cells that exhibit lower levels of DDB2 (Ford & Hanawalt, 1997; Itoh et al, 2004; Itoh et al, 2007).

Upon UV irradiation, DDB2 rapidly translocates to chromatin (Otrin et al, 1997; Wang et al, 2004) where it associates tightly with UV lesions ahead of XPC protein (Fitch et al, 2003b; Moser et al, 2005; Yasuda et al, 2007) and with the highest binding affinity among all NER factors (Reardon et al, 1993; Fujiwara et al, 1999; Wittschieben et al, 2005). However, the mechanism by which this affinity for UV lesions translates to a stimulatory effect in DNA repair is controversial. In most reports, the UV-DDB complex is dispensable for the excision of UV lesions in cell-free NER reactions (Aboussekhra et al, 1995; Mu et al, 1995; Araujo et al, 2000; Wakasugi et al, 2001; Wakasugi et al, 2002), strongly pointing to a specialized function in the chromatin context of vertebrate organisms.

In biochemical assays, UV-DDB displays a strong binding affinity for DNA substrates containing 6-4PPs but it binds with lower affinity to CPDs (Hwang & Chu, 1993; Reardon et al, 1993; Wittschieben et al, 2005). Besides these UV lesions, UV-DDB has also a modest affinity for abasic sites and base mismatches, as well as for DNA lesions caused by cisplatin, nitrogen mustard or 4-nitroquinoline 1-oxide (4-NQO) (Payne & Chu, 1994; Fujiwara et al, 1999; Sugasawa et al, 2005; Wittschieben et al, 2005; Scrima et al, 2008). On the other hand, UV-DDB is not required for the repair of cisplatin-induced DNA damage (Barakat et al, 2010) and the contribution of UV-DDB to the repair of other forms of base damage remains to be elucidated.

The recent co-crystal structure of the UV-DDB complex with a DNA substrate (Scrima et al, 2008) demonstrated that the DDB2 subunit displays a flat and

positively charged surface for the interaction with double-stranded DNA. By insertion of a β-hairpin into the minor groove, DDB2 extrudes the photodimer into a specific binding pocket of the protein and induces a 40º kink of the DNA duplex (**Fig. 7A**). Interestingly, this kink mimics the bending of DNA in nucleosomal core particles, suggesting that UV-DDB might be able to recognize UV lesions in the context of nucleosomal DNA. The N-terminal helix-loop-helix (HLH) domain of DDB2 associates with the DDB1 partner, which on its own does not make any contacts with DNA and, instead, mediates the interaction with the Cullin 4 ubiquitin ligase. By ubiquitination, DDB2 becomes rapidly degraded upon UV irradiation (Rapic-Otrin et al, 2002; Fitch et al, 2003a), raising the question of why DDB2 is almost totally destroyed even before the removal of CPDs is completed.

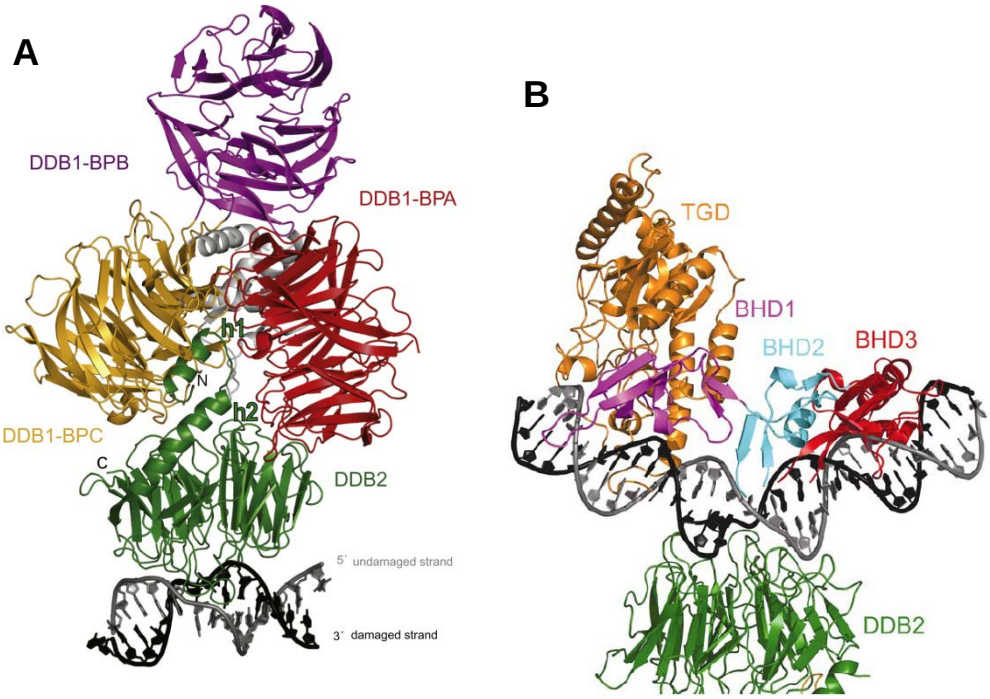

Figure 7. Ribbon structure illustration of UV-DDB in complex with DNA. (A) DDB1-DDB2 bound to a DNA substrate. DDB1 consists of three WD40 beta propeller domains (BPA, BPB and BPC). (B) Model of how DDB2 and XPC protein may interact simultaneously with a lesion site. Yeast homologues of human XPC consists of a single piece of TGD domain and three constitutive beta hairpin domains (Scrima et al, 2008).

A further question is raised by the comparison between co-crystals formed by RAD4/XPC and the UV-DDB complex with DNA (compare Fig. 6A with Fig. 4). Because of the opposite orientation of the protein-induced kink in the DNA double helix, it is unlikely that DDB2 and XPC may form a stable ternary

complex with damaged DNA. A possible model, proposed by Scrima et al. (2008), of how these two proteins may interact at least transiently with the same lesion site is shown in **Fig. 7B**. However, the insertion of a β-hairpin from DDB2 may physically clash with the β-hairpin of XPC protein. Therefore, it was unclear how DDB2 may hand over the lesion site to XPC in order to initiate the NER reaction.

4.5 The ubiquitination system

Protein ubiquitination is a type of post-translational modification carried out by covalent attachment of ubiquitin moieties to the lysine residue of protein substrates through an enzymatic cascade. This reaction is catalyzed by ubiquitin-activating (E1), ubiquitin-conjugating (E2) and ubiquitin-ligating (E3) enzymes as illustrated in **Fig. 8**.

This ubiquitination system is highly conserved in eukaryotic evolution and occurs when an activated ubiquitin monomer is transferred from E1 to E2 and, if E3 binds to specific substrates, the ubiquitin polypeptide is further transferred to the acceptor protein. In eukaryotes, there are two major E3 systems: the HECT domain-containing E3s and RING domain-containing E3s. The attachment of one ubiquitin molecule to single lysine residues of proteins is a mono-ubiquitination reaction. This protein modification is involved in many cellular processes including endocytosis, regulation of gene expression, modulation of chromatin structure, translesion DNA synthesis and DNA repair (Ulrich & Walden, 2010). Poly-ubiquitination is defined as the consecutive linkage of more than one ubiquitin giving rise to a ubiquitin chain. In principle, all seven lysine residues of ubiquitin could be used for the formation of such ubiquitin polymers (Xu et al, 2009). In addition, the N-terminal residue is also used as an acceptor site for the formation of linear chains (Kirisako et al, 2006).

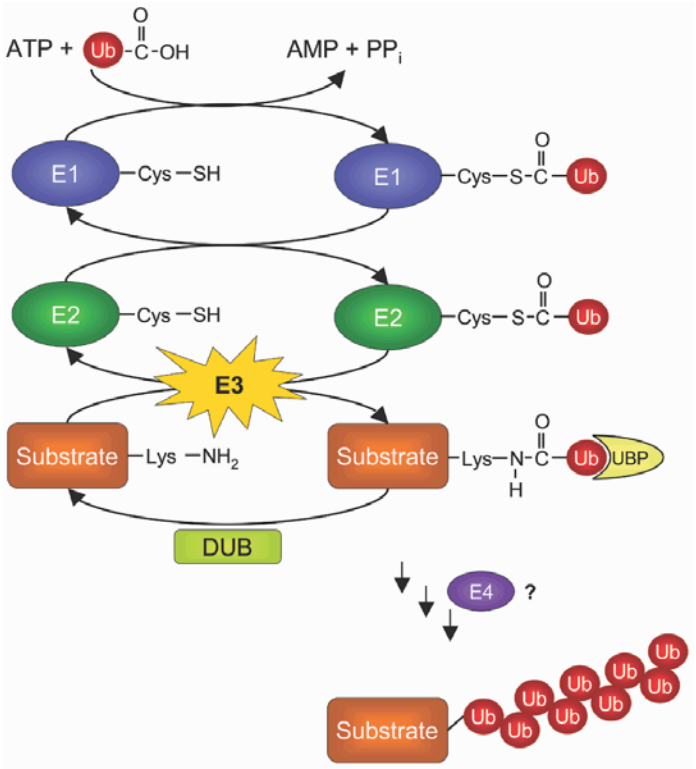

Figure 8. The ubiquitination cascade. E1 transfers ubiquitin monomers to E2, which in turn leads to activation of E2. Under the guidance of substrate-specific E3 enzymes, E2 transfers ubiquitin to target proteins. De-ubiquitination enzymes (DUBs) remove ubiquitin moieties from proteins. E4 is responsible for the ubiquitin chain elongation. Figure adapted from (Passmore & Barford, 2004)

Biophysical studies revealed that the conformation of poly-ubiquitin chains differs as a function of their linkage pattern, which translates to different signals associated with the modified proteins. For example, more than four ubiquitin residues elongated via the Lys48 linkage is a signal to direct the substrate protein to the 26S proteasome for degradation, which is the most widely known function of ubiquitin. Instead, linear and Lys63-linked ubiquitin chains mediate non-proteolytic signals for example by regulating the intracellular trafficking of acceptor proteins. In addition to these single linkage-mediated poly-ubiquitination reactions, protein substrates are also modified by a mixture of linkage patterns, which make functional predictions as to the fate of the modified acceptor more difficult (Hoege et al, 2002; Sugasawa et al, 2005; Kerscher et al, 2006; Jin et al, 2008). Also, non-covalent interactions between poly-ubiquitin chains and proteins have been shown to have an important modulatory function on cellular proteins and the manifold reaction pathways in which they are involved (Zeng et al, 2010). So far, a common

mechanism of how eukaryotic cells decode these different poly-ubiquitin signals has not been discovered.

4.6 Ubiquitination during the GGR pathway

UV-DDB has been shown to interact with several non-repair proteins such as transcription factor E2F1 and the histone acetytransferase CBP/p300 (Hayes et al, 1998; Shiyanov et al, 1999a; Datta et al, 2001). However, the most well-known partners of UV-DDB are Cullin-RING ligases (CRL). In vertebrates, there are seven Cullins (CUL1, CUL2, CUL3, CUL4A, CUL4B, CUL5 and CUL7) that share a structural similarity. These Cullins bridge the interaction between the RING domain protein RBX1 (also known as ROC1 or HRT1) and E2 ubiquitin-conjugating enzyme-adaptor complexes as well as their substrates. Cullin 4A (CUL4A) is one of these CRLs assembled into multiprotein ubiquitin ligase (E3) complexes (Petroski & Deshaies, 2005).

Overexpression of Cullins has been observed in human cancer cells, indicating that their regulation is important for normal cell physiology (Chen et al, 1998). In fact, the activation of CUL4 ubiquitin ligases occurs upon dissociation from the COP9 signalosome (CSN) and, concomitantly, modification (neddylation) with a ubiquitin-like residue called NEDD8 (Groisman et al, 2003; Takedachi et al, 2010). This covalent modification of a conserved domain in the C-terminal region of CUL4A changes its conformation to allow for the recruitment of a ubiquitin-charged E2 enzyme. As a result, the ubiquitin is transferred from E2 to E3 and, finall, to the protein substrate (Saha & Deshaies, 2008). An additional control of CUL4A activity occurs by neddylation-dependent dissociation of the Cullin inhibitor CAND1 (Liu et al, 2002; Goldenberg et al, 2004). These activating events are reversed by de-neddylation executed by a metalloprotease activity of the CSN5 subunit of the COP9 signalosome (Lyapina et al, 2001; Cope et al, 2002). Besides this CSN and neddylation pathway, Cullin activity is also regulated by c-Abl and Arg (Abl-related gene) non-receptor tyrosine kinases and the p38 stress-induced protein kinase (Chen et al, 2006; Zhao et al, 2008) (Galan-Moya et al, 2008).

Based on the aforementioned findings, Sugasawa and coworkers proposed that, under normal conditions, the activity of the UV-DDB-E3 ligase complex, containing DDB1, DDB2, CUL4A or CUL4B, and ROC1, is suppressed by CSN. Upon UV irradiation, UV-DDB translocates to damaged-DNA, which leads to dissociation from CSN and neddylation of the Cullin ubiquitin ligase (Sugasawa et al, 2005). This activated UV-DDB-E3 recruits XPC protein, ubiquitinates DDB2, the Cullin itself, XPC and surrounding histones (**Fig. 9**) (Sugasawa et al, 2005; Wang et al, 2006; Takedachi et al, 2010). The crystal structure analysis of CUL4A-DDB-DNA complexes led to the hypothesis that the Cullin displays a highly flexible domain whose movements demarcate a "ubiquitination zone". Within the reach of this ubiquitination zone, proteins are modified upon UV treatment (Scrima et al, 2008).

Interestingly, the cellular signals and functional consequences arising from the ubiquitination of H2A, H3, H4, XPC and DDB2 are diverging. Histone H3 and H4 mono-ubiquitination is thought to play a role in chromatin relaxation (Wang et al, 2006). Mono-ubiquitination of histone H2A has been linked to gene silencing and chromatin compaction (Baarends et al, 2005). H2A is constitutively mono-ubiquitinated under normal physiological conditions (Kapetanaki et al, 2006), but de-ubiquitination of H2A has been observed within the first two hours after UV irradiation. Thereafter, the mono-ubiquitination of histone H2A is restored by the action of various ubiquitin ligases (Bergink et al, 2006; Kapetanaki et al, 2006), which target different lysine residues depending on the location in either euchromatin or heterochromatin (Dr. Kevin Hiom, personal communication). However, the function of histone ubiquitination and deubiquitination is not yet fully understood.

The role of XPC ubiquitination is equally intriguing, particularly in view of its possible impact on DNA damage recognition during the NER system process. Interestingly, the ubiquitination of XPC protein potentiates its DNA-binding activity, whereas UV-DDB, once ubiquitinated, binds to DNA with lower affinity (Sugasawa et al, 2005). Because poly-ubiquitin chains mark DDB2 for proteasomal degradation, this reaction leads to the removal of the UV-DDB-CUL4A ubiquitin ligase complex from damaged DNA sites, possibly allowing

for the recruitment of more downstream NER factors. Several *in vitro* findings from biochemical reconstitution assays led to a currently accepted model (**Fig. 9**) by which DDB1-CUL4A promotes the destruction of DDB2 at lesion sites to facilitate the recruitment of the XPC-RAD23B complex (Hwang et al, 1999; Harper & Elledge, 2007; O'Connell & Harper, 2007; Sugasawa, 2010).

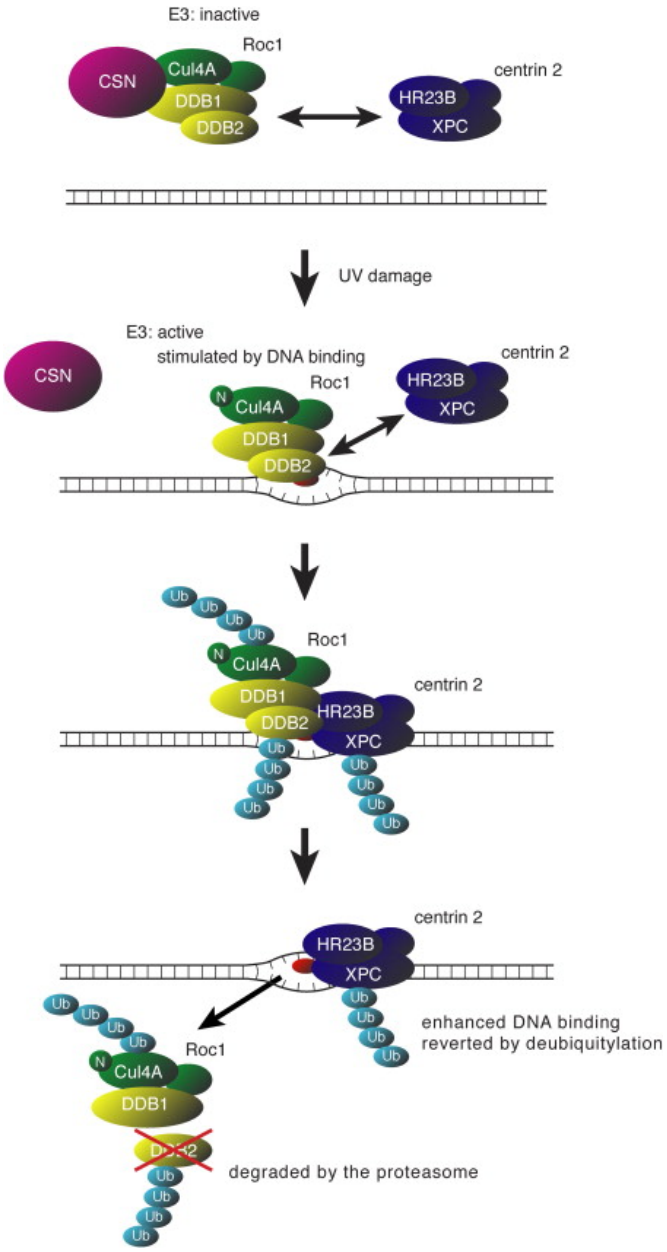

Figure 7. Hypothetical model describing the handover of UV lesions from UV-DDB to XPC protein (adapted from Sugasawa et al, 2005).

However, the mechanism of this critical DDB2-XPC lesion handover remains controversial. First, XPC and DDB2 may clash with each other at damaged sites because both of them use a β-hairpin to anchor themselves onto the

DNA duplex (Scrima et al, 2008). Second, in electrophoretic mobility shift assays with purified UV-DDB, XPC-RAD23B and damaged DNA fragments, it has not been possible to induce the formation of a ternary complex comprising protein complexes as well as the DNA substrate (Batty et al, 2000; Sugasawa, 2009). Third, UV-DDB is absolutely required for the excision of CPDs but is dispensable for the repair of 6-4PPs, despite the fact that it binds with much higher affinity to 6-4PPs than CPDs (Hwang & Chu, 1993; Reardon et al, 1993; Wittschieben et al, 2005). It is also not clear why DDB2 is almost completely degraded in response to UV radiation even before the majority of inflicted CPDs are removed. To accommodate these observations, it has been proposed that the ubiquitin-dependent degradation of DDB2 is necessary to allow for the recruitment of XPC (Chen et al, 2001a; Rapic-Otrin et al, 2002; El-Mahdy et al, 2006). However, it is not clear how DDB2, once degraded, may still stimulate the recognition of UV lesions, particularly CPDs, by its XPC partner. Another hypothesis contends that the CUL4A-mediated ubiquitylation is needed to potentiate the DNA-binding affinity of XPC protein (Sugasawa et al, 2005). The concomitant ubiquitylation of histones, mediated by the CUL4A ligase, may facilitate the access to damaged sites (Kapetanaki et al, 2006; Wang et al, 2006; Scrima et al, 2008). Yet, these hypotheses have been challenged by the finding that CUL4A activity suppresses the NER response (Chen et al, 2006) and that CUL4A-deleted mice show enhanced DNA repair in response to UV irradiation and also an increased resistance to the process of UV-induced skin carcinogenesis (Liu et al, 2009). In CUL4A-knockout mice, these authors found that the cell cycle checkpoint factor p21, another substrate of CUL4A, was greatly stabilized thus potentiating the G1-S checkpoint following DNA damage and increasing the repair capability despite the lack of DDB2 and XPC ubiquitylation (Liu et al, 2009). In addition, studies with mouse cells (both mouse embryonic fibroblasts and mouse dermal fibroblasts) demonstrated that the over-expression of DDB2 stimulates the repair of both CPDs and 6-4PPs (Itoh et al, 2004; Alekseev et al, 2005; Moser et al, 2005), thus questioning the conclusion that DDB2 needs to be degraded to allow for the recruitment of the NER machinery.

4.7 Aim of the thesis

On the basis of the existing literature, discussed in the previous sections, it is difficult to reconcile the cellular and molecular consequences of a DDB2 defect in XP-E cells with the known biochemical properties of this DNA damage recognition factor. Therefore, we used a combined approach with biochemical and cell biological methods to understand the function of DDB2 in inducing the repair of UV lesions. A particular focus was to elucidate the role of protein ubiquitination during the DNA repair response. The specific objectives were as follows:

- To monitor the interactions of DDB2 with damaged DNA in the chromatin of living cells
- To analyze how RAD23B, the constitutive interaction partner of XPC protein that displays a ubiquitin-binding domain influences the DNA damage recognition function
- To monitor the role of DDB2 and XPC ubiquitination in DNA repair
- To demonstrate UV-DDB-XPC interactions in the chromatin context of living cells
- To identify specific protein domains that mediate the UV-DDB-XPC interaction
- To measure how the presence of UV lesions modulates UV-DDB-XPC interactions
- To determine how the molecular handoff from UV-DDB to XPC takes place at UV lesion sites

4.8 References

Aboussekhra A, Biggerstaff M, Shivji MK, Vilpo JA, Moncollin V, Podust VN, Protic M, Hubscher U, Egly JM, Wood RD (1995) Mammalian DNA nucleotide excision repair reconstituted with purified protein components. *Cell* **80:** 859-868

Alekseev S, Kool H, Rebel H, Fousteri M, Moser J, Backendorf C, de Gruijl FR, Vrieling H, Mullenders LH (2005) Enhanced DDB2 expression protects mice from carcinogenic effects of chronic UV-B irradiation. *Cancer Res* **65:** 10298-10306

Anantharaman V, Koonin EV, Aravind L (2001) Peptide-N-glycanases and DNA repair proteins, Xp-C/Rad4, are, respectively, active and inactivated enzymes sharing a common transglutaminase fold. *Hum Mol Genet* **10:** 1627-1630

Anindya R, Mari PO, Kristensen U, Kool H, Giglia-Mari G, Mullenders LH, Fousteri M, Vermeulen W, Egly JM, Svejstrup JQ (2010) A ubiquitin-binding domain in Cockayne syndrome B required for transcription-coupled nucleotide excision repair. *Mol Cell* **38:** 637-648

Araujo SJ, Nigg EA, Wood RD (2001) Strong functional interactions of TFIIH with XPC and XPG in human DNA nucleotide excision repair, without a preassembled repairosome. *Mol Cell Biol* **21:** 2281-2291

Araujo SJ, Tirode F, Coin F, Pospiech H, Syvaoja JE, Stucki M, Hubscher U, Egly JM, Wood RD (2000) Nucleotide excision repair of DNA with recombinant human proteins: definition of the minimal set of factors, active forms of TFIIH, and modulation by CAK. *Genes Dev* **14:** 349-359

Baarends WM, Wassenaar E, van der Laan R, Hoogerbrugge J, Sleddens-Linkels E, Hoeijmakers JH, de Boer P, Grootegoed JA (2005) Silencing of unpaired chromatin and histone H2A ubiquitination in mammalian meiosis. *Mol Cell Biol* **25:** 1041-1053

Barakat BM, Wang QE, Han C, Milum K, Yin DT, Zhao Q, Wani G, Arafa el SA, El-Mahdy MA, Wani AA (2010) Overexpression of DDB2 enhances the sensitivity of human ovarian cancer cells to cisplatin by augmenting cellular apoptosis. *Int J Cancer* **127:** 977-988

Barreto G, Schafer A, Marhold J, Stach D, Swaminathan SK, Handa V, Doderlein G, Maltry N, Wu W, Lyko F, Niehrs C (2007) Gadd45a promotes epigenetic gene activation by repair-mediated DNA demethylation. *Nature* **445:** 671-675

Batty D, Rapic'-Otrin V, Levine AS, Wood RD (2000) Stable binding of human XPC complex to irradiated DNA confers strong discrimination for damaged sites. *J Mol Biol* **300:** 275-290

Bennett D, Itoh T (2008) The XPE gene of xeroderma pigmentosum, its product and biological roles. *Adv Exp Med Biol* **637:** 57-64

Bergink S (2006) Interplay of the ubiquitin proteasome system with nucleotide excision repair. *PhD thesis, Erasmus University, Rotterdam*

Bergink S, Salomons FA, Hoogstraten D, Groothuis TA, de Waard H, Wu J, Yuan L, Citterio E, Houtsmuller AB, Neefjes J, Hoeijmakers JH, Vermeulen W, Dantuma NP (2006) DNA damage triggers nucleotide excision repair-dependent monoubiquitylation of histone H2A. *Genes Dev* **20:** 1343-1352

Bertolaet BL, Clarke DJ, Wolff M, Watson MH, Henze M, Divita G, Reed SI (2001) UBA domains of DNA damage-inducible proteins interact with ubiquitin. *Nat Struct Biol* **8:** 417-422

Bootsma A, Kraemer KH, Cleaver JE, Hoeijmakers JH. (2001) Nucleotide excision repair syndromes: xeroderma pigmentosum, Cockayne syndrome, and trichothiodystrophy. In Scriver CR, Beaudet a, Sly WS, Valle D (eds.), *The metabolic and molecular basis of inherited disease*. McGraw-Hill Book Co., New York, NY, Vol. 1, pp. 677-703.

Bunick CG, Miller MR, Fuller BE, Fanning E, Chazin WJ (2006) Biochemical and structural domain analysis of xeroderma pigmentosum complementation group C protein. *Biochemistry* **45:** 14965-14979

Buterin T, Meyer C, Giese B, Naegeli H (2005) DNA quality control by conformational readout on the undamaged strand of the double helix. *Chem Biol* **12:** 913-922

Camenisch U, Trautlein D, Clement FC, Fei J, Leitenstorfer A, Ferrando-May E, Naegeli H (2009) Two-stage dynamic DNA quality check by xeroderma pigmentosum group C protein. *EMBO J* **28:** 2387-2399

Cang Y, Zhang J, Nicholas SA, Bastien J, Li B, Zhou P, Goff SP (2006) Deletion of DDB1 in mouse brain and lens leads to p53-dependent elimination of proliferating cells. *Cell* **127:** 929-940

Chen L, Shinde U, Ortolan TG, Madura K (2001) Ubiquitin-associated (UBA) domains in Rad23 bind ubiquitin and promote inhibition of multi-ubiquitin chain assembly. *EMBO Rep* **2:** 933-938

Chen LC, Manjeshwar S, Lu Y, Moore D, Ljung BM, Kuo WL, Dairkee SH, Wernick M, Collins C, Smith HS (1998) The human homologue for the Caenorhabditis elegans cul-4 gene is amplified and overexpressed in primary breast cancers. *Cancer Res* **58:** 3677-3683

Chen X, Zhang J, Lee J, Lin PS, Ford JM, Zheng N, Zhou P (2006) A kinase-independent function of c-Abl in promoting proteolytic destruction of damaged DNA binding proteins. *Mol Cell* **22:** 489-499

Chu G, Chang E (1988) Xeroderma pigmentosum group E cells lack a nuclear factor that binds to damaged DNA. *Science* **242:** 564-567

Chu G, Yang W (2008) Here comes the sun: recognition of UV-damaged DNA. *Cell* **135:** 1172-1174

Cleaver JE, Lam ET, Revet I (2009) Disorders of nucleotide excision repair: the genetic and molecular basis of heterogeneity. *Nat Rev Genet* **10:** 756-768

Clement FC, Camenisch U, Fei J, Kaczmarek N, Mathieu N, Naegeli H (2010a) Dynamic two-stage mechanism of versatile DNA damage recognition by xeroderma pigmentosum group C protein. *Mutat Res* **685:** 21-28

Clement FC, Kaczmarek N, Mathieu N, Tomas M, Leitenstorfer A, Ferrando-May E, Naegeli H (2010b) Dissection of the xeroderma pigmentosum group C protein function by site-directed mutagenesis. *Antioxid Redox Signal*

Cope GA, Suh GS, Aravind L, Schwarz SE, Zipursky SL, Koonin EV, Deshaies RJ (2002) Role of predicted metalloprotease motif of Jab1/Csn5 in cleavage of Nedd8 from Cul1. *Science* **298:** 608-611

Dantuma NP, Heinen C, Hoogstraten D (2009) The ubiquitin receptor Rad23: at the crossroads of nucleotide excision repair and proteasomal degradation. *DNA Repair (Amst)* **8:** 449-460

Datta A, Bagchi S, Nag A, Shiyanov P, Adami GR, Yoon T, Raychaudhuri P (2001) The p48 subunit of the damaged-DNA binding protein DDB associates with the CBP/p300 family of histone acetyltransferase. *Mutat Res* **486:** 89-97

Dualan R, Brody T, Keeney S, Nichols AF, Admon A, Linn S (1995) Chromosomal localization and cDNA cloning of the genes (DDB1 and DDB2) for the p127 and p48 subunits of a human damage-specific DNA binding protein. *Genomics* **29:** 62-69

El-Mahdy MA, Zhu Q, Wang QE, Wani G, Praetorius-Ibba M, Wani AA (2006) Cullin 4A-mediated proteolysis of DDB2 protein at DNA damage sites regulates in vivo lesion recognition by XPC. *J Biol Chem* **281:** 13404-13411

Evans E, Moggs JG, Hwang JR, Egly JM, Wood RD (1997) Mechanism of open complex and dual incision formation by human nucleotide excision repair factors. *EMBO J* **16:** 6559-6573

Fan L, Fuss JO, Cheng QJ, Arvai AS, Hammel M, Roberts VA, Cooper PK, Tainer JA (2008) XPD helicase structures and activities: insights into the cancer and aging phenotypes from XPD mutations. *Cell* **133:** 789-800

Feldberg RS, Grossman L (1976) A DNA binding protein from human placenta specific for ultraviolet damaged DNA. *Biochemistry* **15:** 2402-2408

Fitch ME, Cross IV, Turner SJ, Adimoolam S, Lin CX, Williams KG, Ford JM (2003a) The DDB2 nucleotide excision repair gene product p48 enhances global genomic repair in p53 deficient human fibroblasts. *DNA Repair (Amst)* **2:** 819-826

Fitch ME, Nakajima S, Yasui A, Ford JM (2003b) In vivo recruitment of XPC to UV-induced cyclobutane pyrimidine dimers by the DDB2 gene product. *J Biol Chem* **278:** 46906-46910

Ford JM, Hanawalt PC (1997) Expression of wild-type p53 is required for efficient global genomic nucleotide excision repair in UV-irradiated human fibroblasts. *J Biol Chem* **272:** 28073-28080

Friedberg EC (2001) How nucleotide excision repair protects against cancer. *Nat Rev Cancer* **1:** 22-33

Friedberg EC, Aguilera A, Gellert M, Hanawalt PC, Hays JB, Lehmann AR, Lindahl T, Lowndes N, Sarasin A, Wood RD (2006a) DNA repair: from molecular mechanism to human disease. *DNA Repair (Amst)* **5:** 986-996

Friedberg EC, Walker GC, Siede W, Wood RD, Schultz RA, Ellenberger T (2006b) *DNA Repair and Mutagenesis.*, Washington DC: ASM Press.

Fujiwara Y, Masutani C, Mizukoshi T, Kondo J, Hanaoka F, Iwai S (1999) Characterization of DNA recognition by the human UV-damaged DNA-binding protein. *J Biol Chem* **274:** 20027-20033

Galan-Moya EM, Hernandez-Losa J, Aceves Luquero CI, de la Cruz-Morcillo MA, Ramirez-Castillejo C, Callejas-Valera JL, Arriaga A, Aranburo AF, Ramon y Cajal S, Silvio Gutkind J, Sanchez-Prieto R (2008) c-Abl activates p38 MAPK independently of its tyrosine kinase activity: Implications in cisplatin-based therapy. *Int J Cancer* **122:** 289-297

Gillet LC, Scharer OD (2006) Molecular mechanisms of mammalian global genome nucleotide excision repair. *Chem Rev* **106:** 253-276

Goldenberg SJ, Cascio TC, Shumway SD, Garbutt KC, Liu J, Xiong Y, Zheng N (2004) Structure of the Cand1-Cul1-Roc1 complex reveals regulatory mechanisms for the assembly of the multisubunit cullin-dependent ubiquitin ligases. *Cell* **119:** 517-528

Groisman R, Polanowska J, Kuraoka I, Sawada J, Saijo M, Drapkin R, Kisselev AF, Tanaka K, Nakatani Y (2003) The ubiquitin ligase activity in the DDB2 and CSA complexes is differentially regulated by the COP9 signalosome in response to DNA damage. *Cell* **113:** 357-367

Guo C, Tang TS, Friedberg EC (2010) SnapShot: nucleotide excision repair. *Cell* **140:** 754-754 e751

Harper JW, Elledge SJ (2007) The DNA damage response: ten years after. *Mol Cell* **28:** 739-745

Hayes S, Shiyanov P, Chen X, Raychaudhuri P (1998) DDB, a putative DNA repair protein, can function as a transcriptional partner of E2F1. *Mol Cell Biol* **18:** 240-249

Hengge UR, Emmert S (2008) Clinical features of xeroderma pigmentosum. *Adv Exp Med Biol* **637:** 10-18

Hess MT, Gunz D, Luneva N, Geacintov NE, Naegeli H (1997a) Base pair conformation-dependent excision of benzo[a]pyrene diol epoxide-guanine adducts by human nucleotide excision repair enzymes. *Mol Cell Biol* **17:** 7069-7076

Hess MT, Schwitter U, Petretta M, Giese B, Naegeli H (1997b) Bipartite substrate discrimination by human nucleotide excision repair. *Proc Natl Acad Sci U S A* **94:** 6664-6669

Hoege C, Pfander B, Moldovan GL, Pyrowolakis G, Jentsch S (2002) RAD6-dependent DNA repair is linked to modification of PCNA by ubiquitin and SUMO. *Nature* **419:** 135-141

Hoeijmakers JH (2001) Genome maintenance mechanisms for preventing cancer. *Nature* **411:** 366-374

Hoeijmakers JH (2009) DNA damage, aging, and cancer. *N Engl J Med* **361:** 1475-1485

Holstege FC, van der Vliet PC, Timmers HT (1996) Opening of an RNA polymerase II promoter occurs in two distinct steps and requires the basal transcription factors IIE and IIH. *EMBO J* **15:** 1666-1677

Huang JC, Svoboda DL, Reardon JT, Sancar A (1992) Human nucleotide excision nuclease removes thymine dimers from DNA by incising the 22nd phosphodiester bond 5' and the 6th phosphodiester bond 3' to the photodimer. *Proc Natl Acad Sci U S A* **89:** 3664-3668

Hwang BJ, Chu G (1993) Purification and characterization of a human protein that binds to damaged DNA. *Biochemistry* **32:** 1657-1666

Hwang BJ, Ford JM, Hanawalt PC, Chu G (1999) Expression of the p48 xeroderma pigmentosum gene is p53-dependent and is involved in global genomic repair. *Proc Natl Acad Sci U S A* **96:** 424-428

Hwang BJ, Liao JC, Chu G (1996) Isolation of a cDNA encoding a UV-damaged DNA binding factor defective in xeroderma pigmentosum group E cells. *Mutat Res* **362:** 105-117

Itoh T, Cado D, Kamide R, Linn S (2004) DDB2 gene disruption leads to skin tumors and resistance to apoptosis after exposure to ultraviolet light but not a chemical carcinogen. *Proc Natl Acad Sci U S A* **101:** 2052-2057

Itoh T, Iwashita S, Cohen MB, Meyerholz DK, Linn S (2007) Ddb2 is a haploinsufficient tumor suppressor and controls spontaneous germ cell apoptosis. *Hum Mol Genet* **16:** 1578-1586

Itoh T, Mori T, Ohkubo H, Yamaizumi M (1999) A newly identified patient with clinical xeroderma pigmentosum phenotype has a non-sense mutation in the DDB2 gene and incomplete repair in (6-4) photoproducts. *J Invest Dermatol* **113:** 251-257

Jackson SP, Bartek J (2009) The DNA-damage response in human biology and disease. *Nature* **461:** 1071-1078

Janicijevic A, Sugasawa K, Shimizu Y, Hanaoka F, Wijgers N, Djurica M, Hoeijmakers JH, Wyman C (2003) DNA bending by the human damage recognition complex XPC-HR23B. *DNA Repair (Amst)* **2:** 325-336

Jin L, Williamson A, Banerjee S, Philipp I, Rape M (2008) Mechanism of ubiquitin-chain formation by the human anaphase-promoting complex. *Cell* **133:** 653-665

Johnson KA, Fink SP, Marnett LJ (1997) Repair of propanodeoxyguanosine by nucleotide excision repair in vivo and in vitro. *J Biol Chem* **272:** 11434-11438

Johnson RE, Kondratick CM, Prakash S, Prakash L (1999) hRAD30 mutations in the variant form of xeroderma pigmentosum. *Science* **285:** 263-265

Kapetanaki MG, Guerrero-Santoro J, Bisi DC, Hsieh CL, Rapic-Otrin V, Levine AS (2006) The DDB1-CUL4ADDB2 ubiquitin ligase is deficient in xeroderma pigmentosum group E and targets histone H2A at UV-damaged DNA sites. *Proc Natl Acad Sci U S A* **103:** 2588-2593

Keeney S, Wein H, Linn S (1992) Biochemical heterogeneity in xeroderma pigmentosum complementation group E. *Mutat Res* **273:** 49-56

Kerscher O, Felberbaum R, Hochstrasser M (2006) Modification of proteins by ubiquitin and ubiquitin-like proteins. *Annu Rev Cell Dev Biol* **22:** 159-180

Kirisako T, Kamei K, Murata S, Kato M, Fukumoto H, Kanie M, Sano S, Tokunaga F, Tanaka K, Iwai K (2006) A ubiquitin ligase complex assembles linear polyubiquitin chains. *EMBO J* **25:** 4877-4887

Kirkwood TB (2005) Understanding the odd science of aging. *Cell* **120:** 437-447

Klein UR, Nigg EA (2009) SUMO-dependent regulation of centrin-2. *J Cell Sci* **122:** 3312-3321

Kraemer KH, Lee MM, Scotto J (1987) Xeroderma pigmentosum. Cutaneous, ocular, and neurologic abnormalities in 830 published cases. *Arch Dermatol* **123:** 241-250

Kuraoka I, Bender C, Romieu A, Cadet J, Wood RD, Lindahl T (2000) Removal of oxygen free-radical-induced 5',8-purine cyclodeoxynucleosides from DNA by the nucleotide excision-repair pathway in human cells. *Proc Natl Acad Sci U S A* **97:** 3832-3837

Lambertson D, Chen L, Madura K (2003) Investigating the importance of proteasome-interaction for Rad23 function. *Curr Genet* **42:** 199-208

Le May N, Mota-Fernandes D, Velez-Cruz R, Iltis I, Biard D, Egly JM (2010) NER factors are recruited to active promoters and facilitate chromatin modification for transcription in the absence of exogenous genotoxic attack. *Mol Cell* **38:** 54-66

Legerski R, Peterson C (1992) Expression cloning of a human DNA repair gene involved in xeroderma pigmentosum group C. *Nature* **360:** 610

Li T, Chen X, Garbutt KC, Zhou P, Zheng N (2006) Structure of DDB1 in complex with a paramyxovirus V protein: viral hijack of a propeller cluster in ubiquitin ligase. *Cell* **124:** 105-117

Lindahl T (1993) Instability and decay of the primary structure of DNA. *Nature* **362:** 709-715

Lindahl T, Wood RD (1999) Quality control by DNA repair. *Science* **286:** 1897-1905

Liu H, Rudolf J, Johnson KA, McMahon SA, Oke M, Carter L, McRobbie AM, Brown SE, Naismith JH, White MF (2008) Structure of the DNA repair helicase XPD. *Cell* **133:** 801-812

Liu J, Furukawa M, Matsumoto T, Xiong Y (2002) NEDD8 modification of CUL1 dissociates p120(CAND1), an inhibitor of CUL1-SKP1 binding and SCF ligases. *Mol Cell* **10:** 1511-1518

Liu L, Lee S, Zhang J, Peters SB, Hannah J, Zhang Y, Yin Y, Koff A, Ma L, Zhou P (2009) CUL4A abrogation augments DNA damage response and protection against skin carcinogenesis. *Mol Cell* **34:** 451-460

Ljungman M, Zhang F (1996) Blockage of RNA polymerase as a possible trigger for u.v. light-induced apoptosis. *Oncogene* **13:** 823-831

Luch A (2005) Nature and nurture - lessons from chemical carcinogenesis. *Nat Rev Cancer* **5:** 113-125

Lyapina S, Cope G, Shevchenko A, Serino G, Tsuge T, Zhou C, Wolf DA, Wei N, Deshaies RJ (2001) Promotion of NEDD-CUL1 conjugate cleavage by COP9 signalosome. *Science* **292:** 1382-1385

Maillard O, Camenisch U, Clement FC, Blagoev KB, Naegeli H (2007a) DNA repair triggered by sensors of helical dynamics. *Trends Biochem Sci* **32:** 494-499

Maillard O, Solyom S, Naegeli H (2007b) An aromatic sensor with aversion to damaged strands confers versatility to DNA repair. *PLoS Biol* **5:** e79

Masutani C, Kusumoto R, Yamada A, Dohmae N, Yokoi M, Yuasa M, Araki M, Iwai S, Takio K, Hanaoka F (1999) The XPV (xeroderma pigmentosum variant) gene encodes human DNA polymerase eta. *Nature* **399:** 700-704

Mathieu N, Kaczmarek N, Naegeli H (2010) Strand- and site-specific DNA lesion demarcation by the xeroderma pigmentosum group D helicase. *Proc Natl Acad Sci U S A* **In print**

Min JH, Pavletich NP (2007) Recognition of DNA damage by the Rad4 nucleotide excision repair protein. *Nature* **449:** 570-575

Mitchell DL, Nguyen TD, Cleaver JE (1990) Nonrandom induction of pyrimidine-pyrimidone (6-4) photoproducts in ultraviolet-irradiated human chromatin. *J Biol Chem* **265:** 5353-5356

Mocquet V, Kropachev K, Kolbanovskiy M, Kolbanovskiy A, Tapias A, Cai Y, Broyde S, Geacintov NE, Egly JM (2007) The human DNA repair factor XPC-HR23B distinguishes stereoisomeric benzo[a]pyrenyl-DNA lesions. *EMBO J* **26:** 2923-2932

Moggs JG, Yarema KJ, Essigmann JM, Wood RD (1996) Analysis of incision sites produced by human cell extracts and purified proteins during nucleotide excision repair of a 1,3-intrastrand d(GpTpG)-cisplatin adduct. *J Biol Chem* **271:** 7177-7186

Moser J, Kool H, Giakzidis I, Caldecott K, Mullenders LH, Fousteri MI (2007) Sealing of chromosomal DNA nicks during nucleotide excision repair requires XRCC1 and DNA ligase III alpha in a cell-cycle-specific manner. *Mol Cell* **27:** 311-323

Moser J, Volker M, Kool H, Alekseev S, Vrieling H, Yasui A, van Zeeland AA, Mullenders LH (2005) The UV-damaged DNA binding protein mediates efficient targeting of the nucleotide excision repair complex to UV-induced photo lesions. *DNA Repair (Amst)* **4:** 571-582

Mouret S, Baudouin C, Charveron M, Favier A, Cadet J, Douki T (2006) Cyclobutane pyrimidine dimers are predominant DNA lesions in whole human skin exposed to UVA radiation. *Proc Natl Acad Sci U S A* **103:** 13765-13770

Mu D, Park CH, Matsunaga T, Hsu DS, Reardon JT, Sancar A (1995) Reconstitution of human DNA repair excision nuclease in a highly defined system. *J Biol Chem* **270:** 2415-2418

Nance MA, Berry SA (1992) Cockayne syndrome: review of 140 cases. *Am J Med Genet* **42:** 68-84

Ng JM, Vermeulen W, van der Horst GT, Bergink S, Sugasawa K, Vrieling H, Hoeijmakers JH (2003) A novel regulation mechanism of DNA repair by damage-induced and RAD23-dependent stabilization of xeroderma pigmentosum group C protein. *Genes Dev* **17:** 1630-1645

Ng JM, Vrieling H, Sugasawa K, Ooms MP, Grootegoed JA, Vreeburg JT, Visser P, Beems RB, Gorgels TG, Hanaoka F, Hoeijmakers JH, van der Horst GT (2002) Developmental defects and male sterility in mice lacking the ubiquitin-like DNA repair gene mHR23B. *Mol Cell Biol* **22:** 1233-1245

Nishi R, Okuda Y, Watanabe E, Mori T, Iwai S, Masutani C, Sugasawa K, Hanaoka F (2005) Centrin 2 stimulates nucleotide excision repair by interacting with xeroderma pigmentosum group C protein. *Mol Cell Biol* **25:** 5664-5674

O'Connell BC, Harper JW (2007) Ubiquitin proteasome system (UPS): what can chromatin do for you? *Curr Opin Cell Biol* **19:** 206-214

O'Donovan A, Davies AA, Moggs JG, West SC, Wood RD (1994) XPG endonuclease makes the 3' incision in human DNA nucleotide excision repair. *Nature* **371:** 432-435

Ogi T, Limsirichaikul S, Overmeer RM, Volker M, Takenaka K, Cloney R, Nakazawa Y, Niimi A, Miki Y, Jaspers NG, Mullenders LH, Yamashita S, Fousteri MI, Lehmann AR (2010) Three DNA polymerases, recruited by different mechanisms, carry out NER repair synthesis in human cells. *Mol Cell* **37:** 714-727

Okuda Y, Nishi R, Ng JM, Vermeulen W, van der Horst GT, Mori T, Hoeijmakers JH, Hanaoka F, Sugasawa K (2004) Relative levels of the two mammalian Rad23 homologs determine composition and stability of the xeroderma pigmentosum group C protein complex. *DNA Repair (Amst)* **3:** 1285-1295

Otrin VR, McLenigan M, Takao M, Levine AS, Protic M (1997) Translocation of a UV-damaged DNA binding protein into a tight association with chromatin after treatment of mammalian cells with UV light. *J Cell Sci* **110 (Pt 10):** 1159-1168

Paoletti A, Moudjou M, Paintrand M, Salisbury JL, Bornens M (1996) Most of centrin in animal cells is not centrosome-associated and centrosomal centrin is confined to the distal lumen of centrioles. *J Cell Sci* **109 (Pt 13):** 3089-3102

Passmore LA, Barford D (2004) Getting into position: the catalytic mechanisms of protein ubiquitylation. *Biochem J* **379:** 513-525

Payne A, Chu G (1994) Xeroderma pigmentosum group E binding factor recognizes a broad spectrum of DNA damage. *Mutat Res* **310:** 89-102

Petroski MD, Deshaies RJ (2005) Function and regulation of cullin-RING ubiquitin ligases. *Nat Rev Mol Cell Biol* **6:** 9-20

Popescu A, Miron S, Blouquit Y, Duchambon P, Christova P, Craescu CT (2003) Xeroderma pigmentosum group C protein possesses a high affinity binding site to human centrin 2 and calmodulin. *J Biol Chem* **278:** 40252-40261

Raasi S, Pickart CM (2003) Rad23 ubiquitin-associated domains (UBA) inhibit 26 S proteasome-catalyzed proteolysis by sequestering lysine 48-linked polyubiquitin chains. *J Biol Chem* **278:** 8951-8959

Rapic-Otrin V, McLenigan MP, Bisi DC, Gonzalez M, Levine AS (2002) Sequential binding of UV DNA damage binding factor and degradation of the p48 subunit as early events after UV irradiation. *Nucleic Acids Res* **30:** 2588-2598

Rapic-Otrin V, Navazza V, Nardo T, Botta E, McLenigan M, Bisi DC, Levine AS, Stefanini M (2003) True XP group E patients have a defective UV-damaged DNA binding protein complex and mutations in DDB2 which reveal the functional domains of its p48 product. *Hum Mol Genet* **12:** 1507-1522

Reardon JT, Bessho T, Kung HC, Bolton PH, Sancar A (1997) In vitro repair of oxidative DNA damage by human nucleotide excision repair system: possible explanation for neurodegeneration in xeroderma pigmentosum patients. *Proc Natl Acad Sci U S A* **94:** 9463-9468

Reardon JT, Nichols AF, Keeney S, Smith CA, Taylor JS, Linn S, Sancar A (1993) Comparative analysis of binding of human damaged DNA-binding protein (XPE) and Escherichia coli damage recognition protein (UvrA) to the major ultraviolet

photoproducts: T[c,s]T, T[t,s]T, T[6-4]T, and T[Dewar]T. *J Biol Chem* **268:** 21301-21308

Reardon JT, Sancar A (2006) Repair of DNA-polypeptide crosslinks by human excision nuclease. *Proc Natl Acad Sci U S A* **103:** 4056-4061

Riedl T, Hanaoka F, Egly JM (2003) The comings and goings of nucleotide excision repair factors on damaged DNA. *EMBO J* **22:** 5293-5303

Russell SJ, Reed SH, Huang W, Friedberg EC, Johnston SA (1999) The 19S regulatory complex of the proteasome functions independently of proteolysis in nucleotide excision repair. *Mol Cell* **3:** 687-695

Saha A, Deshaies RJ (2008) Multimodal activation of the ubiquitin ligase SCF by Nedd8 conjugation. *Mol Cell* **32:** 21-31

Salisbury JL (2007) A mechanistic view on the evolutionary origin for centrin-based control of centriole duplication. *J Cell Physiol* **213:** 420-428

Salisbury JL, Suino KM, Busby R, Springett M (2002) Centrin-2 is required for centriole duplication in mammalian cells. *Curr Biol* **12:** 1287-1292

Sancar A (1996) DNA excision repair. *Annu Rev Biochem* **65:** 43-81

Satoh MS, Jones CJ, Wood RD, Lindahl T (1993) DNA excision-repair defect of xeroderma pigmentosum prevents removal of a class of oxygen free radical-induced base lesions. *Proc Natl Acad Sci U S A* **90:** 6335-6339

Schaeffer L, Moncollin V, Roy R, Staub A, Mezzina M, Sarasin A, Weeda G, Hoeijmakers JH, Egly JM (1994) The ERCC2/DNA repair protein is associated with the class II BTF2/TFIIH transcription factor. *EMBO J* **13:** 2388-2392

Schaeffer L, Roy R, Humbert S, Moncollin V, Vermeulen W, Hoeijmakers JH, Chambon P, Egly JM (1993) DNA repair helicase: a component of BTF2 (TFIIH) basic transcription factor. *Science* **260:** 58-63

Schauber C, Chen L, Tongaonkar P, Vega I, Lambertson D, Potts W, Madura K (1998) Rad23 links DNA repair to the ubiquitin/proteasome pathway. *Nature* **391:** 715-718

Scrima A, Konickova R, Czyzewski BK, Kawasaki Y, Jeffrey PD, Groisman R, Nakatani Y, Iwai S, Pavletich NP, Thoma NH (2008) Structural basis of UV DNA-damage recognition by the DDB1-DDB2 complex. *Cell* **135:** 1213-1223

Shiyanov P, Hayes SA, Donepudi M, Nichols AF, Linn S, Slagle BL, Raychaudhuri P (1999) The naturally occurring mutants of DDB are impaired in stimulating nuclear import of the p125 subunit and E2F1-activated transcription. *Mol Cell Biol* **19:** 4935-4943

Sijbers AM, de Laat WL, Ariza RR, Biggerstaff M, Wei YF, Moggs JG, Carter KC, Shell BK, Evans E, de Jong MC, Rademakers S, de Rooij J, Jaspers NG, Hoeijmakers JH, Wood RD (1996) Xeroderma pigmentosum group F caused by a defect in a structure-specific DNA repair endonuclease. *Cell* **86:** 811-822

Staresincic L, Fagbemi AF, Enzlin JH, Gourdin AM, Wijgers N, Dunand-Sauthier I, Giglia-Mari G, Clarkson SG, Vermeulen W, Scharer OD (2009) Coordination of dual incision and repair synthesis in human nucleotide excision repair. *EMBO J* **28:** 1111-1120

Sugasawa K (2009) UV-DDB: a molecular machine linking DNA repair with ubiquitination. *DNA Repair (Amst)* **8:** 969-972

Sugasawa K (2010) Regulation of damage recognition in mammalian global genomic nucleotide excision repair. *Mutat Res* **685:** 29-37

Sugasawa K, Akagi J, Nishi R, Iwai S, Hanaoka F (2009) Two-step recognition of DNA damage for mammalian nucleotide excision repair: Directional binding of the XPC complex and DNA strand scanning. *Mol Cell* **36:** 642-653

Sugasawa K, Hanaoka F (2007) Sensing of DNA damage by XPC/Rad4: one protein for many lesions. *Nat Struct Mol Biol* **14:** 887-888

Sugasawa K, Ng JM, Masutani C, Iwai S, van der Spek PJ, Eker AP, Hanaoka F, Bootsma D, Hoeijmakers JH (1998) Xeroderma pigmentosum group C protein complex is the initiator of global genome nucleotide excision repair. *Mol Cell* **2:** 223-232

Sugasawa K, Okamoto T, Shimizu Y, Masutani C, Iwai S, Hanaoka F (2001) A multistep damage recognition mechanism for global genomic nucleotide excision repair. *Genes Dev* **15:** 507-521

Sugasawa K, Okuda Y, Saijo M, Nishi R, Matsuda N, Chu G, Mori T, Iwai S, Tanaka K, Hanaoka F (2005) UV-induced ubiquitylation of XPC protein mediated by UV-DDB-ubiquitin ligase complex. *Cell* **121:** 387-400

Sugasawa K, Shimizu Y, Iwai S, Hanaoka F (2002) A molecular mechanism for DNA damage recognition by the xeroderma pigmentosum group C protein complex. *DNA Repair (Amst)* **1:** 95-107

Sun NK, Sun CL, Lin CH, Pai LM, Chao CC (2010) Damaged DNA-binding protein 2 (DDB2) protects against UV irradiation in human cells and Drosophila. *J Biomed Sci* **17:** 27

Svejstrup JQ (2002) Mechanisms of transcription-coupled DNA repair. *Nat Rev Mol Cell Biol* **3:** 21-29

Takao M, Abramic M, Moos M, Jr., Otrin VR, Wootton JC, McLenigan M, Levine AS, Protic M (1993) A 127 kDa component of a UV-damaged DNA-binding complex, which is defective in some xeroderma pigmentosum group E patients, is homologous to a slime mold protein. *Nucleic Acids Res* **21:** 4111-4118

Takedachi A, Saijo M, Tanaka K (2010) DDB2 complex-mediated ubiquitylation around DNA damage is oppositely regulated by XPC and Ku and contributes to the recruitment of XPA. *Mol Cell Biol* **30:** 2708-2723

Tang JY, Hwang BJ, Ford JM, Hanawalt PC, Chu G (2000) Xeroderma pigmentosum p48 gene enhances global genomic repair and suppresses UV-induced mutagenesis. *Mol Cell* **5:** 737-744

Tantin D (1998) RNA polymerase II elongation complexes containing the Cockayne syndrome group B protein interact with a molecular complex containing the transcription factor IIH components xeroderma pigmentosum B and p62. *J Biol Chem* **273:** 27794-27799

Tornaletti S, Hanawalt PC (1999) Effect of DNA lesions on transcription elongation. *Biochimie* **81:** 139-146

Troelstra C, van Gool A, de Wit J, Vermeulen W, Bootsma D, Hoeijmakers JH (1992) ERCC6, a member of a subfamily of putative helicases, is involved in Cockayne's syndrome and preferential repair of active genes. *Cell* **71:** 939-953

Uchida A, Sugasawa K, Masutani C, Dohmae N, Araki M, Yokoi M, Ohkuma Y, Hanaoka F (2002) The carboxy-terminal domain of the XPC protein plays a

crucial role in nucleotide excision repair through interactions with transcription factor IIH. *DNA Repair (Amst)* **1:** 449-461

Ulrich HD, Walden H (2010) Ubiquitin signalling in DNA replication and repair. *Nat Rev Mol Cell Biol* **11:** 479-489

van der Spek PJ, Eker A, Rademakers S, Visser C, Sugasawa K, Masutani C, Hanaoka F, Bootsma D, Hoeijmakers JH (1996) XPC and human homologs of RAD23: intracellular localization and relationship to other nucleotide excision repair complexes. *Nucleic Acids Res* **24:** 2551-2559

van Hoffen A, Natarajan AT, Mayne LV, van Zeeland AA, Mullenders LH, Venema J (1993) Deficient repair of the transcribed strand of active genes in Cockayne's syndrome cells. *Nucleic Acids Res* **21:** 5890-5895

van Oosten M, Rebel H, Friedberg EC, van Steeg H, van der Horst GT, van Kranen HJ, Westerman A, van Zeeland AA, Mullenders LH, de Gruijl FR (2000) Differential role of transcription-coupled repair in UVB-induced G2 arrest and apoptosis in mouse epidermis. *Proc Natl Acad Sci U S A* **97:** 11268-11273

Venema J, Mullenders LH, Natarajan AT, van Zeeland AA, Mayne LV (1990) The genetic defect in Cockayne syndrome is associated with a defect in repair of UV-induced DNA damage in transcriptionally active DNA. *Proc Natl Acad Sci U S A* **87:** 4707-4711

Volker M, Mone MJ, Karmakar P, van Hoffen A, Schul W, Vermeulen W, Hoeijmakers JH, van Driel R, van Zeeland AA, Mullenders LH (2001) Sequential assembly of the nucleotide excision repair factors in vivo. *Mol Cell* **8:** 213-224

Wakasugi M, Kawashima A, Morioka H, Linn S, Sancar A, Mori T, Nikaido O, Matsunaga T (2002) DDB accumulates at DNA damage sites immediately after UV irradiation and directly stimulates nucleotide excision repair. *J Biol Chem* **277:** 1637-1640

Wakasugi M, Matsuura K, Nagasawa A, Fu D, Shimizu H, Yamamoto K, Takeda S, Matsunaga T (2007) DDB1 gene disruption causes a severe growth defect and apoptosis in chicken DT40 cells. *Biochem Biophys Res Commun* **364:** 771-777

Wakasugi M, Shimizu M, Morioka H, Linn S, Nikaido O, Matsunaga T (2001) Damaged DNA-binding protein DDB stimulates the excision of cyclobutane pyrimidine dimers in vitro in concert with XPA and replication protein A. *J Biol Chem* **276:** 15434-15440

Wang H, Zhai L, Xu J, Joo HY, Jackson S, Erdjument-Bromage H, Tempst P, Xiong Y, Zhang Y (2006) Histone H3 and H4 ubiquitylation by the CUL4-DDB-ROC1 ubiquitin ligase facilitates cellular response to DNA damage. *Mol Cell* **22:** 383-394

Wang QE, Zhu Q, Wani G, Chen J, Wani AA (2004) UV radiation-induced XPC translocation within chromatin is mediated by damaged-DNA binding protein, DDB2. *Carcinogenesis* **25:** 1033-1043

Wang QE, Zhu Q, Wani G, El-Mahdy MA, Li J, Wani AA (2005) DNA repair factor XPC is modified by SUMO-1 and ubiquitin following UV irradiation. *Nucleic Acids Res* **33:** 4023-4034

Wilkinson CR, Seeger M, Hartmann-Petersen R, Stone M, Wallace M, Semple C, Gordon C (2001) Proteins containing the UBA domain are able to bind to multi-ubiquitin chains. *Nat Cell Biol* **3:** 939-943

Wittschieben BO, Iwai S, Wood RD (2005) DDB1-DDB2 (xeroderma pigmentosum group E) protein complex recognizes a cyclobutane pyrimidine dimer, mismatches, apurinic/apyrimidinic sites, and compound lesions in DNA. *J Biol Chem* **280:** 39982-39989

Wold MS (1997) Replication protein A: a heterotrimeric, single-stranded DNA-binding protein required for eukaryotic DNA metabolism. *Annu Rev Biochem* **66:** 61-92

Wolski SC, Kuper J, Hanzelmann P, Truglio JJ, Croteau DL, Van Houten B, Kisker C (2008) Crystal structure of the FeS cluster-containing nucleotide excision repair helicase XPD. *PLoS Biol* **6:** e149

Wood RD (1999) DNA damage recognition during nucleotide excision repair in mammalian cells. *Biochimie* **81:** 39-44

Xu P, Duong DM, Seyfried NT, Cheng D, Xie Y, Robert J, Rush J, Hochstrasser M, Finley D, Peng J (2009) Quantitative proteomics reveals the function of unconventional ubiquitin chains in proteasomal degradation. *Cell* **137:** 133-145

Yasuda G, Nishi R, Watanabe E, Mori T, Iwai S, Orioli D, Stefanini M, Hanaoka F, Sugasawa K (2007) In vivo destabilization and functional defects of the xeroderma pigmentosum C protein caused by a pathogenic missense mutation. *Mol Cell Biol* **27:** 6606-6614

Yokoi M, Masutani C, Maekawa T, Sugasawa K, Ohkuma Y, Hanaoka F (2000) The xeroderma pigmentosum group C protein complex XPC-HR23B plays an important role in the recruitment of transcription factor IIH to damaged DNA. *J Biol Chem* **275:** 9870-9875

Zeng W, Sun L, Jiang X, Chen X, Hou F, Adhikari A, Xu M, Chen ZJ (2010) Reconstitution of the RIG-I pathway reveals a signaling role of unanchored polyubiquitin chains in innate immunity. *Cell* **141:** 315-330

Zhao Q, Barakat BM, Qin S, Ray A, El-Mahdy MA, Wani G, Arafa el S, Mir SN, Wang QE, Wani AA (2008) The p38 mitogen-activated protein kinase augments nucleotide excision repair by mediating DDB2 degradation and chromatin relaxation. *J Biol Chem* **283:** 32553-32561

5. Polyvalent DDB2 (XPE) orchestrates DNA repair in mammalian chromatin

(Manuscript submitted)

Polyvalent DDB2 (XPE) orchestrates DNA repair in mammalian chromatin

Jia Fei[1], Nina Kaczmarek[1], Andreas Luch[2], Andreas Glas[3], Thomas Carell[3], Hanspeter Naegeli[1,#]

DDB2 binds avidly to chromatin of UV-irradiated cells but, until now, inconsistent data have been reported as to how this factor stimulates DNA repair. Here, we demonstrate a previously unknown ubiquitin-dependent function whereby DDB2 sorts out solubilizable chromatin as hotspot for DNA excision activity. Through DDB1-CUL4A-mediated ubiquitylation, DDB2 prevents the XPC partner from migrating to insoluble nucleosomes refractory to the rapid assembly of downstream repair complexes. Also, by ubiquitin-independent, direct but transient interactions with two DNA-binding domains, DDB2 recruits XPC protein to UV lesions and, finally, promotes thermodynamically unfavorable insertions of its beta-hairpin into the double helix. This study identifies a new task of ubiquitin in controlling the spatiotemporal chromatin distribution of a key genome caretaker and describes DDB2 as a polyvalent DNA repair organizer.

1 Institute of Pharmacology and Toxicology, University of Zurich-Vetsuisse, Winterthurerstrasse 260, CH-8057 Zürich, Switzerland

2 German Federal Institute for Risk Assessment (BfR), Department of Product Safety & Center for Alternatives to Animal Testing, Thielallee 88-92, 14195 Berlin, Germany

3 Center for Integrated Protein Science CIPS at the Department of Chemistry, Ludwig-Maximilians University, D-81377 Munich, Germany.

#To whom correspondence should be addressed. E-mail: naegelih@vetpharm.uzh.ch

Introduction

UV light generates hazardous DNA lesions in the skin, primarily cyclobutane pyrimidine dimers (CPDs) and 6-4 pyrimidine-pyrimidone photoproducts (6-4PPs) (Mitchell et al, 1990; Mouret et al, 2006) whose cytotoxic, inflammatory and carcinogenic consequence are mitigated by a genome-wide DNA quality control system (Friedberg et al, 2006; Hoeijmakers, 2009). Genetic defects in the ensuing nucleotide excision repair (NER) pathway cause xeroderma pigmentosum (XP), a syndrome characterized by UV hypersensitivity and predisposition to skin cancer (Cleaver, 2005). Although all basic NER steps are understood in detail (Aboussekhra et al, 1995; Mu et al, 1995; Araujo et al, 2000), it is not yet known how this DNA repair reaction is coordinated in the physiologic context, where the damaged substrate is packaged in chromosomes. Indeed, how the whole genome of living cells is thoroughly inspected for DNA damage remains one of the fundamental unanswered questions in biology.

The damaged DNA-binding (DDB) and XPC-RAD23B complexes are the initial sensors of DNA lesions that trigger NER activity (Sugasawa et al, 1998; Fitch et al, 2003b; Sugasawa et al, 2005). XPC protein is essential for the recruitment of transcription factor TFIIH, with its XPB and XPD subunits, followed by XPA, replication protein A (RPA) and the incision enzymes XPF-ERCC1 and XPG (Volker et al, 2001). DDB is a dimer of DDB1 and DDB2 that binds avidly to UV-irradiated DNA (Feldberg & Grossman, 1976; Chu & Chang, 1988; Takao et al, 1993; Dualan et al, 1995) and also associates with the CUL4A ubiquitin ligase (Shiyanov et al, 1999; Nag et al, 2001; Groisman et al, 2003; Li et al, 2006). Mutations in DDB2, the DNA-binding subunit that recognizes UV lesions (Kulaksiz et al, 2005; Scrima et al, 2008), give rise to XP complementation group E (Itoh et al, 1999; Rapic-Otrin et al, 2003). In response to UV damage, DDB2 translocates to chromatin (Otrin et al, 1997; Fitch et al, 2003b; Wang et al, 2004; Moser et al, 2005; Yasuda et al, 2007) where it binds to UV lesions with higher affinity than all other NER factors (Reardon et al, 1993; Fujiwara et al, 1999; Wittschieben et al, 2005). The absence of functional DDB2 in XP-E cells results in delayed excision of 6-4PPs and an overall slow repair of CPDs (Hwang et al, 1999; Moser et al, 2005).

A widely accepted model is that DDB assists in DNA repair by first recognizing UV lesions and then delivering the substrate to XPC protein, which in turn initiates the NER reaction (Hwang et al, 1999; Sugasawa, 2010). However, this handover mechanism remained elusive because previous studies failed to detect a ternary complex in which DDB2 and XPC bind to damaged sites simultaneously (Batty et al, 2000; Wakasugi et al, 2001; Scrima et al, 2008; Sugasawa, 2009). One hypothetical scenario predicts that XPC protein is recruited to UV lesions only after the removal of DDB2 by DDB1-CUL4A-dependent proteolysis (Chen et al, 2001; Rapic-Otrin et al, 2002; El-Mahdy et al, 2006). Another hypothesis contends that CUL4A-mediated ubiquitylation is needed to potentiate the DNA-binding affinity of XPC protein (Sugasawa et al, 2005). The concomitant ubiquitylation of histones is thought to facilitate the access to target sites (Kapetanaki et al, 2006; Wang et al, 2006; Scrima et al, 2008). Yet, these hypotheses have

been challenged by the finding that the CUL4A ubiquitin ligase suppresses NER activity (Chen et al, 2006) and that *CUL4A*-deleted mice show enhanced DNA repair and resistance to UV-induced skin carcinogenesis (Liu et al, 2009).

Here, the so far enigmatic link between DDB, XPC and CUL4A has been elucidated by chromatin partitioning, *in situ* mapping of interaction domains and live-cell imaging of protein dynamics. This approach disclosed an unforeseen bimodal coordination of DNA repair in UV-irradiated chromatin. First, DDB2 sorts out nucleosomes according to accessibility and, by recruiting the DDB1-CUL4A ubiquitylation system, guides the XPC partner to those sites that are most amenable to the assembly of NER complexes. This ubiquitin-dependent demarcation of repair hotspots counteracts the default-mode binding of XPC protein to less repair-permissive chromatin. Second, as a baseline function that is independent of ubiquitin, DDB2 interacts with the DNA-binding domain of XPC protein to promote an effective engagement with UV lesions.

Results

Dissection of chromatin into hot and cold spots of NER assembly

After UV irradiation, the DDB2 and XPC proteins translocate from a free form into tight binding to chromatin (Fig. 1A; (Otrin et al, 1997; Wang et al, 2004; Kapetanaki et al, 2006). Reflecting the different abundance of each factor (Wittschieben et al, 2005; Nishi et al, 2009), a nearly complete chromatin association of DDB2 (~10^5 molecules per human cell) is detected at a UV dose of 15 J/m^2 whereas, in the case of XPC (~2.5 x 10^4 molecules), this chromatin binding is saturated at a lower dose of 10 J/m^2 (Fig. 1B).

Most chromatin-associated DDB2 is released by treatment with micrococcal nuclease (MNase), which digests nuclear DNA into nucleosomes (Fig. S1A). Even a mild MNase treatment with only partial digestion results in the same efficient release (Fig. S1B and S1C), indicating that DDB2 binds preferentially to highly accessible chromatin regions. The same chromatin fraction prone to solubilization by MNase also favors the UV-dependent recruitment of downstream NER subunits like XPB (a TFIIH subunit), XPA and XPG (Fig. 1A). In contrast, the majority of XPC molecules co-localize with a distinct nucleosome population that is not solubilized by MNase digestion (Figs. 1A and 1B). This unique binding of XPC protein to insoluble nucleosomes is observed in all cell lines examined including U2OS fibroblasts (Fig. 1C) and is in agreement with earlier microscopy studies where part of XPC protein relocates to condensed chromatin (Solimando et al, 2009). The presence of histone variants H1.0 and trimethylated H3 (H3K9m3), correlating with chromatin condensation and gene silencing (Roche et al, 1985; Gunjan et al, 1999; Clausell et al, 2009), support the notion that the insoluble component arises from dense nucleosome packing (Fulmer & Bloomfield, 1981; Zlatanova et al, 1994). To summarize, after UV irradiation, up to ~70% of

DDB2 subunits move to the most accessible hotspots of NER assembly. In contrast, ~60% of XPC protein (but < 20% of DDB2) associate with insoluble nucleosomes representing a less permissive DNA repair cold spot with limited recruitment of downstream NER subunits.

Distinct characteristics of XPC protein at different chromatin locations

At least three features distinguish the XPC molecules accumulating at the just described DNA repair hot and cold spots. First, the immunoblots generated with antibodies against human XPC reveal higher molecular weight forms (>150 kDa) representing ubiquitylated protein generated in response to UV irradiation (Sugasawa et al, 2005; Wang et al, 2005). Intriguingly, the proportion of these ubiquitylated species, relative to unmodified XPC, is higher in the soluble hotspot than in the insoluble cold spot (Fig. 1A and 1C). A second difference appeared by probing the samples with antibodies against RAD23B. As observed in cell extracts, where nearly all XPC is complexed with RAD23B (van der Spek et al, 1996), XPC protein carries the RAD23B partner to solubilizable nucleosomes after UV irradiation. However, in contrast to the intact XPC-RAD23B complexes found in this DNA repair hotspot, the remaining XPC molecules migrate to insoluble chromatin without being accompanied by RAD23B (Fig. 1A). The third difference involves the kinetics of XPC accumulation. At solubilizable hotspot locations, DNA damage recognition by XPC protein reaches a peak ~1 h after each UV stimulus. Instead, the recruitment of XPC protein to the insoluble cold spot persists for many hours after DNA damage (Figs. 1D and 1E), thus reflecting a continued DNA repair response. At 6 h after UV irradiation, when a large proportion of DDB2 is degraded, most of the remaining XPC protein is sequestered in this insoluble chromatin component (Figs. 1D, S1D and S1E).

Ubiquitin-dependent chromatin distribution of XPC protein

Another difference between the aforementioned nucleosome fractions is that, in response to UV light, DDB2 recruits its DDB1 partner only to solubilizable nucleosomes. A depletion of DDB2, by transfection with specific siDDB2, abolishes this UV-induced translocation of DDB1 without influencing the constitutive DDB1 level in the insoluble part (Fig. 2A). In addition, this DDB2 depletion suppresses the ubiquitylation (Fig. S2A) and recruitment of XPC protein to solubilizable nucleosomes, but without affecting its UV-dependent relocation to insoluble counterparts (Figs. 2A and 2B). A similar aversion of XPC protein for solubilizable chromatin is also observed in DDB2-defective XP-E cells (Fig. S2B). However, the normal UV-dependent accumulation of XPC protein at solubilizable nucleosomes is restored by complementing siDDB2-treated cells with a DDB2 construct fused to green-fluorescent protein (DDB2-GFP; Fig. S2C).

The role of XPC ubiquitylation was further tested in mouse ts20 cells that harbor a temperature-sensitive ubiquitin-activating E1 enzyme (Sugasawa et al, 2005; Wang et al, 2005). Due to their ubiquitylation defect when incubated

at the restrictive temperature (39°C), these ts20 cells respond to UV light with an essentially complete translocation of XPC protein to insoluble nucleosomes (Fig. 2C). Instead, in the control H38-5 cells corrected by complementation with wild-type E1, the intact ubiquitylation system is able to retain XPC protein in solubilizable chromatin at both 32°C and 39°C. An identical outcome, i.e., defective XPC ubiquitylation in response to UV light (Fig. S2D) and an XPC accumulation only in insoluble chromatin results from the treatment of HeLa cells with the E1 inhibitor PYR-41 (Figs. 2B and 2D).

Uncoupling of DDB2 from ubiquitylation

Two different approaches were used to dissociate DDB2 from the ubiquitylation system. An siRNA-mediated down regulation of the CUL4A ligase suppresses XPC ubiquitylation (Fig. S2E) and increases the steady-state level of DDB2 (Fig. 2E). However, the missing CUL4A activity translates to a reduced accumulation of XPC in the solubilizable fraction of UV-irradiated chromatin, which in turn causes a diminished recruitment of XPA protein tested as an example of downstream NER subunit. Accordingly, this CUL4A depletion inhibits mainly the initially fast excision of 6-4PPs (Fig. S3), which are enriched in the solubilizable (MNase-sensitive) fraction of chromatin (Mitchell et al, 1990).

The proteasome inhibitor MG132 raises the level of DDB2 that in turn stimulates the movement of DDB1 to UV-irradiated chromatin (Fig. 2F). However, by causing a depletion of free ubiquitin, MG132 also inhibits the ubiquitylation of nuclear substrates (Dantuma et al, 2006) including XPC protein (Fig. S2F). As a consequence, DDB2 is now unable to keep the XPC partner in solubilizable chromatin, while its UV-dependent recruitment to the insoluble counterpart is enhanced (Figs. 2B and 2F). In summary, different approaches to block the CUL4A pathway reveal an unexpected property of XPC protein, i.e., that by default-mode this DNA damage recognition subunit migrates to UV lesions located in poorly accessible nucleosomes. This finding challenges the long-held notion that chromatin poses a general barrier to the recognition of UV lesions and discloses a critical function of DDB2 in recruiting the DDB1-CUL4A ligase. Only the resulting ubiquitylated XPC proteins are retained at solubilizable sites that are more amenable than insoluble chromatin to the assembly of downstream NER subunits.

DDB2-XPC interactions in chromatin

To distinguish the effects of XPC ubiquitylation from those of other CUL4A targets (DDB2 or histones), we took advantage of an ectopically expressed XPC-GFP fusion that, unlike endogenous XPC, is poorly ubiquitylated in response to UV light (Fig. 3A). Although this XPC-GFP construct complements the overt DNA repair defect of XP-C cells in UV survival (Ng et al, 2003) and host-cell reactivation assays (Maillard et al, 2007), upon UV irradiation it is mainly localized to insoluble chromatin (Fig. 3B), a distribution

that is reminiscent of that observed before (Fig. 2) in the background of a defective DDB1-CUL4A pathway.

This non-ubiquitylated XPC-GFP was expressed in Chinese hamster ovary (CHO) cells that lack endogenous DDB2 (Tang & Chu, 2002). Its interactions in chromatin were monitored by inducing local sites of damage whereby only parts of the nuclei are exposed to UV light through a polycarbonate filter (Fitch et al, 2003b). Subsequently, the fluorescence intensity in the UV-irradiated areas was measured over the surrounding nuclear background. As illustrated in Fig. 3C, the accumulation of XPC-GFP at UV lesions is enhanced by co-expression of DDB2, which was tagged with red-fluorescent protein (RFP). This stimulation of lesion recognition was insensitive to the E1 inhibitor PYR-41 (Fig. 3D) and was maintained with an XPC truncate (XPC_{1-831}) that, on its own, is defective in the binding to damaged sites (Fig. 3E). In view of finding, the filter irradiation assay was used, in conjunction with appropriate GFP constructs (Fig. 3F and Fig. S4), to map DDB2-XPC interaction domains. Compared to the full-length control, the truncate XPC_{1-741}, like XPC_{1-831}, exhibits a reduced ability to redistribute to damaged sites but is nevertheless attracted to UV lesions when co-expressed with DDB2-RFP. Instead, the N-terminal fragment XPC_{1-495} is recruited to the UV spots much less efficiently than the full-length control or an even shorter C-terminal fragment ($XPC_{607-940}$; Fig. 3G). Collectively, this *in situ* mapping suggested that the XPC residues 496-741, which comprise a transglutaminase homology domain (TGD) and part of the beta-hairpin domains (BHDs; see Fig. 3F), mediate the association with DDB2.

Next, the contribution of these different protein motifs to DDB2-XPC interactions was tested by deletion of the respective XPC sequences. The TGD-deleted (Δ TGD) and BHD1-deleted XPC constructs (Δ BHD1) display the same intrinsic damage recognition activity as the full-length control, but their accumulation in UV foci is not stimulated by co-expression of DDB2 (Fig. 3H). In contrast to these TGD and BHD1 motifs, the BHD3 sequence is dispensable for DDB2-XPC interactions as the corresponding Δ BHD3 construct is efficiently recruited to UV lesions when co-expressed with DDB2 (Fig. 3H).

DDB2-XPC interactions stimulated by DNA damage

The DDB2-XPC association has been further analyzed by transfection of HEK293 cells with DDB2-FLAG and XPC-GFP fusions, followed by the isolation of protein complexes using anti-FLAG antibodies (Fig. S5A). An N-terminal DDB2 truncate ($DDB2_{79-427}$), which looses the ability to interact with DDB1 (Fig. S5B), still binds to XPC protein, supporting the notion that DDB1 is not implicated in the binary DDB2-XPC interaction. Using appropriate polypeptide fragments ($XPC_{520-633}$-GFP, $XPC_{607-831}$-GFP), these co-immunoprecipitation studies in HEK293 cells confirmed that DDB2 forms complexes with both the TGD (Fig. S5C) and BHD region (Fig. S5D) of XPC protein.

Subsequently, polypeptides of 135-204 amino acids, containing the TGD ($XPC_{428-633}$), BHD1/2 ($XPC_{607-741}$) or BHD2/3 ($XPC_{679-831}$) sequences, were expressed in *E. coli* as glutathione-*S*-transferase (GST) fusions to demonstrate that the TGD (Fig. 4A) and BHD1/2 motifs (Fig. 4B) make direct contacts with purified DDB. In contrast, a fragment comprising the BHD2/3 sequence does not associate with DDB, thus excluding this part of XPC protein as a main interaction motif. Next, we found that the association of the TGD fragment with DDB is inhibited by the addition of either undamaged or damaged double-stranded DNA (Fig. 4C). Instead, the interaction between BHD1/2 fragments and DDB is stimulated by short DNA duplexes carrying site-specific photoproducts. In line with the distinct affinity of DDB2 for UV lesions, DNA duplexes with 6-4PPs stimulate this interaction more efficiently than those carrying a CPD (Fig. 4D). These findings point to a stepwise process whereby DDB2 recognizes UV lesions, then attracts XPC protein through a DNA-independent interaction with the TGD region and, finally, positions the XPC partner onto the lesion site through a DNA-stimulated interaction primarily with the BHD1 motif.

Transient immobilization of XPC protein on damaged DNA

The identification of a specific XPC domain, whose association with DDB2 is stimulated by damaged DNA (Fig. 4D), suggested that the two factors are able to bind the same lesion simultaneously. To characterize the dynamics of this dual interaction in the chromatin context, CHO cells were transfected with the XPC-GFP construct alone or in combination with DDB2-RFP. Following the induction of local UV damage through polycarbonate filters, the stability of XPC-DNA interactions was tested by bleaching the green fluorescence signal at lesion sites, thus reducing its intensity to that of the surrounding nuclear background (Luijsterburg et al, 2007; Alekseev et al, 2008). The subsequent analysis by fluorescence recovery after photobleaching on local damage (FRAP-LD) revealed that XPC molecules are only transiently immobilized at DNA lesions and that DDB2 doubles the half-life of this dynamic interaction between XPC protein and damaged DNA from ~10 s to ~20 s (Fig. 4E). Conversely, the dissociation of DDB2 (tested as a GFP fusion) from UV lesions is accelerated by XPC-RFP (Fig. S6).

From a published crystal structure of the yeast RAD4 homolog (Min & Pavletich, 2007), it can be inferred that the recognition of damaged substrates by XPC protein involves the insertion of a beta-hairpin of the BHD3 motif into the DNA double helix. To test the role of this critical rearrangement during the DDB2-XPC handover, we constructed an appropriate deletion by removing amino acids 789-815 from the human XPC sequence. The resulting beta-hairpin-deleted mutant (Δ hairpin), although unable to detect DNA damage on its own, is very effectively recruited to UV foci by co-expression with DDB2 (Fig. 3G). However, the steep slope of its fluorescence redistribution, determined in FRAP-LD analyses (Fig. 4F), shows that DDB2 fails to stabilize the interaction of this Δ hairpin construct with damaged DNA. Taken together, these results indicate that DDB2 not only attracts XPC protein to lesion sites,

but also prolongs its residence time at damaged targets to facilitate the helical insertion of a beta-hairpin subdomain that is crucial for NER activity.

Discussion

Until now, the manifestations of a DDB2 defect in XP-E patients have been difficult to reconcile with the biochemical properties of this auxiliary factor. For example, DDB2 is generally thought to be needed only for the excision of CPDs (Fujiwara et al, 1999; Hwang et al, 1999; Wittschieben et al, 2005), although it binds with much higher affinity to 6-4PPs (Fujiwara et al, 1999; Wittschieben et al, 2005). *In vitro* reconstitution assays demonstrated that DDB2 is not needed at all for the processing of naked DNA (Aboussekhra et al, 1995; Mu et al, 1995; Araujo et al, 2000), thus pointing to a yet unidentified function in the chromatin context. The accompanying DDB1-CUL4A-mediated ubiquitylation has been proposed to induce the clearance of DDB2 from lesion sites (Rapic-Otrin et al, 2002; Fitch et al, 2003a; Sugasawa et al, 2005), potentiate the DNA-binding affinity of XPC protein (Sugasawa et al, 2005) or open chromatin (Wang et al, 2006; Scrima et al, 2008). However, other reports indicate that CUL4A activity inhibits DNA repair and that a *CUL4A* deletion in mice protects from skin carcinogenesis (Chen et al, 2006; Liu et al, 2009).

In this study, we discovered that DDB2 is required for the early UV response to delineate high-priority DNA repair hotspots coinciding with MNase-sensitive and, hence, accessible nucleosomes. This DDB2 function is critical for an effective DNA repair reaction because XPC protein, the initiator of NER activity, by default migrates preferentially to UV lesions in less permissive chromatin environments distinguished by MNase resistance and inefficient recruitment of downstream NER subunits. While sorting out accessible nucleosomes, DDB2 associates with the DDB1-CUL4A ligase and only the resulting ubiquitylated XPC molecules are retained at these repair hotspots where they launch the fast excision of UV lesions, particularly the more easily recognizable 6-4PPs (Mitchell et al, 1990). This recruitment of XPC protein to DNA repair hotspots is abolished by down regulation of DDB2 or CUL4A, by inhibition of the E1 ubiquitin-activating enzyme or by depletion of the nuclear ubiquitin pool, thus explaining why even the excision of 6-4PPs is delayed in XP-E cells (Ford & Hanawalt, 1997; Hwang et al, 1999; Moser et al, 2005). That the chromatin location of XPC protein is determined by its own ubiquitylation, rather than concurrent DDB2 or histone modifications, is demonstrated by an XPC-GFP fusion that is refractory to ubiquitylation and whose chromatin distribution is identical to that observed with a defective ubiquitylation system. Thus, neither the polyubiquitylation of DDB2 (Chen et al, 2001; Rapic-Otrin et al, 2002; El-Mahdy et al, 2006) nor the monoubiquitylation of histones (Bergink et al, 2006; Kapetanaki et al, 2006; Wang et al, 2006; Scrima et al, 2008) are major determinants of XPC chromatin distribution. Ubiquitin moieties linked to XPC may prevent protein-protein interactions that are needed to infiltrate chromatin and, in support of this conclusion, chromatin-penetrating XPC molecules dissociate from RAD23B, which carries a ubiquitin-like domain. In any case, the DDB1-

CUL4A-dependent proteolysis of DDB2 terminates the just described phase of fast DNA repair. Due to progressive DDB2 degradation, a growing proportion of XPC protein evades ubiquitylation and, hence, gains access to lesions buried in bulk chromatin that is slowly processed. This XPC relocation to less permissive sites appears necessary to maximize the recruitment of downstream factors like XPA to regions of high chromatin compaction.

Next we discovered that, independently of ubiquitin, DDB2 interacts directly with XPC protein to facilitate its engagement with DNA damage. The evidence underlying this conclusion is that DDB2 recruits non-ubiquitylated XPC-GFP fusions to UV lesions and that this association is not affected by inhibition of the ubiquitylation system. Direct interactions have been detected between DDB2 and the TGD/BHD1 motifs, two adjacent DNA-binding domains of XPC protein. The interaction with BHD1 is stimulated by damaged substrates, indicating that DDB2 and XPC undergo physical contacts to transfer the UV lesion from one factor to another. Analyses of protein dynamics show that this damage-specific DDB2-XPC interaction takes place transiently, that it serves to stabilize the association of XPC protein with UV lesions and that this stabilization depends on the insertion of a beta-hairpin subdomain of XPC protein into the DNA double helix. Such a helical insertion occurs at a substantial energetic cost as it requires the local disruption of base stacking and Watson-Crick hydrogen bonds (Min & Pavletich, 2007). While 6-4PPs reduce the thermodynamic threshold of this conformational change by lowering the melting temperature of damaged DNA, CPDs cause minimal DNA-destabilizing effects (Kim et al, 1995; McAteer et al, 1998). Thus, the dependence on DDB2 for a beta-hairpin insertion at CPDs explains the overall defect of XP-E cells in repairing this more abundant type of UV lesion. The finding that CUL4A ligase plays only an accessory role, by triggering an early wave of DNA repair, also reconciles the conflicting results as to the role of this ubiquitin ligase in stimulating (El-Mahdy et al, 2006; Wang et al, 2006) or inhibiting (Chen et al, 2006; Liu et al, 2009) UV responses. Because the same ligase also regulates the cellular level of DNA repair proteins and other transactions including cell cycle (Liu et al, 2009; Sugasawa, 2010), it is conceivable that an interference with CUL4A activity may yield opposing effects depending on the organism, cellular context or genetic background.

To summarize, we discovered a bimodal action (Fig. S7) by which DDB2 optimizes in space and time the genome-wide NER reaction to ensure both an initially fast (ubiquitin-dependent) removal of easily accessible lesions as well as the prolonged (ubiquitin-independent) excision of more intractable damage buried in chromatin. Lower eukaryotes with minimal heterochromatin lack DDB2 (Tan & Chu, 2002), indicating that this bivalent coordinator of DNA repair becomes critical in vertebrates, where a large genome necessitate multiple levels of chromatin compaction. We propose that the advent of DDB2 in evolution correlates with the need for a spatiotemporal organizer that optimizes NER activity within complex chromatin architectures.

My contribution is designed experiments with Dr. Naegeli, cloned all the constructs and performed experiments of Fig. 1, 2, 3(A, B & F), 4(A-D), S1-S5 and S7.

Materials and methods

Reagents

The 15-mer oligonucleotide 5'-ACAGCGGTTGCAGGT-3', carrying a CPD at the central pyrimidines was synthesized according to a published procedure and incorporated by standard DNA synthesis (Butenandt et al, 1998). The oligonucleotide containing the T(6-4)T lesion was produced by irradiation of purchased DNA (Metabion, Martinsried, Germany) using published procedures (Glas et al, 2009). Control oligonucleotides (5'-ACAGCGGTTGCAGGT-3') were synthesized by Microsynth. The siRNA directed to CUL4A (target sequence 5'-TTCGAAGGACATCATGGTTCA-3') and DDB2 (target sequence 5'-AGGGATCAAGCAGTTATTTGA-3') as well as the corresponding control, were purchased from Qiagen. The negative control (siCTRL) consists of a pool of scrambled siRNA designed to have at least four mismatches for all the sequences present in the human genome. The MG132 proteosome inhibitor was obtained from Sigma-Aldrich and added to the cell culture medium 6 h before each assay, at a final concentration of 10 μM. The E1 inhibitor, PYR-41 (Santa Cruz) was used at concentration of 50 μM and added to the medium 5 h before the assays. Restriction enzymes and micrococcal nuclease (MNase) were obtained from New England Biolabs.

Plasmids and cloning

The full-length human *DDB2* sequence, obtained from plasmid DDB2-GFP-C1 (a gift from Dr. S. Linn, University of California, Berkeley, USA) by *BamH*I restriction, was inserted into the expression vectors p3XFLAG-CMV-14 (Sigma-Aldrich) and pmRFP1-C3 (a gift of Dr. Elisa May, University of Konstanz, Germany). To construct the $DDB2_{79-427}$-FLAG fusion, *Nde*I restriction sites were generated by site directed mutagenesis at the start codon and at the position 78 of the DDB2 coding sequence. Subsequently, residues 1-78 were removed by *Nde*I digestion. For the cloning of XPC truncations and deletions, *Nde*I restriction sites were generated at the appropriate positions of vector XPC-pEGFP-N3 (Maillard et al, 2007; Camenisch et al, 2009). XPC-RFP was cloned by insertion of the XPC sequence into vector pmRFP1-C3 using the *Kpn*I and *Sma*I sites. All final plasmids were sequenced (Microsynth) to exclude accidental mutations.

Proteins and antibodies

The recombinant human DDB heterodimer (containing His_6-tagged DDB2) was kindly provided by Dr. A. Scrima and Dr. N. Thomä (FMI, Basel, Switzerland). Antibodies against the following proteins were used for Western blots following the manufacturers' recommendations: human DDB2 (dilution 1:50, ab51017, Abcam), human XPC (1:1,000, ab6264, Abcam), mouse XPC (1:100, sc-74411, Santa Cruz), human RAD23B (1:500, HPA029718, Sigma-

Aldrich), human XPB (1:200, sc-293, Santa Cruz), human XPG (1:500, X1629, Sigma-Aldrich), human XPA (1:100, sc-853, Santa Cruz), human GAPDH (1:4,000, No. 4300, Ambion), human histone H1.0 (1:1,000, ab11079, Abcam), human H3 (1:10,000, No. 07-690, Millipore) and H3K9m3 (1:10,000, No. 17-625, Millipore), human DDB1 (1:4,000, No. 612488, BD Bioscience), human CUL4A (1:1,000, ab34897, Abcam), FLAG peptide (1:4,000, F3165, Sigma-Aldrich) and GFP (1:4,000, No. 632375, Clontech). Horse radish peroxidase- (HRP)-conjugated secondary antibodies against mouse or rabbit IgG were from Sigma-Aldrich. HRP-conjugated antibodies against the His_6 sequence (1:500, sc-8036) were from Santa Cruz.

Cell lines and culture conditions

All cell lines were grown in humidified incubators containing 5% CO_2. HeLa, HEK293, U2OS and the Chinese hamster ovary (CHO) cells V79 were obtained from Dr. G. Marra, University of Zurich, Switzerland. Human XP-C (GM16093) and XP-E fibroblasts (GM02415) were purchased from the Coriell Institute for Medical Research (Camden, New Jersey, USA). These cells were grown at 37°C in Dulbecco's modified Eagle's medium (DMEM) supplemented with 10% (v/v) fetal bovine serum (FBS; Gibco), 100 U/ml penicillin and 0.1 mg/ml streptomycin. For XP-E fibroblasts, the FBS concentration was raised to 15% (v/v). The mouse embryonic fibroblast (MEF) cell line ts-20 (thermosensitive for the E1 ubiquitin-activating enzyme) and the stably corrected H38-5 were kindly provided by Dr. C. Borner, University of Freiburg, Germany and Dr. H. Ozer, New Jersey Medical School, USA. The ts-20 cells were grown at 32°C in DMEM with 10% (v/v) FBS (Chowdary et al, 1994). H38-5 cells were cultured at 37°C in the presence of hygromycin (50 □g/ml) to maintain expression of the complementing wild-type E1 enzyme. These MEFs were transferred to the restrictive temperature (39°C) 18 h before starting the experiments.

UV irradiation

After removal of the culture medium, the cells were rinsed with phosphate-buffered saline (PBS) and irradiated with the indicated doses of UV-C from a germicidal lamp (254 nm wavelength). For local damage induction, a 5-µm polycarbonate filter (Millipore) presoaked in PBS was placed over the cells followed by irradiation with 100 J/m^2. After removal of the filter, the cells were incubated in fresh medium before being processed for chromatin segregation assays, immunocytochemistry or FRAP-LD analyses.

Transfections

For gene silencing, 6 x 10^5 HeLa cells were seeded into a 10-cm cell culture dish. Transfections with siRNA were carried out 72 h before the experiments, using the Lipofectamine RNAiMAX reagent (Invitrogen) according to the

manufacturer's protocol. The siRNA final concentration was 15 nM. To complement silenced DDB2, HeLa cells were first transfected with siDDB2 and, 48 h later, transfected with the DDB2-GFP-C1 plasmid (5 µg) using the FuGENE HD reagent (Roche). Experiments were conducted following another 24-h incubation period, at a cell confluence of 90-95%. For immunoprecipitations, 6 x 10^6 HEK293 cells were transfected in 10-cm dishes with 2.5 µg FLAG-DDB2 and 2.5 µg XPC-GFP vectors using the FuGENE reagent. For immunocytochemistry and live-cell imaging experiments, 6 x 10^5 CHO cells were seeded into 6-well plates containing glass cover slips and transfected (FuGENE) with 1 µg each of the XPC-GFP, XPC-RFP, DDB2-GFP or DDB2-RFP vectors as indicated.

Chromatin segregation assay

A combined strategy of salt extraction and nuclease treatment at physiologic ionic strength was applied to separate the nuclei into fractions enriched for soluble proteins, open chromatin proteins (nuclease-susceptible) and compacted (nuclease-resistant) chromatin proteins (Groisman et al, 2003; Goodarzi et al, 2008). The cells were seeded on 10-cm culture dishes, grown to confluence and UV-irradiated. One dish was used per condition. After the indicated time periods, the cells were washed twice with 10 ml ice-cold PBS and scraped into a 1.5-ml tube with 0.3 ml of NP-40 lysis buffer [25 mM Tris-HCl (pH 8.0), 0.3 M NaCl, 1 mM EDTA, 10% (v/v) glycerol, 1% (v/v) NP-40, 0.25 mM phenylmethylsulfonyl fluoride and the Complete, Mini, EDTA-free protease inhibitor cocktail (Roche)] (Sugasawa et al, 2005). After a 30-min incubation on a turning wheel, the fraction of free, i.e., non-chromatin-bound proteins was recovered by centrifugation (15,000 g, 4°C). The volume of these fractions of free proteins was adjusted to 500 µl by adding NP-40 lysis buffer. The remaining nuclear pellet was washed twice with 0.5 ml ice-cold CS buffer (Kapetanaki et al, 2006) consisting of 20 mM Tris-HCl, pH 7.5, 100 mM KCl, 2 mM $MgCl_2$, 1 mM $CaCl_2$, 0.3 M sucrose and 0.1% (v/v) Triton X-100. The resulting chromatin pellet was resuspended in 40 µl CS buffer and, after the addition of 5 µl reaction buffer [500 mM Tris-HCl (pH 7.9), 50 mM $CaCl_2$], 1 µl of bovine serum albumin (BSA; 1 mg/ml) and MNase (final concentration of 4 U/µl in a volume of 50 µl), incubated at 37°C for 20 min. The MNase digestion was stopped by the addition of EDTA (5 mM) and the solubilized supernatant (50 µl) was separated from the insoluble chromatin by centrifugation at 15,000 g (10 min, 4°C). The insoluble pellet was dissolved in 80 µl denaturing buffer [20 mM Tris-HCl, pH 7.4, 50 mM NaCl, 1 mM EDTA, 0.5% (v/v) NP-40, 0.5% (v/v) deoxycholate and 0.5% (w/v) sodium dodecyl sulfate (SDS)] (Yuan et al, 2009) and sonicated (1 x 12 s). To obtain the MNase dose dependence, chromatin pellets obtained from 6 x 10^6 cells each were digested for 20 min at 37ºC with increasing concentrations of MNase ranging from 0.1 to 8 U/µl. For the subsequent DNA analysis, the nuclesome fractions were extracted using the QIAamp Blood Kit (QIAGEN) and resolved on 2% agarose gels stained by ethidium bromide.

Quantification of UV lesions

Antibodies against 6-4PPs and CPDs (MBL International Corporation) were used in an enzyme-linked immunosorbent assay (ELISA) to quantify UV lesions according to the manufacturer's instructions. Briefly, DNA purified from each nucleosome fraction (obtained by MNase digestion) and from the whole genome (before MNase digestion) was denatured by heating to 95ºC (10 min) followed by a 15-min incubation in ice-cold water. A volume of 50 µl per well of denatured DNA (4 µg/ml) was distributed into a 96-well micotiter plate coated with protamine sulfate (BD Biosciences) and dried overnight at 37ºC. The DNA-coated plates were washed five times with PBST [0.05% (v/v) Tween-20 in PBS] and blocked with 2% FBS in PBS at 37ºC for 30 min. The antibodies against either 6-4PPs (64M-2) or CPDs (TDM-2) were used for 30 min (37ºC) at a dilution of 1:2,000. The primary antibodies bound to DNA molecules were recognized by biotin-labeled $F(ab')_2$ fragments of anti-mouse IgG (dilution 1:2,000; Invitrogen) added for 30 min at 37ºC. After washing the plates, 100 µl of a peroxidase-streptavidin conjugate (dilution 1:10,000; Invitrogen) was distributed into each well. The reaction was started by the addition 0.5 mg/ml o-phenylenediamine, 0.007% H_2O_2 and 0.1 M citrate-phosphate buffer (pH 5.0), stopped with 2 M H_2SO_4, and monitored by measuring the absorbance at 490 nm in a PLUS384 microplate spectrophotometer (Molecular Devices).

Immunoprecipitation

One day after transfection, the medium was aspirated and HEK293 cells were washed twice with ice-cold PBS and harvested by scraping in 0.5 ml of ice-cold NP-40 lysis buffer. After 30 min, the cells were snap frozen in liquid nitrogen and the resulting lysates were centrifuged at 10,000 g for 10 min at 4°C. The supernatant was mixed with 30 µl anti-FLAG M2 affinity gel (Sigma) and incubated under rotation overnight at 4°C. After two washes each with ice-cold TNT buffer [50 mM Tris-HCl (pH 7.5), 140 mM NaCl, 1% (v/v) Triton X-100] and TN buffer [50 mM Tris-HCl (pH 7.5), 140 mM NaCl], the immunoprecipitates were eluted with 0.5 mg/ml 3xFLAG peptides (Sigma), boiled in loading buffer [60 mM Tris-HCl, pH 6.8, 2% (w/v) SDS, 10% (v/v) glycerol, 4% (v/v) 2-mercaptoethanol and 0.002% (w/v) bromphenol blue] and resolved by denaturing polyacrylamide gel electrophoresis.

Immunoblotting

The electrophoretically resolved samples were transferred to a polyvinylidene (PVDF) membrane (BioRad) that was blocked by incubation for 2 h at room temperature with TBST buffer (Tris-buffered saline with Tween-20) containing 5% (w/v) nonfat dry milk. The primary antibodies were used at the indicated dilutions in TBST/2.5% (w/v) nonfat dry milk. The HRP-conjugated secondary antibody was diluted 10,000-fold in TBST containing 2.5% milk. The reactions were developed with the SuperSignal West Pico or Femto substrate (Pierce) and documented with a FUJI LAS-3000 imaging system. The resulting data

were quantified using the Quantity One software (BioRad) to calculate mean values and standard deviations from the blots of at least three independent experiments.

Protein pull-down assay

GST-XPC$_{607-741}$, GST-XPC$_{607-766}$, GST-XPC$_{679-832}$ and GST-XPC$_{428-633}$ were cloned and expressed in *E. coli* as described (Uchida et al, 2002). These GST-tagged polypeptides (120 pmol) were incubated for 1 h at 4°C with 25 µl glutathione-Sepharose beads in 500 µl washing buffer [50 mM Tris-HCl (pH 8.0), 1 mM EDTA, 1 mM dithriothreitol, 10% (v/v) glycerol, 0.5% (v/v) Nonidet P-40, 150 mM NaCl and 200 g/ml bovine serum albumin] containing 0.5% (w/v) nonfat dry milk. In the experiments with DNA, DDB (120 pmol) was pre-incubated with the indicated amounts of undamaged or damaged duplexes in a separate tube containing 500 µl washing buffer for 1 h at 4°C. The bead suspension containing the GST-tagged polypeptides were washed three times with 1 ml washing buffer and incubated with DDB for 20 min at room temperature in a total volume of 500 µl. The beads were then washed 3 times with 1 ml washing buffer containing nonfat dry milk, twice with washing buffer without nonfat dry milk, resuspended in loading buffer and processed for 10% denaturing polyacrylamide gel electrophoresis.

Live-cell analysis of protein dynamics

FRAP-LD measurements were performed on a Leica TCS SP5 confocal microscope equipped with an Ar^+ laser (488 nm) and a 63x oil immersion lens as previously described (Camenisch et al, 2009). The assays were performed in a controlled environment at 37°C and a CO_2 supply of 5%. Briefly, cells transfected with the indicated GFP and RFP constructs were UV-irradiated (254 nm, 100 J/m^2) through 5-µm polycarbonate filters. After 15-min incubations in complete medium (37°C), regions of interest (ROIs) corresponding to spots of GFP accumulation were photobleached at 50% laser intensity to reduce their fluorescence to that of the surrounding nuclear background. Fluorescence recovery was monitored 10 times using 0.7 s intervals followed by 10 frames at 5 s and 6 frames at 20 s. The results were adjusted for the overall bleaching by correction with a reference ROI of the same size monitored at each time point. The values were used to calculate ratios between the damaged area in the foci and the corresponding intensity before bleaching. In the data display, the first fluorescence measurement after photobleaching is set to 0, while all following data points are plotted as a function of time.

Immunocytochemistry

Following a 15-min incubation after local UV damage induction, the medium was aspirated, the cells were rinsed with PBS and fixed for 15 min at room

temperature using 4% (v/v) paraformaldehyde (Sigma-Aldrich) in PBS. The cells were then permeabilized twice with PBS containing 0.1% (v/v) Tween-20 for 10 min and DNA was denatured with 0.07 M NaOH for 8 min. Next, the samples were washed three times with 0.1% Tween-20 and incubated (30 min, 37°C) with 20% FBS in PBS to inhibit unspecific binding. The samples were incubated (1 h at 37°C in 5% FBS) with the primary antibodies directed against CPDs (TDM-2; dilution 1:1'000). The samples were then washed with 0.1% Tween-20, blocked twice for 10 min with 20% FBS, and treated with Alexa Fluor 594 dye-conjugated secondary antibodies (Invitrogen; dilution 1:400) for 30 min at 37°C. After washing with 0.1% Tween-20 in PBS, the nuclei were stained for 10 min with Hoechst dye 33258 (200 ng/ml). Finally, the samples were washed three times and analyzed in a Leica SP5 confocal microscope equipped with a ×63 oil immersion lens. For quantification of the immunocytochemistry results, a minimum of 30 cells were analyzed per experiment.

Figure legends

Fig. 1. Nucleosome sorting and demarcation of DNA repair hotspots by DDB2. (**A**) The chromatin segregation of NER factors and histone markers was analyzed 1 h after exposure of HeLa cells to UV light. Following MNase digestion, chromatin was separated according to solubility and the translocation of NER factors from the pool of free proteins to either soluble or insoluble nucleosomes was monitored by Western blotting. GAPDH, glyceraldehyde-3-phosphate dehydrogenease (loading control). H3K9m3, trimethylated histone H3 (marker of heterochromatin). The asterisks denote the position of ubiquitylated XPC. (**B**) UV dose-dependent translocation of from the free (F) pool to soluble (S) and insoluble (I) nucleosomes. The relative amount of DDB2 and XPC was calculated by the quantification of Western blots and correction for loading differences (mean values of three independent determinations). (**C**) UV-dependent translocation of DDB2 and XPC to chromatin of U2OS cells. (**D**) Time course of DDB2 and XPC segregation in the chromatin of UV-exposed (30 J/m^2) HeLa cells. (**E**) Time-dependent distribution of XPC protein in chromatin of UV-irradiated HeLa cells (30 J/m^2). The amount of XPC in each fraction was quantified from three separate Western blots.

Fig. 2. Ubiquitin-dependent targeting of XPC protein to DNA repair hotspots. (**A**) Depletion of DDB2 alters the chromatin distribution of DDB1, XPC and XPA. HeLa cells were UV-irradiated (30 J/m^2) after transfection with specific siRNA against DDB2 (siDDB2) or control RNA (siCTRL). Double amounts of soluble chromatin fractions were loaded to facilitate comparisons with the insoluble counterparts. (**B**) Abnormal chromatin relocation of XPC protein after inhibition of the ubiquitylation system by different treatments. UV-dependent XPC translocations from the free (F) protein pool to either soluble (S) or insoluble (I) chromatin was determined by quantification of Western blots (mean values of 3-5 experiments). (**C**) Inactivation of the E1 ubiquitin-activating enzyme in ts-20 cells (incubated at 39°C) suppresses the UV-dependent accumulation of XPC protein in soluble chromatin. This effect is not observed at the permissive temperature (32°C) or in corrected H38-5 cells. (**D**) Treatment with the E1 inhibitor PYR-41 reduces the UV-dependent relocation of XPC protein to solubilizable nucleosomes of HeLa cells. (**E**) Anomalous distribution of DDB2, XPC and XPA in UV-irradiated chromating following depletion of CUL4A. (**F**) Treatment with MG132 increases the steady-state level of DDB2 but reduces the UV-dependent recruitment of XPC and XPA proteins to solubilizable nucleosomes.

Fig. 3. DDB2-XPC interactions in chromatin. (**A**) Ubiquitylation of endogenous XPC and an ectopic XPC-GFP fusion in U2OS fibroblasts. Untreated or UV-irradiated cells were processed by boiling in lysis buffer, electrophoresis and Western blotting. The 125-kDa and 150-kDa bands represent unmodified XPC and XPC-GFP, respectively. (**B**) Accumulation of XPC-GFP at insoluble

nucleosomes of XP-C cells. For comparison, the XPC-dependent recruitment of XPA occurs mainly in solubilizable chromatin. (**C**) Relocation of XPC-GFP to irradiated areas of CHO cells. The UV lesion spots were visualized with antibodies against CPDs or by monitoring the red fluorescence of DDB2-RFP. (**D**) Redistribution of XPC-GFP to UV lesions stimulated by co-expression of DDB2-RFP. GFP signals at UV lesion spots were quantified, normalized to the nuclear background and expressed as a percentage of control values obtained with XPC alone (average ± s.d., N=30). (**E**) Image illustrating the DDB2-stimulated recruitment of XPC_{1-831}-GFP to UV irradiated areas. (**F**) Domain structure of human XPC. (**G**) Recruitment of XPC truncates. GFP spots co-localizing with UV lesions (N=30) were normalized and expressed as a percentage of the control value (full-length XPC alone). (**H**) Recruitment of XPC-GFP deletions to UV lesions (N=30). The Δ hairpin lacks amino acids 789-815.

Fig. 4. Direct DDB2-XPC interactions. (**A**) Association of DDB2 with the TGD region. Purified DDB heterodimers (120 pmol) were incubated with $XPC_{428-631}$-GST (120 pmol) and probed by the addition of GST beads. $XPC_{428-633}$-GST in the pull-down fraction was visualized by Coomassie staining whereas the fraction of interacting DDB2 was detected by antibodies against its His_6 extension. An input control displays 20% of the total DDB2 in each reaction mixture. (**B**) Association of DDB2 with $XPC_{607-741}$-GST and the slightly longer $XPC_{607-766}$-GST, both containing the BHD1 and BHD2 regions. (**C**) The interaction between DDB2 and $XPC_{428-633}$-GST is inhibited by the addition of a 15-mer DNA duplex (120 pmol). UD, undamaged. The sequence of this DNA fragment is outlined with the position of the 6-4PP or CPD shown in red color. (**D**) The interaction between DDB2 and $XPC_{607-741}$-GST is stimulated by the addition of a 15-mer DNA duplex (top panel: 15-60 pmol; bottom panel: 120 pmol). (**E**) Dissociation kinetics of XPC-GFP proteins from UV lesion sites in the nuclei of CHO cells measured by FRAP-LD (N=15; error bars, s.e.m.). The half-lives were estimated from the fluorescence recovery curves (**F**) DDB2 is unable to stabilize the Δ hairpin construct at UV lesions (N=15).

Supporting figure legends

Fig. S1. Partitioning of NER subunits. (A) Ethidium bromide staining of agarose gels demonstrating the gradual digestion of nuclear DNA with increasing MNase concentrations. Saturation is reached at 4 U/µl, generating nucleosome core fragments of 146 bp. Lanes 1-6 and 9, analysis of whole (W) chromatin mixtures; lane 8, 100-bp size markers; lane 10, solubilized (S) nucleosomes (4 U/µl MNase); lane 11, analysis of the respective insoluble (I) pellet. (B) Chromatin distribution of DDB2 in UV-irradiated (30 J/m^2) HeLa cells determined with different MNase concentrations. Nucleosomes were separated according to solubility and DDB2 translocation to either insoluble or soluble fractions was monitored by Western blotting. (C) Chromatin segregation with limiting Mnase (0.1 U/µl) resulting in partial DNA digestion (see lane 2 of panel S1A). The movement of DDB2 and XPC from the pool of free proteins to either insoluble or soluble nucleosomes was analyzed 1 h after exposure of HeLa cells to UV light. (D) Chromatin segregation of NER factors 6 h after UV irradiation (30 J/m^2). GAPDH and H1.0 are markers of chromatin-free and chromatin-bound proteins, respectively. (E) Distribution of DDB2, XPC and XPA between chromatin-free (F), solubilizable (S) and insoluble (I) chromatin fractions in control cells and 6 h after UV irradiation (30 J/m^2). The amount of each factor was calculated by the quantification of Western blots and correction for loading differences (mean values of three independent determinations).

Fig. S2. Ubiquitin-dependent distribution of XPC protein after UV irradiation. (A) Defective XPC ubiquitylation following DDB2 depletion by transfection of HeLa cells with specific siRNA (longer exposure of the soluble fraction in Fig. 2A). The UV dose was 30 J/m^2; siCTRL, control siRNA. Soluble nucleosomes were recovered after MNase digestion at 4 U/µl and analyzed by Western blotting. The asterisks denote the position of ubiquitylated XPC. (B) Abnormal chromatin distribution of XPC protein in XP-E fibroblasts. After UV exposure (30 J/m^2), essentially all XPC molecules translocate to insoluble nucleosomes resulting from MNase digestion (4 U/µl). (C) Complementation of DDB2-depleted HeLa cells by transfection with a construct coding for DDB2-GFP. This construct reconstitutes DDB2 expression and, hence, restores in part the ubiquitylation of XPC protein and its UV-dependent accumulation at solubilizable nucleosomes (compare lanes 4 and 6). (D) Defective XPC ubiquitylation following treatment of HeLa cells with the E1 inhibitor PYR-41 (longer exposure of the soluble fraction in Fig. 2D). The UV dose was 30 J/m^2. (E) Defective XPC ubiquitylation following a CUL4A depletion by transfection of HeLa cells with specific siRNA (longer exposure of the soluble fraction in Fig. 2E). (F) Defective XPC ubiquitylation in HeLa cells treated with MG132 (longer exposure of the soluble fraction in Fig. 2F).

Fig. S3. DDB2-XPC interactions mapped by co-immunoprecipitation in HEK293 cells. (A) Full-length DDB2 (DDB2$_{1-427}$-FLAG) interacts with XPC-GFP. The lysates of transiently transfected cells were probed by the addition of anti-FLAG affinity beads and the resulting immunoprecipitates were analyzed by Western blotting

using anti-FLAG and anti-GFP antibodies. (B) $DDB2_{79-427}$-FLAG is unable to associate with DDB1 but still interacts with XPC-GFP. (C) DDB2 interacts with a polypeptide ($XPC_{520-633}$-GFP) covering the TGD region of XPC protein. (D) DDB2 binds to a polypeptide ($XPC_{607-831}$-GFP) that represents the BHD region of XPC protein.

Fig. S4. Domains of human XPC protein and constructs used for the *in situ* mapping of DDB2-XPC interactions in chromatin. TGD, transglutaminase homology domain; BHD, beta-hairpin domain.

Fig. S5. Initial excision of UV lesions from different chromatin fractions of HeLa cells transfected with the indicated siRNA reagents. Relative amounts of 6-4PPs (A and B) or CPDs (C and D) were determined at the different time points by immunoassay analysis. This quantification was performed with total genomic DNA or nucleosomal core fragments contained in the insoluble pellet from MNase treatment (4 U/µl). The repair of UV lesions in the MNase-sensitive (solubilizable) fraction was calculated by subtraction from the aforementioned values (average of three independent experiments). The UV dose was 15 J/m^2.

Fig. S6. Protein dynamics measurements reflecting the dissociation of DDB2 from UV lesions. Spots of local DNA damage were generated by UV irradiation of CHO cells through micropore filters. The subsequent FRAP-LD analyses were performed in cells transfected with constructs coding for DDB2-GFP, either in the absence or in the presence of XPC-RFP (N=15; error bars, s.e.m.). The Δ hairpin construct lacks amino acids 789-815 of the human XPC sequence.

Fig. S7. Bimodal role of DDB2 in stimulating DNA damage recognition by the repair-initiating XPC protein. *Left*, DDB2 action over the entire genome. DDB2 recruits XPC protein to UV lesions and, through a transient interaction with its DNA-binding domain, facilitates a beta-hairpin insertion that causes localized unwinding of the DNA double helix. This ubiquitin-independent activity of DDB2 is required mainly for the excision of CPDs that, on their own, induce minimal distortion of the DNA helix. *Right*, ubiquitin-dependent stimulation of DNA repair at accessible hotspots. A UV-induced accumulation of DDB2 at highly accessible chromatin sites leads to the recruitment of DDB1-CUL4A ubiquitin ligases. Only ubiquitylated XPC protein is retained at these DNA repair hotspots whereas non-ubiquitylated XPC protein migrates to UV lesions in bulk chromatin. This ubiquitin-mediated activity of DDB2 is required mainly for the fast excision of helix-distorting 6-4PPs, which are highly enriched in MNase-sensitive repair hotspots (Mitchell et al, 1990) and recognized directly by XPC protein. Ubiquitylated DDB2 is degraded, but XPC protein is protected from proteasome activity by RAD23B (Ng et al, 2003).

References

Aboussekhra A, Biggerstaff M, Shivji MK, Vilpo JA, Moncollin V, Podust VN, Protic M, Hubscher U, Egly JM, Wood RD (1995) Mammalian DNA nucleotide excision repair reconstituted with purified protein components. *Cell* 80: 859-868

Alekseev S, Luijsterburg MS, Pines A, Geverts B, Mari PO, Giglia-Mari G, Lans H, Houtsmuller AB, Mullenders LH, Hoeijmakers JH, Vermeulen W (2008) Cellular concentrations of DDB2 regulate dynamic binding of DDB1 at UV-induced DNA damage. *Mol Cell Biol* 28: 7402-7413

Araujo SJ, Tirode F, Coin F, Pospiech H, Syvaoja JE, Stucki M, Hubscher U, Egly JM, Wood RD (2000) Nucleotide excision repair of DNA with recombinant human proteins: definition of the minimal set of factors, active forms of TFIIH, and modulation by CAK. *Genes Dev* 14: 349-359

Batty D, Rapic'-Otrin V, Levine AS, Wood RD (2000) Stable binding of human XPC complex to irradiated DNA confers strong discrimination for damaged sites. *J Mol Biol* 300: 275-290

Bergink S, Salomons FA, Hoogstraten D, Groothuis TA, de Waard H, Wu J, Yuan L, Citterio E, Houtsmuller AB, Neefjes J, Hoeijmakers JH, Vermeulen W, Dantuma NP (2006) DNA damage triggers nucleotide excision repair-dependent monoubiquitylation of histone H2A. *Genes Dev* 20: 1343-1352

Butenandt J, Eker PMA, Carell T (1998) Synthesis, Crystal Structure, and Enzymatic Evaluation of a DNA-Photolesion Isostere. *Chem Eur J* 4: 642-654

Camenisch U, Trautlein D, Clement FC, Fei J, Leitenstorfer A, Ferrando-May E, Naegeli H (2009) Two-stage dynamic DNA quality check by xeroderma pigmentosum group C protein. *EMBO J* 28: 2387-2399

Chen X, Zhang J, Lee J, Lin PS, Ford JM, Zheng N, Zhou P (2006) A kinase-independent function of c-Abl in promoting proteolytic destruction of damaged DNA binding proteins. *Mol Cell* 22: 489-499

Chen X, Zhang Y, Douglas L, Zhou P (2001) UV-damaged DNA-binding proteins are targets of CUL-4A-mediated ubiquitination and degradation. *J Biol Chem* 276: 48175-48182

Chowdary DR, Dermody JJ, Jha KK, Ozer HL (1994) Accumulation of p53 in a mutant cell line defective in the ubiquitin pathway. *Mol Cell Biol* 14: 1997-2003

Chu G, Chang E (1988) Xeroderma pigmentosum group E cells lack a nuclear factor that binds to damaged DNA. *Science* 242: 564-567

Clausell J, Happel N, Hale TK, Doenecke D, Beato M (2009) Histone H1 subtypes differentially modulate chromatin condensation without preventing ATP-dependent remodeling by SWI/SNF or NURF. *PLoS One* 4: e0007243

Cleaver JE (2005) Cancer in xeroderma pigmentosum and related disorders of DNA repair. *Nat Rev Cancer* 5: 564-573

Dantuma NP, Groothuis TA, Salomons FA, Neefjes J (2006) A dynamic ubiquitin equilibrium couples proteasomal activity to chromatin remodeling. *J Cell Biol* 173: 19-26

Dualan R, Brody T, Keeney S, Nichols AF, Admon A, Linn S (1995) Chromosomal localization and cDNA cloning of the genes (DDB1 and DDB2) for the p127 and p48 subunits of a human damage-specific DNA binding protein. *Genomics* 29: 62-69

El-Mahdy MA, Zhu Q, Wang QE, Wani G, Praetorius-Ibba M, Wani AA (2006) Cullin 4A-mediated proteolysis of DDB2 protein at DNA damage sites regulates in vivo lesion recognition by XPC. *J Biol Chem* 281: 13404-13411

Feldberg RS, Grossman L (1976) A DNA binding protein from human placenta specific for ultraviolet damaged DNA. *Biochemistry* 15: 2402-2408

Fitch ME, Cross IV, Turner SJ, Adimoolam S, Lin CX, Williams KG, Ford JM (2003a) The DDB2 nucleotide excision repair gene product p48 enhances global genomic repair in p53 deficient human fibroblasts. *DNA Repair (Amst)* 2: 819-826

Fitch ME, Nakajima S, Yasui A, Ford JM (2003b) In vivo recruitment of XPC to UV-induced cyclobutane pyrimidine dimers by the DDB2 gene product. *J Biol Chem* 278: 46906-46910

Ford JM, Hanawalt PC (1997) Expression of wild-type p53 is required for efficient global genomic nucleotide excision repair in UV-irradiated human fibroblasts. ***J Biol Chem*** **272: 28073-28080**

Friedberg EC, Walker GC, Siede W, Wood RD, Schultz RA, Ellenberger T (2006) ***DNA Repair and Mutagenesis.*****, Washington DC: ASM Press.**

Fujiwara Y, Masutani C, Mizukoshi T, Kondo J, Hanaoka F, Iwai S (1999) Characterization of DNA recognition by the human UV-damaged DNA-binding protein. ***J Biol Chem*** **274: 20027-20033**

Fulmer AW, Bloomfield VA (1981) Chicken erythrocyte nucleus contains two classes of chromatin that differ in micrococcal nuclease susceptibility and solubility at physiological ionic strength. ***Proc Natl Acad Sci U S A*** **78: 5968-5972**

Glas AF, Schneider S, Maul MJ, Hennecke U, Carell T (2009) Crystal structure of the T(6-4)C lesion in complex with a (6-4) DNA photolyase and repair of UV-induced (6-4) and Dewar photolesions. ***Chem Eur J*** **15: 10387-10396**

Goodarzi AA, Noon AT, Deckbar D, Ziv Y, Shiloh Y, Lobrich M, Jeggo PA (2008) ATM signaling facilitates repair of DNA double-strand breaks associated with heterochromatin. ***Mol Cell*** **31: 167-177**

Groisman R, Polanowska J, Kuraoka I, Sawada J, Saijo M, Drapkin R, Kisselev AF, Tanaka K, Nakatani Y (2003) The ubiquitin ligase activity in the DDB2 and CSA complexes is differentially regulated by the COP9 signalosome in response to DNA damage. ***Cell*** **113: 357-367**

Gunjan A, Alexander BT, Sittman DB, Brown DT (1999) Effects of H1 histone variant overexpression on chromatin structure. ***J Biol Chem*** **274: 37950-37956**

Hoeijmakers JH (2009) DNA damage, aging, and cancer. ***N Engl J Med*** **361: 1475-1485**

Hwang BJ, Ford JM, Hanawalt PC, Chu G (1999) Expression of the p48 xeroderma pigmentosum gene is p53-dependent and is involved in global genomic repair. ***Proc Natl Acad Sci U S A*** **96: 424-428**

Itoh T, Mori T, Ohkubo H, Yamaizumi M (1999) A newly identified patient with clinical xeroderma pigmentosum phenotype has a non-sense mutation in the DDB2 gene and incomplete repair in (6-4) photoproducts. *J Invest Dermatol* 113: 251-257

Kapetanaki MG, Guerrero-Santoro J, Bisi DC, Hsieh CL, Rapic-Otrin V, Levine AS (2006) The DDB1-CUL4ADDB2 ubiquitin ligase is deficient in xeroderma pigmentosum group E and targets histone H2A at UV-damaged DNA sites. *Proc Natl Acad Sci U S A* 103: 2588-2593

Kim JK, Patel D, Choi BS (1995) Contrasting structural impacts induced by cis-syn cyclobutane dimer and (6-4) adduct in DNA duplex decamers: implication in mutagenesis and repair activity. *Photochem Photobiol* 62: 44-50

Kulaksiz G, Reardon JT, Sancar A (2005) Xeroderma pigmentosum complementation group E protein (XPE/DDB2): purification of various complexes of XPE and analyses of their damaged DNA binding and putative DNA repair properties. *Mol Cell Biol* 25: 9784-9792

Li J, Wang QE, Zhu Q, El-Mahdy MA, Wani G, Praetorius-Ibba M, Wani AA (2006) DNA damage binding protein component DDB1 participates in nucleotide excision repair through DDB2 DNA-binding and cullin 4A ubiquitin ligase activity. *Cancer Res* 66: 8590-8597

Liu L, Lee S, Zhang J, Peters SB, Hannah J, Zhang Y, Yin Y, Koff A, Ma L, Zhou P (2009) CUL4A abrogation augments DNA damage response and protection against skin carcinogenesis. *Mol Cell* 34: 451-460

Luijsterburg MS, Goedhart J, Moser J, Kool H, Geverts B, Houtsmuller AB, Mullenders LH, Vermeulen W, van Driel R (2007) Dynamic in vivo interaction of DDB2 E3 ubiquitin ligase with UV-damaged DNA is independent of damage-recognition protein XPC. *J Cell Sci* 120: 2706-2716

Maillard O, Solyom S, Naegeli H (2007) An aromatic sensor with aversion to damaged strands confers versatility to DNA repair. *PLoS Biol* 5: e79

McAteer K, Jing Y, Kao J, Taylor JS, Kennedy MA (1998) Solution-state structure of a DNA dodecamer duplex containing a Cis-syn thymine cyclobutane dimer, the major UV photoproduct of DNA. *J Mol Biol* 282: 1013-1032

Min JH, Pavletich NP (2007) Recognition of DNA damage by the Rad4 nucleotide excision repair protein. *Nature* 449: 570-575

Mitchell DL, Nguyen TD, Cleaver JE (1990) Nonrandom induction of pyrimidine-pyrimidone (6-4) photoproducts in ultraviolet-irradiated human chromatin. *J Biol Chem* 265: 5353-5356

Moser J, Volker M, Kool H, Alekseev S, Vrieling H, Yasui A, van Zeeland AA, Mullenders LH (2005) The UV-damaged DNA binding protein mediates efficient targeting of the nucleotide excision repair complex to UV-induced photo lesions. *DNA Repair (Amst)* 4: 571-582

Mouret S, Baudouin C, Charveron M, Favier A, Cadet J, Douki T (2006) Cyclobutane pyrimidine dimers are predominant DNA lesions in whole human skin exposed to UVA radiation. *Proc Natl Acad Sci U S A* 103: 13765-13770

Mu D, Park CH, Matsunaga T, Hsu DS, Reardon JT, Sancar A (1995) Reconstitution of human DNA repair excision nuclease in a highly defined system. *J Biol Chem* 270: 2415-2418

Nag A, Bondar T, Shiv S, Raychaudhuri P (2001) The xeroderma pigmentosum group E gene product DDB2 is a specific target of cullin 4A in mammalian cells. *Mol Cell Biol* 21: 6738-6747

Ng JM, Vermeulen W, van der Horst GT, Bergink S, Sugasawa K, Vrieling H, Hoeijmakers JH (2003) A novel regulation mechanism of DNA repair by damage-induced and RAD23-dependent stabilization of xeroderma pigmentosum group C protein. *Genes Dev* 17: 1630-1645

Nishi R, Alekseev S, Dinant C, Hoogstraten D, Houtsmuller AB, Hoeijmakers JH, Vermeulen W, Hanaoka F, Sugasawa K (2009) UV-DDB-dependent regulation of nucleotide excision repair kinetics in living cells. *DNA Repair (Amst)* 8: 767-776

Otrin VR, McLenigan M, Takao M, Levine AS, Protic M (1997) Translocation of a UV-damaged DNA binding protein into a tight association with chromatin after treatment of mammalian cells with UV light. *J Cell Sci* 110 (Pt 10): 1159-1168

Rapic-Otrin V, McLenigan MP, Bisi DC, Gonzalez M, Levine AS (2002) Sequential binding of UV DNA damage binding factor and degradation of the p48 subunit as early events after UV irradiation. *Nucleic Acids Res* 30: 2588-2598

Rapic-Otrin V, Navazza V, Nardo T, Botta E, McLenigan M, Bisi DC, Levine AS, Stefanini M (2003) True XP group E patients have a defective UV-damaged DNA binding protein complex and mutations in DDB2 which reveal the functional domains of its p48 product. *Hum Mol Genet* 12: 1507-1522

Reardon JT, Nichols AF, Keeney S, Smith CA, Taylor JS, Linn S, Sancar A (1993) Comparative analysis of binding of human damaged DNA-binding protein (XPE) and Escherichia coli damage recognition protein (UvrA) to the major ultraviolet photoproducts: T[c,s]T, T[t,s]T, T[6-4]T, and T[Dewar]T. *J Biol Chem* 268: 21301-21308

Roche J, Girardet JL, Gorka C, Lawrence JJ (1985) The involvement of histone H1[0] in chromatin structure. *Nucleic Acids Res* 13: 2843-2853

Scrima A, Konickova R, Czyzewski BK, Kawasaki Y, Jeffrey PD, Groisman R, Nakatani Y, Iwai S, Pavletich NP, Thoma NH (2008) Structural basis of UV DNA-damage recognition by the DDB1-DDB2 complex. *Cell* 135: 1213-1223

Shiyanov P, Nag A, Raychaudhuri P (1999) Cullin 4A associates with the UV-damaged DNA-binding protein DDB. *J Biol Chem* 274: 35309-35312

Solimando L, Luijsterburg MS, Vecchio L, Vermeulen W, van Driel R, Fakan S (2009) Spatial organization of nucleotide excision repair proteins after UV-induced DNA damage in the human cell nucleus. *J Cell Sci* 122: 83-91

Sugasawa K (2009) UV-DDB: a molecular machine linking DNA repair with ubiquitination. *DNA Repair (Amst)* 8: 969-972

Sugasawa K (2010) Regulation of damage recognition in mammalian global genomic nucleotide excision repair. *Mutat Res* 685: 29-37

Sugasawa K, Ng JM, Masutani C, Iwai S, van der Spek PJ, Eker AP, Hanaoka F, Bootsma D, Hoeijmakers JH (1998) Xeroderma pigmentosum group C protein complex is the initiator of global genome nucleotide excision repair. *Mol Cell* 2: 223-232

Sugasawa K, Okuda Y, Saijo M, Nishi R, Matsuda N, Chu G, Mori T, Iwai S, Tanaka K, Hanaoka F (2005) UV-induced ubiquitylation of XPC protein mediated by UV-DDB-ubiquitin ligase complex. *Cell* 121: 387-400

Takao M, Abramic M, Moos M, Jr., Otrin VR, Wootton JC, McLenigan M, Levine AS, Protic M (1993) A 127 kDa component of a UV-damaged DNA-binding complex, which is defective in some xeroderma pigmentosum group E patients, is homologous to a slime mold protein. *Nucleic Acids Res* 21: 4111-4118

Tan T, Chu G (2002) p53 Binds and activates the xeroderma pigmentosum DDB2 gene in humans but not mice. *Mol Cell Biol* 22: 3247-3254

Tang J, Chu G (2002) Xeroderma pigmentosum complementation group E and UV-damaged DNA-binding protein. *DNA Repair (Amst)* 1: 601-616

Uchida A, Sugasawa K, Masutani C, Dohmae N, Araki M, Yokoi M, Ohkuma Y, Hanaoka F (2002) The carboxy-terminal domain of the XPC protein plays a crucial role in nucleotide excision repair through interactions with transcription factor IIH. *DNA Repair (Amst)* 1: 449-461

van der Spek PJ, Eker A, Rademakers S, Visser C, Sugasawa K, Masutani C, Hanaoka F, Bootsma D, Hoeijmakers JH (1996) XPC and human homologs of RAD23: intracellular localization and relationship to other nucleotide excision repair complexes. *Nucleic Acids Res* 24: 2551-2559

Volker M, Mone MJ, Karmakar P, van Hoffen A, Schul W, Vermeulen W, Hoeijmakers JH, van Driel R, van Zeeland AA, Mullenders LH (2001) Sequential assembly of the nucleotide excision repair factors in vivo. *Mol Cell* 8: 213-224

Wakasugi M, Shimizu M, Morioka H, Linn S, Nikaido O, Matsunaga T (2001) Damaged DNA-binding protein DDB stimulates the excision of cyclobutane pyrimidine dimers in vitro in concert with XPA and replication protein A. *J Biol Chem* 276: 15434-15440

Wang H, Zhai L, Xu J, Joo HY, Jackson S, Erdjument-Bromage H, Tempst P, Xiong Y, Zhang Y (2006) Histone H3 and H4 ubiquitylation by the CUL4-DDB-ROC1 ubiquitin ligase facilitates cellular response to DNA damage. *Mol Cell* 22: 383-394

Wang QE, Zhu Q, Wani G, Chen J, Wani AA (2004) UV radiation-induced XPC translocation within chromatin is mediated by damaged-DNA binding protein, DDB2. *Carcinogenesis* 25: 1033-1043

Wang QE, Zhu Q, Wani G, El-Mahdy MA, Li J, Wani AA (2005) DNA repair factor XPC is modified by SUMO-1 and ubiquitin following UV irradiation. *Nucleic Acids Res* 33: 4023-4034

Wittschieben BO, Iwai S, Wood RD (2005) DDB1-DDB2 (xeroderma pigmentosum group E) protein complex recognizes a cyclobutane pyrimidine dimer, mismatches, apurinic/apyrimidinic sites, and compound lesions in DNA. *J Biol Chem* 280: 39982-39989

Yasuda G, Nishi R, Watanabe E, Mori T, Iwai S, Orioli D, Stefanini M, Hanaoka F, Sugasawa K (2007) In vivo destabilization and functional defects of the xeroderma pigmentosum C protein caused by a pathogenic missense mutation. *Mol Cell Biol* 27: 6606-6614

Yuan J, Ghosal G, Chen J (2009) The annealing helicase HARP protects stalled replication forks. *Genes Dev* 23: 2394-2399

Zlatanova J, Leuba SH, Yang G, Bustamante C, van Holde K (1994) Linker DNA accessibility in chromatin fibers of different conformations: a reevaluation. *Proc Natl Acad Sci U S A* 91: 5277-5280

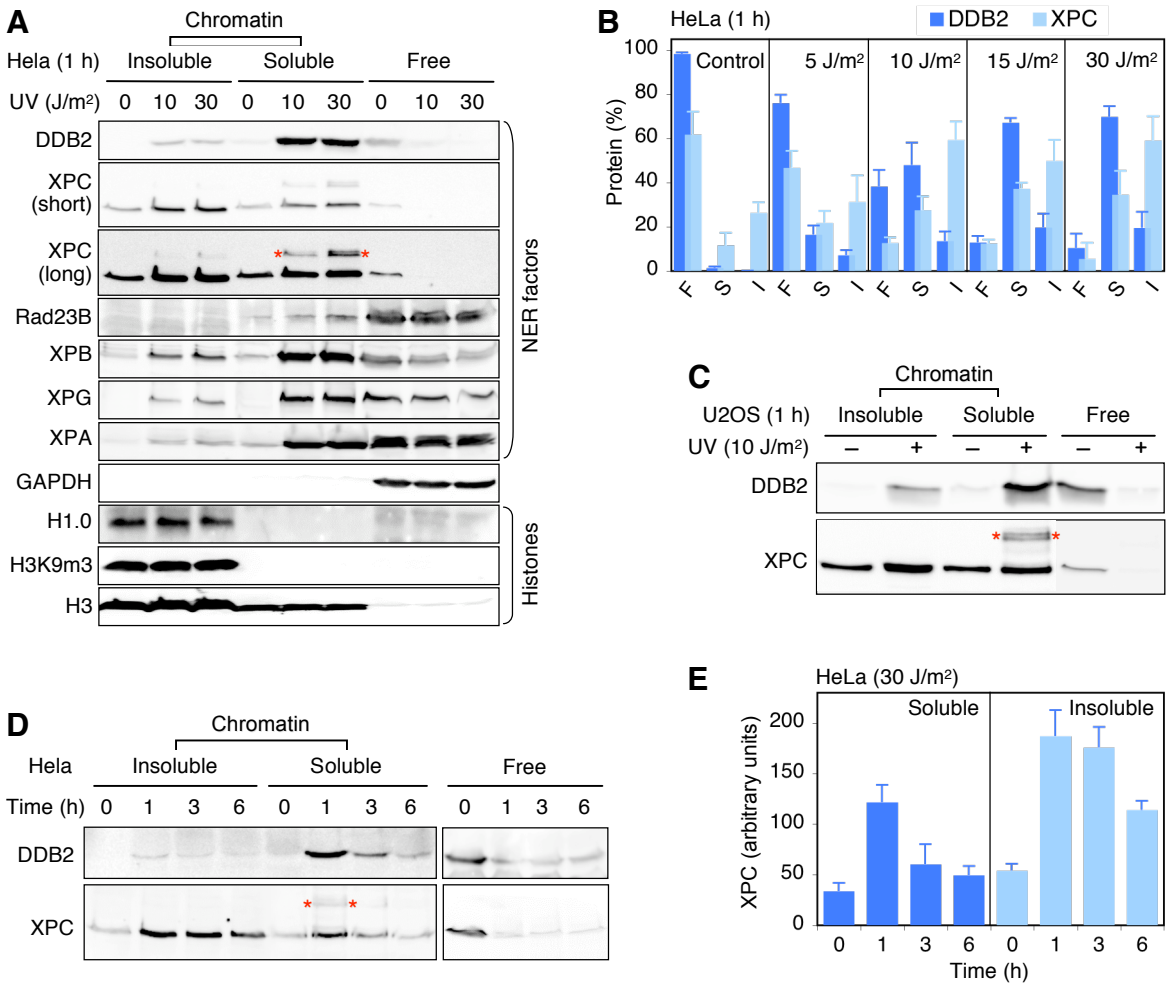
A
Chromatin
Hela (1 h)
Insoluble
Soluble
Free
UV (J/m²)
0 10 30 0 10 30 0 10 30
DDB2
XPC (short)
XPC (long)
Rad23B
XPB
XPG
XPA
GAPDH
H1.0
H3K9m3
H3
NER factors
Histones
B
HeLa (1 h)
DDB2
XPC
Control
5 J/m²
10 J/m²
15 J/m²
30 J/m²
Protein (%)
100
80
60
40
20
0
F S I F S I F S I F S I F S I
C
Chromatin
U2OS (1 h)
Insoluble
Soluble
Free
UV (10 J/m²)
– + – + – +
DDB2
XPC
D
Chromatin
Hela
Insoluble
Soluble
Free
Time (h)
0 1 3 6 0 1 3 6 0 1 3 6
DDB2
XPC
E
HeLa (30 J/m²)
Soluble
Insoluble
XPC (arbitrary units)
200
150
100
50
0
0 1 3 6 0 1 3 6
Time (h)

Figure 1

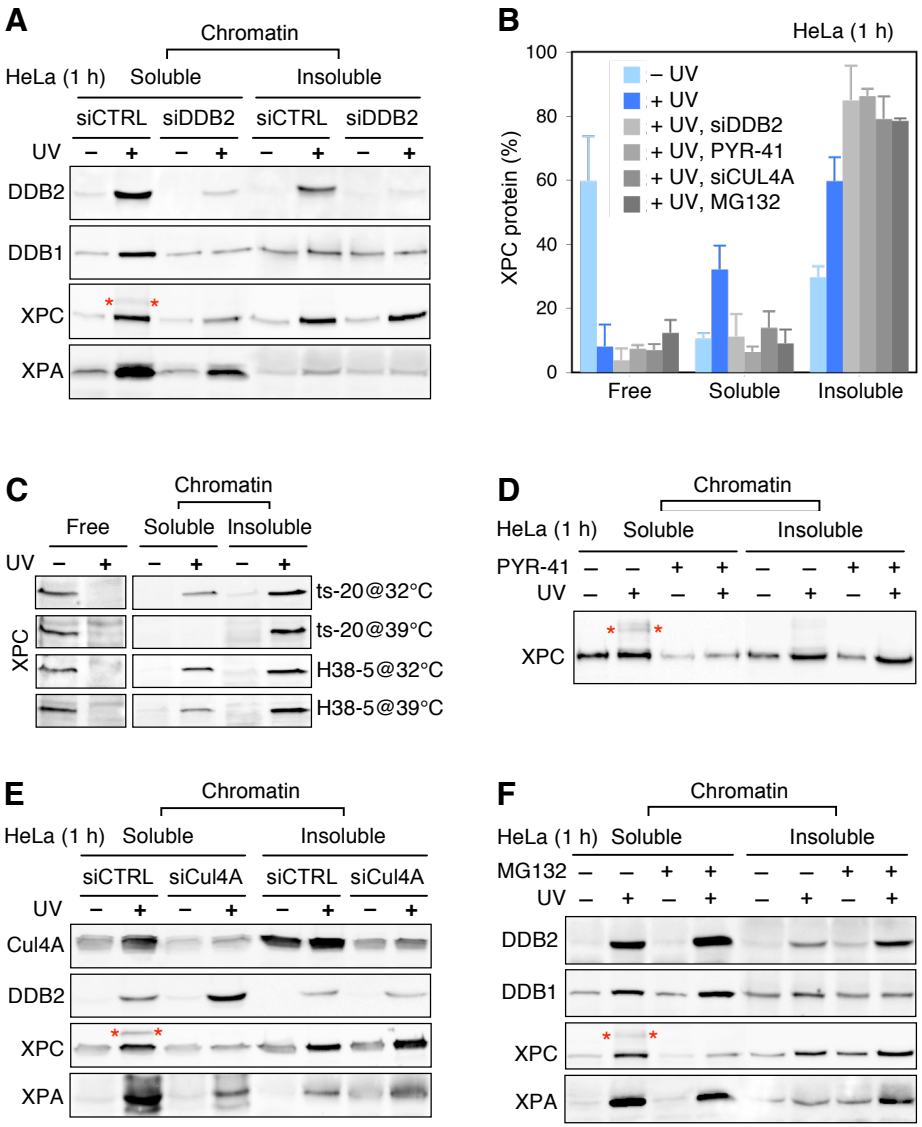
A
Chromatin
HeLa (1 h)
Soluble
Insoluble
siCTRL
siDDB2
siCTRL
siDDB2
UV
– + – + – + – +
DDB2
DDB1
XPC
XPA
B
HeLa (1 h)
100
80
60
40
20
0
XPC protein (%)
– UV
+ UV
+ UV, siDDB2
+ UV, PYR-41
+ UV, siCUL4A
+ UV, MG132
Free
Soluble
Insoluble
C
Chromatin
Free
Soluble
Insoluble
UV
– + – + – +
XPC
ts-20@32°C
ts-20@39°C
H38-5@32°C
H38-5@39°C
D
Chromatin
HeLa (1 h)
Soluble
Insoluble
PYR-41
– – + + – – + +
UV
– + – + – + – +
XPC
E
Chromatin
HeLa (1 h)
Soluble
Insoluble
siCTRL
siCul4A
siCTRL
siCul4A
UV
– + – + – + – +
Cul4A
DDB2
XPC
XPA
F
Chromatin
HeLa (1 h)
Soluble
Insoluble
MG132
– – + + – – + +
UV
– + – + – + – +
DDB2
DDB1
XPC
XPA

Figure 2

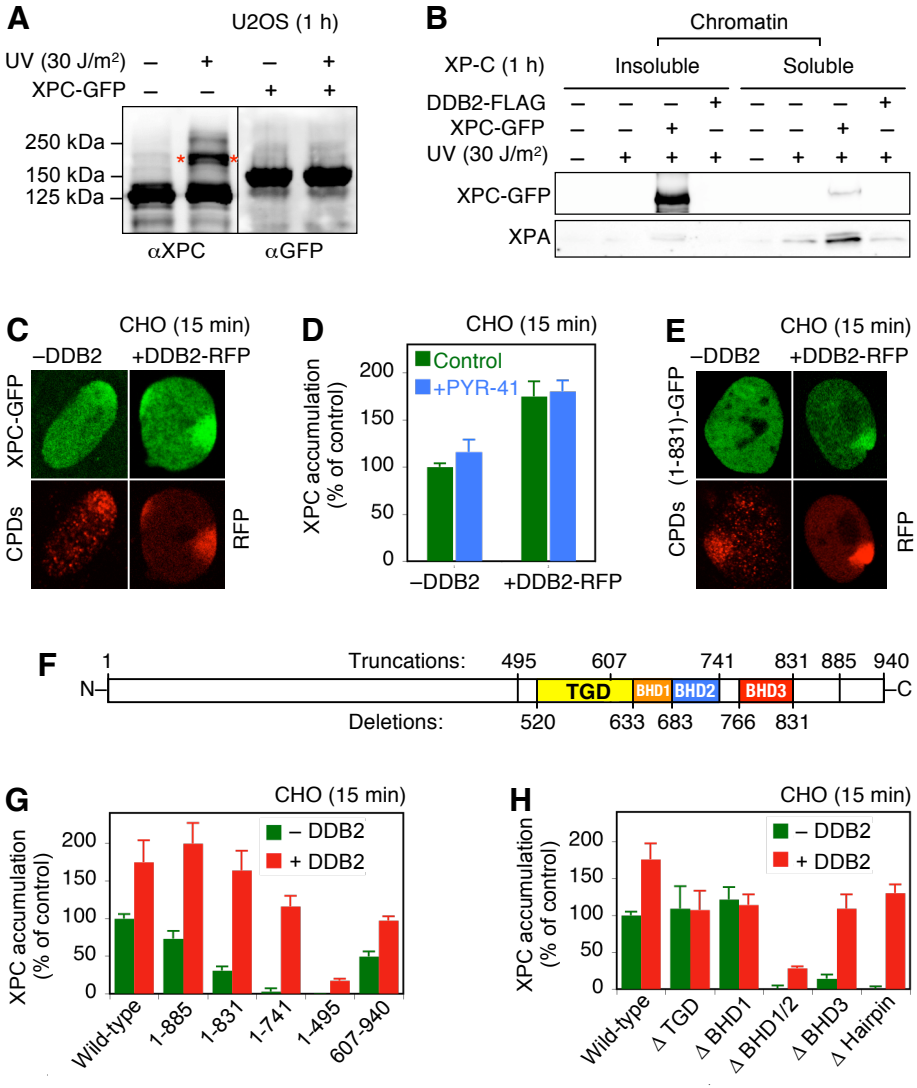
A
U2OS (1 h)
UV (30 J/m²)
XPC-GFP
250 kDa
150 kDa
125 kDa
αXPC
αGFP
B
Chromatin
XP-C (1 h)
Insoluble
Soluble
DDB2-FLAG
XPC-GFP
UV (30 J/m²)
XPC-GFP
XPA
C
CHO (15 min)
–DDB2
+DDB2-RFP
XPC-GFP
CPDs
RFP
D
CHO (15 min)
Control
+PYR-41
XPC accumulation (% of control)
–DDB2
+DDB2-RFP
E
CHO (15 min)
–DDB2
+DDB2-RFP
(1-831)-GFP
CPDs
RFP
F
Truncations:
Deletions:
N
C
TGD
BHD1
BHD2
BHD3
G
CHO (15 min)
– DDB2
+ DDB2
XPC accumulation (% of control)
Wild-type
1-885
1-831
1-741
1-495
607-940
H
CHO (15 min)
– DDB2
+ DDB2
XPC accumulation (% of control)
Wild-type
Δ TGD
Δ BHD1
Δ BHD1/2
Δ BHD3
Δ Hairpin

Figure 3

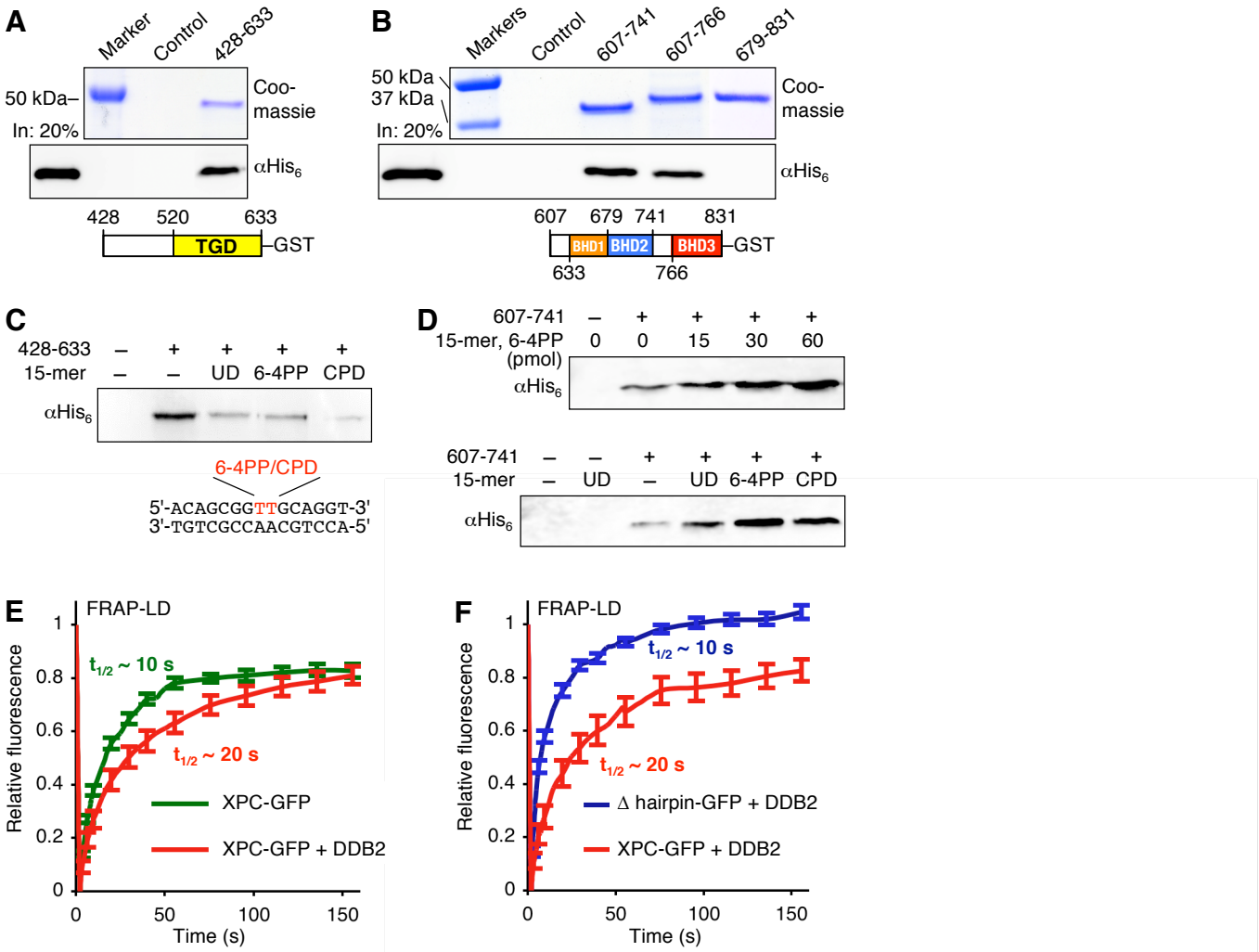
A
Marker
Control
428-633
50 kDa–
In: 20%
Coo-massie
αHis6
428
520
633
TGD
GST
B
Markers
Control
607-741
607-766
679-831
50 kDa
37 kDa
In: 20%
Coo-massie
αHis6
607
679
741
831
BHD1
BHD2
BHD3
GST
633
766
C
428-633 – + + + +
15-mer – – UD 6-4PP CPD
αHis6
6-4PP/CPD
5'-ACAGCGGTTGCAGGT-3'
3'-TGTCGCCAACGTCCA-5'
D
607-741 – + + + +
15-mer, 6-4PP 0 0 15 30 60
(pmol)
αHis6
607-741 – – + + + +
15-mer – UD – UD 6-4PP CPD
αHis6
E
FRAP-LD
Relative fluorescence
t1/2 ~ 10 s
t1/2 ~ 20 s
XPC-GFP
XPC-GFP + DDB2
Time (s)
F
FRAP-LD
Relative fluorescence
t1/2 ~ 10 s
t1/2 ~ 20 s
Δ hairpin-GFP + DDB2
XPC-GFP + DDB2
Time (s)

Figure 4

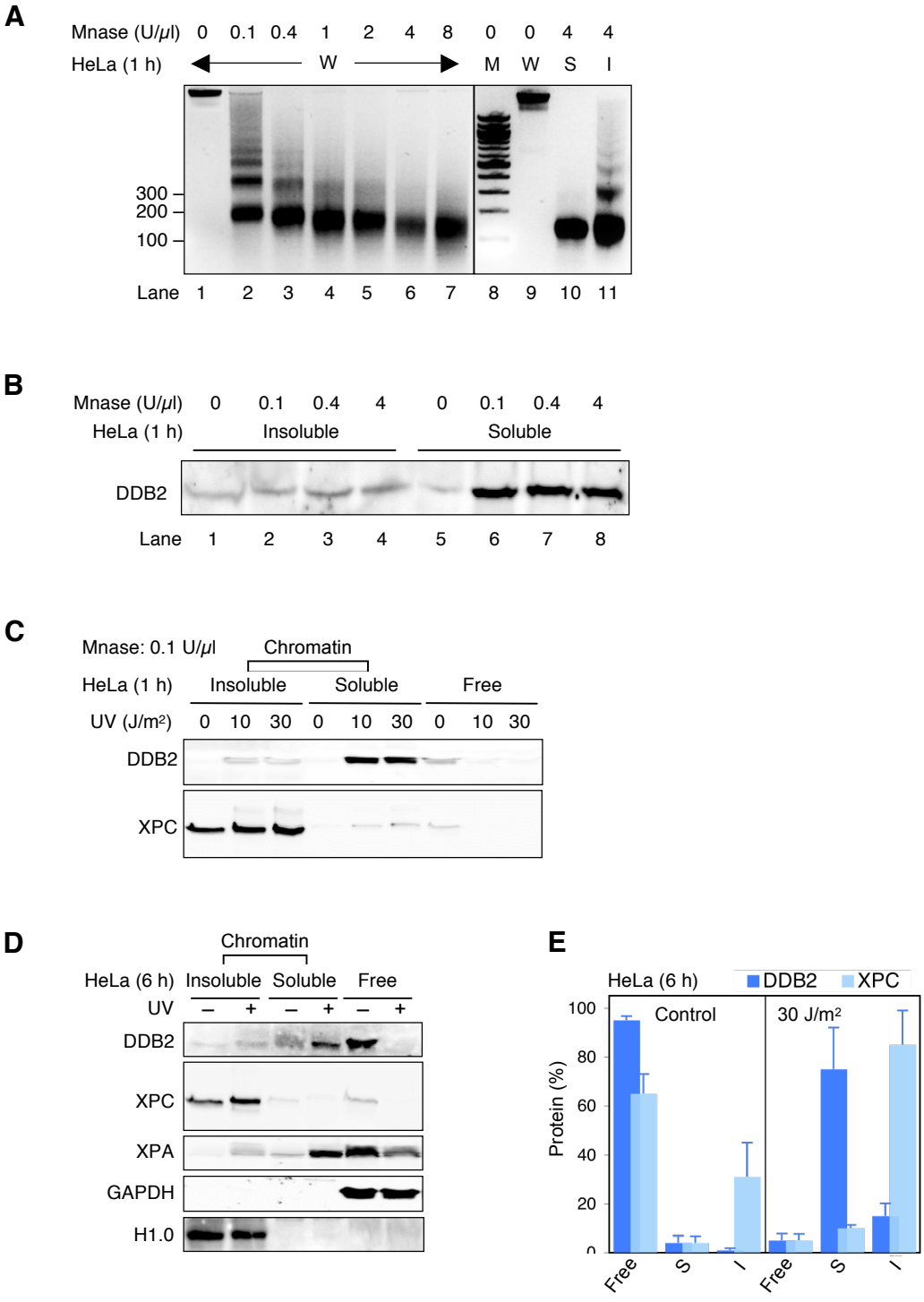
A
Mnase (U/μl) 0 0.1 0.4 1 2 4 8 0 0 4 4
HeLa (1 h) W M W S I
300
200
100
Lane 1 2 3 4 5 6 7 8 9 10 11
B
Mnase (U/μl) 0 0.1 0.4 4 0 0.1 0.4 4
HeLa (1 h) Insoluble Soluble
DDB2
Lane 1 2 3 4 5 6 7 8
C
Mnase: 0.1 U/μl Chromatin
HeLa (1 h) Insoluble Soluble Free
UV (J/m²) 0 10 30 0 10 30 0 10 30
DDB2
XPC
D
Chromatin
HeLa (6 h) Insoluble Soluble Free
UV – + – + – +
DDB2
XPC
XPA
GAPDH
H1.0
E
HeLa (6 h) DDB2 XPC
Control
30 J/m²
Protein (%)
100
80
60
40
20
0
Free S I Free S I

Figure S1

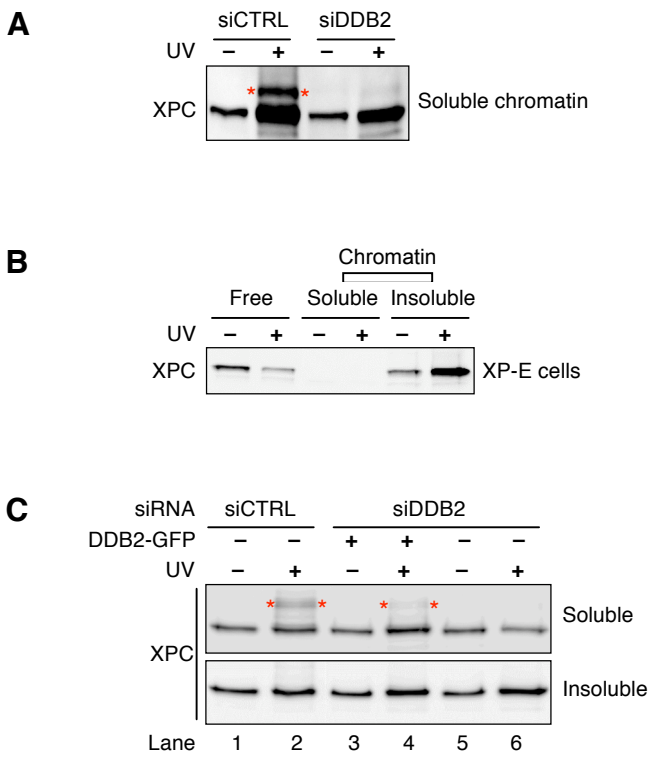
A
siCTRL
siDDB2
UV
– + – +
XPC
Soluble chromatin
B
Chromatin
Free
Soluble
Insoluble
UV
– + – + – +
XPC
XP-E cells
C
siRNA
siCTRL
siDDB2
DDB2-GFP
– – + + – –
UV
– + – + – +
XPC
Soluble
Insoluble
Lane
1 2 3 4 5 6
D
PYR-41
– – + +
UV
– + – +
XPC
Soluble chromatin
E
siCTRL
siCul4A
UV
– + – +
XPC
Soluble chromatin
F
MG132
– – + +
UV
– + – +
XPC
Soluble chromatin

Figure S2

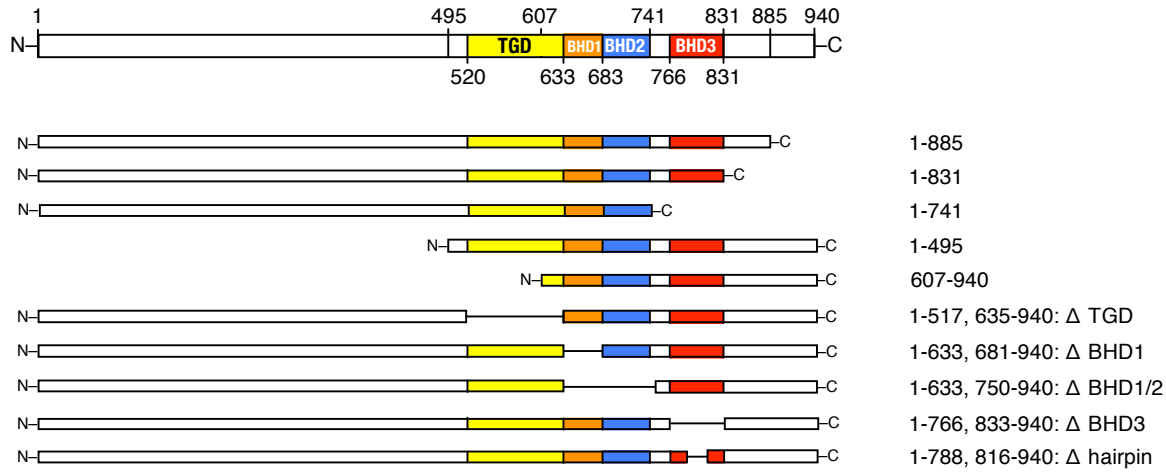
1
495
607
741
831
885
940
N
TGD
BHD1
BHD2
BHD3
C
520
633
683
766
831
1-885
1-831
1-741
1-495
607-940
1-517, 635-940: Δ TGD
1-633, 681-940: Δ BHD1
1-633, 750-940: Δ BHD1/2
1-766, 833-940: Δ BHD3
1-788, 816-940: Δ hairpin

Figure S3

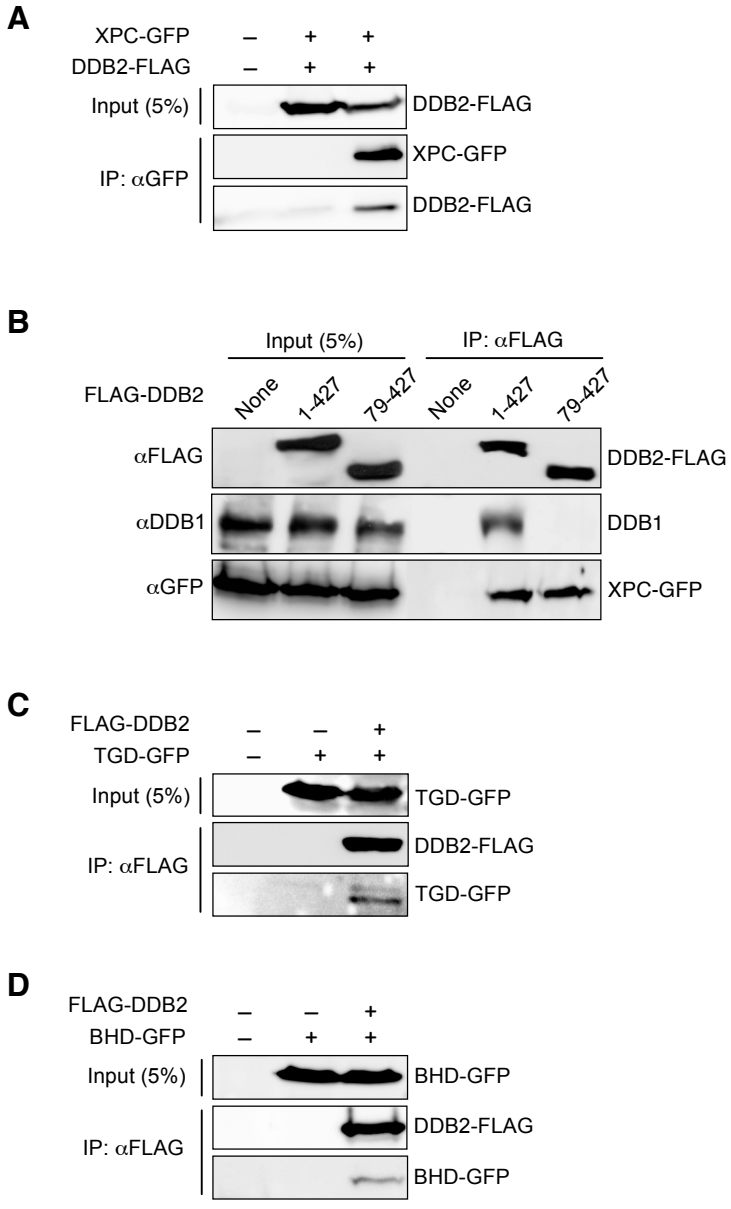
A
XPC-GFP – + +
DDB2-FLAG – + +
Input (5%)
IP: αGFP
DDB2-FLAG
XPC-GFP
DDB2-FLAG
B
Input (5%)
IP: αFLAG
FLAG-DDB2
None
1-427
79-427
None
1-427
79-427
αFLAG
αDDB1
αGFP
DDB2-FLAG
DDB1
XPC-GFP
C
FLAG-DDB2 – – +
TGD-GFP – + +
Input (5%)
IP: αFLAG
TGD-GFP
DDB2-FLAG
TGD-GFP
D
FLAG-DDB2 – – +
BHD-GFP – + +
Input (5%)
IP: αFLAG
BHD-GFP
DDB2-FLAG
BHD-GFP

Figure S4

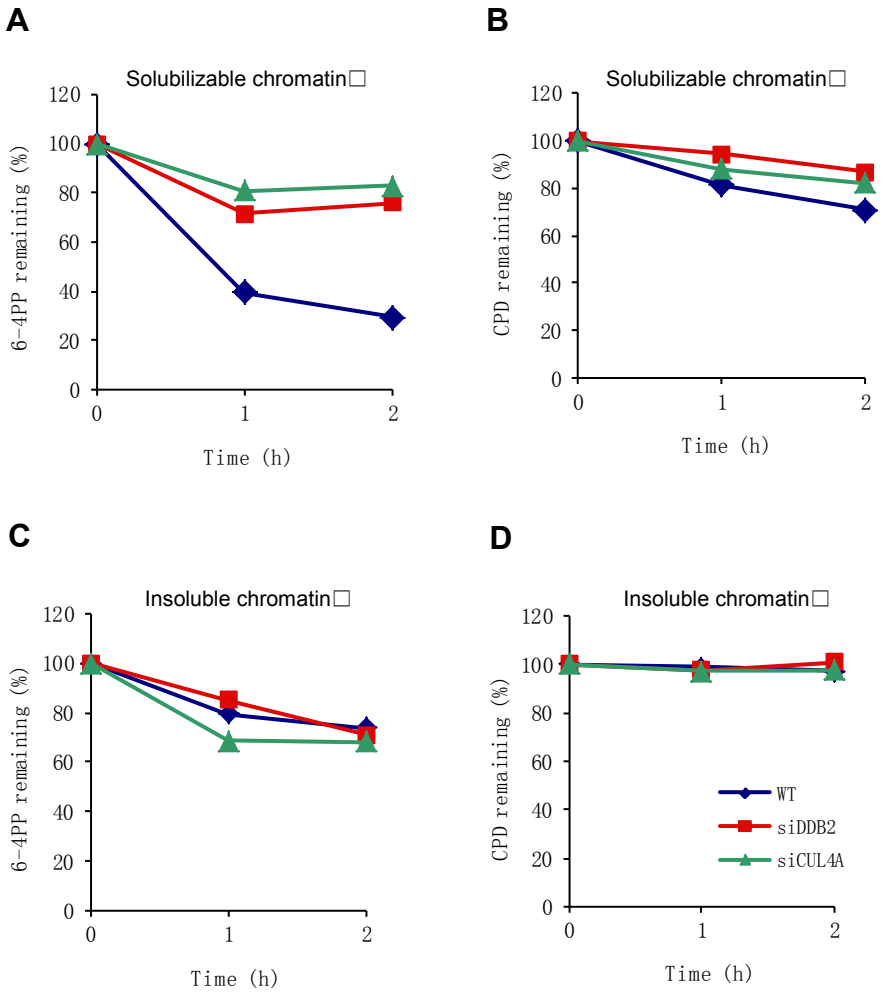
A
Solubilizable chromatin□
6-4PP remaining (%)
120
100
80
60
40
20
0
0
1
2
Time (h)
B
Solubilizable chromatin□
CPD remaining (%)
120
100
80
60
40
20
0
0
1
2
Time (h)
C
Insoluble chromatin□
6-4PP remaining (%)
120
100
80
60
40
20
0
0
1
2
Time (h)
D
Insoluble chromatin□
CPD remaining (%)
120
100
80
60
40
20
0
0
1
2
Time (h)
WT
siDDB2
siCUL4A

Figure S5

A

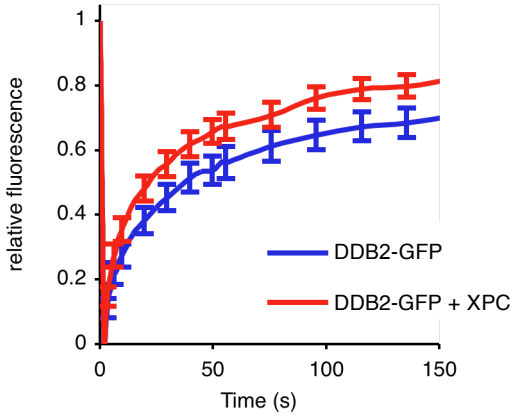
relative fluorescence
1
0.8
0.6
0.4
0.2
0
0
50
100
150
Time (s)
DDB2-GFP
DDB2-GFP + XPC

B

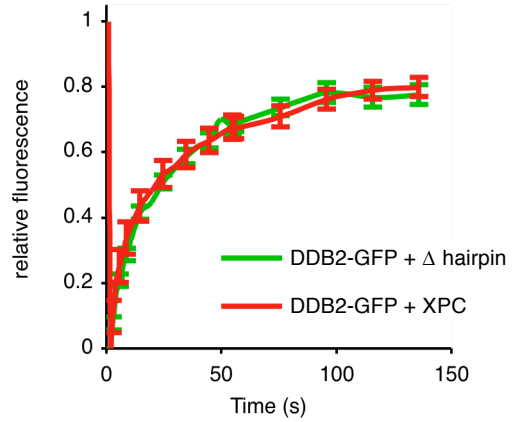
relative fluorescence
1
0.8
0.6
0.4
0.2
0
0
50
100
150
Time (s)
DDB2-GFP + Δ hairpin
DDB2-GFP + XPC

Figure S6

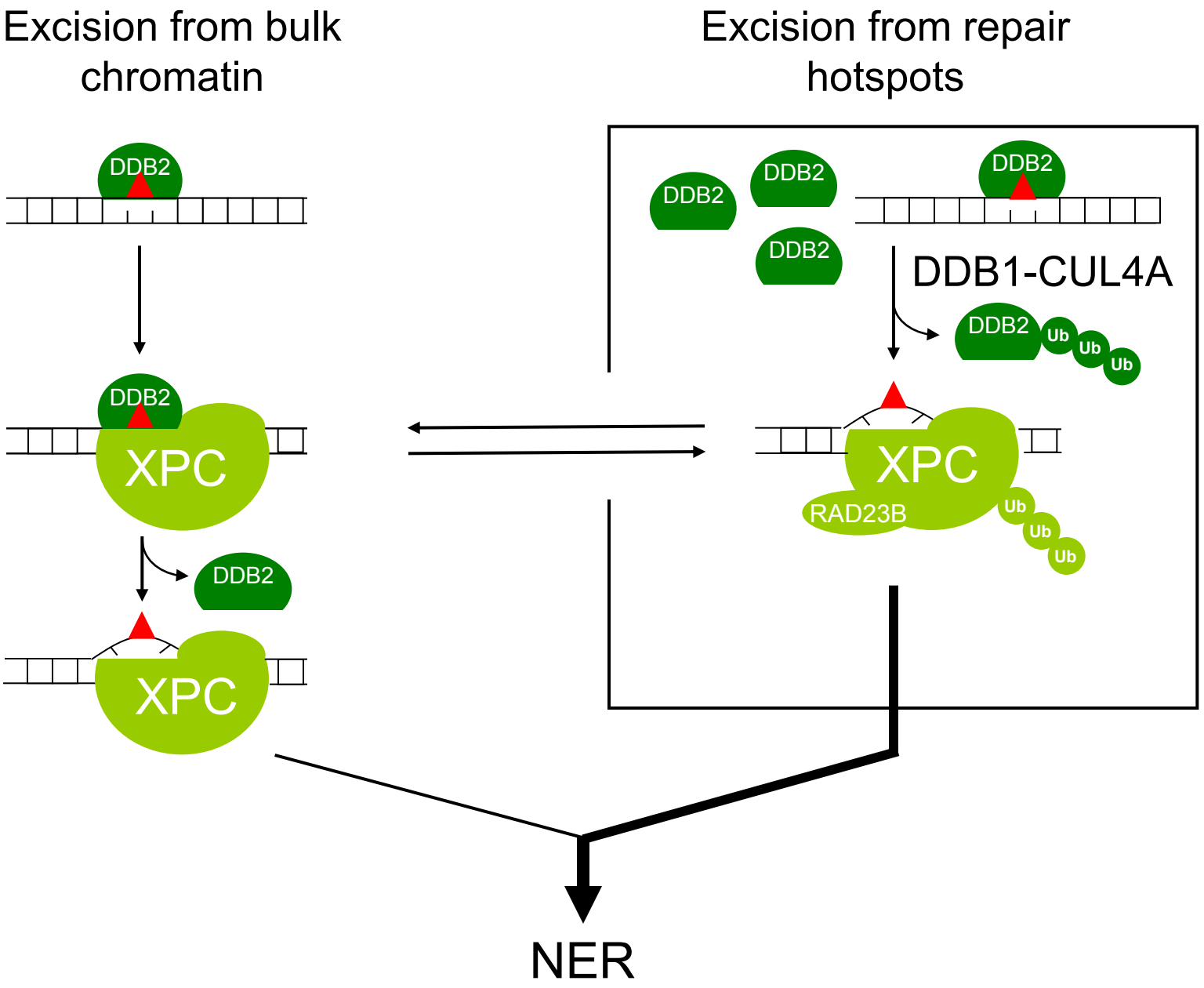
Excision from bulk chromatin
Excision from repair hotspots
DDB2
DDB2
DDB2
DDB2
DDB2
DDB1-CUL4A
DDB2
Ub
Ub
Ub
DDB2
XPC
XPC
RAD23B
Ub
Ub
Ub
DDB2
XPC
NER

Figure S7

6. Two-stage dynamic DNA quality check by xeroderma pigmentosum group C protein

(published in EMBO Journal)

The EMBO Journal (2009) 28, 2387–2399 | © 2009 European Molecular Biology Organization | All Rights Reserved 0261-4189/09
www.embojournal.org

THE EMBO JOURNAL

Two-stage dynamic DNA quality check by xeroderma pigmentosum group C protein

Ulrike Camenisch[1,4], Daniel Träutlein[2,4], Flurina C Clement[1], Jia Fei[1], Alfred Leitenstorfer[2], Elisa Ferrando-May[3] and Hanspeter Naegeli[1,*]

[1]Institute of Pharmacology and Toxicology, University of Zürich-Vetsuisse, Zürich, Switzerland, [2]Department of Physics and Center for Applied Photonics, University of Konstanz, Konstanz, Germany and [3]Bioimaging Center, University of Konstanz, Konstanz, Germany

Xeroderma pigmentosum group C (XPC) protein initiates the DNA excision repair of helix-distorting base lesions. To understand how this versatile subunit searches for aberrant sites within the vast background of normal genomic DNA, the real-time redistribution of fluorescent fusion constructs was monitored after high-resolution DNA damage induction. Bidirectional truncation analyses disclosed a surprisingly short recognition hotspot, comprising ~15% of human XPC, that includes two β-hairpin domains with a preference for non-hydrogen-bonded bases in double-stranded DNA. However, to detect damaged sites in living cells, these DNA-attractive domains depend on the partially DNA-repulsive action of an adjacent β-turn extension that promotes the mobility of XPC molecules searching for lesions. The key function of this dynamic interaction surface is shown by a site-directed charge inversion, which results in increased affinity for native DNA, retarded nuclear mobility and diminished repair efficiency. These studies reveal a two-stage discrimination process, whereby XPC protein first deploys a dynamic sensor interface to rapidly interrogate the double helix, thus forming a transient recognition intermediate before the final installation of a more static repair-initiating complex.

The EMBO Journal (2009) **28,** 2387–2399. doi:10.1038/emboj.2009.187; Published online 16 July 2009
Subject Categories: genome stability & dynamics
Keywords: DNA repair; genome stability; protein dynamics

Introduction

Nucleotide excision repair (NER) is a fundamental protective system that promotes genome stability by eliminating a wide range of DNA lesions (Gillet and Schärer, 2006). In addition to (6-4) photoproducts and cyclobutane pyrimidine dimers (CPDs) caused by ultraviolet (UV) light, the NER pathway removes DNA adducts generated by electrophilic chemicals as well as intrastrand DNA cross-links, DNA-protein cross-links and a subset of oxidative lesions (Huang *et al*, 1994; Kuraoka *et al*, 2000; Reardon and Sancar, 2006). The NER system operates through the cleavage of damaged strands on either side of injured sites, thus releasing defective bases as the component of oligomeric DNA fragments (Evans *et al*, 1997). Subsequently, the excised oligonucleotides are replaced by repair patch synthesis before DNA integrity is restored by ligation. Hereditary defects in this NER process cause devastating syndromes such as xeroderma pigmentosum (XP), a recessive disorder presenting with photosensitivity, a >1000-fold increased risk of skin cancer and, occasionally, internal tumours and neurological complications (Cleaver, 2005; Andressoo *et al*, 2006; Friedberg *et al*, 2006). XP patients are classified into seven repair-deficient complementation groups designated XP-A through XP-G (Cleaver *et al*, 1999; Lehmann, 2003).

In the NER pathway, the initial detection of DNA damage occurs by two alternative mechanisms. One subpathway, referred to as transcription-coupled repair, takes place when the transcription machinery is blocked by obstructing lesions in the transcribed strand (Hanawalt and Spivak, 2008). The second subpathway, known as global genome repair (GGR), is triggered by the binding of a versatile recognition complex, composed of XPC, Rad23B and centrin 2, to damaged DNA anywhere in the genome (Sugasawa *et al*, 1998; Nishi *et al*, 2005). XPC protein, which is the actual damage sensor of this initiator complex, displays a general preference for DNA substrates that contain helix-destabilizing lesions including (6-4) photoproducts (Batty *et al*, 2000; Sugasawa *et al*, 2001). In the particular case of CPDs, this recognition function depends on an auxiliary protein discovered by virtue of its characteristic UV-damaged DNA-binding (UV-DDB) activity (Nichols *et al*, 2000; Fitch *et al*, 2003). The affinity of this accessory factor for UV-irradiated substrates is conferred by a DNA-binding subunit (DDB2) mutated in XP-E cells (Scrima *et al*, 2008).

To achieve its outstanding substrate versatility, XPC protein interacts with an array of normal nucleic acid residues surrounding the lesion in a way that no direct contacts are made with the damaged bases themselves (Buterin *et al*, 2005; Trego and Turchi, 2006; Maillard *et al*, 2007). This exceptional binding strategy has been confirmed by structural analyses of Rad4 protein, a yeast orthologue that shares ~40% similarity with the human XPC sequence. In co-crystals, Rad4 protein associates with DNA through a large transglutaminase-homology domain (TGD) flanked by the three β-hairpin domains BHD1, BHD2 and BHD3 (Supplementary Figure 1; Min and Pavletich, 2007). In view of the position of these structural elements relative to the accompanying model substrate, a recognition mechanism has been proposed in which BHD3 would 'sample the DNA's conformational space to detect a lesion' (Min and Pavletich, 2007).

These earlier studies describing the features of an ultimately stable XPC/Rad4–DNA complex explain its ability

*Corresponding author. Institute of Pharmacology and Toxicology, University of Zurich-Vetsuisse, Winterthurerstrasse 260, Zurich 8057, Switzerland. Tel.: +41 44 635 87 63; Fax: +41 44 635 89 10; E-mail: naegelih@vetpharm.uzh.ch
[4]These authors contributed equally to this work

Received: 3 February 2009; accepted: 17 June 2009; published online: 16 July 2009

to serve as a molecular platform for the recruitment of transcription factor IIH (TFIIH) or other downstream NER players (Yokoi *et al*, 2000; Uchida *et al*, 2002). However, one of the most challenging issues in the DNA repair field is the question of how a versatile sensor-like XPC/Rad4 examines the Watson–Crick double helix and faces the task of actually finding base lesions among a large excess of native DNA in a typical mammalian genome (Schärer, 2007; Sugasawa and Hanaoka, 2007). To address this long-standing question, we exploited fluorescence-based imaging techniques (Houtsmuller *et al*, 1999; Houtsmuller and Vermeulen, 2001; Politi *et al*, 2005) to visualize the mobility of XPC protein at work in the chromatin context of living cells. Our results point to a two-stage discrimination process, in which the rapid DNA quality check driven by a dynamic sensor of non-hydrogen-bonded bases precedes the final engagement of BHD3 with lesion sites.

Results

Instantaneous recognition of DNA lesions in human cells

Damage-induced changes of molecular dynamics in the nuclear compartment have been followed by C-terminal conjugation of the human XPC polypeptide with green-fluorescent protein (GFP). The time-dependent relocation of this fusion product was tested by transfection of repair-deficient XP-C fibroblasts that lack functional *XPC* because of a mutation leading to premature termination at codon 718 (Chavanne *et al*, 2000). Individual nuclei containing low levels of XPC-GFP (similar to the XPC expression in wild-type fibroblasts) were identified on the basis of their overall fluorescence (Supplementary Figure 2). To induce lesions, the nuclei were subjected to near-infrared irradiation using a pulsed multiphoton laser, thereby generating spatially confined and clearly detectable patterns of DNA damage with minimal collateral effects (Meldrum *et al*, 2003). The resulting laser tracks contained (6-4) photoproducts (Figure 1A) and CPDs (Figure 1B), representing the major UV lesions processed by the NER system. As expected, wild-type XPC-GFP was rapidly concentrated at nuclear sites containing such photolesions (Figure 1A and B). As earlier studies showed that the UV-induced accumulation of XPC is stimulated by DDB2 protein (Fitch *et al*, 2003; Moser *et al*, 2005), we applied the same procedure to XP-E cells, in which an R273H mutation generates a DDB2 product that is inactive in DNA binding and fails to be expressed to detectable levels (Nichols *et al*, 2000; Itoh *et al*, 2001). In this XP-E background, XPC-GFP is nevertheless effectively relocated to UV-irradiated tracks (Figure 1C), consistent with the known ability of XPC protein to detect (6-4) photoproducts in the absence of UV-DDB activity (Batty *et al*, 2000; Kusumoto *et al*, 2001).

To determine the kinetics of protein redistribution, DNA photoproducts were formed along a single 10-μm line crossing the nucleus of XP-C cells. Maximal accumulation of XPC protein was detected after treatment with a near-infrared radiation of 300–360 $GW \cdot cm^{-2}$ (Supplementary Figure 3). Subsequently, DNA damage was induced with 314 $GW\,cm^{-2}$ to generate ~5000 UV lesions in each cell or, on the average, 1 UV lesion in $\sim 1.6 \times 10^6$ base pairs (see Materials and methods). Under these conditions, the local fluorescence in irradiated areas increased nearly instantaneously leading to a clearly distinguishable relocation of XPC fusion protein already 3 s after irradiation (Supplementary Movie 1). With progressive accumulation of wild-type XPC, a half-maximal increase in local fluorescence intensity was reached after ~40 s (Figure 1D). A plateau level of fluorescence in the irradiation tracks, reflecting a steady-state situation with constant turnover, was detected after ~300 s.

Concordance of relocation and DNA-binding activity

Besides the truncating *XPC* mutation, the XP-C fibroblasts used in this study (GM16093) are characterized by a

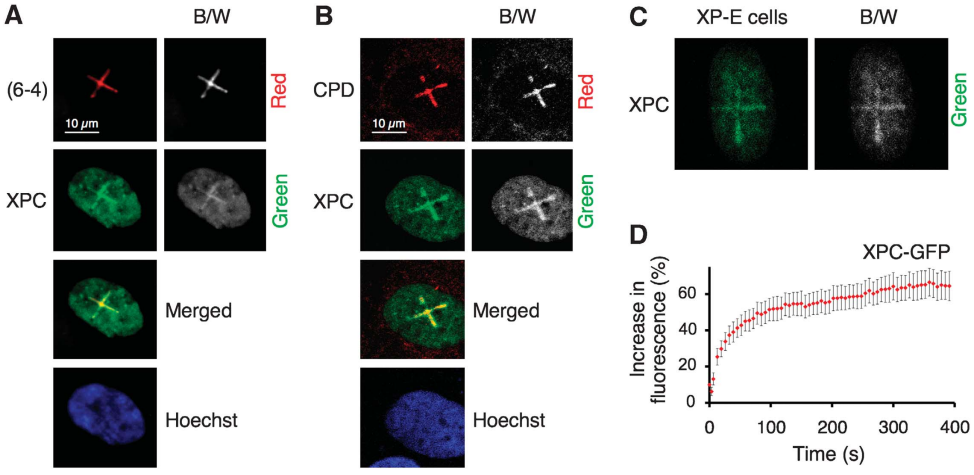

Figure 1 Instantaneous recognition of DNA damage by XPC protein in living cells. (**A**) High-resolution patterns of DNA damage and XPC-GFP accumulation. XP-C fibroblasts expressing low levels of XPC-GFP were laser treated to generate ~5000 UV lesions along each linear irradiation track. The cells were fixed after 6 min and (6-4) photoproducts were detected by immunochemical staining using the red dye Alexa 546. B/W, black-and-white images illustrating the pattern of UV lesions (*upper panel*) and the accumulation of XPC-GFP (*lower panel*). Merged, superimposed images in which the relocation of XPC-GFP matches the pattern of DNA damage. Hoechst, DNA staining visualizing the nuclei. (**B**) Co-localization of XPC-GFP and CPDs. (**C**) Efficient relocation of XPC-GFP to UV irradiation tracks in XP-E cells devoid of UV-DDB activity. (**D**) Real-time kinetics of DNA damage recognition. A single 10-μm line of UV photoproducts was generated across each nucleus of XP-C cells. The accumulation of XPC-GFP at different time points is plotted as a percentage of the average fluorescence before irradiation ($n = 7$). Error bars, standard errors of the mean.

comparably low level of DDB2 protein (Supplementary Figure 4). This reduced DDB2 expression suggested that the GM16093 fibroblasts may provide a cellular context in which, in contrast to an earlier report (Yasuda *et al*, 2007), the damage recognition defect of XPC mutants becomes evident without preceding DDB2 down-regulation. This view was confirmed by testing the nuclear dynamics of a repair-deficient W690S mutant with minimal DNA-binding affinity (Bunick *et al*, 2006; Maillard *et al*, 2007; Hoogstraten *et al*, 2008). In conjunction with the GFP fusion partner, this pathogenic mutant is expressed in similar amounts as the wild-type control and also localizes to the nuclei. However, in the XP-C fibroblasts of this study, the single W690S mutation causes >five-fold reduction in the relocation to UV-damaged areas (Figure 2A; Supplementary Movie 2). These findings were confirmed when another technique was used to inflict genotoxic stress, that is by UV-C irradiation (254 nm wavelength) through the pores of polycarbonate filters (Moné *et al*, 2004). In fact, compared with wild-type XPC, the W690S mutant exhibits only a marginal tendency to accumulate in UV-C radiation-induced foci (data not shown). Oligonucleotide-binding assays with XPC protein expressed in insect cells confirmed that this W690S mutation and the corresponding alanine substitution (W690A) abrogate the interaction with DNA (Figure 2B).

The same analysis was extended to further repair-deficient XPC mutants targeting conserved aromatic residues (Maillard *et al*, 2007). A nearly complete loss of DNA binding is conferred by the F733A mutation, whereas the W531A and W542A substitutions are associated with more moderate defects (Figure 2B). When tested in GM16093 fibroblasts as GFP fusions, the damage-dependent redistribution of these different mutants correlates closely with the respective DNA-binding properties. In fact, the W690S, W690A and F733A derivatives display a poor ability to concentrate at damaged sites. In contrast, the residual DNA-binding activity of W531A and W542A leads to an intermediary level of accumulation in areas containing UV photoproducts (Figure 2C). From this tight correspondence between DNA binding and nuclear redistribution, we concluded that the rapid relocation of XPC protein to UV lesion sites reflects the intrinsic capacity of this sensor subunit to detect DNA damage through direct interactions with the nucleic acid substrate.

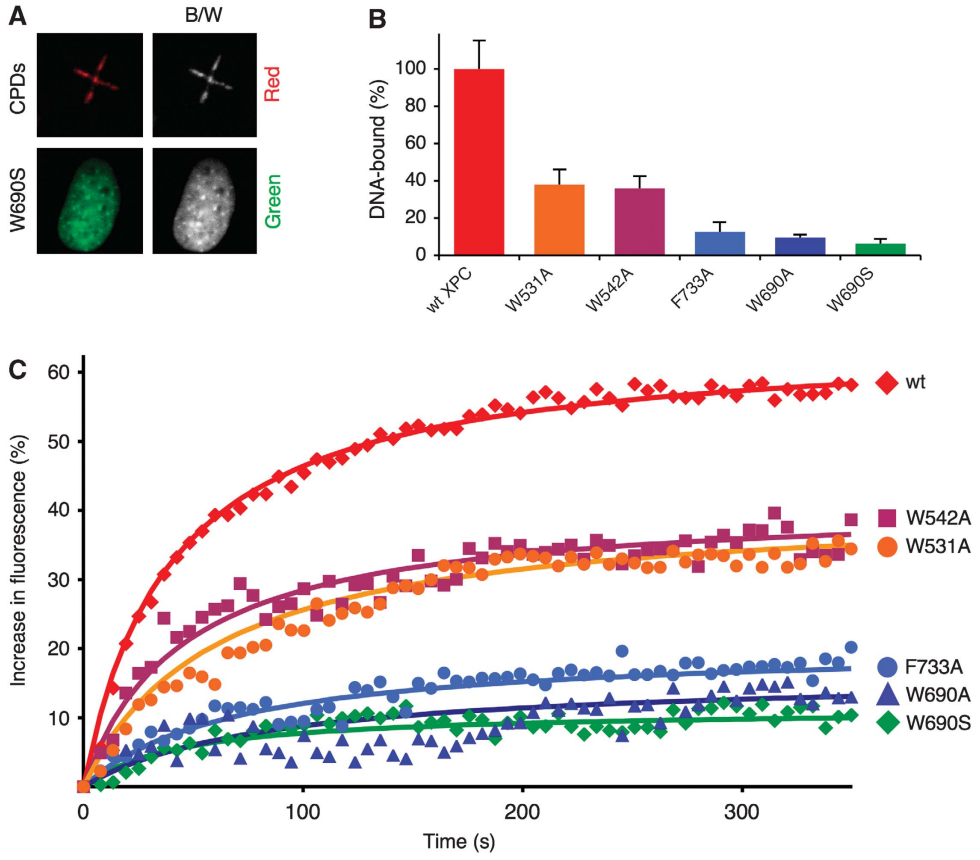

Figure 2 Dependence on intrinsic DNA-binding activity. (**A**) Representative image (in colour and black-and-white) showing the low residual accumulation of the W690S mutant 6 min after irradiation. DNA lesions were counterstained by antibodies against CPDs. (**B**) DNA-binding activity determined by direct pull down. Wild-type (wt) XPC or mutants were expressed in *Sf*9 cells as fusion constructs with maltose-binding protein (MBP). Cell lysates containing similar amounts of XPC protein (Maillard *et al*, 2007) were incubated with a single-stranded 135-mer oligonucleotide. Subsequently, radiolabelled DNA molecules captured by XPC protein were separated from the free probes using anti-MBP antibodies linked to magnetic beads, and the radioactivity in each fraction was quantified in a scintillation counter. DNA binding is represented as the percentage of radioactivity immobilized by wt XPC protein after deduction of a background value determined with empty beads ($n=3$). Error bars, standard deviation. (**C**) Correlation between DNA binding and the kinetics of XPC accumulation in XP-C cells ($n=7$). See legend to Figure 1D for details.

Role of the transglutaminase-like domain

As the transglutaminase-like region maps to the N-terminal part of human XPC (Figure 3A), we generated N-terminal truncations ($XPC_{118-940}$, $XPC_{427-940}$ and $XPC_{607-940}$) to test how the TGD sequences contribute to DNA damage recognition in living cells. The positions 118 and 607 were selected for these truncations to allow for comparisons with an earlier *in vitro* study monitoring the DNA-, Rad23B- and TFIIH-binding activity of XPC fragments (Uchida *et al*, 2002). Another truncate (XPC_{1-495}) was included as a negative control that lacks the entire C-terminal half. The functionality of these constructs, conjugated to GFP at their C-terminus, was compared in a host-cell reactivation assay that has been developed to measure the cellular GGR activity (Carreau *et al*, 1995). Briefly, XP-C fibroblasts were transfected with a dual luciferase reporter system along with an expression vector coding for full-length or truncated XPC fusions. The reporter plasmid, which carries a *Photinus* luciferase gene, was damaged by exposure to UV-C light and supplemented with an undamaged vector that expresses the *Renilla* luciferase. GGR efficiency was assessed after 18-h incubations by determining *Photinus* luciferase activity in cell lysates, followed by normalization against the *Renilla* control.

The full-length protein (XPC_{1-940}) and an $XPC_{118-940}$ derivative, isolated by functional complementation (Legerski and Peterson, 1992), were proficient in correcting the repair defect of XP-C cells (Figure 3B), thus showing that gene reactivation is determined by the ability of the GGR pathway to excise offending UV lesions. However, this repair activity could not be rescued by $XPC_{427-940}$ and $XPC_{607-940}$ (Figure 3B), implying that the N-terminal part of XPC protein is essential for the GGR reaction. All tested fragments were detected in transfected fibroblasts in similar amounts as the full-length control or the functional $XPC_{118-940}$ derivative

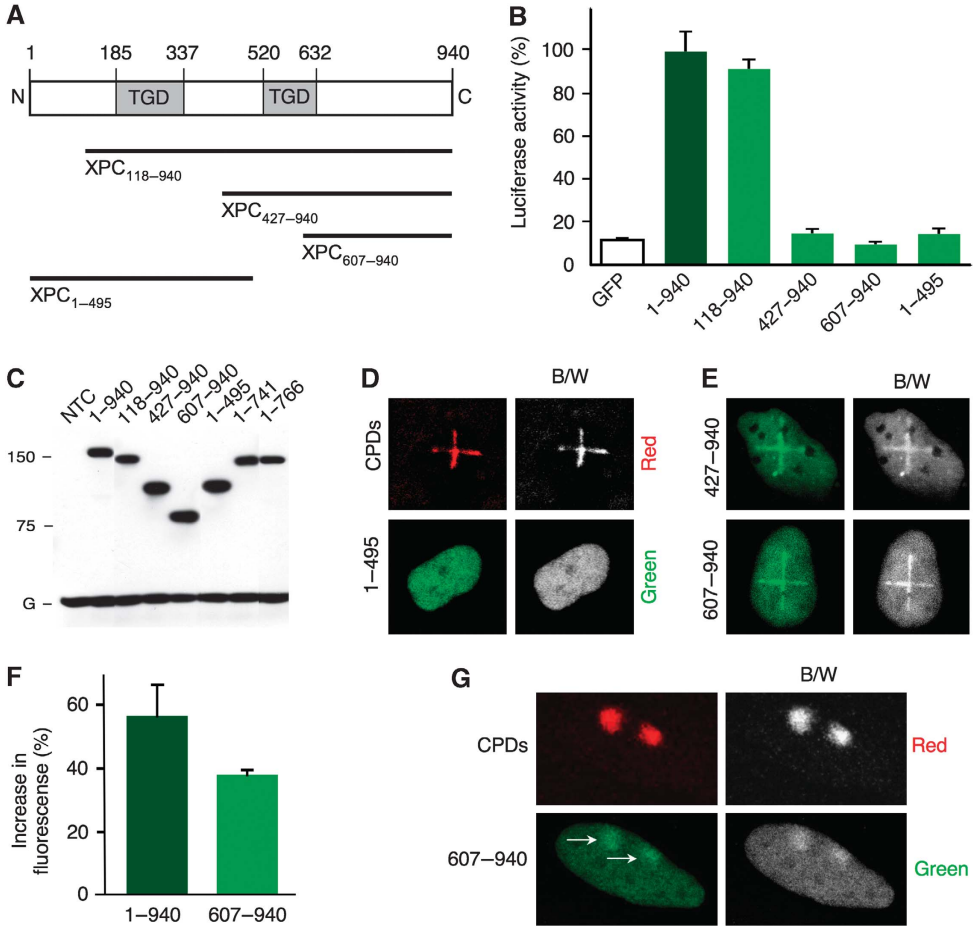

Figure 3 Mapping of the damage sensor domain to the C-terminal part of human XPC. (**A**) Scheme illustrating the position of the TGD sequences relative to the N-terminal XPC truncates. (**B**) GGR activity determined by host-cell reactivation assay ($n = 5$; error bars, standard deviation). (**C**) Immunoblot analysis of XP-C cells transfected with expression vectors coding for the indicated fusions. The protein level was probed using anti-GFP antibodies. G, endogenous GAPDH control. (**D**) Representative image showing that an XPC fragment lacking the C-terminus (XPC_{1-495}) fails to accumulate in laser-damaged areas. The XP-C fibroblasts were fixed 6 min after irradiation. B/W, black-and-white images showing that the tracks of DNA damage (*upper panel*) do not induce an accumulation of truncated XPC fusions (*lower panels*). (**E**) Representative images (in colour and black and white) showing that $XPC_{427-940}$ and $XPC_{607-940}$ accumulate in damaged areas of XP-C fibroblasts. The distribution of fluorescent fusion products was monitored 6 min after irradiation. (**F**) Local increase of fluorescence resulting from the damage-induced redistribution of full-length XPC or $XPC_{607-940}$. A 10-μm line of UV photoproducts was generated across each nucleus and the resulting accumulation of fusion proteins (after a 6-min incubation) is plotted as a percentage of the average fluorescence before irradiation ($n = 7$). Error bars, standard errors of the means. (**G**) Representative image illustrating that $XPC_{607-940}$ accumulates in foci generated by UV-C irradiation (100 J m^{-2}) through the pores of polycarbonate filters. The XP-C cells were fixed 15 min after treatment and CPDs were detected by immunochemical staining. The position of $XPC_{607-940}$ foci is indicated by the arrows.

(Figure 3C), indicating that their repair deficiency does not result from reduced expression or enhanced degradation.

Next, all GGR-deficient truncates were tested for their damage recognition proficiency in XP-C fibroblasts. Neither XPC_{1-495} (Figure 3D) nor XPC_{1-718} (Supplementary Figure 4) were redistributed to sites of photoproduct formation in the irradiated nuclei of living cells, confirming that the C-terminal half of XPC protein is necessary for lesion recognition. However, unlike these C-terminal truncations, fragment $XPC_{427-940}$ retains the ability to concentrate in laser-irradiated areas (Figure 3E). Even more surprising was the observation that the smaller fragment $XPC_{607-940}$ readily accumulates at sites containing UV photolesions (Figure 3E). The quantification of defined 10-μm tracks showed that $XPC_{607-940}$ is only ~30% less efficient than full-length XPC in relocating to damaged sites (Figure 3F). Thus, a large N-terminal part of human XPC (65% of the full-length protein including its TGD regions) stimulates DNA damage recognition, but is not absolutely required for the sensing process itself. This conclusion is confirmed by the accumulation of $XPC_{607-940}$ in UV-C foci generated by irradiation through the pores of polycarbonate filters (Figure 3G).

Differential contribution of β-hairpin domains

According to the Rad4 crystal, three consecutive β-hairpin domains (BHD1, BHD2 and BHD3) mediate the interaction with damaged DNA (see Supplementary Figure 1). In the homologous XPC sequence, these structural elements range from residue 637 (start of BHD1) to residue 831 (end of BHD3). To examine how each of these domains contributes to DNA damage recognition in living cells, we generated the C-terminal truncations XPC_{1-741} (comprising BHD1 and BHD2) and XPC_{1-831}, which includes all three BHDs (Figure 4A). Again, the truncation position 741 was chosen to allow for comparisons with an earlier *in vitro* study (Uchida *et al*, 2002). The constructs were conjugated to GFP at their C-terminus and tested for their ability to initiate the GGR reaction. In the case of XPC_{1-741}, the repair function is reduced to a background level observed with empty GFP vector (Figure 4B). However, the reporter gene was reactivated to ~40% of control in the presence of XPC_{1-831}, indicating that despite its C-terminal truncation, this large fragment retains in part the ability to recruit NER factors to lesion sites. Although attempting to delineate the borders of a minimal sensor domain, we surprisingly found that essentially the same GGR activity was induced by XPC_{1-766}, that is by adding only 25 amino acids to XPC_{1-741} (Figure 4B). A comparison with the Rad4 orthologue indicates that these 25 amino acids (residues 742–766) belong to an N-terminal extension of BHD3, which folds into a β-turn structure (see Figure 4A).

The UV-induced relocation of truncated XPC derivatives was tested in XP-C fibroblasts expressing similar low levels of each GFP construct (Supplementary Figure 5). Consistent with its distinctive functionality in the GGR assay, we observed that XPC_{1-766} accumulates more effectively than XPC_{1-741} to the 10-μm tracks of photolesions generated by laser irradiation (Figure 4C). An unequivocal pattern of XPC_{1-766} accumulation along the radiation tracks was also recorded in XP-E fibroblasts, that is in the absence of UV-DDB activity (Figure 4D). A quantitative comparison in both XP-C and XP-E cells highlights the increase in damage recognition when the truncation was introduced at residue 766 as compared with the truncation at position 741 (Figure 4E), thus showing that the damage-specific accumulation of XPC truncates as well as the effect of the β-turn structure takes place in the absence of DDB2 protein. A clear difference between XPC_{1-766} and XPC_{1-741} was reproduced when foci of fluorescence were monitored after UV-C irradiation through the pores of polycarbonate filters (Figure 4F). Taken together, this efficient redistribution of XPC_{1-766}, irrespective of the cell type or technique used to inflict DNA damage, establishes for the first time that most of BHD3 is not required for the initial damage-sensing process.

The β-turn structure enhances XPC dynamics

The GGR and relocation assays of Figure 4 revealed a striking difference between XPC_{1-741} and XPC_{1-766} because of the 25-amino-acid β-turn extension. To analyse the function of this β-turn structure, we compared the nuclear mobility of different truncates using fluorescence recovery after photobleaching (FRAP; Houtsmuller and Vermeulen, 2001). In cells that express similarly low levels of GFP fusion constructs, a nuclear area of $4\,\mu m^2$ was bleached and, subsequently, protein movements were tested by recording the recovery of local fluorescence, which is dependent on the ability of the GFP fusions to move rapidly within the nuclear compartment.

The control experiment of Figure 5A shows how, in the absence of a fusion partner, the GFP moiety moves freely inside the cells. Instead, the nuclear mobility of full-length XPC-GFP is restrained by its larger size and propensity to undergo macromolecular interactions, as reported earlier (Hoogstraten *et al*, 2008). Surprisingly, in a direct comparison between XPC_{1-741}, XPC_{1-766} and XPC_{1-831}, a larger size correlated with increased nuclear mobility (Figure 5B). The FRAP curves obtained with these different truncates were used to calculate effective diffusion coefficients (D_{eff}; Supplementary Table I). It was unexpected to find that, in undamaged cells, XPC_{1-766} (containing BHD1, BHD2 and the β-turn structure) and XPC_{1-831} (containing all three BHDs) move more rapidly inside the nucleus ($D_{eff} = 0.44$ and $0.49\,\mu m^2\,s^{-1}$, respectively) than the shorter polypeptide XPC_{1-741} lacking the β-turn ($D_{eff} = 0.34\,\mu m^2\,s^{-1}$). We concluded that these C-terminal truncations disclose the existence of a dynamic interface, residing within the β-turn structure, which enhances the constitutive nuclear mobility of XPC protein in the absence of genotoxic stress.

Subsequently, the FRAP approach was used to assess the corresponding responses to UV-C irradiation. In accord with its poor accumulation along DNA damage tracks (Figure 4C), the mobility of XPC_{1-741} is only marginally affected by the induction of photolesions (Figure 5C). In contrast, the diffusion rates of XPC_{1-766} (Figure 5D) and XPC_{1-831} (Figure 5E), which accumulate in UV lesion tracks, are significantly reduced (the respective D_{eff} values are listed in Supplementary Table I). In the case of XPC_{1-831}, the induction of DNA damage had a two-fold effect. First, UV lesions decreased the initial rate of protein diffusion exactly as observed with XPC_{1-766}. Second, similar to the response of full-length XPC (Hoogstraten *et al*, 2008), the overall fluorescence recovery is less complete on UV irradiation (Figure 5E), indicating that a fraction of XPC_{1-831} is immobilized in a damage-specific manner. In summary, these

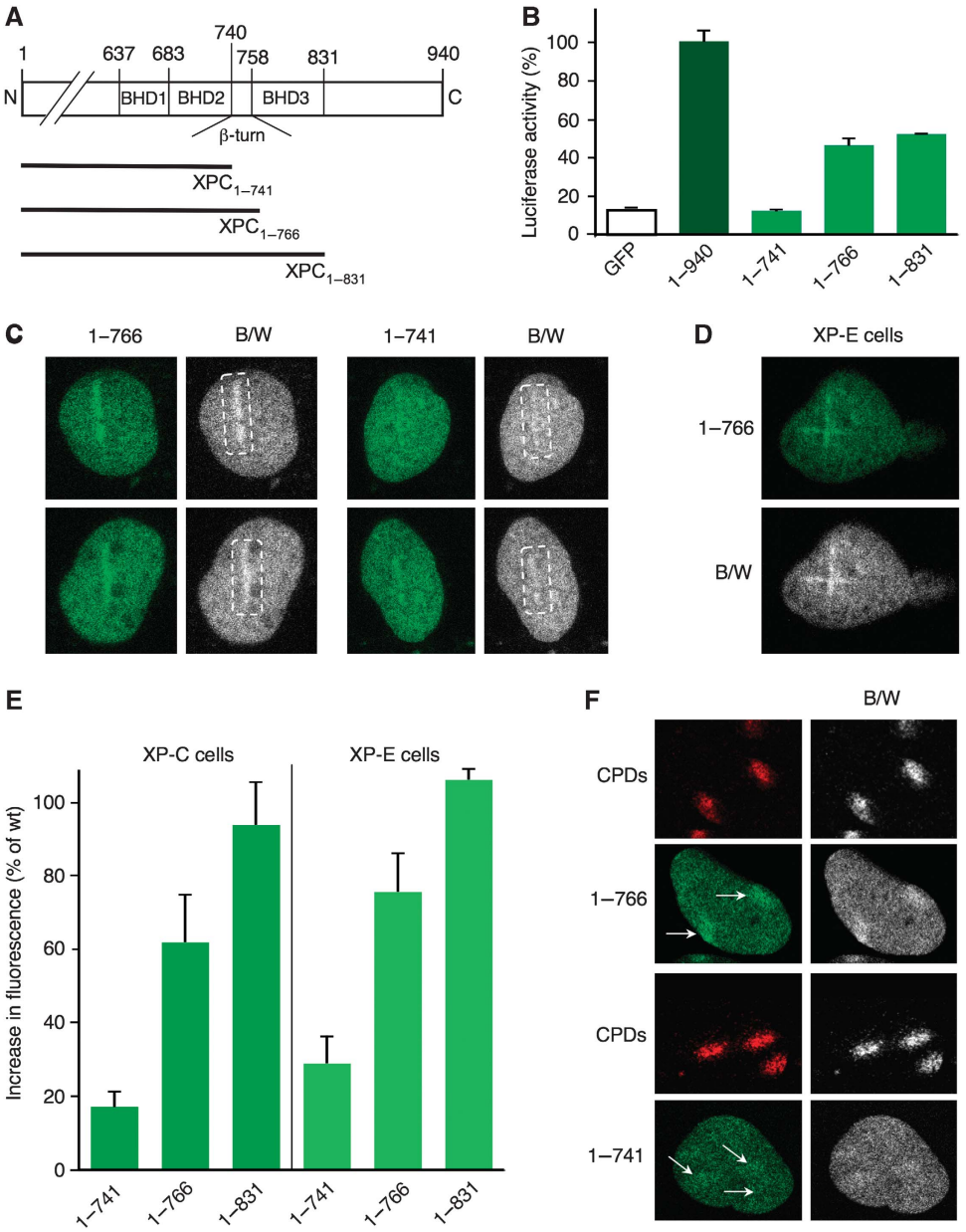

Figure 4 BHD3 is not required for DNA damage detection. (**A**) Scheme illustrating the location of BHD and β-turn sequences relative to the C-terminal XPC truncates of this study. (**B**) GGR activity determined by host-cell reactivation assay in XP-C fibroblasts ($n = 5$; error bars, standard deviation). (**C**) Representative images (taken 6 min after irradiation) comparing the accumulation of XPC_{1-766} and XPC_{1-741} at damaged sites. In the black-and-white representation, the linear irradiation tracks are surrounded by a dashed rectangle. (**D**) Representative image illustrating the accumulation of XPC_{1-766} along UV radiation tracks generated in XP-E fibroblasts devoid of UV-DDB activity. (**E**) The local increase in fluorescence, because of damage-induced redistributions of XPC truncates, was measured in XP-C and XP-E cells and plotted as the percentages of wt control as outlined in Figure 1D ($n = 5$; error bars, standard errors of the mean). (**F**) XPC_{1-766} is also more efficient than XPC_{1-741} in accumulating in DNA damage foci generated by UV-C irradiation through the pores of polycarbonate filters (see Figure 3G for details). XPC_{1-766} (*top*) and XPC_{1-741} foci (*bottom*) are indicated by the arrows.

protein mobility studies show that BHD3 induces the formation of a stable nucleoprotein complex once the lesion has been detected.

Antagonistic composition of the dynamic sensor domain

The truncation studies of Figures 4 and 5 suggested that residues 607–766 may be sufficient to find lesion sites in the genome. This hypothesis was confirmed by expressing short protein fragments in XP-C fibroblasts (Figure 6A). In the case of $XPC_{607-766}$ (consisting of BHD1/BHD2 and the β-turn structure), a clear pattern of damage-induced accumulation was detected immediately after laser irradiation (Figure 6B). In contrast, $XPC_{607-741}$ (lacking the β-turn) failed to accumulate in the tracks of UV lesions. $XPC_{607-741}$ was unable to relocate to damaged areas regardless of whether the GFP moiety was placed at the C- (Figure 6C) or at the N-terminus (data not shown). These results support the conclusion that $XPC_{607-766}$ displays a minimal sensor surface with damage recognition activity in living human cells.

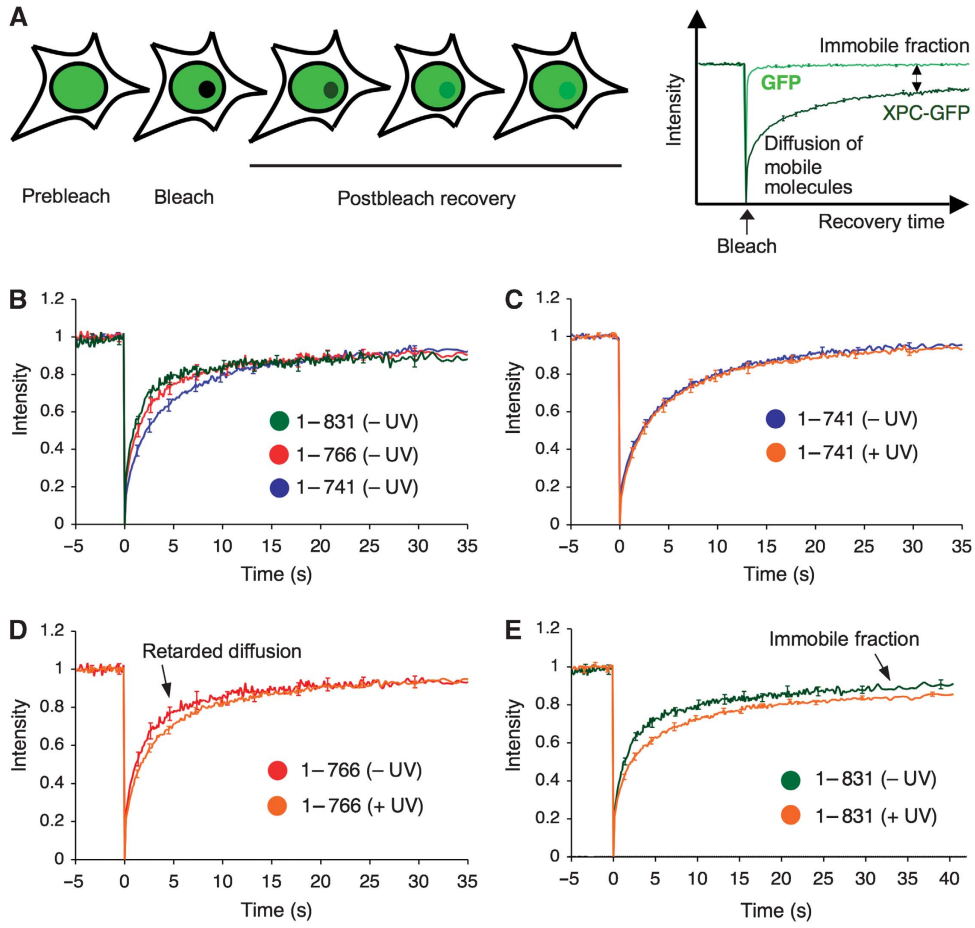

Figure 5 Identification of a dynamic core and two-stage damage recognition. (**A**) Principle of FRAP analysis. An area of 4 μm^2 in the nuclei of XP-C fibroblasts expressing a particular GFP construct is bleached with a 488-nm wavelength laser. The kinetics and extent of fluorescence recovery (shown for GFP and XPC-GFP) depends on diffusion rate, molecular interactions as well as the fraction of immobile molecules. (**B**) Recovery plots of XPC truncates normalized to prebleach intensity ($n = 12$). Error bars, standard errors of the mean. The difference between XPC_{1-766} and XPC_{1-831} is not significant. (**C**) The nuclear mobility of XPC_{1-741} remains unaffected by UV-C irradiation at a dose of 10 J m^{-2} ($n = 12$). (**D**) The initial diffusion of XPC_{1-766} is reduced by UV light (10 J m^{-2}, $n = 12$), reflecting transient molecular interactions during stage 1 of the damage recognition process. (**E**) A fraction of XPC_{1-831} is stably immobilized after UV irradiation (10 J cm^{-2}, $n = 12$), reflecting stage 2 of the damage recognition process.

The fragments $XPC_{607-741}$, $XPC_{607-766}$ and $XPC_{607-831}$ have been isolated to assess their DNA-binding properties using 135-mer DNA substrates. All three fragments were expressed and purified as soluble polypeptides without any signs of aggregation or precipitation that would be indicative of defective protein folding (Figure 6D). We compared their binding with three different DNA conformations: homoduplexes, heteroduplexes with three contiguous base mismatches or single-stranded oligonucleotides of the same length. Although $XPC_{607-741}$ (containing BHD1 and BHD2) is unable to find DNA lesions in living cells, this fragment displays a preference for unpaired bases embedded in double-stranded DNA. In fact, $XPC_{607-741}$ binds with higher affinity to heteroduplex DNA relative to homoduplexes or single-stranded oligonucleotides (Figure 6E).

A similar preference for hetero- over homoduplexes is retained by $XPC_{607-766}$, which includes both BHD1/BHD2 and the β-turn structure (Figure 6F), thus supporting the notion that this minimal sensor is active in living cells by searching for destabilized base pairs. A side-by-side comparison of dose-dependent DNA-binding activities with $XPC_{607-741}$ and $XPC_{607-766}$ showed that the β-turn structure leads to a substantial reduction in nucleic acid binding (Figure 6F). In particular, we found that the association constant representing the interaction with homoduplex DNA decreases nearly 10-fold from $2.7 \times 10^9\,M^{-1}$ for $XPC_{607-741}$ to $2.8 \times 10^8\,M^{-1}$ for $XPC_{607-766}$. This drop in binding to the native double helix implies that the enhanced nuclear mobility conferred by amino acids 742–766 (Figure 5B) results from an antagonistic DNA-repulsive effect.

Finally, to test the contribution of BHD3, the same 135-mer substrates were used to monitor the DNA-binding properties of a longer fragment ($XPC_{607-831}$) comprising all three BHDs. Figure 6G shows that this larger fragment has the characteristics of a single-stranded DNA-binding protein, indicating that BHD3 itself confers a pronounced selectivity for single-stranded conformations. The characteristic DNA-binding profile of this larger fragment $XPC_{607-831}$ corresponds roughly to that detected when identical reactions were carried out with full-length XPC protein (Supplementary Figure 6).

Design of an XPC mutant with retarded nuclear mobility

We postulated that part of the DNA-repulsive action mediated by the β-turn structure (Figure 6F) arises from negatively charged side chains that clash with the phosphates of the nucleic acid backbone. This hypothesis predicts that it should

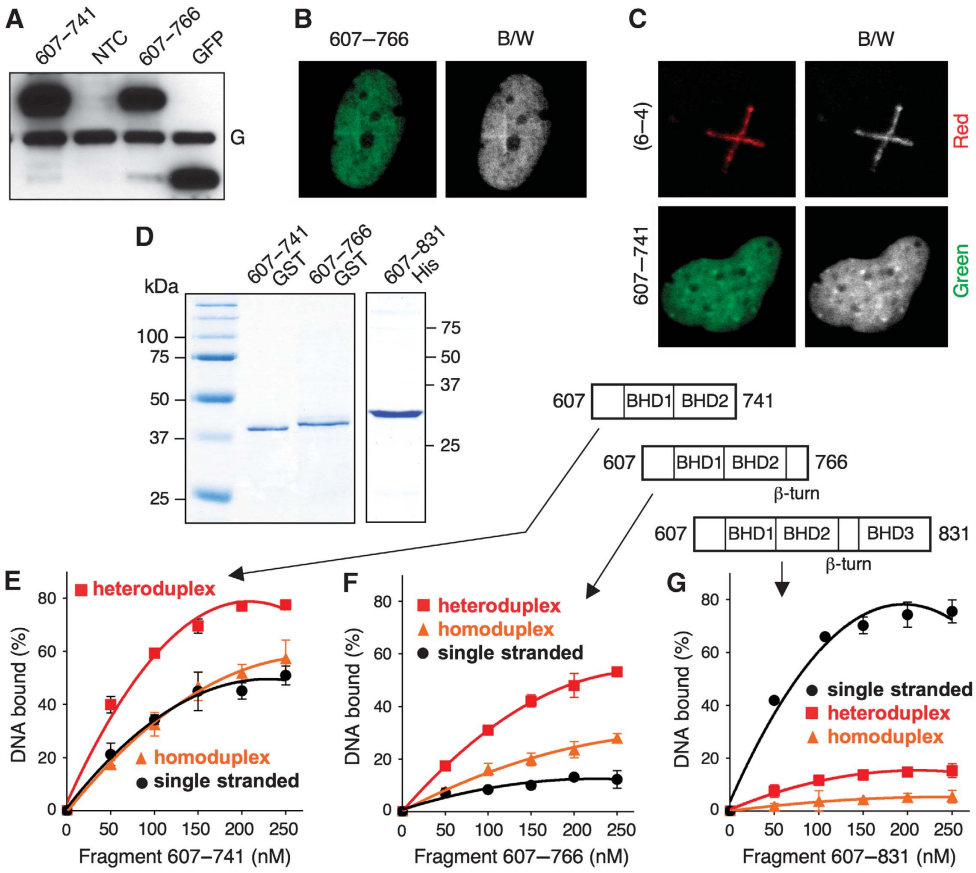

Figure 6 Antagonistic composition of the minimal damage sensor. (**A**) Immunoblot analysis of XP-C fibroblasts after transfection with vectors coding for the indicated XPC-GFP sequences. The expression was probed using anti-GFP antibodies. NTC, non-transfected cells; GFP, cells transfected with the GFP sequence alone; G, GAPDH control. (**B**) Representative image illustrating that fragment $XPC_{607-766}$ readily accumulates in damaged areas containing DNA photolesions. The distribution of fluorescent fusion products was monitored 1 min after laser irradiation. B/W, black-and-white image. (**C**) $XPC_{607-741}$ is unable to recognize UV lesions in living cells. Fibroblasts were subjected to fixation 1 min after irradiation and (6-4) photoproducts were detected by immunochemical staining. B/W, black-and-white images showing that UV lesions (*upper panel*) did not lead to accumulation of the fusion protein (*lower panel*). (**D**) Gel electrophoretic analysis of purified XPC fragments expressed as glutathione-*S*-transferase (GST) fusions in *E. coli* or with a histidine (His) tag in *Sf*9 cells. (**E**) DNA binding of $XPC_{607-741}$ determined by oligonucleotide capture. The indicated concentrations of XPC-GST fragments were incubated with radiolabelled 135-mer oligonucleotides (3-mismatch heteroduplexes, homoduplexes and single strands). Thereafter, DNA molecules immobilized by XPC fragments were separated from the free oligonucleotides using glutathione-Sepharose beads, followed by the quantification of radioactivity associated with the beads. DNA binding is represented as the percentage of total input radioactivity captured by XPC fragments after deduction of a background value determined with empty beads ($n = 6$; error bars, standard deviation). (**F**) DNA-binding profile of the minimal damage sensor ($XPC_{607-766}$) determined as described in the legend to Figure 6E. (**G**) Contribution of BHD3. The DNA-binding profile of $XPC_{607-831}$ was determined as outlined in the legend to Figure 6E, except that pull downs were performed with Ni-NTA agarose beads.

be possible to mitigate this DNA-repellent effect by replacing negatively charged amino acids with positively charged analogues. We identified a glutamate moiety at position 755 of the human β-turn motif that is conserved among higher eukaryotes (Figure 7A) and inverted the charge of this particular side chain by substitution with lysine.

The consequence of this engineered charge inversion was first tested by comparing the interaction with native double-stranded DNA in biochemical assays. For that purpose, the lysine substitution was introduced into $XPC_{607-766}$, thus generating a mutated fragment of 160 amino acids ($E755K_{607-766}$) that, similar to its wild-type counterpart ($XPC_{607-766}$), is amenable to expression and purification as a soluble polypeptide. DNA homoduplexes of 135 base pairs were used to determine the DNA-binding capacity of this mutated fragment in relation to the wild-type control. As illustrated in the comparison of Figure 7B, the E755K mutation was able to partially reverse the drop in DNA binding resulting from the presence of the β-turn structure in $XPC_{607-766}$. Binding saturation studies with homoduplex DNA indicates that the association constant increased from $2.8 \times 10^8\,M^{-1}$ for $XPC_{607-766}$ containing the wild-type sequence (determined in the earlier section) to $7.4 \times 10^8\,M^{-1}$ for the $E755K_{607-766}$ derivative, which carries the single charge inversion.

These findings led us to generate a mutant GFP fusion construct to confirm that the effect of the β-turn structure in enhancing the XPC dynamics, observed with truncated derivatives (Figure 5B), is retained in the full-length protein context. Unlike other repair-defective XPC mutants (W531A, W542A, W690A, W690S and F733A), all of which display a higher nuclear mobility than the wild-type control (Hoogstraten *et al*, 2008 and data not shown), the novel E755K mutant is characterized by a strikingly reduced nuclear mobility (Figure 7C) accompanied by a significant GGR defect (Figure 7D). Collectively, these effects induced by a

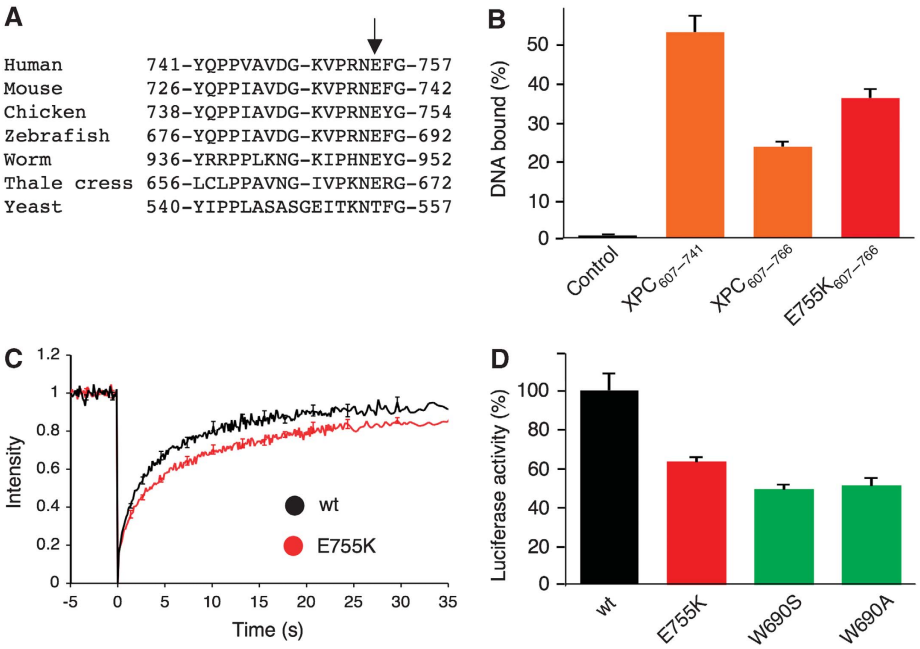

Figure 7 Analysis of the dynamic interface by site-directed mutagenesis. (**A**) Identification of a conserved glutamate (*arrow*) in the β-turn motif of higher eukaryotes. This residue is not conserved in the Rad4 sequence, suggesting that the yeast orthologue may have different dynamic properties. (**B**) A single E755K mutation reduces the DNA-repellent effect of the β-turn structure. The association of $XPC_{607-741}$, $XPC_{607-766}$ and $E755K_{607-766}$ with homoduplex DNA was compared at a polypeptide concentration of 150 nM, as outlined in the legend to Figure 6E. DNA binding is represented as the percentage of total input radioactivity captured by XPC fragments ($n=6$; error bars, standard deviation). A control reaction was carried out with empty beads. (**C**) FRAP analysis showing that, in undamaged cells, the nuclear mobility of the full-length E755K mutant is retarded relative to the wt control ($n=12$; error bars, standard error of the mean). (**D**) Host-cell reactivation assay showing that the E755K mutation confers a significant GGR defect. All results were corrected for the background activity in XP-C cells transfected with the GFP vector ($n=5$; error bars, standard deviation).

single site-directed mutation confirm that the dynamic properties of its minimal sensor surface, conferred by the β-turn structure, are critical for the ability of human XPC protein to act as a sensor of DNA damage.

Discussion

We elucidated the mechanism by which XPC protein scrutinizes DNA quality in living cells. The most outstanding finding is the identification of a two-stage discrimination process triggered by a dynamic sensor interface that detects DNA damage without the involvement of a prominent DNA-binding domain (BHD3), which was thought to represent the primary lesion recognition module on the basis of the Rad4 crystal structure (Min and Pavletich, 2007). The newly identified sensor interface serves to rapidly screen the double helix for the presence of unpaired bases, thus localizing damaged target sites that are amenable to the subsequent installation of an ultimate repair-initiating complex.

Dynamic molecular dialogue with the DNA double helix

According to the aforementioned Rad4 structure, the TGD region cooperates with BHD1 to associate with a portion of double-stranded DNA flanking the lesion (see Supplementary Figure 1). However, we observed that a large N-terminal segment (65% of the human sequence including most TGD sequences) has a stimulatory role, but is not directly required for the relocation of XPC protein to focus on DNA lesions (Figure 3). In the absence of this TGD segment, a strong interaction with the normal duplex is nevertheless mediated by the earlier described (Uchida *et al*, 2002) minimal DNA-binding fragment $XPC_{607-741}$, which consists of BHD1 and BHD2 (Figure 6E). Instead, a longer fragment covering all three BHDs displays a comparably low affinity for the normal duplex (Figure 6G), indicating that the double-stranded DNA-binding activity of BHD1/BHD2 is opposed by the neighbouring BHD3 sequence. The further dissection of this critical XPC region revealed that a short β-turn extension of BHD3 is sufficient to mediate in part such an antagonistic effect (Figure 6F).

Several observations in living cells support the notion that the addition of this β-turn extension conveys a true gain of function rather than causing the destabilization of adjacent structural elements in the respective XPC constructs. First, XPC_{1-766} and XPC_{1-831} display a residual GGR function that is missing in the case of XPC_{1-741}, which lacks the β-turn structure (Figure 4B). The fact that XPC_{1-766} and XPC_{1-831} exert a similarly low complementing activity is likely because of the absence of at least some components of the TFIIH-recruiting domain in their C-terminal region (Uchida *et al*, 2002). Second, a side-by-side comparison of the same C-terminal truncates shows that the enhanced nuclear mobility conferred by the β-turn structure (Figure 5B) correlates with a more efficient relocation to UV lesions (Figure 4E). Third, the nuclear mobility of XPC_{1-766}, but not XPC_{1-741}, is retarded by UV damage (Figure 5C and D), confirming that the former detects DNA lesions more effectively. Fourth, in living cells, the damage-induced accumulation of an earlier defined minimal DNA-binding fragment ($XPC_{607-741}$) is strictly dependent on the presence of the β-turn structure (Figure 6B). Finally,

the critical role of this dynamic β-turn subdomain is supported by a site-directed E755K substitution that reverts in part its DNA-repellent action. The increased affinity of this novel mutant for the native double helix results in decreased nuclear mobility and markedly reduced repair activity (Figure 7). According to the Rad4 structure, the critical position 755 maps to an amino-acid sequence that is in close contact with the DNA substrate (Min and Pavletich, 2007). Thus, our findings indicate that the β-turn structure displays both DNA-attractive and DNA-repulsive forces that dictate the dynamic interplay with duplex DNA such that, in the full genome context, this subdomain facilitates damage recognition by providing sufficient mobility to the XPC molecules searching for lesions.

Identification of a transient recognition intermediate

On binding to damaged substrates, XPC protein induces local DNA melting and kinking (Evans *et al*, 1997; Janicijevic *et al*, 2003; Mocquet *et al*, 2007). A structural basis for these rearrangements is again provided by the Rad4 crystal, in which the β-hairpin of BHD3 is inserted through the DNA duplex, causing two base pairs to entirely flip out of the double helix (see Supplementary Figure 1). In view of these features of the Rad4–DNA complex, it was unexpected to find that most of BHD3 including the protruding β-hairpin is actually not necessary to sense DNA damage in living cells. In fact, an XPC fragment that contains the β-turn structure, but is devoid of the remaining BHD3 sequence because of a truncation at position 766 (XPC_{1-766}), accumulates in UV foci with remarkable efficiency (~60% of the full-length control; Figure 4E), but without forming stable nucleoprotein complexes (Figure 5D). Similar to the W690S mutant, this truncated XPC_{1-766} derivative is even able to induce GGR activity (Figure 4B), although to moderate levels that are not sufficient to complement the repair defect of XP-C cells. A damage-specific accumulation of XPC_{1-766} was also detected in DDB2-deficient XP-E fibroblasts (Figure 4D and E) and V79 hamster cells (data not shown), thus excluding that the BHD3-independent relocation occurs in an indirect manner by association with UV-DDB. Finally, the conclusion that XPC protein forms a transient damage recognition intermediate without the involvement of BHD3 is supported by the finding that a small fragment ($XPC_{607-766}$) consisting only of BHD1/BHD2 and the β-turn structure (together ~15% of the human XPC sequence) still functions as a cellular DNA damage sensor (Figure 6B). This minimal sensor surface displays a binding preference for duplexes containing non-hydrogen-bonded bases, a generic feature of damaged DNA, and hence functions as a molecular caliper of thermodynamic base-pair stability.

A two-stage quality-control inspection

Although the BHD3 segment (residues 767–831) and its β-hairpin are not required to attract XPC protein to lesion sites, this additional domain favours the subsequent formation of stable nucleoprotein complexes, resulting in an immobile fraction of XPC protein in response to DNA damage (Figure 5E). The biochemical analysis of purified fragments shows that, unlike the BHD1/BHD2/β-turn minimal sensor, which displays a preference for duplexes with unpaired bases, BHD3 confers an exquisite selectivity for single-stranded DNA conformations (Figure 6G). In conjunction with the earlier mentioned Rad4 structure, these findings indicate that BHD3 does not participate in the early and transient recognition intermediate, but, instead, facilitates the subsequent stabilization of a repair-initiating complex using its single-stranded DNA-binding activity to encircle the undamaged strand across lesion sites.

To conclude, this is the first report providing evidence for a two-stage discrimination mechanism by which XPC protein carries out its versatile recognition function (Figure 8). This two-stage process obviates the difficulty of probing every genomic base pair for its susceptibility to undergo a BHD3-mediated β-hairpin insertion. Instead, the energetically less demanding search conducted by the dynamic BHD1/BHD2/β-turn interface is likely to precede more extensive BHD3-dependent structural adjustments. This initial search leads to the detection of non-hydrogen-bonded residues that are more prone than native base pairs to be flipped out of the double helix and, hence, become an interaction partner for the single-stranded DNA-binding activity of BHD3. A critical step of this two-stage quality-control process is the transition from an initially labile sensor intermediate to the more stable ultimate recognition complex. Two constitutive interaction partners of XPC protein, Rad23B and centrin 2, are thought to exert an accessory function not only by inhibiting XPC degradation, but also by stimulating its DNA-binding activity (Ng *et al*, 2003; Xie *et al*, 2004; Nishi *et al*, 2005). Such an auxiliary role is supported for Rad23B by the observation that $XPC_{607-940}$, a fragment that fails to associate with Rad23B (Uchida *et al*, 2002), has a reduced DNA damage recognition capacity in living cells (Figure 3F). In addition, the two-step discrimination process identified in this study raises the possibility that Rad23B, centrin 2 or other binding partners may facilitate the installation of an ultimate XPC–DNA complex by lowering the energetic cost of critical nucleoprotein rearrangements required for the final β-hairpin insertion.

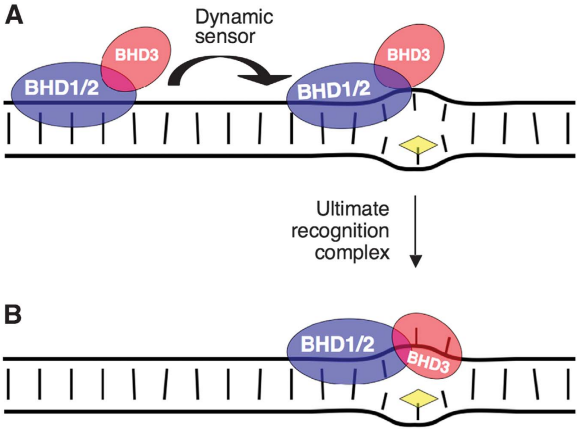

Figure 8 Two-stage detection of DNA lesions by XPC protein. Model depicting the switch from a dynamic damage sensor intermediate to the ultimate recognition complex. (**A**) This study identifies a minimal sensor interface that rapidly scrutinizes base-pair integrity. This initial search, carried out by BHD1/BHD2 in conjunction with the β-turn structure, results in the formation of a labile nucleoprotein intermediate. (**B**) The single-stranded DNA-binding activity of BHD3 promotes the subsequent transition to a stable recognition complex by capturing extruded nucleotides in the undamaged strand.

Materials and methods

XPC constructs

The human *XPC* complementary DNA was cloned into pEGFP-N3 (Clontech) using the restrictions enzymes *Kpn*I and *Xma*I. The same enzymes were used to generate the truncated XPC fragments. Primers for the insertion of restrictions sites and site-directed mutagenesis (QuickChange, Stratagene) are listed in the Supplementary Table II. All clones were sequenced (Microsynth) to exclude accidental mutations.

Cell culture

Simian virus 40-transformed human XP-C fibroblasts (GM16093) and untransformed XP-E fibroblasts (GM02415), derived from patients XP14BR and XP2RO, respectively, were purchased from the Coriell Institute for Medical Research (Camden, New Jersey, USA). The XP-C cells carry a homozygous C→T transition at position 2152 of the *XPC* sequence (Chavanne *et al*, 2000). The GM02415 cells carry a G→A transition in the *DDB2* sequence generating an inactive R273H mutant that is not expressed to detectable levels (Nichols *et al*, 2000; Itoh *et al*, 2001). These fibroblasts, as well as V79 hamster cells deficient in UV-DDB activity (Tang *et al*, 2000) were cultured in Dulbecco's modified Eagle's medium (DMEM; Gibco), supplemented with 10% fetal calf serum (FCS), penicillin G (100 units ml^{-1}) and streptomycin (100 μg ml^{-1}). The cells were maintained at 37°C in a humidified incubator containing 5% CO_2.

Transfections

One day before transfection, 600 000 cells were seeded into 6-well plates containing glass cover slips. At a confluence of 90–95%, the cells were transfected with 1 μg XPC-pEGFP-N3 (or truncated constructs) using 4 μl FuGENE HD reagent (Roche) and incubated for another 18 h. Expression of XPC polypeptides was monitored by western blotting (Maillard *et al*, 2007).

High-resolution DNA damage induction

The growth medium was replaced by phenol red-free DMEM (Gibco) supplemented with 10% FCS and 25 mM HEPES (pH 7.2). Single cells were irradiated with a femtosecond fibre laser (Träutlein *et al*, 2008) coupled to a confocal microscope (LSM Pascal, Zeiss) that generates pulses of 775 nm (duration 230 fs, repetition rate 107 MHz). The peak power density at the focal plane was 350 GW cm^{-2} and the pixel dwell time was 44.2 ms. Nuclei were irradiated along a single track or two intersecting lines. The area of each irradiation track was $<10\,\mu m^2$ and its volume $<20\,\mu m^3$.

By multiphoton excitation, three photons of low energy (775 nm wavelength) cause DNA lesions normally produced by the absorption of a single photon of higher energy (equivalent to 258 nm wavelength). Irradiation in the near-infrared range induces CPDs, (6-4) photoproducts and oxidative lesions (Lan *et al*, 2004; Dinant *et al*, 2007). In an earlier report (Meldrum *et al*, 2003), it has been calculated that three-photon irradiation with a peak power density of 350 GW cm^{-2} generates ~7000 UV lesions in each treated cell. Taking into account our slightly modified parameters, we calculated that in this study, the same power density produced ~5000 UV lesions along each linear 10-μm track.

Image analysis

Fluorescence measurements were carried out through a ×40 oil immersion objective lens with a numerical aperture of 1.4 (EC-Plan-Neo-Fluar, Zeiss) using an Ar^+ source (488 nm). The selected parameters, including laser power and magnification factor, were kept constant throughout all experiments. To monitor the distribution of fluorescent fusions, at least 60 images were taken for up to 10 min after irradiation and analysed using the ImageJ software (http://rsb.info.nih.gov/ij). An initial-control image was taken immediately before damage induction. Signals were corrected for bleaching (http://www.embl-heidelberg.de/eamnet/html/body_bleach_correction.html) and cell movements (http://bigwww.epfl.ch/thevenaz/stackreg). For every time point, the average fluorescence intensities were measured in the area of accumulation and, as a background reference, in a neighbouring area of identical size. Finally, the background-corrected values were normalized to the mean intensity of the same nuclear region before irradiation.

Induction of UV foci

After removal of the culture medium, the cells were rinsed with phosphate-buffered saline (PBS), covered by a polycarbonate filter (Millipore) with 5-μm pores and irradiated using a UV-C source (254 nm, 100 J m^{-2}). Subsequently, the filter was removed and the cells were returned to complete DMEM for 15 min at 37°C before paraformaldehyde fixation.

Immunocytochemistry

All wash steps and incubations were performed in PBS. At the indicated times after irradiation, cells were washed and fixed for 15 min at room temperature using 4% (v/v) paraformaldehyde. The cells were then permeabilized twice with 0.1% (v/v) TWEEN 20 for 10 min and DNA was denatured with 0.07 M NaOH for 8 min. Subsequently, the samples were washed five times with 0.1% TWEEN 20 and incubated (30 min at 37°C) with 20% FCS to inhibit unspecific binding. The samples were incubated (1 h at 37°C in 5% FCS) with primary antibodies (MBL International Corporation) directed against CPDs (TDM-2, dilution 1:3000) or (6-4) photoproducts (64M-2, dilution 1:1000). Next, the samples were washed with 0.1% TWEEN 20, blocked twice for 10 min with 20% FCS and treated with Alexa Fluor 546 dye-conjugated secondary antibodies (Invitrogen, dilution 1:400) for 30 min at 37°C. After washing with 0.1% TWEEN 20, the nuclei were stained for 10 min with Hoechst dye 33258 (200 ng ml^{-1}). Finally, the samples were washed three times and analysed using an oil immersion objective.

GGR assay

Triplicate samples of XP-C fibroblasts, at a confluence of 90–95%, were transfected in a 6-well plate. The total amount of plasmid DNA (1 μg) included 0.45 μg pGL3 (UV irradiated at 1000 J m^{-2}, coding for *Photinus* luciferase), 0.05 μg phRL-TK (unirradiated, coding for *Renilla* luciferase) and 0.5 μg of XPC-pEGFP expression vector. After 4 h, the transfection mixture was replaced by complete culture medium. After another 18 h, the cells were disrupted in 500 μl Passive Lysis Buffer (Promega). The lysates were cleared by centrifugation and the ratio of *Photinus* and *Renilla* luciferase activity was determined in a Dynex microtiter luminometer using the Dual-Luciferase assay system (Promega).

FRAP analysis

Protein mobility was analysed at high time resolution using a Leica TCS SP5 confocal microscope equipped with an Ar^+ laser (488 nm, not inducing DNA lesions) and a ×60 oil immersion lens (numerical aperture of 1.4). The assays were performed in a controlled environment at 37°C and CO_2 supply of 5%. A region of interest (ROI) covering 4 μm^2 was photobleached for 2.3 s at 100% laser intensity. Fluorescence recovery within the ROI was monitored 200 times using 115-ms intervals followed by 30 frames at 250-ms and 10 frames at 500 ms. Simultaneously, a reference ROI of the same size was measured for each time point to correct for overall bleaching. All data were normalized to the prebleach intensity and the effective diffusion model (Sprague *et al*, 2004) was used to estimate diffusion coefficients (see Supplementary Table I).

DNA-binding assays

Full-length MBP-XPC fusions were expressed in *Sf*9 cells (Maillard *et al*, 2007). Insect cell lysates (5–20 μl) were incubated with ^{32}P-labelled 135-mer oligonucleotides (4 nM) in 200 μl buffer A (25 mM Tris–HCl, pH 7.5, 0.3 M NaCl, 10% glycerol, 0.01% Triton X-100, 0.25 mM phenylmethane sulfonyl fluoride and 1 mM EDTA). After 1 h at 4°C, the reaction mixtures were supplemented with monoclonal antibodies against MBP linked to paramagnetic beads (0.2 mg, New England BioLabs). After another 2 h at 4°C, the beads were washed four times with 200 μl buffer A and the oligonucleotides associated with paramagnetic beads were quantified by liquid scintillation counting. All values were corrected for the background radioactivity resulting from unspecific binding to empty beads. The amount of immobilized XPC protein was controlled by denaturing gel electrophoresis.

GST-$XPC_{607-741}$, GST-$XPC_{607-766}$ and GST-$K755E_{607-766}$ (expressed in *Escherichia coli*) as well as His-$XPC_{607-831}$ (expressed in *Sf*9 cells) were purified as described (Uchida *et al*, 2002). The indicated concentrations of XPC fragments were incubated with radiolabelled 135-mer oligonucleotides (4 nM) in 200 μl buffer B (25 mM Tris–HCl, pH 7.5, 0.15 M NaCl, 10% glycerol, 0.01% Triton X-100, 0.25 mM phenylmethane sulfonyl fluoride and 1 mM EDTA).

After 1 h at 4°C, the reaction mixtures were supplemented with glutathione-Sepharose (10 μl, Amersham) or Ni-NTA agarose beads (10 μl, Qiagen). After another 1 h at 4°C, the beads were washed twice with 200 μl buffer B and the immobilized oligonucleotides were quantified by liquid scintillation counting. All values were corrected for the background radioactivity resulting from unspecific binding to empty beads. To estimate binding constants, the data from saturation experiments (50–250 nM protein) were subjected to Scatchard analysis by plotting the ratio of bound and free XPC fragments as a function of the fraction of bound protein (Husain and Sancar, 1987). The double-stranded homoduplex or heteroduplex probes were obtained by hybridization of complementary 135-mers in 50 mM Tris–HCl (pH 7.4), 10 mM $MgCl_2$ and 1 mM dithiothreitol. Equal amounts of each oligonucleotide were heated at 95°C for 10 min followed by slow cooling (3 h at 25°C).

Supplementary data
Supplementary data are available at *The EMBO Journal* Online (http://www.embojournal.org).

Acknowledgements

We thank D Hermann, A Lenisa, M Träxler and M Vitanescu for excellent technical assistance and W Vermeulen for introduction into the FRAP technique. We also thank CT Craescu, A Scrima and N Thomä for critical reading and discussion of the manuscript. This work was supported by the Swiss National Science Foundation (grant 3100A0-113694), Oncosuisse (grant KLS-01827-02-2006), the German Research Foundation (grant DFG MA/2385/2-3) and the Ministry of Science, Research and the Arts of Baden-Württemberg.

References

Andressoo JO, Hoeijmakers JH, Mitchell JR (2006) Nucleotide excision repair disorders and the balance between cancer and aging. *Cell Cycle* **5:** 2886–2888

Batty D, Rapic'-Otrin V, Levine AS, Wood RD (2000) Stable binding of human XPC complex to irradiated DNA confers strong discrimination for damaged sites. *J Mol Biol* **300:** 275–290

Bunick CG, Miller MR, Fuller BE, Fanning E, Chazin WJ (2006) Biochemical and structural domain analysis of xeroderma pigmentosum complementation group C protein. *Biochemistry* **45:** 14965–14979

Buterin T, Meyer C, Giese B, Naegeli H (2005) DNA quality control by conformational readout on the undamaged strand of the double helix. *Chem Biol* **12:** 913–922

Carreau M, Eveno E, Quilliet X, Chevalier-Lagent O, Benoit A, Tanganelli B, Stefanini M, Vermeulen W, Hoeijmakers JH, Sarasin A, Mezzina M (1995) Development of a new easy complementation assay for DNA repair deficient human syndromes using cloned repair genes. *Carcinogenesis* **16:** 1003–1009

Chavanne F, Broughton BC, Pietra D, Nardo T, Browitt A, Lehmann AR, Stefanini M (2000) Mutations in the XPC gene in families with xeroderma pigmentosum and consequenced at the cell, protein and transcription level. *Cancer Res* **60:** 1974–1982

Cleaver JE (2005) Cancer in xeroderma pigmentosum and related disorders of DNA repair. *Nat Rev Cancer* **5:** 564–573

Cleaver JE, Thompson LH, Richardson AS, States JC (1999) A summary of mutations in the UV-sensitive disorders: xeroderma pigmentosum, Cockayne syndrome, and trichothiodystrophy. *Hum Mutat* **14:** 9–22

Dinant C, de Jager M, Essers J, van Cappellen WA, Kanaar R, Houtsmuller AB, Vermeulen W (2007) Activation of multiple DNA repair pathways by subnuclear damage induction methods. *J Cell Sci* **120:** 2731–2740

Evans E, Moggs JG, Hwang JR, Egly JM, Wood RD (1997) Mechanism of open complex and dual incision formation by human nucleotide excision repair factors. *EMBO J* **16:** 6559–6573

Fitch ME, Nakajima S, Yasui A, Ford JM (2003) *In vivo* recruitment of XPC to UV-induced cyclobutane pyrimidine dimers by the DDB2 gene product. *J Biol Chem* **278:** 46906–46910

Friedberg EC, Walker GC, Siede W, Wood RD, Schultz RA, Ellenberger T (2006) *DNA Repair and Mutagenesis*. Washington DC: ASM Press

Gillet LC, Schärer OD (2006) Molecular mechanisms of mammalian global genome nucleotide excision repair. *Chem Rev* **106:** 253–276

Hanawalt PC, Spivak G (2008) Transcription-coupled DNA repair: two decades of progress and surprises. *Nat Rev Mol Cell Biol* **9:** 958–970

Hoogstraten D, Bergink S, Verbiest VH, Luijsterburg MS, Geverts B, Raams A, Dinant C, Hoeijmakers JH, Vermeulen W, Houtsmuller AB (2008) Versatile DNA damage detection by the global genome nucleotide excision repair protein XPC. *J Cell Sci* **121:** 2850–2859

Houtsmuller AB, Rademakers S, Nigg AL, Hoogstraten D, Hoeijmakers JH, Vermeulen W (1999) Action of DNA repair endonuclease ERCC1/XPF in living cells. *Science* **284:** 958–961

Houtsmuller AB, Vermeulen W (2001) Macromolecular dynamics in living cell nuclei revealed by fluorescence redistribution after photobleaching. *Histochem Cell Biol* **115:** 13–21

Huang JC, Hsu DS, Kazantsev A, Sancar A (1994) Substrate spectrum of human excinuclease: repair of abasic sites, methylated bases, mismatches and bulky adducts. *Proc Natl Acad Sci USA* **91:** 12213–12217

Husain I, Sancar A (1987) Binding of E. coli DNA photolyase to a defined substrate containing a single T<>T dimer. *Nucleic Acids Res* **15:** 1109–1120

Itoh T, Nichols A, Linn S (2001) Abnormal regulation of DDB2 gene expression in xeroderma pigmentosum group E strains. *Oncogene* **20:** 7041–7050

Janicijevic A, Sugasawa K, Shimizu Y, Hanaoka F, Wijgers N, Djurica M, Hoeijmakers JH, Wyman C (2003) DNA bending by the human damage recognition complex XPC-HR23B. *DNA Rep* **2:** 325–336

Kuraoka I, Bender C, Romieu A, Cadet J, Wood RD, Lindahl T (2000) Removal of oxygen free-radical-induced 5′,8-purine cyclodeoxynucleosides from DNA by the nucleotide excision-repair pathway in human cells. *Proc Natl Acad Sci USA* **97:** 3832–3837

Kusumoto R, Masutani C, Sugasawa K, Iwai S, Araki M, Uchida A, Mizukoshi T, Hanaoka F (2001) Diversity of the damage recognition step in the global genomic nucleotide excision repair *in vitro*. *Mutat Res* **485:** 219–227

Lan L, Nakajima S, Oohata Y, Takao M, Okano S, Masutani M, Wilson SH, Yasui A (2004) *In situ* analysis of repair processes for oxidative DNA damage in mammalian cells. *Proc Natl Acad Sci USA* **101:** 13738–13743

Legerski R, Peterson C (1992) Expression cloning of a human DNA repair gene involved in xeroderma pigmentosum group C. *Nature* **359:** 70–73

Lehmann AR (2003) DNA repair-deficient diseases, xeroderma pigmentosum, Cockayne syndrome and trichothiodystrophy. *Biochimie* **85:** 1101–1111

Maillard O, Solyom S, Naegeli H (2007) An aromatic sensor with aversion to damaged strands confers versatility to DNA repair. *PLoS Biol* **5:** e79

Meldrum RA, Botchway SW, Wharton CW, Hirst GJ (2003) Nanoscale spatial induction of ultraviolet photoproducts in cellular DNA by three-photon near-infrared absorption. *EMBO Rep* **4:** 1144–1149

Min J-H, Pavletich NP (2007) Recognition of DNA damage by the Rad4 nucleotide excision repair protein. *Nature* **449:** 570–575

Mocquet V, Kropachev K, Kolbanovskiy M, Kolbanovskiy A, Tapias A, Cay Y, Broyde S, Geacintov NE, Egly JM (2007) The human DNA repair factor XPC-HR23B distinguishes stereoisomeric benzo[a]pyrenyl-DNA lesions. *EMBO J* **26:** 2923–2932

Moné JJ, Bernas T, Dinant C, Goedvree FA, Manders EM, Volker M, Houtsmuller AB, Hoeijmakers JH, Vermeulen W, van Driel R (2004) *In vivo* dynamics of chromatin-associated complex formation in mammalian nucleotide excision repair. *Proc Natl Acad Sci USA* **101:** 15933–15937

Moser J, Volker M, Kool H, Alekseev S, Vrieling H, Yasui A, van Zeeland AA, Mullenders LH (2005) The UV-damaged DNA binding protein mediates efficient targeting of the nucleotide excision repair complex to UV-induced photo lesions. *DNA Rep* **4:** 571–582

Ng JM, Vermeulen W, van der Horst GT, Bergink S, Sugasawa K, Vrieling H, Hoeijmakers JH (2003) A novel regulation mechanism of DNA repair by damage-induced and RAD23-dependent stabi-

lization of xeroderma pigmentosum group C protein. *Genes Dev* **17:** 1630–1645

Nichols AF, Itoh T, Graham JA, Liu W, Yamaizumi M, Linn S (2000) Human damage-specific DNA-binding protein p48. *J Biol Chem* **275:** 21422–21428

Nishi R, Okuda Y, Watanabe E, Mori T, Iwai S, Masutani C, Sugasawa K, Hanaoka F (2005) Centrin 2 stimulates nucleotide excision repair by interacting with xeroderma pigmentosum group C protein. *Mol Cell Biol* **25:** 5664–5674

Politi A, Moné MJ, Houtsmuller AB, Hoogstraaten D, Vermeulen W, Heinrich R, van Driel R (2005) Mathematical modeling of nucleotide excision repair reveals efficiency of sequential assembly strategies. *Mol Cell* **19:** 679–690

Reardon JT, Sancar A (2006) Repair of DNA-polypeptide crosslinks by human excision nuclease. *Proc Natl Acad Sci USA* **103:** 4056–4061

Schärer OD (2007) Achieving broad substrate specificity in damage recognition by binding accessible nondamaged DNA. *Mol Cell* **28:** 184–185

Scrima A, Konickova R, Czyzewski BK, Kawasaki Y, Jeffrey PD, Groisman R, Nakatani Y, Iwai S, Pavletich NP, Thomä NH (2008) Structural basis of UV DNA-damage recognition by the DDB1-DDB2 complex. *Cell* **135:** 1213–1223

Sprague BL, Pego RL, Stavreva DA, McNally JG (2004) Analysis of binding reactions by fluorescence recovery after photobleaching. *Biophys J* **86:** 3473–3495

Sugasawa K, Hanaoka F (2007) Sensing of DNA damage by XPC/Rad4: one protein for many lesions. *Nat Struct Mol Biol* **14:** 887–888

Sugasawa K, Ng JM, Masutani C, Iwai S, van der Spek PJ, Eker AP, Hanaoka F, Bootsma D, Hoeijmakers JH (1998) Xeroderma pigmentosum group C protein complex is the initiator of global genome nucleotide excision repair. *Mol Cell* **2:** 223–232

Sugasawa K, Okamoto T, Shimizu Y, Masutani C, Iwai S, Hanaoka F (2001) A multistep damage recognition mechanism for global genomic nucleotide excision repair. *Genes Dev* **15:** 507–521

Tang JY, Hwang BJ, Ford JM, Hanawalt PC, Chu G (2000) Xeroderma pigmentosum p48 gene enhances global gemomic repair and suppresses UV-induced mutagenesis. *Mol Cell* **5:** 737–744

Träutlein D, Adler F, Moutzouris K, Jeromin A, Leitenstorfer A, Ferrando-May E (2008) Highly versatile confocal microscopy system based on a tunable femtosecond Er:fiber source. *J Biophoton* **1:** 53–61

Trego KS, Turchi JJ (2006) Pre-steady-state binding of damaged DNA by XPC-hHR23B reveals a kinetic mechanism for damage discrimination. *Biochemistry* **45:** 1961–1969

Uchida A, Sugasawa K, Masutani C, Dohmae N, Araki M, Yokoi M, Ohkuma Y, Hanaoka F (2002) The C-terminal domain of the XPC protein plays a crucial role in nucleotide excision repair through interactions with transcription factor IIH. *DNA Rep* **1:** 449–461

Xie Z, Liu S, Zhang Y, Wang Z (2004) Roles of Rad23 protein in yeast nucleotide excision repair. *Nucl Acids Res* **15:** 5981–5990

Yasuda G, Nishi R, Watanabe E, Mori T, Iwai S, Orioli D, Stefanini M, Hanaoka F, Sugasawa K (2007) *In vivo* destabilization and functional defects of the xeroderma pigmentosum C protein caused by a pathogenic missense mutation. *Mol Cell Biol* **27:** 6606–6614

Yokoi M, Masutani C, Maekawa T, Sugasawa K, Ohkuma Y, Hanaoka F (2000) The xeroderma pigmentosum group C protein complex XPC-HR23B plays an important role in the recruitment of transcription factor IIH to damaged DNA. *J Biol Chem* **275:** 9870–9875

SUPPLEMENTARY INFORMATION

Two-stage dynamic DNA quality check by xeroderma pigmentosum group C protein

Ulrike Camenisch[1,4], Daniel Träutlein[2,4], Flurina C. Clement[1], Jia Fei[1], Alfred Leitenstorfer[2], Elisa Ferrando-May[3] and Hanspeter Naegeli[1,*]

[1]Institute of Pharmacology and Toxicology, University of Zürich-Vetsuisse, CH-8057 Zürich, Switzerland

[2]Department of Physics and Center for Applied Photonics, University of Konstanz, D-78457 Konstanz, Germany

[3]Bioimaging Center, University of Konstanz, D-78457 Konstanz, Germany

[4]These authors contributed equally to this work

TABLE OF CONTENTS

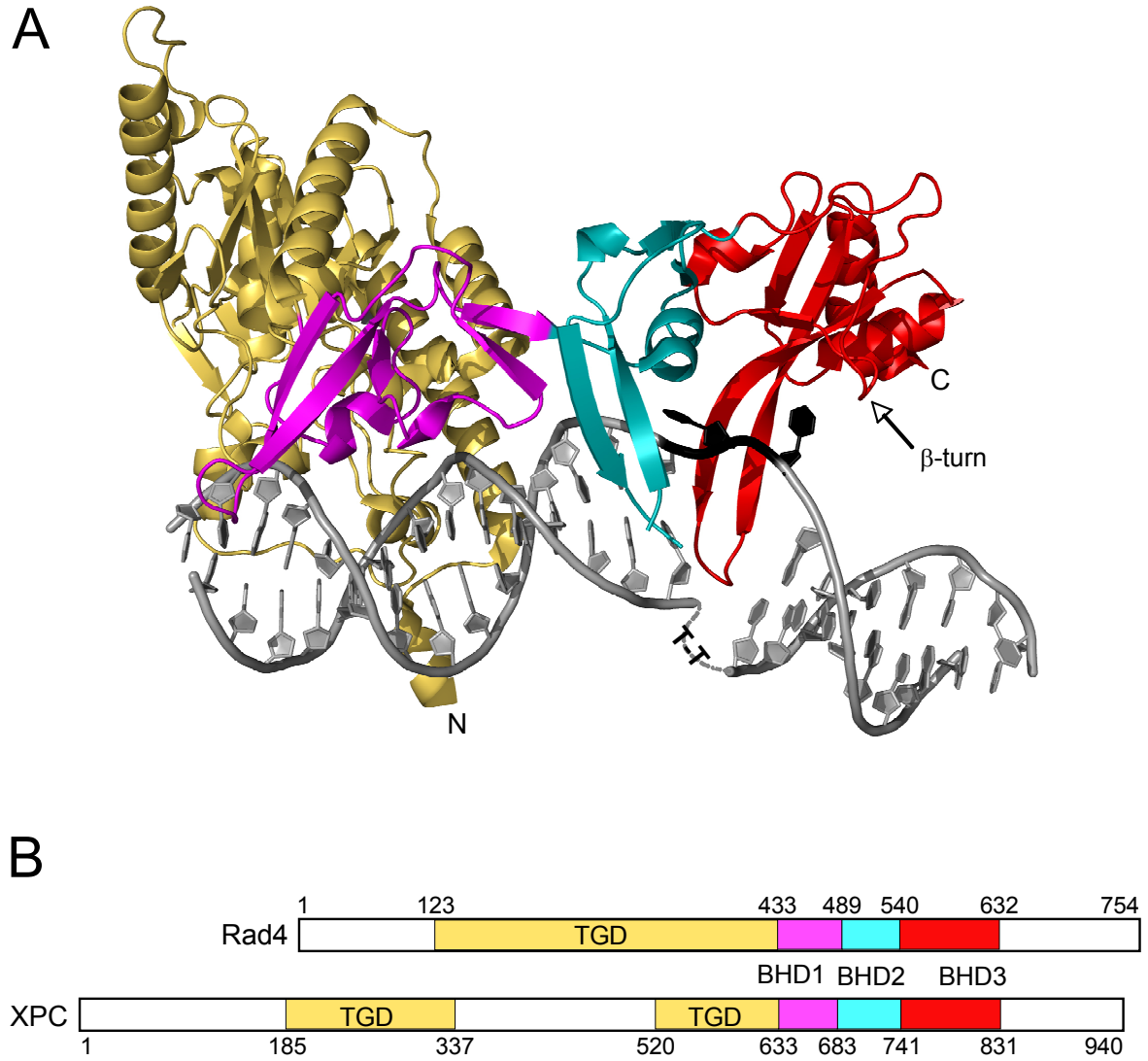

Supplementary Figure 1. Structure of XPC protein inferred from the yeast (*Saccaromyces cerevisiae*) Rad4 homolog. (**A**) Ribbon diagram of the crystal structure of Rad4 protein in complex with DNA containing a cyclobutane pyrimidine dimer (CPD) embedded in 3 base mismatches (Min & Pavletich, 2007). Gold, transglutaminase-homology domain (TGD); magenta, β-hairpin domain 1 (BHD1); cyan, BHD2; red, BHD3. The arrow indicates the location of the β-turn structure where the E755K mutation is introduced. T-T denotes the CPD, which is expelled from the double helix. The figure was made with the PyMol Molecular Viewer using the coordinates PDB 2QSG (**B**). Schematic representation of the aforementioned Rad4 domains and the respective XPC sequences. In human XPC protein, the TGD is divided into two distinct parts by a disordered ~180-residue insertion (Bunick et al, 2006).

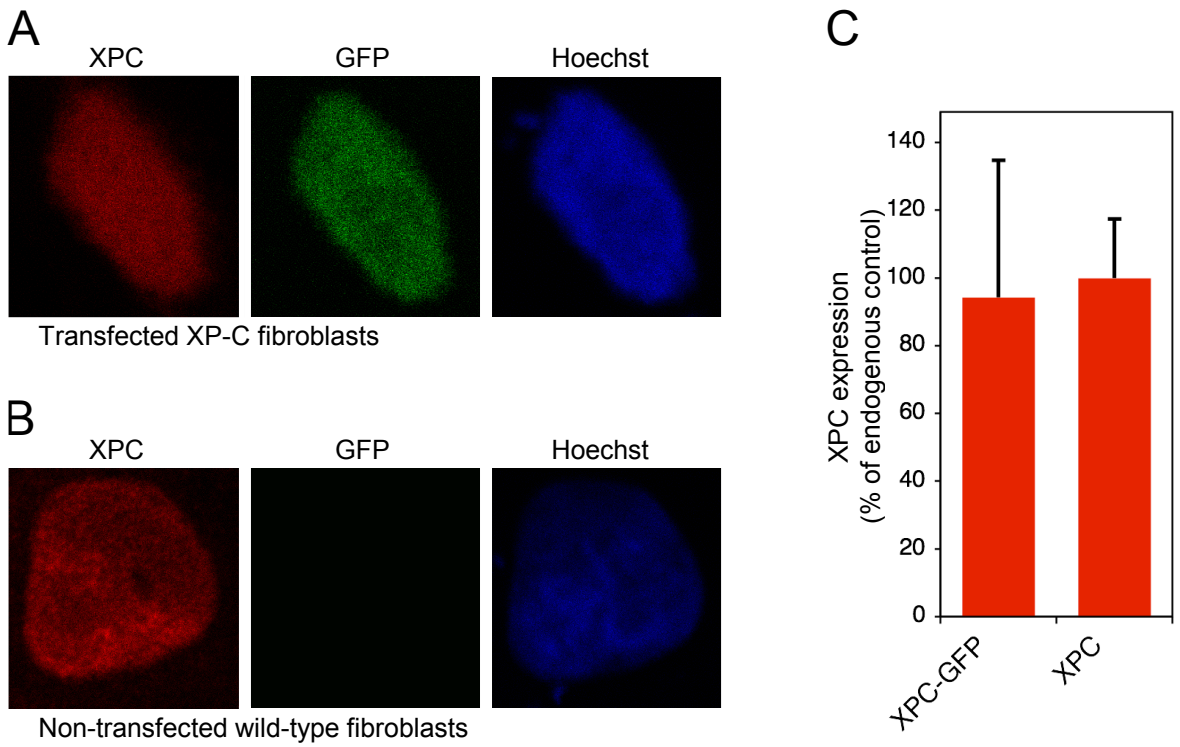

Supplementary Figure 2. Immunocytochemical analysis of XPC protein expression. (**A**) Visualization of XPC-GFP in a typical XP-C fibroblast expressing a low level of fusion protein. The immunological detection was performed with mouse monoclonal antibodies against human XPC (Abcam) followed by secondary antibodies conjugated to the Alexa Fluor 546 red dye (Invitrogen). The nuclear compartment is indicated by the Hoechst reagent. (**B**) Immunochemical detection of endogenous XPC in a representative wild-type fibroblast (GM00637). (**C**) Quantitative assessement of XPC-GFP expression in XP-C cells displaying the low green fluorescence level used as the criterion for imaging studies, in comparison to the endogenous XPC protein in wild-type fibroblasts (n = 10; error bars, standard deviation). Expression levels were compared by immunochemical analysis using antibodies against XPC and represented as the percentage of red fluorescence in normal fibroblasts. These results demonstrate that the XP-C cells targeted for live-cell imaging contain XPC protein in the same expression range as the endogenous protein in wild-type counterparts.

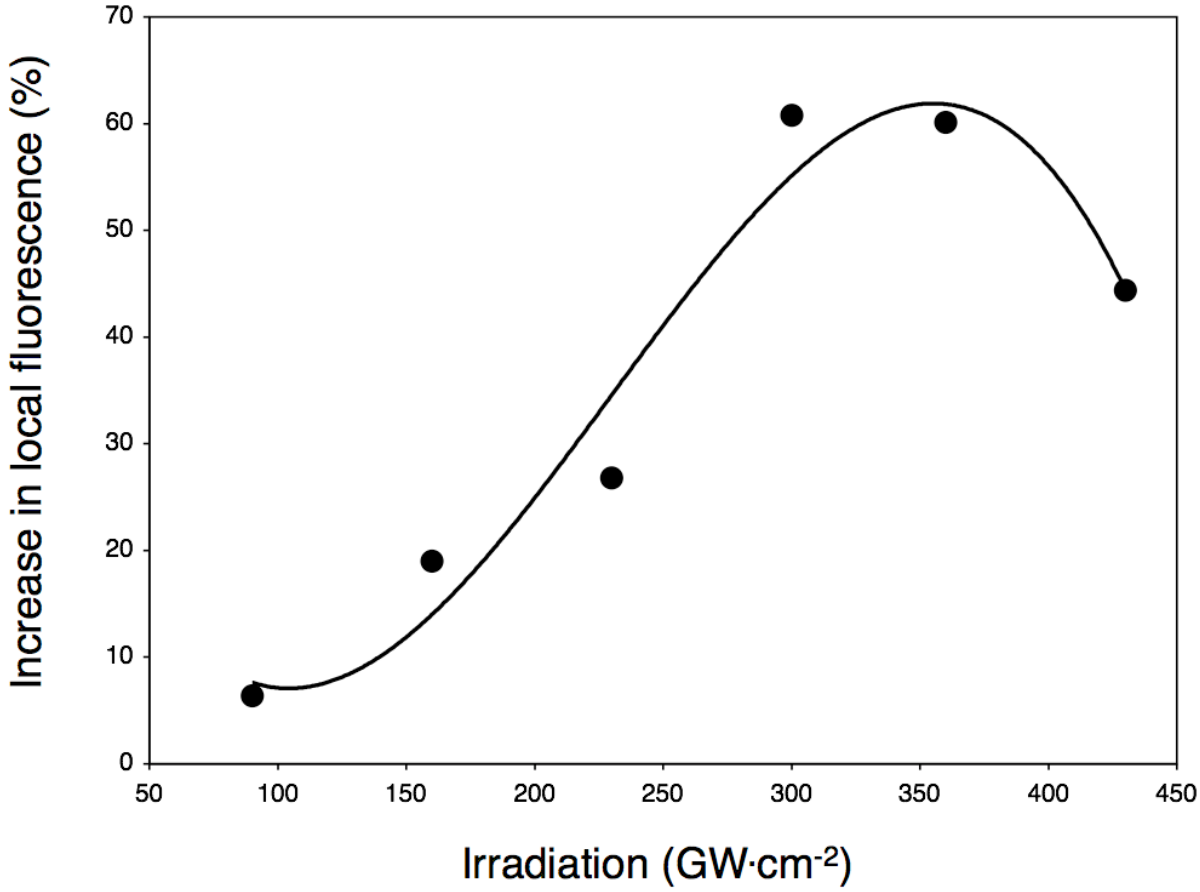

Supplementary Figure 3. Dose-dependent accumulation of XPC-GFP fusion protein in damaged chromatin areas of human XP-C fibroblasts. A single 10-µm line of UV photoproducts was generated at different dose levels of near-infrared irradiation. The local increase in fluorescence, determined 6 min after irradiation, was plotted as a percentage of the average fluorescence measured before irradiation (mean values of 5 experiments).

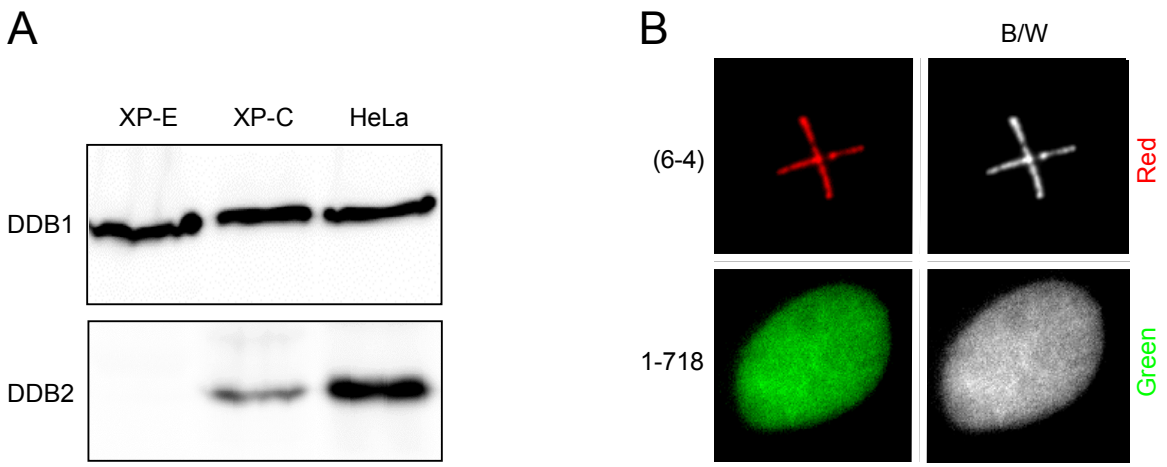

Supplementary Figure 4. Characterization of the XP-C fibroblasts GM16093. (**A**) Immunoblot analysis of endogenous DDB1 and DDB2 expression in the GM16093 cell line compared to HeLa cells and XP-E (GM02415) fibroblasts. Each lane contains 60 µg of cell lysate proteins. The antibodies against DDB1 and DDB2 were from BD Biosciences and Abcam, respectively. (**B**) Defective DNA damage recognition by fragment $XPC_{1\text{-}718}$. The cells GM16093, derived from patient XP14BR, lack functional *XPC* due to a nonsense mutation leading to premature termination at codon 718. The representative images (in color and black-and-white) demonstrate that, if expressed, the truncated XPC protein is unable to relocate to nuclear tracks of UV lesions. The distribution of GFP fusion protein was visualized 6 min after irradiation and DNA lesions were counterstained with antibodies against (6-4) photoproducts.

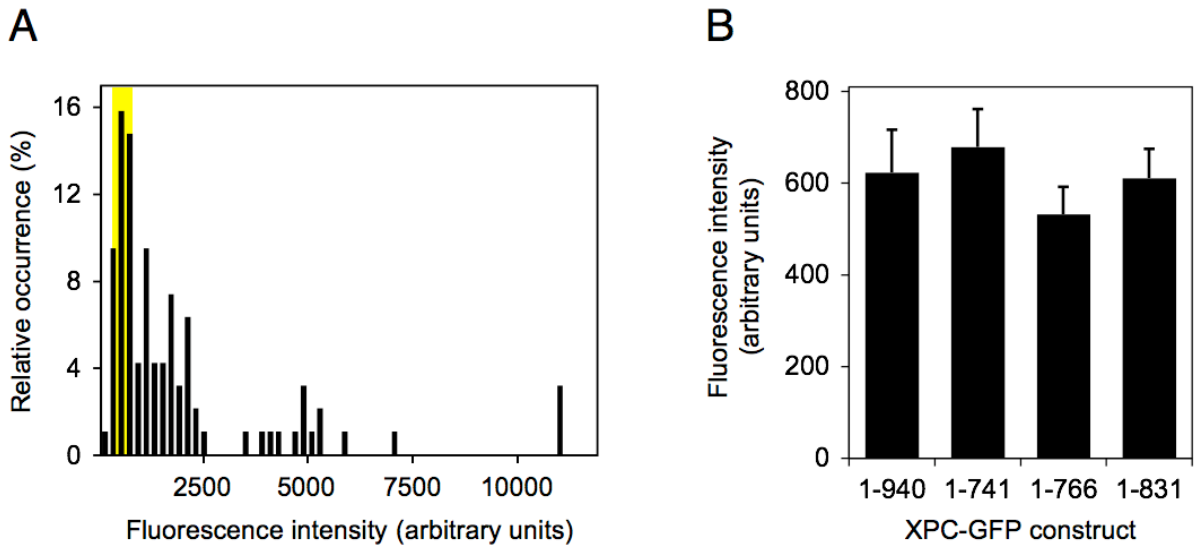

Supplementary Figure 5. Level of XPC-GFP truncates inside individual nuclei. (**A**) Overall fluorescence intensity in 95 representative nuclei of XP-C fibroblasts transfected with the full-length XPC-GFP sequence. The green fluorescence intensity of each nucleus is expressed in arbitrary units and the Y-axis indicates the proportion of cells in each fluorescence category. The yellow box illustrates the narrow range of cells selected for live-cell imaging. A comparison between the level of XPC-GFP in the selected XP-C cells and the normal XPC expression in wild-type fibroblasts is shown in the supplementary Figure 2. (**B**) Expression of wild-type XPC protein and truncated derivatives in nuclei used for live-cell imaging studies (n = 20; error bars, standard errors of the mean). These quantifications of overall fluorescence demonstrate that cells containing comparably low amounts of each construct were used for the experiments.

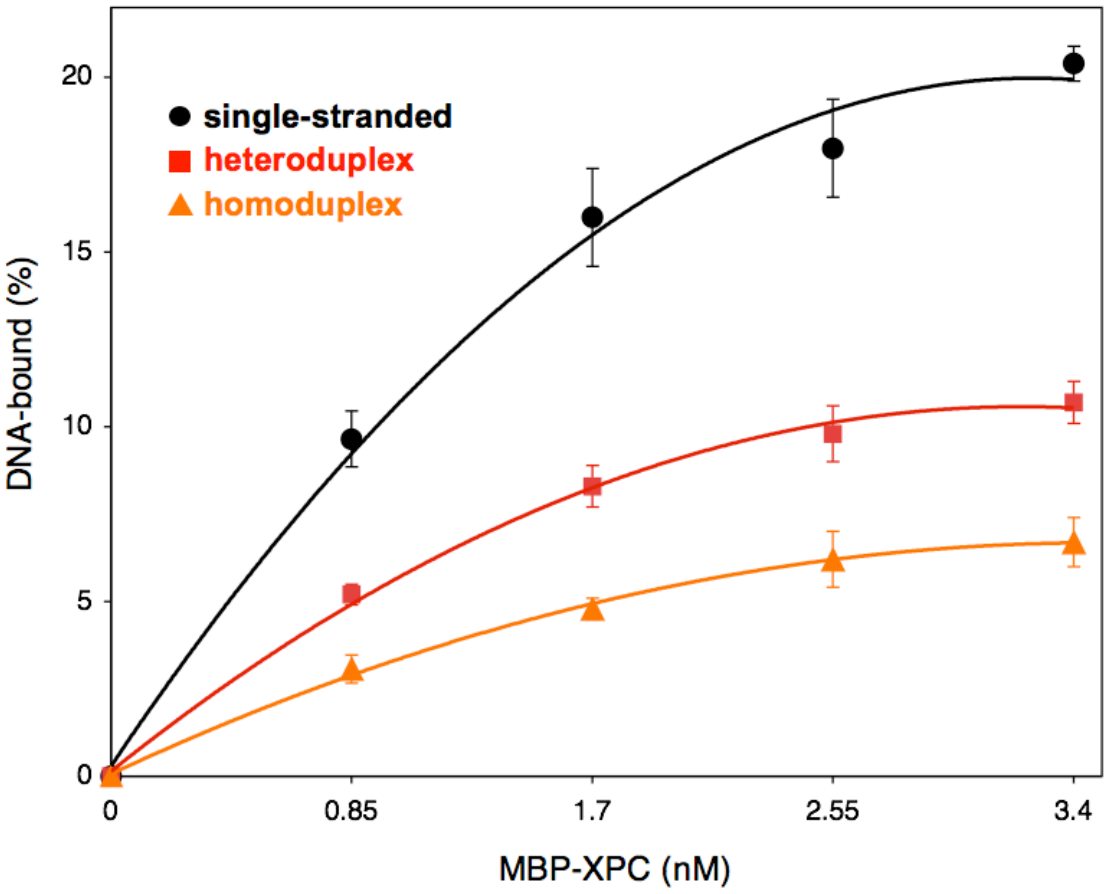

Supplementary Figure 6. DNA-Binding of full-length XPC protein. The indicated amounts of immunoprecipitated MBP-XPC fusion protein linked to magnetic beads (Maillard et al, 2007) were incubated with 2 nM ^{32}P-labeled 135-mer oligonucleotides (single-stranded, 3-mismatch heteroduplexes or homoduplexes). The DNA molecules captured by XPC protein were separated from free oligonucleotides and DNA-binding activity (n = 3) is reported as the percentage of immobilized radioactivity after deduction of the background determined with empty beads. Error bars, standard deviation.

Supplementary Table I. Effective diffusion coefficients (D_{eff}) and equilibrium constants (k^*_{on}/k_{off}) were computed from the FRAP curves of Figure 5 using the effective diffusion model (Sprague et al, 2004). The fit between experimental data and the mathematical model is indicated by the correlation coefficient (R).

XPC construct	***R***	$\boldsymbol{D_{eff}}$ **(μm²/s)[a]**	$\mathbf{k^*_{on}/k_{off}}$ **[b]**
Control (XPC_{1-940})	0.91	0.30	36.3
XPC_{1-831}	0.94	0.49	22.7
XPC_{1-831} + UV[c]	0.91	0.34	33.1
XPC_{1-766}	0.98	0.44	26.1
XPC_{1-766} + UV	0.99	0.37	31.2
XPC_{1-741}	0.99	0.34	34.3
XPC_{1-741} + UV	0.99	0.32	36.5

[a]D_{eff} values were calculated in Matlab (The Math Works, Natick, MA, USA) using the model: $f(t) = e^{-\tau_D/2t} \cdot [I_0(\tau_D/2t) + I_1(\tau_D/2t)]$, where $\tau_D = \omega^2/D_{eff}$ (ω, radius of the bleach spot); I_0 and I_1 are modified Bessel functions.

[b]k^*_{on}/k_{off} (the ratio of bound/free molecules) was calculated from $D_{eff} = D_f / 1 + (k^*_{on}/k_{off},)$, where D_f is the expected free diffusion coefficient if the FRAP curve is determined by free movement (11.2 μm²/s for full-length XPC protein, 11.6 μm²/s for XPC_{1-831}, 11.9 μm²/s for XPC_{1-766} and 12.0 μm²/s for XPC_{1-741}) and k^* is the pseudo-on rate. The D_f values were calculated assuming a diffusion coefficient of 20 μm²/s for GFP (Sprague et al, 2004).

[c]The cells were exposed to UV-C light (254 nm) at a dose of 10 J/m².

Supplementary Table II. Forward and reverse oligonucleotide primers used for the construction of truncated XPC derivatives and for site-directed mutagenesis.

$XPC_{118-940}$	Forward: 5'-GGGGTACCGCTACC**ATG**AATGAAGAC-3' Reverse: 5'-ATACCCGGGTT**CAG**CTTCTCAA-3'
XPC_{1-495}	Forward: 5'-ATGGTACCGCCACC**ATG**GCTCGGAAAC-3' Reverse: 5'-ACACCCGGGTC**TGG**GTCCTTACGATG-3'
XPC_{1-718}	Forward: 5'-ATGGTACCGCCACC**ATG**GCTCGGAAAC-3' Reverse: 5'-ACACCCGGGAG**TCG**GGCTTTCCGAGCACG-3'
XPC_{1-741}	Forward: 5'-ATGGTACCGCCACC**ATG**GCTCGGAAAC-3' Reverse: 5'-ATACCCGGGTC**ATA**CTCCTCTGTCTGCC-3'
XPC_{1-766}	Forward: 5'-ATGGTACCGCCACC**ATG**GCTCGGAAAC-3' Reverse: 5'-ATACCCGGGTT**CAT**GCTGGGCAGGAA-3'
XPC_{1-831}	Forward: 5'-ATGGTACCGCCACC**ATG**GCTCGGAAAC-3' Reverse: 5'-ATGGTACC**GAC**TGCCTGCTCATTTTCCCAGG-3'
$XPC_{427-940}$	Forward: 5'-AAGGTACCGCCACC**ATG**GTGTCTTATAAA-3' Reverse: 5-'ATACCCGGGTT**CAG**CTTCTCAA-3'
$XPC_{607-940}$	Forward: 5'-ATGGTACCGCCACC**ATG**TTGAGACCATA-3' Reverse: 5-'ATACCCGGGTT**CAG**CTTCTCAA-3'
$XPC_{607-741}$	Forward: 5'-ATGGTACCGCCACC**ATG**TTGAGACCATA-3' Reverse: 5'-ATACCCGGGTC**ATA**CTCCTCTGTCTGCC-3'
$XPC_{607-766}$	Forward: 5'-ATGGTACCGCCACC**ATG**TTGAGACCATA-3' Reverse: 5'-ATACCCGGGTT**CAT**GCTGGGCAGGAA-3'
W690S	Forward: 5'-GCATTCCAGGGACACGT**C**GCTGAAGAAAGCAAGAG-3' Reverse: 5'-CTCTTGCTTTCTTCAGC**G**ACGTGTCCCTGGAATGC-3'
W690A	Forward: 5'-GCATTCCAGGGACACG**G**CGCTGAAGAAAGCAAGAG-3' Reverse: 5'-CTCTTGCTTTCTTCAGCG**C**CGTGTCCCTGGAATGC-3'
W531A	Forward: 5'-GCTGGTATAGACCAG**GC**GCTAGAGGTGTTC-3' Reverse: 5'-GAACACCTCTAGC**GC**CTGGTCTATACCAGC-3'
W542A	Forward: 5'-GAGCAGGAGGAAAAG**GC**GGTATGTGTAGAC-3' Reverse: 5'-GTCTACACATACC**GC**CTTTTCCTCCTGCTC-3'
F733A	Forward: 5'-GAAAATGACCTGGGCCTG**GC**TGGCTACTGGCAGACAGAG-3' Reverse: 5'-CTCTGTCTGCCAGTAGCCA**GC**CAGGCCCAGGTCATTTTC-3'
E755K	Forward: 5'-GTGCCCCGGAAC**A**AGTTTGGGAATGTGTACC-3' Reverse: 5'-GGTACACATTCCCAAACT**T**GTTCCGGGGCA-3'

Legends to supplementary movies

Movie 1. Accumulation of wild-type XPC in UV-damaged nuclear tracks. XPC-GFP protein was expressed in human XP-C fibroblasts and the near-infrared laser (314 GW·cm^{-2}) was used to generate a single 10-μm track of UV photoproducts across the nucleus. The damaged area is indicated by the white bar shown at the beginning of the movie. Subsequently, the dynamic distribution of XPC-GFP was monitored over a 6-min time period. A clearly distinguishable pattern of XPC-GFP accumulation is already formed 3 seconds after the induction of UV lesions.

Movie 2. Representative video illustrating that the W690S mutant is defective in the accumulation in irradiated areas containing UV lesions. An XP-C fibroblast expressing the W690S mutant was treated with a near-infrared irradiation of 314 GW·cm^{-2} to generate a 10-μm track of UV lesions identical to that of Movie 1. Subsequently, the dynamic distribution of mutant XPC-GFP was monitored over a 6-min time period.

7. Dynamic two-stage mechanism of versatile DNA damage recognition by xeroderma pigmentosum group C protein

(Review, Published in Mutation Research/Fundamental and Molecular Mechanisms of Mutagenesis)

Mutation Research 685 (2010) 21–28

Contents lists available at ScienceDirect

Mutation Research/Fundamental and Molecular Mechanisms of Mutagenesis

journal homepage: www.elsevier.com/locate/molmut
Community address: www.elsevier.com/locate/mutres

Review

Dynamic two-stage mechanism of versatile DNA damage recognition by xeroderma pigmentosum group C protein

Flurina C. Clement, Ulrike Camenisch, Jia Fei, Nina Kaczmarek, Nadine Mathieu, Hanspeter Naegeli*

Institute of Pharmacology and Toxicology, University of Zürich-Vetsuisse, Winterthurerstrasse 260, CH-8057 Zürich, Switzerland

ARTICLE INFO

Article history:
Received 3 August 2009
Accepted 7 August 2009
Available online 15 August 2009

Keywords:
Aging
Carcinogenesis
DNA damage
Mutagenesis
Xeroderma pigmentosum

ABSTRACT

The recognition and subsequent repair of DNA damage are essential reactions for the maintenance of genome stability. A key general sensor of DNA lesions is xeroderma pigmentosum group C (XPC) protein, which recognizes a wide variety of helix-distorting DNA adducts arising from ultraviolet (UV) radiation, genotoxic chemicals and reactive metabolic byproducts. By detecting damaged DNA sites, this unique molecular sensor initiates the global genome repair (GGR) pathway, which allows for the removal of all the aforementioned lesions by a limited repertoire of excision factors. A faulty GGR activity causes the accumulation of DNA adducts leading to mutagenesis, carcinogenesis, neurological degeneration and other traits of premature aging. Recent findings indicate that XPC protein achieves its extraordinary substrate versatility by an entirely indirect readout strategy implemented in two clearly discernible stages. First, the XPC subunit uses a dynamic sensor interface to monitor the double helix for the presence of non-hydrogen-bonded bases. This initial screening generates a transient nucleoprotein intermediate that subsequently matures into the ultimate recognition complex by trapping undamaged nucleotides in the abnormally oscillating native strand, in a way that no direct contacts are made between XPC protein and the offending lesion itself. It remains to be elucidated how accessory factors like Rad23B, centrin-2 or the UV-damaged DNA-binding complex contribute to this dynamic two-stage quality control process.

Contents

Abbreviations: 6-4PPs, (6-4) photoproducts; B[*a*]P, benzo[*a*]pyrene; BHD, β-hairpin domain; CPDs, cyclobutane pyrimidine dimers; ERCC1, excision repair cross complementing-1; GGR, global genome repair; NER, nucleotide excision repair; PCNA, proliferating cell nuclear antigen; RFC, replication factor C; RPA, replication protein A; TGD, transglutaminase homology domain; TFIIH, transcription factor IIH; UV, ultraviolet; UV-DDB, UV-damaged DNA-binding; XP, xeroderma pigmentosum.

* Corresponding author. Tel.: +41 44 635 87 63; fax: +41 44 635 89 10.
E-mail address: naegelih@vetpharm.uzh.ch (H. Naegeli).

0027-5107/$ – see front matter © 2009 Elsevier B.V. All rights reserved.
doi:10.1016/j.mrfmmm.2009.08.005

1. Introduction

Nucleotide excision repair (NER) is a central component of the DNA damage response network that protects the genetic integrity against permanent attacks from both environmental mutagens and endogenous reactive metabolites. In humans, NER is the only system that promotes the error-free removal of UV-induced crosslinks between adjacent bases, mainly (6-4) pyrimidine–pyrimidone photoproducts (6-4PPs) and cyclobutane pyrimidine dimers (CPDs) [1–4]. The same excision system eliminates other intrastrand crosslinks, produced for example by the antitumor drug cisplatin, and a wide diversity of bulky carcinogen–DNA adducts. In addition, this versatile reaction eliminates a subset of oxidative base lesions like 8,5′-cyclopurine nucleosides, which are not amenable to excision by DNA glycosylases [5,6], as well as DNA adducts formed from lipid peroxidation products such as malondialdehyde [7]. A common feature of these different lesions channeled into the same repair pathway is their ability to cause helical distortions, leading to abnormal oscillations of non-hydrogen-bonded nucleotides primarily in the undamaged strand [8].

The NER process operates in two distinct subpathways that differ only in the initial mechanism of DNA damage recognition. One subpathway, known as transcription-coupled repair, takes place when the transcriptional activity is obstructed by DNA lesions in the transcribed strand (reviewed by Hanawalt and Spivak [9]). In contrast, the global genome repair (GGR) subpathway is triggered by the recognition of damaged sites anywhere in the genome, including non-transcribed strands and silent chromatin regions (reviewed by Friedberg [10]). Many core factors participating in the GGR reaction are encoded by genes that, when mutated, give rise to xeroderma pigmentosum (XP), an autosomal recessive disorder characterized by photosensitivity, skin atrophy, hyperpigmentation and sunlight-induced skin cancer [1,2]. XP patients also have an increased risk of developing internal tumors and the disease is often associated with neurological manifestations attributable to oxidative damage [5–7]. Indeed, various clinical and pathological features of XP patients are similar to those seen in elderly people and, hence, reflect premature aging triggered by the accumulation of unrepaired DNA lesions [11].

Over 30 gene products are employed in the GGR pathway, which is thought to proceed by the stepwise assembly of a multiprotein excision machinery, followed by the recruitment of dedicated DNA synthesis and DNA ligation factors [1,4,10]. In higher eukaryotes, this sequential reaction is initiated by a versatile DNA damage sensor composed of XPC, Rad23B and centrin-2 [12,13]. XPC is the actual sensor subunit of this initiator complex, whereas Rad23B and centrin-2 exert accessory functions (see Section 3). The present review addresses the central question of how XPC protein examines the Watson–Crick double helix to search for base lesions and how this factor faces the task of actually finding rare sites of DNA damage among the vast excess of native DNA in a typical mammalian genome.

2. Overview of the GGR pathway

Individual steps of the GGR reaction, *i.e.*, DNA damage sensing, local DNA melting, dual DNA incision, damage excision, repair patch synthesis and DNA ligation are illustrated in Fig. 1. Upon recognition of lesion sites, the XPC complex acts as a landing platform for the recruitment of TFIIH, which among its 10 subunits comprises the two DNA helicases XPB and XPD responsible for strand separation. Further GGR players that are sequentially recruited to target sites include XPA, RPA, XPG and, finally, XPF-ERCC1 [14,15]. The DNA unwinding activity of TFIIH generates a central nucleoprotein intermediate, in which the duplex undergoes partial melting by

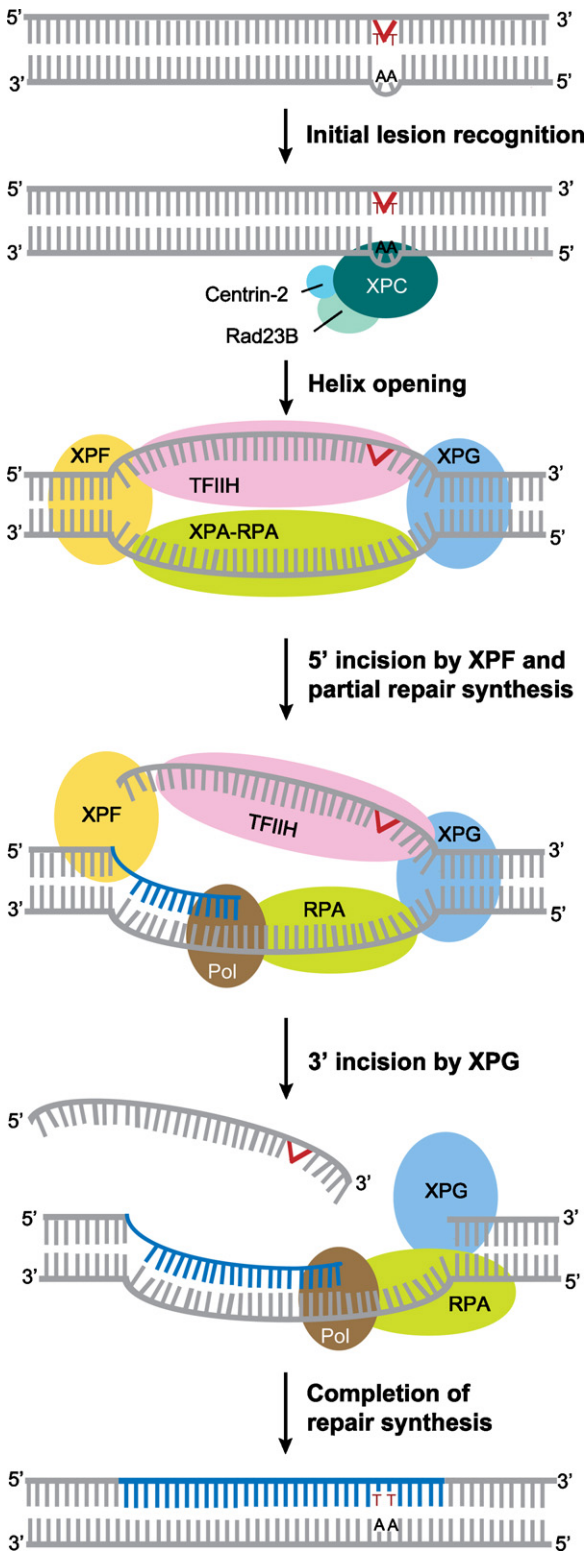

Fig. 1. Mammalian GGR pathway. Target DNA sites containing an offending lesion, for example a UV-induced 6-4PP, are detected by the XPC-Rad23B-centrin-2 complex. Subsequently, this XPC complex triggers a sequential reaction involving local DNA unwinding by TFIIH, stabilization of the open intermediate by XPA-RPA and dual DNA incision by XPF-ERCC1 and XPG. Excision and DNA repair patch synthesis occur in a coordinated manner. After completion of this cut-and-patch process, the duplex integrity is restored by DNA ligation.

about 25 nucleotides [16–18]. This open intermediate is framed by "Y-shaped" double- to single-stranded junctions, which constitute a preferred substrate for the structure-specific DNA endonucleases XPF and XPG [19,20]. The 5′ incision by XPF-ERCC1 precedes the 3′ incision by XPG [21]. Through double cleavage of the damaged strand, the combined action of these two endonucleases leads to excision of the offending lesion in the form of an oligonucleotide segment of 24–32 residues [22,23]. Duplex integrity is reestablished by the action of DNA polymerases δ, ε and κ [24,25], in conjunction with RFC and PCNA. This DNA repair synthesis is carried out in line with the initial 5′ incision, thus avoiding that excision of an oligonucleotide fragment causes the transient exposure of single-stranded DNA, which is at risk to be converted to a double-stranded break by inadvertent nuclease activity [21]. Finally, the newly synthesized repair patch is joined to the pre-existing strand by DNA ligase I and DNA ligase III [26,27].

3. Initiation of GGR activity by the XPC complex

In the cellular context, the XPC polypeptide (125 kDa) is found in association with Rad23B, a 58-kDa homolog of the yeast Rad23 protein [28], and centrin-2, a 18-kDa centrosomal factor [29]. XPC protein itself possesses DNA-binding activity, whereas the ubiquitin-binding Rad23B and the calcium-binding centrin-2 protect the initiator complex from degradation and stimulate its activity in DNA repair [28,30]. In double-mutant mouse cells lacking Rad23B as well as the functionally redundant Rad23A ortholog, XPC protein is completely degraded by proteasomal activity [31].

The XPC subunit alone or in combination with Rad23B binds preferentially to damaged DNA substrates containing, for example, 6-4PPs, B[*a*]P diol epoxide adducts, acetylaminofluorene adducts or cisplatin crosslinks [32–34]. More detailed biochemical analyses with defined nucleic acid substrates revealed that XPC protein displays a general affinity for DNA sites that deviate from the canonical Watson–Crick geometry, including single-stranded loops, mismatched bubbles or single-stranded overhangs [35,36]. According to scanning force microscopy studies, the binding of XPC protein to DNA induces a kink of 39–49° in the nucleic acid backbone regardless of whether the substrate is damaged or not [37]. Permanganate footprinting studies demonstrate that the observed sharp bending is accompanied by partial melting of the duplex extending over 4–7 base pairs [34,38].

These conformational changes in the DNA helix have been further examined at atomic resolution by crystallization of parts of Rad4 protein, a yeast ortholog that shares ∼40% similarity and ∼25% identity with the human XPC sequence. In co-crystals with heteroduplex DNA carrying a single CPD, Rad4 protein binds to the substrate in a bimodal manner [39]. One portion of Rad4 protein, consisting of its large transglutaminase homology domain (TGD) in conjunction with a short β-hairpin domain (BHD1), forms a C-clamp-like structure that interacts with 11 base pairs of native double-stranded DNA located on the 3′ side of the lesion (Fig. 2A). The TGD region, which provides one tip of the C-clamp, displays an intriguing similarity to the transglutaminase fold of peptide-*N*-glycanases that remove glycan modifications from proteins. Unlike other members of this enzyme family, however, Rad4 lacks the predicted catalytic triad (Cys-His-Asp) [40]. As illustrated in the scheme of Fig. 2B, the homologous TGD segment of human XPC protein is separated into two individual parts by a disordered ∼180 residue insertion [41].

Another portion of Rad4 protein, composed of the β-hairpin domains BHD2 and BHD3, folds into a hand-like structure that associates with a 4-nucleotide DNA segment at the lesion site. As will be discussed in Section 4, most of these interactions made by BHD2/BHD3 are van der Waals contacts with the undamaged strand of the substrate. We previously found that there is ∼75% amino acid similarity and ∼30% identity between this central DNA-binding region of XPC protein (Fig. 2B) and the oligonucleotide/oligosaccharide-binding fold (OB-fold) of RPA-B, one of the single-stranded DNA-binding motifs of human RPA [42]. Such an intriguing sequence similarity extends to two OB-folds of breast cancer protein-2, another factor with selectivity for single-stranded conformations, thus suggesting that the damage sensor core of XPC protein may have emerged during evolution from an ancient single-stranded DNA-binding protein.

In proximity to the CPD lesion, the Rad4 protein-DNA structure is characterized by two characteristic features (Fig. 2A). First, a long β-hairpin protruding from BHD3 is inserted into the double helix, thus inducing a kink of 42° in the DNA backbone. Second, this β-hairpin invasion causes extrahelical displacements involving not only the crosslinked pyrimidines, making up the CPD, but also the opposing native bases in the undamaged strand (Fig. 2A). Each one of these flipped-out normal residues is sandwiched between aromatic side chains provided by the BHD2/BHD3 motifs. Finally, the crystallized Rad4 complex also includes a polypeptide fragment representing Rad23 protein and, therefore, has been able to solve the previous ambiguity [43,44] over the precise amino acids mediating the Rad4–Rad23 association. In fact, the incorporated Rad23 polypeptide interacts with several residues mapping to the beginning and the end of the TGD region, in the N-terminal region of Rad4. These particular Rad4–Rad23 interaction sites are consistent with an earlier report demonstrating that an XPC fragment extending from residues 607 to 940, not containing the TGD region, fails to form complexes with the human Rad23 homolog [44]. The N-terminal region of human XPC is responsible for an association with XPA [41]. On the other hand, the carboxy-terminal tail of XPC protein harbors domains that interact with centrin-2 (residues 847–863) and TFIIH (residues 816–940) [30,44].

4. The molecular basis for substrate versatility

A long unanswered question has been the mechanism by which Rad4/XPC protein achieves its ability to detect a wide spectrum of damaged substrates. There is no common chemical feature of the different DNA adducts that would permit a classic "lock and key" recognition scheme. Instead, the observed substrate versatility of the GGR pathway implies that its promiscuous initiator, XPC protein, acts by recognizing damage-induced distortions of the DNA helix rather than specific base modifications. In support of this hypothesis, it has been observed that the GGR system exhibits a general preference for base adducts that lower the melting temperature of double-stranded DNA [45], suggesting that XPC protein may detect the single-stranded character of damaged sites carrying bulky lesions. However, not in all cases the degree of duplex destabilization correlates with excision efficiency. For example, the more helix-destabilizing (+)- or (−)-*trans*-B[*a*]P-dG adducts are excised at lower rates in reconstituted GGR systems compared to their (+)- or (−)-*cis*-B[*a*]P-dG isomers, where the pyrenyl ring moiety exerts helix-stabilizing effects by intercalating between neighboring base pairs [34,46].

A straightforward approach to address the mechanism of bulky lesion recognition has been to identify a critical structural determinant of damaged DNA that provides the initial binding site for the assembly of GGR complexes. Towards that goal, Hess et al. [47] constructed a series of synthetic DNA duplexes to show that a non-distorting adduct is only amenable to excision in a reconstituted GGR system when the substrate also contains a DNA bulge generated by the insertion of 1–3 base pair mismatches. Subsequently, Buterin et al. [48] elaborated on this molecular strategy to generate substrates where a non-distorting adduct is accompanied by

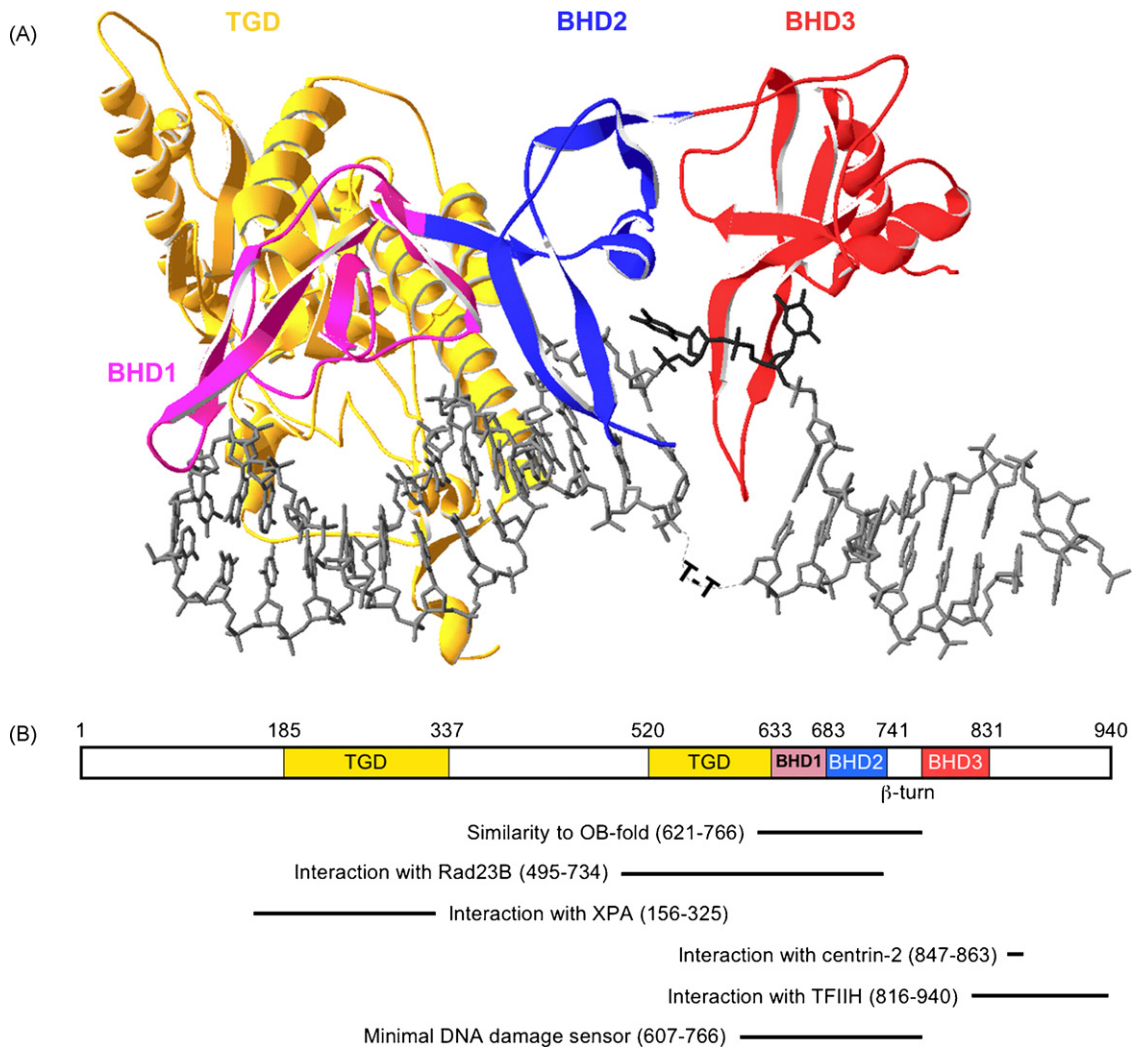

Fig. 2. Structure of XPC protein inferred from the yeast (*Saccaromyces cerevisiae*) Rad4 homolog. (A) Ribbon diagram of the crystal structure of a Rad4 protein fragment (residues 123–632) in complex with heteroduplex DNA carrying a CPD lesion [39]. Multiple Rad4 domains interact with the DNA substrate: TGD (gold), BHD1 (magenta), BHD2 (blue) and BHD3 (red). T-T denotes the CPD, which is totally expelled from the duplex. The figure was made with the Swiss-PdbViewer using the coordinates PDB 2QSG. (B) Scheme of the homologous domains in the human XPC sequence. Also shown are the region of sequence similarity with OB-folds [42], the domains involved in interactions with Rad23B [44], XPA [41], centrin-2 [30] and TFIIH [44], as well as the newly identified minimal DNA damage sensor interface [54].

local duplex deformations in opposite directions relative to the long axis of DNA. They discovered that the target adduct becomes refractory to GGR activity when, by deletion of 3 nucleotides in the undamaged strand, only the adduct-carrying sequence is bulged out of the double helix. In contrast, the same non-distorting adduct is efficiently excised when, by insertion of 3 nucleotides in the undamaged strand, the opposing native strand is bulged out of the double helix. These findings obtained with artificial constructs were confirmed by the observation that at least one destabilized nucleotide in the undamaged strand is necessary to attract the GGR system to B[*a*]P or acetylaminofluorene carcinogen–DNA adducts. Also, excision activity was suppressed by various backbone or base modifications introduced in the undamaged strand across lesion sites indicating that adduct removal involves intimate contacts with the distorted but chemically intact complementary strand [48].

Collectively, these findings converge on the conclusion that XPC protein initiates the GGR reaction by detecting non-hydrogen-bonded bases on the undamaged side of the double helix. In agreement with the identification of an amino acid sequence related to single-stranded DNA-binding motifs (see Section 3), we found that purified XPC protein indeed displays a strong preference for single-stranded oligonucleotides over duplexes of the same length. Surprisingly, XPC exhibits an unfavorable binding to damaged single-stranded oligonucleotides compared to the more efficient interaction with native counterparts [33,42]. This exquisite affinity for single-stranded conformations, in combination with its aversion to interact with damaged single strands, confirms that XPC protein binds primarily to non-hybridizing nucleotides in the undamaged strand, where it makes close interactions with backbone moieties and bases of the normal complementary sequence, in order to load downstream GGR subunits onto damaged substrates. This mechanism has been defined as "indirect conformational readout" because XPC protein detects an abnormal conformational feature in the undamaged strand rather than recognizing specifically modified groups in the damaged sequence [42]. Further support for this unprecedented mode of DNA lesion recognition has been provided by the Rad4 crystal structure, where the BHD2/BHD3 region interacting with the target site makes contacts exclusively with the native complementary strand (Fig. 2A). Conversely, absolutely no interactions occur between Rad4 protein and the modified bases, which are expelled from the recognition complex [39]. This inverted mode of DNA quality control presents the obvious advantage that the

initial sensor does not need to recognize the adducts themselves and, as outlined before, actually avoids close contacts with damaged residues. The general affinity for destabilized DNA sites may facilitate other repair processes, as XPC has been shown to interact with 3-methyladenine DNA glycosylase [49], thymine DNA glycosylase [50] and 8-oxoguanine DNA glycosylase [6]. It is relevant to note that even a subtle 8-oxoguanine lesion perturbs the thermodynamic stability of the duplex [51]. Accordingly, the XPC complex may provide a molecular platform not only for the loading of GGR players onto damaged DNA, but also for the recruitment of a battery of enzymes involved in base excision or other repair pathways.

5. Dynamic search for DNA lesions in the physiologic chromatin context

In cultured mammalian cells, the nuclear distribution of XPC protein correlates with the degree of DNA condensation yielding a typical chromatin-like pattern. Photobleaching experiments indicate that this non-homogenous distribution reflects a tight association with native DNA. In fact, unlike other GGR subunits, XPC protein is not freely mobile in the nuclear compartment, presumably due to constitutive interactions with the normal DNA helix [52,53].

The apparently tight association of XPC protein with undamaged DNA raises the question of how this recognition factor scrutinizes the genome to detect rare aberrant sites among a vast background of the native nucleic acid. In order to address this fundamental issue, we took advantage of fluorescence-based imaging techniques to visualize the mobility of XPC molecules at work in the chromatin context. Real-time kinetics (based on laser-induced high-resolution tracks of UV lesions) and protein dynamics studies (based on fluorescence recovery after photobleaching) were combined to bidirectional truncation analyses, thus revealing that a surprisingly short recognition hotspot, comprising ~15% of human XPC, is necessary and sufficient to detect UV lesions in living cells [54]. This minimal sensor interface of human XPC includes BHD1 and BHD2, together with a short adjacent motif that folds into a β-turn structure (Fig. 2B), but not BHD3, which was thought to represent the primary lesion recognition module on the basis of the Rad4 crystal structure [39]. On its own, a purified polypeptide fragment consisting only of BHD1 and BHD2 displays a preference for heteroduplex over homoduplex and single-stranded oligonucleotides, confirming that the newly identified minimal sensor interface recognizes damaged sites using its inherent affinity for non-hydrogen-bonded bases. However, in living cells, the efficacy of this minimal recognition hotspot depends on the DNA-repulsive action exerted by an additional motif that coincides with the adjacent β-turn structure [54].

In brief, the evidence for a dynamic DNA-repulsive role of the β-turn motif (residues 742–766) in enhancing the efficiency of DNA damage recognition is as follows. First, C-terminal XPC truncates containing this motif display a residual GGR activity, determined by host-cell reactivation assays, that is missing with shorter truncates lacking the β-turn sequence. Second, the partial GGR proficiency observed in the presence of the β-turn structure correlates with a more efficient relocation to tracks of UV lesions. Third, protein dynamics assays performed by photobleaching demonstrate that the β-turn motif confers an increased nuclear mobility in living cells. Fourth, again in photobleaching experiments, only the nuclear mobility of C-terminal XPC truncates containing the β-turn motif is retarded upon UV irradiation, confirming that this critical subdomain increases the rate of DNA damage recognition. Fifth, as outlined before, a polypeptide fragment comprising BHD1 and BHD2 acts as a minimal sensor of DNA damage in living cells only in conjunction with the accompanying β-turn structure. Sixth, biochemical experiments indicate that the nuclear mobility mediated by this β-turn structure is the consequence of a repulsion from native double-stranded DNA. Finally, in the context of full-length XPC protein, the dynamic role of this β-turn structure is supported by a site-directed glutamic acid to lysine substitution. This charge inversion was introduced on the assumption that it may mitigate repulsive electrostatic forces between the negatively charged protein side chain and phosphate moieties in the DNA backbone. As expected, the tested charge inversion increases the affinity for native DNA, thus generating mutant XPC molecules that display a reduced nuclear mobility and diminished GGR activity [54]. In conclusion, these novel findings converge on a key role of the β-turn structure in regulating the dynamic interplay with normal duplex DNA. By virtue of its DNA-repellent activity, this subdomain facilitates damage recognition by providing sufficient mobility to XPC molecules searching for lesions in the genome.

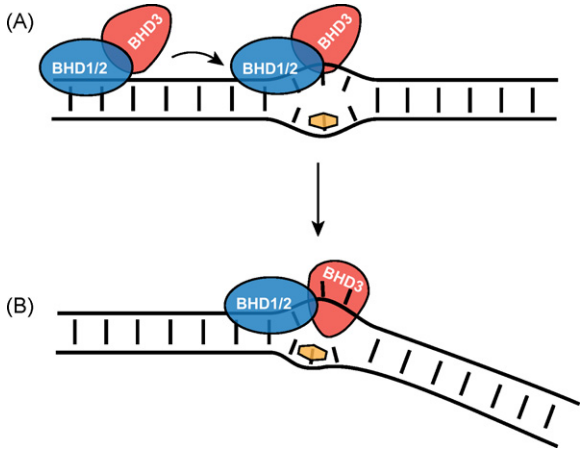

Fig. 3. Two-stage detection of DNA lesions by XPC protein. (A) The minimal sensor interface, consisting of BHD1, BHD2 and the β-turn structure, scrutinizes base pair integrity and forms a labile nucleoprotein intermediate in the proximity to non-hydrogen-bonded bases. (B) The single-stranded DNA-binding activity of BHD3 promotes the subsequent transition to a stable recognition complex by capturing extrahelically oscillating nucleotides in the undamaged strand.

6. Two-stage discrimination process

Although the BHD3 segment of XPC protein and its long protruding β-hairpin are not required for the initial damage sensing process (Section 5), photobleaching experiments in living cells demonstrate that this additional domain is responsible for the formation of stable nucleoprotein complexes, thus generating an immobile fraction of XPC protein in response to UV irradiation [54]. The biochemical analysis of purified fragments shows that, in contrast to the BHD1/BHD2/β-turn minimal sensor, which displays a preference for non-hydrogen-bonded bases in duplex DNA, BHD3 confers an exquisite selectivity for single-stranded DNA conformations. In fact, like full-length XPC protein [42], a polypeptide fragment covering BHD1–BHD3 binds preferentially to single-stranded oligonucleotides. From these findings, it appears that BHD3 does not participate in the early and transient recognition intermediate but, instead, facilitates the subsequent stabilization of a repair-initiating nucleoprotein complex using its single-stranded DNA-binding activity to encircle the strand across lesion sites.

Taken together, our recent studies of XPC kinetics and dynamics point to a two-stage discrimination mechanism by which XPC protein carries out its versatile recognition function (Fig. 3). This two-stage process obviates the difficulty of probing every genomic base pair for its susceptibility to undergo β-hairpin insertion, which is one of the principal features of the reported Rad4 crystal structure

[39]. Instead, the rapid and energetically less demanding search conducted by the dynamic BHD1/BHD2/β-turn interface is likely to precede the more extensive conformational adjustments required for the β-hairpin intrusion. As illustrated in Fig. 3, this initial search leads to the detection of non-hydrogen-bonded bases that are more prone than native residues to be displaced from the double helix by engagement of the β-hairpin. A critical step of this two-stage quality control process is the transition from an initially labile sensor intermediate to the more stable ultimate recognition complex. It is likely that the energetic cost of this nucleoprotein transition is lowered by damage-induced strand oscillations appearing primarily on the undamaged side of the double helix [8], thus displacing the unstable nucleotides into an extrahelical position where they are easily captured by the single-stranded DNA-binding motif of XPC protein. However, it is also possible that Rad23B or centrin-2 may promote the two-stage discrimination process of XPC protein by accelerating the nucleoprotein rearrangements required for engagement of the β-hairpin with damaged sites.

7. The special case of CPD recognition

Another interaction partner of XPC is the UV-damaged DNA-binding (UV-DDB) protein. This factor has been isolated from tissue extracts in view of its characteristic binding to UV-irradiated DNA [55] and, indeed, UV-DDB displays the highest reported affinity for substrates containing 6-4PPs and CPDs [56–58]. UV-DDB consists of p127 (DDB1) and p48 (DDB2), with the small subunit being encoded by the *XPE* gene [59–61]. A recent crystallographic analysis demonstrated that the binding of UV-DDB to UV lesions is entirely mediated by the DDB2 subunit, which accommodates the crosslinked pyrimidines into a specialized binding pocket and inserts a three-amino acid hairpin into the DNA minor groove [62]. DDB1, on the other hand, is an adaptor that connects the Cul4A-RBX1 ubiquitin ligase to WD40-repeat target proteins [63,64], including DDB2 itself [65,66]. Other known substrates of the Cul4A-RBX1-DDB1 ubiquitin ligase include XPC [67] as well as the core histones H2A, H3 and H4 [68,69].

Although CPDs represent the most frequent lesions generated by sunlight, this particular type of DNA injury escapes direct detection by the XPC complex because it causes only a low degree of structural perturbation. The problem of CPD recognition is exemplified by XP-E cells, which are heavily compromised in the repair of CPDs due to their defective UV-DDB activity, but nevertheless retain the ability to excise 6-4PPs [70,71]. Similarly, rodent cells that fail to express DDB2 protein, as a consequence of promoter methylation, are inefficient in CPD repair [72]. The DDB2 subunit rapidly accumulates at sites of UV-induced DNA lesions and the recruitment of XPC protein to DNA repair foci containing exclusively CPDs is dependent on the UV-DDB complex [73,74]. Two major hypotheses have been forwarded for the mechanism by which UV-DDB contributes to the recognition of UV lesions. The handover hypothesis has been proposed on the basis of *in vitro* assays indicating that ubiquitin modulates the DNA-binding affinity of DDB2 and XPC [67]. In this scenario, UV-DDB recognizes UV lesions and recruits XPC protein through direct protein–protein interactions. Subsequently, polyubiquitylation of DDB2 reduces its affinity for DNA and results in degradation, whereas polyubiquitylation of XPC preserves its affinity for the DNA substrate [67]. The chromatin remodeling hypothesis is prompted by the observation that DDB2 is not absolutely required for the excision of CPDs by reconstituted GGR systems using naked DNA as the substrate [74]. This finding may be taken as evidence in favor of a function of UV-DDB in mediating a local relaxation of chromatin, which in turn facilitates XPC binding to damaged sites [68,69]. Additionally, the recently discovered two-stage discrimination process of XPC protein (Fig. 3) raises the possibility that UV-DDB may act in an analogous two-step manner. First, UV-DDB may bypass the initial sensing process, which is ineffective for CPDs, through direct XPC recruitment as postulated in the handover hypothesis. Subsequently, UV-DDB may coordinate the correct positioning of the BHD1–BHD3 motifs onto the undamaged strand and trigger the β-hairpin insertion at CPD sites.

8. Conclusion

The earlier hypothesis that XPC protein simply detects the single-stranded character of lesion sites [42] has been revisited in light of recent findings that this versatile sensor adopts a two-stage mechanism of substrate discrimination [54]. As illustrated in Fig. 3, XPC protein deploys a dynamic interface to screen for non-hydrogen-bonded bases in duplex DNA before undergoing tight interactions mediated by its intrinsic single-stranded DNA-binding activity. Both stages of this substrate discrimination process are directed to the native complementary strand across lesion sites, such that this early recognition step becomes independent of the variable chemistry of damaged sites, thereby broadening the spectrum of DNA lesions that can be channeled into the versatile GGR system. It is important to point out that XPC protein detects non-hydrogen-bonded bases even in the absence of DNA lesions, implying the existence of "proofreading" or "damage verification" factors in the GGR pathway. Candidate mechanisms for this downstream function are the enzymatic scanning by DNA helicases [75] or the sensing of DNA bendability by XPA protein [76,77]. The participation of a scanning mechanism, involving active translocation along the DNA molecule, is supported by our observation that an effective double check process, leading to excision, still takes place on composite substrates where the site of XPC binding is physically dislocated from the target adduct [78].

Acknowledgments

Work in the authors' laboratory is supported by the Swiss National Science Foundation (grant 31003A-127499) and by Oncosuisse (grant KLS-01827-02-2006).

References

[1] E.C. Friedberg, G.C. Walker, W. Siede, R.D. Wood, R.A. Schultz, T. Ellenberger, DNA Repair and Mutagenesis, ASM Press, Washington, D.C., 2006.
[2] J.H. Hoeijmakers, Genome maintenance mechanisms for preventing cancer, Nature 411 (2001) 366–374.
[3] A. Sancar, DNA excision repair, Annu. Rev. Biochem. 65 (1996) 43–81.
[4] R.D. Wood, Nucleotide excision repair in mammalian cells, J. Biol. Chem. 272 (1997) 23465–23468.
[5] I. Kuraoka, C. Bender, A. Romieu, J. Cadet, R.D. Wood, T. Lindahl, Removal of oxygen free-radical-induced 5′,8-purine cyclodeoxynucleosides from DNA by the nucleotide excision-repair pathway in human cells, Proc. Natl. Acad. Sci. U.S.A. 97 (2000) 3832–3837.
[6] M. D'Errico, E. Parlanti, M. Teson, B.M. de Jesus, P. Degan, A. Calcagnile, P. Jaruga, M. Bjoras, M. Crescenzi, A.M. Pedrini, J.M. Egly, G. Zambruno, M. Stefanini, M. Dizdaroglu, E. Dogliotti, New functions of XPC in the protection of human skin cells from oxidative damage, EMBO J. 25 (2006) 4305–4315.
[7] K.A. Johnson, S.P. Fink, L.J. Marnett, Repair of propanodeoxyguanosine by nucleotide excision repair *in vivo* and *in vitro*, J. Biol. Chem. 272 (1997) 11434–11438.
[8] O. Maillard, U. Camenisch, F.C. Clement, K.B. Blagoev, H. Naegeli, DNA repair triggered by sensors of helical dynamics, Trends Biochem. Sci. 32 (2007) 494–499.
[9] P.C. Hanawalt, G. Spivak, Transcription-coupled DNA repair: two decades of progress and surprises, Nat. Rev. Mol. Cell Biol. 9 (2008) 958–970.
[10] E.C. Friedberg, How nucleotide excision repair protects against cancer, Nat. Rev. Cancer 1 (2001) 22–33.
[11] L.J. Niedernhofer, Tissue-specific accelerated aging in nucleotide excision repair deficiency, Mech. Ageing Dev. 129 (2008) 408–415.
[12] K. Sugasawa, J.M. Ng, C. Masutani, S. Iwai, P.J. van der Spek, A.P. Eker, F. Hanaoka, D. Bootsma, J.H. Hoeijmakers, Xeroderma pigmentosum group C protein complex is the initiator of global genome nucleotide excision repair, Mol. Cell 2 (1998) 223–232.

[13] M. Volker, M.J. Mone, P. Karmakar, A. van Hoffen, W. Schul, W. Vermeulen, J.H. Hoeijmakers, R. van Driel, A.A. van Zeeland, L.H. Mullenders, Sequential assembly of the nucleotide excision repair factors in vivo, Mol. Cell 8 (2001) 213–224.
[14] D. Mu, D.S. Hsu, A. Sancar, Reaction mechanism of human DNA repair excision nuclease, J. Biol. Chem. 271 (1996) 8285–8294.
[15] S.J. Araujo, F. Tirode, F. Coin, H. Pospiech, J.E. Syväoja, M. Stucki, U. Hübscher, J.-M. Egly, R.D. Wood, Nucleotide excision repair of DNA with recombinant human proteins: definition of the minimal set of factors, active forms of TFIIH, and modulation by CAK, Genes Dev. 14 (2000) 349–359.
[16] E. Evans, J. Fellows, A. Coffer, R.D. Wood, Open complex formation around a lesion during nucleotide excision repair provides a structure for cleavage by human XPG protein, EMBO J. 16 (1997) 625–638.
[17] M. Wakasugi, A. Sancar, Assembly, subunit composition, and footprint of human DNA repair excision nuclease, Proc. Natl. Acad. Sci. U.S.A. 95 (1998) 6669–6674.
[18] F. Tirode, D. Busso, F. Coin, J.M. Egly, Reconstitution of the transcription factor TFIIH: assignment of functions for the three enzymatic subunits, XPB, XPD, and cdk7, Mol. Cell 3 (1999) 87–95.
[19] A.M. Sijbers, W.L. de Laat, R.R. Ariza, M. Biggerstaff, Y.F. Wei, J.C. Moggs, K.C. Carter, B.K. Shell, E. Evans, M.C. de Jong, S. Rademakers, J. de Rooij, N.G. Jaspers, J.H. Hoeijmakers, R.D. Wood, Xeroderma pigmentosum group F caused by a defect in a structure-specific DNA repair endonuclease, Cell 86 (1996) 811–822.
[20] A. O'Donovan, A.A. Davies, J.C. Moggs, S.C. West, R.D. Wood, XPG endonuclease makes the 3′ incision in human DNA nucleotide excision repair, Nature 371 (1994) 432–435.
[21] L. Staresincic, A.F. Fagbemi, J.H. Enzlin, A.M. Gourdin, N. Wijgers, I. Dunand-Sauthier, G. Giglia-Mari, S.G. Clarkson, W. Vermeulen, O.D. Schärer, Coordination of dual incision and repair synthesis in human nucleotide excision repair, EMBO J. 28 (2009) 1111–1120.
[22] J.C. Huang, D.L. Svoboda, J.T. Reardon, A. Sancar, Human nucleotide excision nuclease removes thymine dimers from DNA by incising the 22nd phosphodiester bond 5′ and the 6th phosphodiester bond 3′ to the photodimer, Proc. Natl. Acad. Sci. U.S.A. 89 (1992) 3664–3668.
[23] J.G. Moggs, K.J. Yarema, J.M. Essigmann, R.D. Wood, Analysis of incision sites produced by human cell extracts and purified proteins during nucleotide excision repair of a 1,3-intrastrand d(GpTpG)-cisplatin adduct, J. Biol. Chem. 271 (1996) 7177–7186.
[24] M.K. Shivji, V.N. Podust, U. Hübscher, R.D. Wood, Nucleotide excision repair DNA synthesis by DNA polymerase epsilon in the presence of PCNA, RCF, and RPA, Biochemistry 34 (1995) 5011–5017.
[25] T. Ogi, A.R. Lehmann, The Y-family DNA polymerase kappa (pol kappa) functions in mammalian nucleotide-excision repair, Nat. Cell Biol. 8 (2006) 640–642.
[26] A. Aboussekhra, M. Biggerstaff, M.K. Shivji, J.A. Vilpo, V. Moncollin, V.N. Podust, M. Protic, U. Hübscher, J.M. Egly, R.D. Wood, Mammalian DNA nucleotide excision repair reconstituted with purified protein components, Cell 80 (1995) 859–868.
[27] J. Moser, H. Kool, I. Giakzidis, K. Caldecott, L.H. Mullenders, M.I. Fousteri, Sealing of chromosomal DNA nicks during nucleotide excision repair requires XRCC1 and DNA ligase III alpha in a cell-cycle-specific manner, Mol. Cell 27 (2007) 311–323.
[28] C. Masutani, K. Sugasawa, J. Yanagisawa, T. Sonoyama, M. Ui, T. Enomoto, K. Takio, K. Tanaka, P.J. van der Spek, D. Bootsma, J.H. Hoeijmakers, F. Hanaoka, Purification and cloning of a nucleotide excision repair complex involving the xeroderma pigmentosum group C protein and a human homologue of yeast RAD23, EMBO J. 13 (1994) 1831–1843.
[29] M. Araki, C. Masutani, M. Takemura, A. Uchida, K. Sugasawa, J. Kondoh, Y. Ohkuma, F. Hanaoka, Centrosome protein centrin 2/caltractin 1 is part of the xeroderma pigmentosum group C complex that initiates global genome nucleotide excision repair, J. Biol. Chem. 276 (2001) 18665–18672.
[30] R. Nishi, Y. Okuda, E. Watanabe, T. Mori, S. Iwai, C. Masutani, K. Sugasawa, F. Hanaoka, Centrin 2 stimulates nucleotide excision repair by interacting with xeroderma pigmentosum group C protein, Mol. Cell. Biol. 25 (2005) 5664–5674.
[31] J.M. Ng, W. Vermeulen, G.T. van der Horst, S. Bergink, K. Sugasawa, H. Vrieling, J.H. Hoeijmakers, A novel regulation mechanism of DNA repair by damage-induced and RAD23-dependent stabilization of xeroderma pigmentosum group C protein, Genes Dev. 17 (2003) 1630–1645.
[32] D. Batty, V. Rapic'-Otrin, A.S. Levine, R.D. Wood, Stable binding of human XPC complex to irradiated DNA confers strong discrimination for damaged sites, J. Mol. Biol. 300 (2000) 275–290.
[33] K.S. Trego, J.J. Turchi, Pre-steady-state binding of damaged DNA by XPC-hHR23B reveals a kinetic mechanism for damage discrimination, Biochemistry 45 (2006) 1961–1969.
[34] V. Mocquet, K. Kropachev, M. Kolbanovskiy, A. Kolbanovskiy, A. Tapias, Y. Cai, S. Broyde, N.E. Geacintov, J.M. Egly, The human DNA repair factor XPC-HR23B distinguishes stereoisomeric benzo[*a*]pyrenyl-DNA lesions, EMBO J. 26 (2007) 2923–2932.
[35] K. Sugasawa, T. Okamoto, Y. Shimizu, C. Masutani, S. Iwai, F. Hanaoka, A multistep damage recognition mechanism for global genomic nucleotide excision repair, Genes Dev. 15 (2001) 507–521.
[36] K. Sugasawa, Y. Shimizu, S. Iwai, F. Hanaoka, A molecular mechanism for DNA damage recognition by the xeroderma pigmentosum group C protein complex, DNA Repair 1 (2002) 95–107.
[37] A. Janicijevic, K. Sugasawa, Y. Shimizu, F. Hanaoka, N. Wijgers, M. Djurica, J.H. Hoeijmakers, C. Wyman, DNA bending by the human damage recognition complex XPC-HR23B, DNA Repair (Amst) 2 (2003) 325–336.
[38] E. Evans, J.G. Moggs, J.R. Hwang, J.M. Egly, R.D. Wood, Mechanism of open complex and dual incision formation by human nucleotide excision repair factors, EMBO J. 16 (1997) 6559–6573.
[39] J.-H. Min, N.P. Pavletich, Recognition of DNA damage by the Rad4 nucleotide excision repair protein, Nature 449 (2007) 570–575.
[40] V. Anantharaman, E.V. Koonin, L. Aravind, Peptide-N-glycanases and DNA repair proteins, Xp-C/Rad4, are, respectively, active and inactivated enzymes sharing a common transglutaminase fold, Hum. Mol. Genet. 10 (2001) 1627–1630.
[41] C.G. Bunick, M.R. Miller, B.E. Fuller, E. Fanning, W.J. Chazin, Biochemical and structural domain analysis of xeroderma pigmentosum complementation group C protein, Biochemistry 45 (2006) 14965–14979.
[42] O. Maillard, S. Solyom, H. Naegeli, An aromatic sensor with aversion to damaged strands confers versatility to DNA repair, PLoS Biol. 5 (2007) e79.
[43] L. Li, X. Lu, C. Peterson, R. Legerski, XPC interacts with both HHR23B and HHR23A in vivo, Mutat. Res. 383 (1997) 197–203.
[44] A. Uchida, K. Sugasawa, C. Masutani, N. Dohmae, M. Araki, M. Yokoi, Y. Ohkuma, F. Hanaoka, The carboxy-terminal domain of the XPC protein plays a crucial role in nucleotide excision repair through interactions with transcription factor IIH, DNA Repair 1 (2002) 449–461.
[45] D. Gunz, M.T. Hess, H. Naegeli, Recognition of DNA adducts by human nucleotide excision repair. Evidence for a thermodynamic probing mechanism, J. Biol. Chem. 271 (1996) 25089–25098.
[46] M.T. Hess, D. Gunz, N. Luneva, N.E. Geacintov, H. Naegeli, Base pair conformation-dependent excision of benzo[a]pyrene diol epoxide-guanine adducts by human nucleotide excision repair enzymes, Mol. Cell. Biol. 17 (1997) 7069–7076.
[47] M.T. Hess, U. Schwitter, M. Petretta, B. Giese, H. Naegeli, Bipartite substrate discrimination by human nucleotide excision repair, Proc. Natl. Acad. Sci. U.S.A. 94 (1997) 6664–6669.
[48] T. Buterin, C. Meyer, B. Giese, H. Naegeli, DNA quality control by conformational readout on the undamaged strand of the double helix, Chem. Biol. 12 (2005) 913–922.
[49] F. Miao, M. Bouziane, R. Dammann, C. Masutani, F. Hanaoka, G. Pfeifer, T.R. O'Connor, 3-Methyladenine-DNA glycosylase (MPG protein) interacts with human RAD23 proteins, J. Biol. Chem. 275 (2000) 28433–28438.
[50] Y. Shimizu, S. Iwai, F. Hanaoka, K. Sugasawa, Xeroderma pigmentosum group C protein interacts physically and functionally with thymine DNA glycosylase, EMBO J. 22 (2003) 164–173.
[51] G.E. Plum, A.P. Grollman, F. Johnson, K.J. Breslauer, Influence of the oxidatively damaged adduct 8-oxodeoxyguanosine on the conformation, energetics, and thermodynamic stability of a DNA duplex, Biochemistry 34 (1995) 16148–16160.
[52] D. Hoogstraten, S. Bergink, V.H.M. Verbiest, M.S. Luijsterburg, B. Geverts, A. Raams, C. Dinant, J.H.J. Hoeijmakers, W. Vermeulen, A.B. Houtsmuller, Versatile DNA damage detection by the global genome nucleotide excision repair protein XPC, J. Cell Sci. 121 (2008) 2850–2859.
[53] L. Solimando, M.S. Luijsterburg, L. Vecchio, W. Vermeulen, R. van Driel, S. Fakan, Spatial organization of nucleotide excision repair proteins after UV-induced DNA damage in the human cell nucleus, J. Cell Sci. 122 (2009) 83–91.
[54] U. Camenisch, D. Träutlein, F. Clement, J. Fei, A. Leitenstorfer, E. Ferrando-May, H. Naegeli, Two-stage dynamic DNA quality check by xeroderma pigmentosum group C protein, EMBO J. 28 (2009) 2387–2399.
[55] R.S. Feldberg, L. Grossman, A DNA binding protein from human placenta specific for ultraviolet damaged DNA, Biochemistry 15 (1976) 2402–2408.
[56] B.J. Hwang, G. Chu, Purification and characterization of a human protein that binds to damaged DNA, Biochemistry 32 (1993) 1657–1666.
[57] J.T. Reardon, A.F. Nichols, S. Keeney, C.A. Smith, J.S. Taylor, S. Linn, A. Sancar, Comparative analysis of binding of human damaged DNA-binding protein (XPE) and *Escherichia coli* damage recognition protein (UvrA) to the major ultraviolet photoproducts: T[c,s]T, T[t,s]T, T[6-4]T, and T[Dewar]T, J. Biol. Chem. 268 (1993) 21301–21308.
[58] B.O. Wittschieben, S. Iwai, R.D. Wood, DDB1–DDB2 (xeroderma pigmentosum group E) protein complex recognizes a cyclobutane pyrimidine dimer, mismatches, apurinic/apyrimidinic sites, and compound lesions in DNA, J. Biol. Chem. 280 (2005) 39982–39989.
[59] R. Dualan, T. Brody, S. Keeney, A.F. Nichols, A. Admon, S. Linn, Chromosomal localization and cDNA cloning of the genes (*DDB1* and *DDB2*) for the p127 and p48 subunits of a human damage-specific DNA binding protein, Genomics 29 (1995) 62–69.
[60] A.F. Nichols, P. Ong, S. Linn, Mutations specific to the xeroderma pigmentosum group E DDB$^{(-)}$ phenotype, J. Biol. Chem. 271 (1996) 24317–24320.
[61] V. Rapic-Otrin, V. Navazza, T. Nardo, E. Botta, M. McLenigan, D.C. Bisi, A.S. Levine, M. Stefanini, True XP group E patients have a defective UV-damaged DNA binding protein complex and mutations in *DDB2* which reveal the functional domains of its p48 product, Hum. Mol. Genet. 12 (2003) 1507–1522.
[62] A. Scrima, R. Konickova, B.K. Czyzewski, Y. Kawasaki, P.D. Jeffrey, R. Groisman, Y. Nakatani, S. Iwai, N.P. Pavletich, N.H. Thomä, Structural basis of UV DNA-damage recognition by the DDB1– DDB2 complex, Cell 135 (2008) 1213–1223.
[63] P. Shiyanov, A. Nag, P. Raychaudhuri, Cullin 4A associates with the UV-damaged DNA-binding protein DDB, J. Biol. Chem. 274 (1999) 35309–35312.
[64] R. Groisman, J. Polanowska, I. Kuraoka, J. Sawada, M. Saijo, R. Drapkin, A.F. Kisselev, K. Tanaka, Y. Nakatani, The ubiquitin ligase activity in the DDB2 and CSA

complexes is differentially regulated by the COP9 signalosome in response to DNA damage, Cell 113 (2003) 357–367.
[65] X. Chen, Y. Zhang, L. Douglas, P. Zhou, UV-damaged DNA-binding proteins are targets of CUL-4A-mediated ubiquitination and degradation, J. Biol. Chem. 276 (2001) 48175–48182.
[66] A. Nag, T. Bondar, S. Shiv, P. Raychaudhuri, The xeroderma pigmentosum group E gene product *DDB2* is a specific target of cullin 4A in mammalian cells, Mol. Cell. Biol. 21 (2001) 6738–6747.
[67] K. Sugasawa, Y. Okuda, M. Saijo, R. Nishi, N. Matsuda, G. Chu, T. Mori, S. Iwai, K. Tanaka, K. Tanaka, F. Hanaoka, UV-induced ubiquitylation of XPC protein mediated by UV-DDB-ubiquitin ligase complex, Cell 121 (2005) 387–400.
[68] H. Wang, L. Zhai, J. Xu, H.Y. Joo, S. Jackson, H. Erdjument-Bromage, P. Tempst, Y. Xiong, Y. Zhang, Histone H3 and H4 ubiquitylation by the CUL4-DDB-ROC1 ubiquitin ligase facilitates cellular response to DNA damage, Mol. Cell 22 (2006) 383–394.
[69] M.G. Kapetanaki, J. Guerrero-Santoro, D.C. Bisi, C.L. Hsieh, V. Rapic-Otrin, A.S. Levine, The DDB1-CUL4ADDB2 ubiquitin ligase is deficient in xeroderma pigmentosum group E and targets histone H2A at UV-damaged DNA sites, Proc. Natl. Acad. Sci. U.S.A. 103 (2006) 2588–2593.
[70] B.J. Hwang, S. Toering, U. Francke, G. Chu, p48 activates a UV-damaged-DNA binding factor and is defective in xeroderma pigmentosum group E cells that lack binding activity, Mol. Cell. Biol. 18 (1998) 4391–4399.
[71] J.Y. Tang, B.J. Hwang, J.M. Ford, P.C. Hanawalt, G. Chu, Xeroderma pigmentosum p48 gene enhances global genomic repair and suppresses UV-induced mutagenesis, Mol. Cell 5 (2000) 737–744.
[72] M.E. Fitch, S. Nakajima, A. Yasui, J.M. Ford, In vivo recruitment of XPC to UV-induced cyclobutane pyrimidine dimers by the DDB2 gene product, J. Biol. Chem. 278 (2003) 46906–46910.
[73] J. Moser, M. Volker, H. Kool, S. Alekseev, H. Vrieling, A. Yasui, A.A. van Zeeland, L.H. Mullenders, The UV-damaged DNA binding protein mediates efficient targeting of the nucleotide excision repair complex to UV-induced photo lesions, DNA Repair 4 (2005) 571–582.
[74] J.T. Reardon, A. Sancar, Recognition and repair of the cyclobutane thymine dimer, a major cause of skin cancers, by the human excision nuclease, Genes Dev. 17 (2003) 2539–2551.
[75] H. Naegeli, L. Bardwell, E.C. Friedberg, The DNA helicase and adenosine triphosphatase activities of yeast Rad3 protein are inhibited by DNA damage, J. Biol. Chem. 267 (1992) 392–398.
[76] U. Camenisch, R. Dip, S.B. Schumacher, B. Schuler, H. Naegeli, Recognition of helical kinks by xeroderma pigmentosum group A protein triggers DNA excision repair, Nat. Struct. Mol. Biol. 13 (2006) 278–284.
[77] U. Camenisch, R. Dip, M. Vitanescu, H. Naegeli, Xeroderma pigmentosum complementation group A protein is driven to nucleotide excision repair sites by the electrostatic potential of distorted DNA, DNA Repair 6 (2007) 1819–1828.
[78] N. Buschta-Hedayat, T. Buterin, M.T. Hess, M. Missura, H. Naegeli, Recognition of nonhybridizing base pairs during nucleotide excision repair of DNA, Proc. Natl. Acad. Sci. U.S.A. 96 (1999) 6090–6095.

8. Conclusion and perspectives

The xeroderma pigmentosum (XP) syndrome has been used as a model disease to investigate the cancer-inducing effects of UV exposure since 1967, when it was discovered that the major molecular defect underlying this disease is a deficient DNA excision repair activity (Cleaver, 2005; Friedberg, 2008; Cleaver et al, 2009). Cell fusion studies performed with fibroblasts from XP patients led to the identification of eight complementation groups, seven of which reflect mutations in different nucleotide excision repair (NER) genes. Among these complementation groups, XP-E arises from mutations in the *DDB2* (for damaged DNA-binding 2) gene (Chu & Chang, 1988; Keeney et al, 1992). Patients assigned to the XP-E complementation group present with a milder form of the disease consistent with the finding that the *DDB2* gene product is not a component of the core NER machinery and, instead, constitutes an accessory factor that stimulates the excision of UV lesions (CPDs and 6-4PPs) (Ford & Hanawalt, 1997; Hwang et al, 1999; Bennett & Itoh, 2008).

Until now, the clinical and biological consequences of *DDB2* mutations in XP-E patients and cells, respectively, have been difficult to reconcile with the known biochemical properties of DDB2 protein (Sugasawa, 2010). For example, DDB2 protein displays a much higher binding affinity for DNA containing 6-4PPs than for comparable substrates containing only CPDs (Hwang & Chu, 1993; Reardon et al, 1993; Wittschieben et al, 2005). However, the absence of DDB2 in XP-E cells affects the excision of CPDs more severely compared to 6-4PPs. In fact, in XP-E cells, the removal of CPDs is nearly abrogated whereas the repair of 6-4PPs is only initially delayed (Ford & Hanawalt, 1997; Hwang et al, 1999). Also, the excision of both 6-4PPs and CPDs can be reconstituted *in vitro* without the need for DDB2 protein (Araujo et al, 2000; Kulaksiz et al, 2005). It is also not clear what is the true impact on DNA repair of the interaction partner DDB1, which acts as a molecular adaptor to recruit the CUL4A and CUL4B ubiquitin ligases (Chen et al, 2006; Liu et al, 2009).

For these reasons, the function of DDB2 in the NER process remained enigmatic. Upon binding to UV lesions, DDB2 is rapidly ubiquitinated by the DDB1-CUL4A ubiquitin ligase and degraded by proteasomal activity, which

leads to the clearance of this factor from damaged sites (Chen et al, 2001a; Rapic-Otrin et al, 2002; El-Mahdy et al, 2006). The currently most widely accepted model predicts that DDB2 also recruits XPC protein to UV lesions, thus inducing the XPC ubiquitination by the same ubiquitin ligase complex (Sugasawa, 2009). Unlike DDB2, which is rapidly degraded upon ubiquitination, the ubiquitin modification of XPC is at least in part reversible and, according to *in vitro* binding assays, potentiates its DNA-binding activity (Rapic-Otrin et al, 2002; Sugasawa et al, 2005; El-Mahdy et al, 2006). However, the interaction between DDB2 and XPC that can be detected in solution are rather weak and, in biochemical assays, it has never been possible to isolate a ternary complex containing DDB2, XPC and damaged DNA (Batty et al, 2000; Wakasugi et al, 2001; Scrima et al, 2008; Sugasawa, 2009). As a consequence, it was not clear how the DNA substrate handover from DDB2 to XPC takes place in the chromatin of living cells. Also, NER activity in response to UV lesions can be biochemically reconstituted without any concomitant ubiquitination reactions (Aboussekhra et al, 1995; Mu et al, 1995; Araujo et al, 2000; Sugasawa et al, 2005). Ironically, CUL4A knockout mice, which are unable to ubiquitinate DDB2, XPC and other protein substrates, show much higher repair efficiency of both 6-4PPs and CPDs than wild-type controls and, as a consequence, are protected from UV-induced skin carcinogenesis (Chen et al, 2006; Liu et al, 2009).

To resolve these controversial issues, at the start of this project, we set up a working hypothesis by which DDB2 plays a role mainly in the context of chromatin where it regulates the excision of UV lesion by a direct and dynamic interaction with the XPC partner. A second important hypothesis was that ubiquitination modulates the distribution of XPC protein in chromatin rather than its overall affinity for damaged DNA. When assembled in chromatin, the eukaryotic DNA filament is known to be wrapped around histone core particles to form nucleosome structures. Each nucleosome is comprised of approximately 147 base pairs of DNA wrapped in 1.67 left-handed superhelical turns around a histone octamer which is made of two copies of histone H2A, H2B, H3 and H4. Nucleosome core particles are linked to each other by linker DNA of 60-80 base pairs to form a 10-nm “beads on a

string" fiber, which can be further organized into a 30-nm fiber probably through the participation of linker histone H1, histone modifications and other chromatin proteins (Ramakrishnan et al, 1993; Zlatanova et al, 1994; Luger et al, 1997; Robinson et al, 2006). Although the structure of more highly compacted chromatin is not yet understood, currently the chromatin is classified into two main species, *i.e.*, euchromatin and heterochromatin. Euchromatin is the less compacted form and is thought to be transcriptionally active. Heterochromatin is a highly compacted and less accessible form of chromatin that is important for gene silencing and cell division (Zlatanova et al, 1994; Allis et al, 2006; Bernstein et al, 2006).

Micrococcal nuclease (MNase, also called staphylococcal nuclease) is major biochemical tool often used to dissect the complex chromatin of eukaryotic cells (Heins et al, 1967). This nuclease digests preferentially the linker DNA regions between nucleosomes. When carried out under conditions of physiologic ionic strength, the MNase digestion of chromatin generates two distinct fractions that correlated with the kinetics of DNA repair synthesis. Generally, DNA damages located in MNase-sensitive regions are rapidly repaired, whereas DNA lesions in MNase-resistant sites are more refractory to repair (Smerdon & Lieberman, 1978; Smerdon et al, 1978). Another frequently used enzyme, DNase I, digests the DNA preferentially in the minor groove of both nucleosome core fragments and linker segments and, therefore, does not show a marked preference of DNA repair sites (Smerdon et al, 1978; Smerdon & Lieberman, 1980).

In this project, the UV-irradiated chromatin of mammalian cells was dissected by MNase digestion yielding two separate fractions, namely MNase-sensitive chromatin consisting of solubilizable nucleosome core particles and linker DNA and MNase-resistant chromatin consisting of insoluble core particles. This analysis of UV-irradiated chromatin disclosed novel mechanisms by which DDB2 stimulates the repair of both 6-4PPs and CPDs by the global-genome NER subpathway.

A key finding of the present thesis work is that DDB2 sorts out highly accessible nucleosomes as DNA repair hotspots. This activity is achieved by

recruitment of the DDB1-CUL4A ubiquitin ligase and poly-ubiquitination of the XPC partner. Only the ubiquitinated XPC molecules are retained in this accessible chromatin region that is amenable to the subsequent recruitment of downstream NER factors. In the absence of this ubiquitination activity, XPC protein by default migrates to repair cold spots that represent a highly compacted chromatin environment much less permissive to the assembly of downstream NER complexes. This newly discovered regulatory mechanism is important because the majority of inflicted 6-4PPs (~90%) are generated in MNase-sensitive chromatin regions (Mitchell et al, 1990). Although in wild-type cells, ~75% of 6-4PPs are removed rapidly during the first 1 hour after UV irradiation, the repair of 6-4PPs is initially delayed in XP-E cells lacking functional DDB2 (Ford & Hanawalt, 1997; Hwang et al, 1999), thus provoking higher levels of mutagenesis (Gentil et al, 1996). It can be concluded that the initially delayed excision of 6-4PPs in XP-E cells is due to the inaccessibility of XPC protein to 6-4PPs in the absence of ubiquitination.

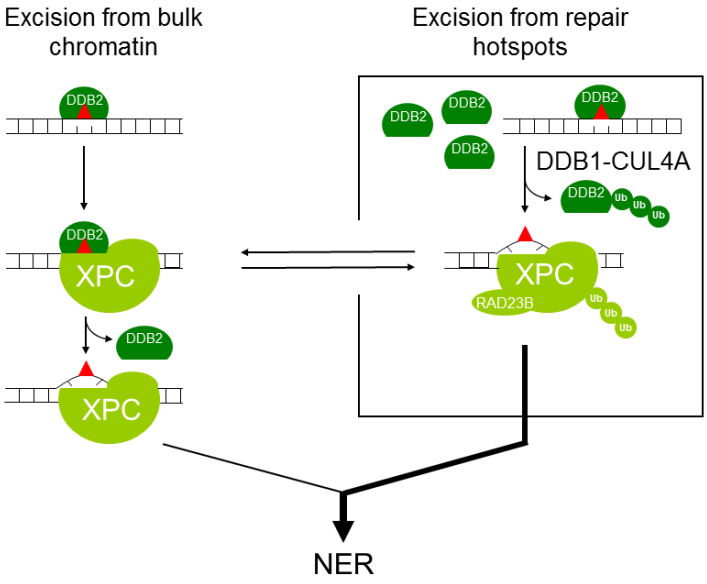

Figure 1. Bimodal action of DDB2 in stimulating DNA damage recognition by the repair-initiating XPC protein.

Our findings also contradict the notion that the DDB1-CUL4A activity is mainly needed to relax chromatin by ubiquitination of histones H2A, H3 and H4, thus facilitating the access of DNA repair factors to damaged sites (Kapetanaki et al, 2006; Wang et al, 2006). The concomitant ubiquitination of DDB2 is thought to mediate its clearance from lesion sites, again to facilitate the recruitment of XPC protein and other downstream NER factors (Chen et al, 2001b; Rapic-Otrin et al, 2002; El-Mahdy et al, 2006). In some studies, the inhibition of CUL4A ubiquitination reduced the ability of XPC protein to accumulate in nuclear spots of UV lesions and inhibited the subsequent excision of these lesions (El-Mahdy et al, 2006; Wang et al, 2006). However, in other studies, the suppression of CUL4A activity resulted in enhanced removal of photolesions (Liu et al, 2009). In this thesis, we provide a different explanation for the role of DDB1-CUL4A-mediated modifications as we show that the ubiquitination of XPC protein is the main determinant of its distribution in chromatin. We found that the ubiquitination of DDB2 (Chen et al, 2001b; Rapic-Otrin et al, 2002; El-Mahdy et al, 2006) and histones (Bergink et al, 2006; Kapetanaki et al, 2006; Wang et al, 2006; Scrima et al, 2008) has no impact on the overall affinity of XPC protein for UV-irradiated chromatin. This conclusion is supported by the finding that a XPC-GFP fusion protein, which escapes ubiquitination, displays the same chromatin distribution as endogenous XPC in the presence of a defective ubiquitylation system. In summary, by mediating the ubiquitination of XPC protein, DDB2 indirectly facilitates the fast removal of 6-4PPs during the initial response after UV irradiation.

The second key finding of this project is that DDB2, independently of ubiquitin, is able to enhance the recruitment of the XPC partner to UV lesions through direct protein-protein interactions with the TGD and BHD1 motifs of XPC protein. It has been shown before that UV-DDB interacts physically with XPC protein in solution (Sugasawa et al, 2005). However, so far it has never been possible to isolate a ternary complex comprising UV-DDB, XPC and DNA, raising doubts about whether UV-DDB may be able to directly recruit the XPC partner to DNA lesions (Batty et al, 2000). In addition, the crystal structures of UV-DDB-DNA and RAD4-DNA complexes (RAD4 is the yeast XPC homolog)

showed that both proteins insert a beta-hairpin into the DNA duplex and it has been noted that these two competing beta-hairpins may clash with each other if both factors interact with the same lesion (Scrima et al, 2008).

In this thesis, we demonstrate that two separate domains of XPC protein (the TGD and BHD1 motifs) interacts with DDB2 in the absence of DNA. Interestingly, the association with TGD is abolished in the presence of UV-damaged DNA substrates. In contrast, the interaction with BHD1 is stimulated by damaged DNA duplexes. The identification of a separable domain, whose interaction with DDB2 is inhibited in the presence of damaged DNA, suggested that DDB2-XPC associations occur only transiently at lesion sites. Indeed, protein dynamics analysis by fluorescence recovery after photobleaching on local damage show that DDB2-XPC interactions do occur in the chromatin of living cells but only transiently. These dynamic DDB2-XPC interactions serve to prolong the residence time of XPC protein at UV lesions and facilitates the insertion of the beta-hairpin of the BHD3 motif into the DNA duplex. Taking together, the interaction studies indicated that DDB2 and XPC undergo physical contacts to transfer the UV lesion from one factor to the other. This transition process provides for the first time a mechanistic framework by which DDB2 promotes CPD recognition by XPC protein and explains the overall defect of XP-E cells in repairing CPDs.

In summary, we discovered a bimodal mechanism by which DDB2 spatially and temporally organizes NER reactions in mammalian chromatin to ensure an initial (ubiquitin-dependent) fast repair (mainly of easily recognizable 6-4PPs) as well as the prolonged (ubiquitin-independent) excision of more intractable DNA lesions buried in chromatin (**Fig. 1**). We propose that DDB2 is a master organizer of DNA repair for the effective removal of UV lesions from mammalian chromatin. Despite the progress of this thesis, there are still a number of unanswered questions to be solved. Some of these open issues are outlined below.

1. DDB2 levels and function are regulated by ubiquitin-mediated proteasomal degradation (Rapic-Otrin et al, 2002; Sugasawa et al, 2005; El-Mahdy et al, 2006). However, DDB2 is also subject to other

posttranslational protein modifications such as, for example, acetylation at the position K278 (Choudhary et al, 2009). It is not known to what extent this acetylation or other modifications alter the stability, distribution and activity of DDB2.

2. It is not even clear why DDB2 is degraded upon UV exposure. Is this degradation necessary to allow for the binding of XPC protein to damaged DNA sites? Or is DDB2 degradation necessary to prevent excessive DDB2-mediated apoptosis following exposure to UV light? Indeed, it has been reported that a *DDB2* gene deletion leads to tumor progression and resistance to apoptosis by abrogating a p53 dependent pathway (Itoh et al, 2004; Stoyanova et al, 2008). However, it is not yet know whether the degradation of DDB2 upon UV radiation has the same effect on the apoptotic endpoint.
3. What is the function of UV-dependent alterations of the histone code (Tjeertes et al, 2009)? Do these changes of the histone modification pattern promote the opening of compact chromatin structures to allow for the recognition and removal of UV-lesions, as suggested previously (Huang & Sancar, 1994)? Or are these modifications able to attract directly damage recognition factors like UV-DDB or XPC? It has been reported that histone H2A becomes rapidly deubiquitinated upon UV irradiation even in the absence of DDB2 (Kapetanaki et al, 2006). This observation suggests that DDB2 is not the first factor that senses UV lesions and initiates the cellular DNA damage response. As a consequence, it will be important to know the function of UV-dependent histone modification signatures and understand how they are formed. These future studies might change the current view of how cells sense UV damage in their genome.
4. It has been inferred from an *in vitro* studies that the ATP-dependent chromatin assembly and remodeling factor (ACF) stimulates the removal of 6-4PPs in the linker DNA region (Ura et al, 2001). Therefore, it will be of interest to determine in the future if ACF also regulates recruitment of XPC in nucleosome core particles and whether ACF activity is regulated by the DDB1-CUL4 ubiquitin ligase.

5. Reconstitution assays *in vitro* suggested that XPC protein cannot access DNA lesions located on the nucleosome core fragment (Yasuda et al, 2005). However, several findings indicate that, in living cells, XPC co-localizes with condensed chromatin regions (Luijsterburg et al, 2007; Solimando et al, 2009). In agreement with these reports, we showed here that, in response to UV damage, XPC protein by default migrates to repair cold spots consisting of fully compacted nucleosomes. However, it is not yet known how XPC protein is able to migrate into such crowded and apparently compact chromatin. Are there any other factors besides UV-DDB that assists XPC in the binding to heterochromatin?
6. In this study, the distribution of RAD23B, the apparently constitutive interaction partner of XPC, is different to what has been described in previous reports (see for example van der Spek et al, 1996). In biochemical reconstitution experiments, RAD23B interacts with XPC to stimulate its DNA binding activity and, *in vivo*, RAD23B protects XPC from proteasome degradation (Sugasawa et al, 1996; Ng et al, 2003). However, we found in UV-irradiated HeLa cells that RAD23B is only recruited to the solubilizable DNA repair hotspots, where XPC protein is preferentially ubiquitinated. Instead, XPC migrates to the insoluble highly condensed chromatin fraction without being accompanied by RAD23B. Using the FRET technique, Bergink (2006) observed that the proportion of RAD23B in complex with XPC drops dramatically after UV irradiation (Bergink, 2006). This earlier finding is consistent with our observation that XPC dissociates from RAD23B to reach UV lesions buried in compacted chromatin.
7. As mentioned before, DDB2 is degraded upon UV in a CUL4A-DDB1 dependent manner (Rapic-Otrin et al, 2002; Sugasawa et al, 2005; El-Mahdy et al, 2006). However, we found that, in the insoluble chromatin fraction, the DDB2 proteolysis could not be blocked by CUL4A knockdown using specific siRNA. On the other hand, the proteasome inhibitor MG132 prevented DDB2 degradation in this chromatin region. This observation points to the existence of alternative mechanisms by which DDB2 levels are regulated. In this respect, it may be interesting

that the amino-truncated $DDB2_{79-427}$ construct, which cannot associate with DDB1, is effectively ubiquitinated and degraded upon UV (data not shown).

8. What are functions of other post-translational modifications, i.e. SUMOylation or phosphorylation of XPC protein? Is there any crosstalk between these different types of protein modifications? It has been shown that XPC can be phosphorylated at residues S350 and S892 by ATM (ataxia telangiectasia-mutated) and ATR (ATM and Rad3-related) upon exposure to ionizing radiation (Matsuoka et al, 2007). UV irradiation also triggers activation of ATR due to replication stress (Ward et al, 2004). Does UV-activated ATR phosphorylate XPC? What are the consequences of this putative modification?
9. As stated before, it has been established that the UV-induced arrest of replication forks during cell division triggers ATR activity (Ward et al, 2004; Stokes et al, 2007), which has been reported to be required for the removal of 6-4PPs in S phase cells (Auclair et al, 2008). However, it is not known how ATR may modulate this proposed cell division phase-specific removal of 6-4PPs. It has been suggested that, in the absence of ATR, UV light is unable to trigger the translocation of XPA protein from cytoplasma to the nucleus (Wu et al, 2007). Our own results suggest that an inhibition of kinase activities by caffeine changes the chromatin distribution of XPC protein. Work is now in progress to confirm this observation with more specific small-molecule kinase inhibitors or with specific respective siRNA knockdown techniques.
10. Another open question in the field is whether ubiquitinated XPC protein is degraded by proteasomal activity or, alternatively, deubiquitinated by deubiquitinase (DUB) enzymes? What DUBs are involved in this XPC deubiquitination reaction?
11. Finally, it has never been investigated how cells cope with UV lesions generated during ongoing mitosis, particularly during the metaphase and anaphase, when chromosomes are highly compacted and very limited replication or transcription takes place (Giunta et al, 2010). Is

the a DNA repair activity on such highly compacted chromosomal structures?

To summarize, although the basic biochemical steps of the NER pathway have been elucidated in detail, there is still ongoing research on how this multistep process is carried out in the context of complex chromatin substrates or how it is coordinated with ongoing cell division cycle in proliferating tissues.

Aboussekhra A, Biggerstaff M, Shivji MK, Vilpo JA, Moncollin V, Podust VN, Protic M, Hubscher U, Egly JM, Wood RD (1995) Mammalian DNA nucleotide excision repair reconstituted with purified protein components. *Cell* **80:** 859-868

Allis CD, Jenuwein T, Reinberg D, Caparros ML (2006) *Epigenetics*, Cold Spring Harbor: Cold Spring Harbor Laboratory Press.

Araujo SJ, Tirode F, Coin F, Pospiech H, Syvaoja JE, Stucki M, Hubscher U, Egly JM, Wood RD (2000) Nucleotide excision repair of DNA with recombinant human proteins: definition of the minimal set of factors, active forms of TFIIH, and modulation by CAK. *Genes Dev* **14:** 349-359

Auclair Y, Rouget R, Affar el B, Drobetsky EA (2008) ATR kinase is required for global genomic nucleotide excision repair exclusively during S phase in human cells. *Proc Natl Acad Sci U S A* **105:** 17896-17901

Batty D, Rapic'-Otrin V, Levine AS, Wood RD (2000) Stable binding of human XPC complex to irradiated DNA confers strong discrimination for damaged sites. *J Mol Biol* **300:** 275-290

Bennett D, Itoh T (2008) The XPE gene of xeroderma pigmentosum, its product and biological roles. *Adv Exp Med Biol* **637:** 57-64

Bergink S (2006) Interplay of the ubiquitin proteasome system with nucleotide excision repair. *PhD thesis, Erasmus University, Rotterdam*

Bergink S, Salomons FA, Hoogstraten D, Groothuis TA, de Waard H, Wu J, Yuan L, Citterio E, Houtsmuller AB, Neefjes J, Hoeijmakers JH, Vermeulen W, Dantuma NP (2006) DNA damage triggers nucleotide excision repair-dependent monoubiquitylation of histone H2A. *Genes Dev* **20:** 1343-1352

Bernstein BE, Mikkelsen TS, Xie X, Kamal M, Huebert DJ, Cuff J, Fry B, Meissner A, Wernig M, Plath K, Jaenisch R, Wagschal A, Feil R, Schreiber SL, Lander ES (2006) A bivalent chromatin structure marks key developmental genes in embryonic stem cells. *Cell* **125:** 315-326

Chen L, Shinde U, Ortolan TG, Madura K (2001a) Ubiquitin-associated (UBA) domains in Rad23 bind ubiquitin and promote inhibition of multi-ubiquitin chain assembly. *EMBO Rep* **2:** 933-938

Chen X, Zhang J, Lee J, Lin PS, Ford JM, Zheng N, Zhou P (2006) A kinase-independent function of c-Abl in promoting proteolytic destruction of damaged DNA binding proteins. *Mol Cell* **22:** 489-499

Chen X, Zhang Y, Douglas L, Zhou P (2001b) UV-damaged DNA-binding proteins are targets of CUL-4A-mediated ubiquitination and degradation. *J Biol Chem* **276:** 48175-48182

Choudhary C, Kumar C, Gnad F, Nielsen ML, Rehman M, Walther TC, Olsen JV, Mann M (2009) Lysine acetylation targets protein complexes and co-regulates major cellular functions. *Science* **325:** 834-840

Chu G, Chang E (1988) Xeroderma pigmentosum group E cells lack a nuclear factor that binds to damaged DNA. *Science* **242:** 564-567

Cleaver JE (2005) Cancer in xeroderma pigmentosum and related disorders of DNA repair. *Nat Rev Cancer* **5:** 564-573

Cleaver JE, Lam ET, Revet I (2009) Disorders of nucleotide excision repair: the genetic and molecular basis of heterogeneity. *Nat Rev Genet* **10:** 756-768

El-Mahdy MA, Zhu Q, Wang QE, Wani G, Praetorius-Ibba M, Wani AA (2006) Cullin 4A-mediated proteolysis of DDB2 protein at DNA damage sites regulates in vivo lesion recognition by XPC. *J Biol Chem* **281:** 13404-13411

Ford JM, Hanawalt PC (1997) Expression of wild-type p53 is required for efficient global genomic nucleotide excision repair in UV-irradiated human fibroblasts. *J Biol Chem* **272:** 28073-28080

Friedberg EC (2008) A brief history of the DNA repair field. *Cell Res* **18:** 3-7

Gentil A, Le Page F, Margot A, Lawrence CW, Borden A, Sarasin A (1996) Mutagenicity of a unique thymine-thymine dimer or thymine-thymine pyrimidine pyrimidone (6-4) photoproduct in mammalian cells. *Nucleic Acids Res* **24:** 1837-1840

Giunta S, Belotserkovskaya R, Jackson SP (2010) DNA damage signaling in response to double-strand breaks during mitosis. *J Cell Biol* **190:** 197-207

Heins JN, Suriano JR, Taniuchi H, Anfinsen CB (1967) Characterization of a nuclease produced by Staphylococcus aureus. *J Biol Chem* **242:** 1016-1020

Huang JC, Sancar A (1994) Determination of minimum substrate size for human excinuclease. *J Biol Chem* **269:** 19034-19040

Hwang BJ, Chu G (1993) Purification and characterization of a human protein that binds to damaged DNA. *Biochemistry* **32:** 1657-1666

Hwang BJ, Ford JM, Hanawalt PC, Chu G (1999) Expression of the p48 xeroderma pigmentosum gene is p53-dependent and is involved in global genomic repair. *Proc Natl Acad Sci U S A* **96:** 424-428

Itoh T, Cado D, Kamide R, Linn S (2004) DDB2 gene disruption leads to skin tumors and resistance to apoptosis after exposure to ultraviolet light but not a chemical carcinogen. *Proc Natl Acad Sci U S A* **101:** 2052-2057

Kapetanaki MG, Guerrero-Santoro J, Bisi DC, Hsieh CL, Rapic-Otrin V, Levine AS (2006) The DDB1-CUL4ADDB2 ubiquitin ligase is deficient in xeroderma pigmentosum group E and targets histone H2A at UV-damaged DNA sites. *Proc Natl Acad Sci U S A* **103:** 2588-2593

Keeney S, Wein H, Linn S (1992) Biochemical heterogeneity in xeroderma pigmentosum complementation group E. *Mutat Res* **273:** 49-56

Kulaksiz G, Reardon JT, Sancar A (2005) Xeroderma pigmentosum complementation group E protein (XPE/DDB2): purification of various complexes of XPE and analyses of their damaged DNA binding and putative DNA repair properties. *Mol Cell Biol* **25:** 9784-9792

Liu L, Lee S, Zhang J, Peters SB, Hannah J, Zhang Y, Yin Y, Koff A, Ma L, Zhou P (2009) CUL4A abrogation augments DNA damage response and protection against skin carcinogenesis. *Mol Cell* **34:** 451-460

Luger K, Mader AW, Richmond RK, Sargent DF, Richmond TJ (1997) Crystal structure of the nucleosome core particle at 2.8 A resolution. *Nature* **389:** 251-260

Luijsterburg MS, Goedhart J, Moser J, Kool H, Geverts B, Houtsmuller AB, Mullenders LH, Vermeulen W, van Driel R (2007) Dynamic in vivo interaction of DDB2 E3 ubiquitin ligase with UV-damaged DNA is independent of damage-recognition protein XPC. *J Cell Sci* **120:** 2706-2716

Matsuoka S, Ballif BA, Smogorzewska A, McDonald ER, 3rd, Hurov KE, Luo J, Bakalarski CE, Zhao Z, Solimini N, Lerenthal Y, Shiloh Y, Gygi SP, Elledge SJ (2007) ATM and ATR substrate analysis reveals extensive protein networks responsive to DNA damage. *Science* **316:** 1160-1166

Mitchell DL, Nguyen TD, Cleaver JE (1990) Nonrandom induction of pyrimidine-pyrimidone (6-4) photoproducts in ultraviolet-irradiated human chromatin. *J Biol Chem* **265:** 5353-5356

Mu D, Park CH, Matsunaga T, Hsu DS, Reardon JT, Sancar A (1995) Reconstitution of human DNA repair excision nuclease in a highly defined system. *J Biol Chem* **270:** 2415-2418

Ng JM, Vermeulen W, van der Horst GT, Bergink S, Sugasawa K, Vrieling H, Hoeijmakers JH (2003) A novel regulation mechanism of DNA repair by damage-induced and RAD23-dependent stabilization of xeroderma pigmentosum group C protein. *Genes Dev* **17:** 1630-1645

Ramakrishnan V, Finch JT, Graziano V, Lee PL, Sweet RM (1993) Crystal structure of globular domain of histone H5 and its implications for nucleosome binding. *Nature* **362:** 219-223

Rapic-Otrin V, McLenigan MP, Bisi DC, Gonzalez M, Levine AS (2002) Sequential binding of UV DNA damage binding factor and degradation of the p48 subunit as early events after UV irradiation. *Nucleic Acids Res* **30:** 2588-2598

Reardon JT, Nichols AF, Keeney S, Smith CA, Taylor JS, Linn S, Sancar A (1993) Comparative analysis of binding of human damaged DNA-binding protein (XPE) and Escherichia coli damage recognition protein (UvrA) to the major ultraviolet

photoproducts: T[c,s]T, T[t,s]T, T[6-4]T, and T[Dewar]T. *J Biol Chem* **268:** 21301-21308

Robinson PJ, Fairall L, Huynh VA, Rhodes D (2006) EM measurements define the dimensions of the "30-nm" chromatin fiber: evidence for a compact, interdigitated structure. *Proc Natl Acad Sci U S A* **103:** 6506-6511

Scrima A, Konickova R, Czyzewski BK, Kawasaki Y, Jeffrey PD, Groisman R, Nakatani Y, Iwai S, Pavletich NP, Thoma NH (2008) Structural basis of UV DNA-damage recognition by the DDB1-DDB2 complex. *Cell* **135:** 1213-1223

Smerdon MJ, Lieberman MW (1978) Nucleosome rearrangement in human chromatin during UV-induced DNA- reapir synthesis. *Proc Natl Acad Sci U S A* **75:** 4238-4241

Smerdon MJ, Lieberman MW (1980) Distribution within chromatin of deoxyribonucleic acid repair synthesis occurring at different times after ultraviolet radiation. *Biochemistry* **19:** 2992-3000

Smerdon MJ, Tlsty TD, Lieberman MW (1978) Distribution of ultraviolet-induced DNA repair synthesis in nuclease sensitive and resistant regions of human chromatin. *Biochemistry* **17:** 2377-2386

Solimando L, Luijsterburg MS, Vecchio L, Vermeulen W, van Driel R, Fakan S (2009) Spatial organization of nucleotide excision repair proteins after UV-induced DNA damage in the human cell nucleus. *J Cell Sci* **122:** 83-91

Stokes MP, Rush J, Macneill J, Ren JM, Sprott K, Nardone J, Yang V, Beausoleil SA, Gygi SP, Livingstone M, Zhang H, Polakiewicz RD, Comb MJ (2007) Profiling of UV-induced ATM/ATR signaling pathways. *Proc Natl Acad Sci U S A* **104:** 19855-19860

Stoyanova T, Roy N, Kopanja D, Bagchi S, Raychaudhuri P (2009) DDB2 decides cell fate following DNA damage. *Proc Natl Acad Sci U S A* **106:** 10690-10695

Stoyanova T, Yoon T, Kopanja D, Mokyr MB, Raychaudhuri P (2008) The xeroderma pigmentosum group E gene product DDB2 activates nucleotide excision repair by regulating the level of p21Waf1/Cip1. *Mol Cell Biol* **28:** 177-187

Sugasawa K (2009) UV-DDB: a molecular machine linking DNA repair with ubiquitination. *DNA Repair (Amst)* **8:** 969-972

Sugasawa K (2010) Regulation of damage recognition in mammalian global genomic nucleotide excision repair. *Mutat Res* **685:** 29-37

Sugasawa K, Masutani C, Uchida A, Maekawa T, van der Spek PJ, Bootsma D, Hoeijmakers JH, Hanaoka F (1996) HHR23B, a human Rad23 homolog, stimulates XPC protein in nucleotide excision repair in vitro. *Mol Cell Biol* **16:** 4852-4861

Sugasawa K, Okuda Y, Saijo M, Nishi R, Matsuda N, Chu G, Mori T, Iwai S, Tanaka K, Hanaoka F (2005) UV-induced ubiquitylation of XPC protein mediated by UV-DDB-ubiquitin ligase complex. *Cell* **121:** 387-400

Tjeertes JV, Miller KM, Jackson SP (2009) Screen for DNA-damage-responsive histone modifications identifies H3K9Ac and H3K56Ac in human cells. *EMBO J* **28:** 1878-1889

Ura K, Araki M, Saeki H, Masutani C, Ito T, Iwai S, Mizukoshi T, Kaneda Y, Hanaoka F (2001) ATP-dependent chromatin remodeling facilitates nucleotide excision repair of UV-induced DNA lesions in synthetic dinucleosomes. *EMBO J* **20:** 2004-2014

van der Spek PJ, Eker A, Rademakers S, Visser C, Sugasawa K, Masutani C, Hanaoka F, Bootsma D, Hoeijmakers JH (1996) XPC and human homologs of RAD23: intracellular localization and relationship to other nucleotide excision repair complexes. *Nucleic Acids Res* **24:** 2551-2559

Wakasugi M, Shimizu M, Morioka H, Linn S, Nikaido O, Matsunaga T (2001) Damaged DNA-binding protein DDB stimulates the excision of cyclobutane pyrimidine dimers in vitro in concert with XPA and replication protein A. *J Biol Chem* **276:** 15434-15440

Wang H, Zhai L, Xu J, Joo HY, Jackson S, Erdjument-Bromage H, Tempst P, Xiong Y, Zhang Y (2006) Histone H3 and H4 ubiquitylation by the CUL4-DDB-ROC1 ubiquitin ligase facilitates cellular response to DNA damage. *Mol Cell* **22:** 383-394

Ward IM, Minn K, Chen J (2004) UV-induced ataxia-telangiectasia-mutated and Rad3-related (ATR) activation requires replication stress. *J Biol Chem* **279:** 9677-9680

Wittschieben BO, Iwai S, Wood RD (2005) DDB1-DDB2 (xeroderma pigmentosum group E) protein complex recognizes a cyclobutane pyrimidine

dimer, mismatches, apurinic/apyrimidinic sites, and compound lesions in DNA. *J Biol Chem* **280:** 39982-39989

Wu X, Shell SM, Liu Y, Zou Y (2007) ATR-dependent checkpoint modulates XPA nuclear import in response to UV irradiation. *Oncogene* **26:** 757-764

Yasuda T, Sugasawa K, Shimizu Y, Iwai S, Shiomi T, Hanaoka F (2005) Nucleosomal structure of undamaged DNA regions suppresses the non-specific DNA binding of the XPC complex. *DNA Repair (Amst)* **4:** 389-395

Zlatanova J, Leuba SH, Yang G, Bustamante C, van Holde K (1994) Linker DNA accessibility in chromatin fibers of different conformations: a reevaluation. *Proc Natl Acad Sci U S A* **91:** 5277-5280

9. Abbreviations

DNA	Deoxyribonucleic acid
NER	Nucleotide excision repair
BER	Base excision repair
MMR	Mismatch repair
HR	Homologous recombination
NHEJ	Non-homologous-end-joining
UV light	Ultraviolet light
CPD	Cyclobutane pyrimidine dimers
6-4PP	(6-4)-pyrimidone photoproduct
GGR	Global genomic repair
TCR	Transcription coupled repair
RNAPII	RNA polymerase II
CS	Cockayne syndrome
CSA	Cockayne syndrome protein A
TFIIH	Transcription factor IIH
UBD	Ubiquitin binding domain
XP	Xeroderma pigmentosum
Rad23	Radiation sensitive23 protein
TLS	Translesion synthesis
XPC	Xeroderma pigmentosum complementation group C
ERCC1	DNA excision repair protein 1
RPA	Replication protein A
PCNA	*Proliferating cell nuclear antigen*
RFC	Replication factor C
Polη	Polymerase-[η,eta]
TTD	Trichothiodystrophy

UPS	Ubiquitin proteasome system
UBL	Ubiquitin like domain
UBA	Ubiquitin association domains
K	Lysine
FRET	Fluorescence resonance energy transfer
SUMO	Small ubiquitin-related modifier
EMSA	Electrophoretic mobility shift assay
B[a]P	*Benzo(a)pyrene*
AAF	N-acetoxy 2-acetylaminofluorescence
TGD	Transglutaminase homology domain
BHD	Beta-hairpin domain
OB-fold	Oligonucleotide/oligosaccharide-binding fold
BRCA2	Breast and ovarian cancer type 2 susceptibility protein
UV-DDB	UV damaged DNA binding protein
E	Glutamat
CHO cell	Chinese hamster ovarian cell
4-NQO	4-nitroquinoline 1-oxide
HLH	Helix-loop-helix
BP	Beta propeller domains
E1	Ubiquitin-activating enzyme
E2	Ubiquitin-conjugating enzyme
E3	Ubiquitin-ligating enzyme
Cul4	Cullin 4

10. Acknowledgements

I would like to express the sincere gratitude from the bottom of my heart to the people who made this thesis possible.

Firstly, I would like to deeply thank my supervisor, Prof. Dr. Hanspeter Naegeli for taking me in his group and pertinently guiding me throughout the whole PhD project. His scientific prominence and expertise encouraged me all the time.

I would also thank Prof. Dr. Josef Jiricny and Prof. Dr. Michael Hengartner for giving me the opportunity of being part of the excellent cancer biology PhD program and life science Zurich graduate school, for joining my PhD committee and giving constructive suggestions on the project.

Many thanks to Dr. Nicolas Thomae, Dr. Andrea Scrima, Dr. Giancarlo Marra, Dr. Andreas Luch, Dr. Thomas Carrel, Dr. Christopher Borner, Dr. Harvey Ozer and Dr. Stuart Linn for kindly sharing materials and ideas.

Thanks to Prof. Dr. Felix Althaus and Susanne Bachmann for their support in the institute.

Thanks to the past and present members of Naegeli group, especially to Dr. Kiki Camenisch and Dr. Flurina Clement for introducing lab techniques and Nina Kaczmarek for helps on this project. I would like also thank to the other members of the IVPT for helps and accompany.

Thanks to Mirela Vitanescu, Müriel Träxler, Maja Bollhalder, Jessica Bader and Aymone Lenisa for excellent technical assistances and to Dr. Daniel Demuth and Dr. Cedric Müntener for their IT support.

Thanks to Frau Sabina Podgorski for excellent Deutsch tuitions.

Thank George Kwok, Yungang Zi, Jia Xue, Yi Zhong and Yu Hong for being life-long friends and sharing remarkable moments with me.

Last but not least, a very special thank goes to my parents, Qiongxian Li and Jincai Fei for their love.

11. Curriculum Vitae

Name	Jia Fei Born 24th March 1983, P.R. China Single
Nationality	Chinese
Languages	Chinese, English, German
Address	Institute of Veterinary Pharmacology and Toxicology Winterthurerstrasse 260, CH-8057 Zürich Tel. +41-44-635 87 65; Fax. +41-1-635 89 10; email: jia.fei@vetpharm.uzh.ch

Education and academic positions

Since 2007	PhD-student (Cancer Biology PhD Program, Life Science Zurich Graduate School, Zurich) at the Institute of Veterinary Pharmacology and Toxicology, University of Zurich, Zurich
2006	MSc in Medical and Molecular Biosciences, Newcastle University, England
2005	BSc in Biological Sciences, Yunnan University, China
2001	Graduation from Yuxi No.1 middle school (high school)
1998	Graduation from Yuxi No.3 middle school (middle school)
1995	Graduation from Yuxi No.2 primary school (primary school)